eman ta zabal zazu

Universidad del País Vasco
Euskal Herriko Unibertsitatea

DOCTORAL THESIS

NEW INSIGHTS INTO THE TREATMENT OF DEPRESSION: ROLE OF GIRK CHANNELS AND THE GLUTAMATERGIC ANTAGONIST KETAMINE IN THE NEUROPHYSIOLOGY OF THE DORSAL RAPHE NUCLEUS

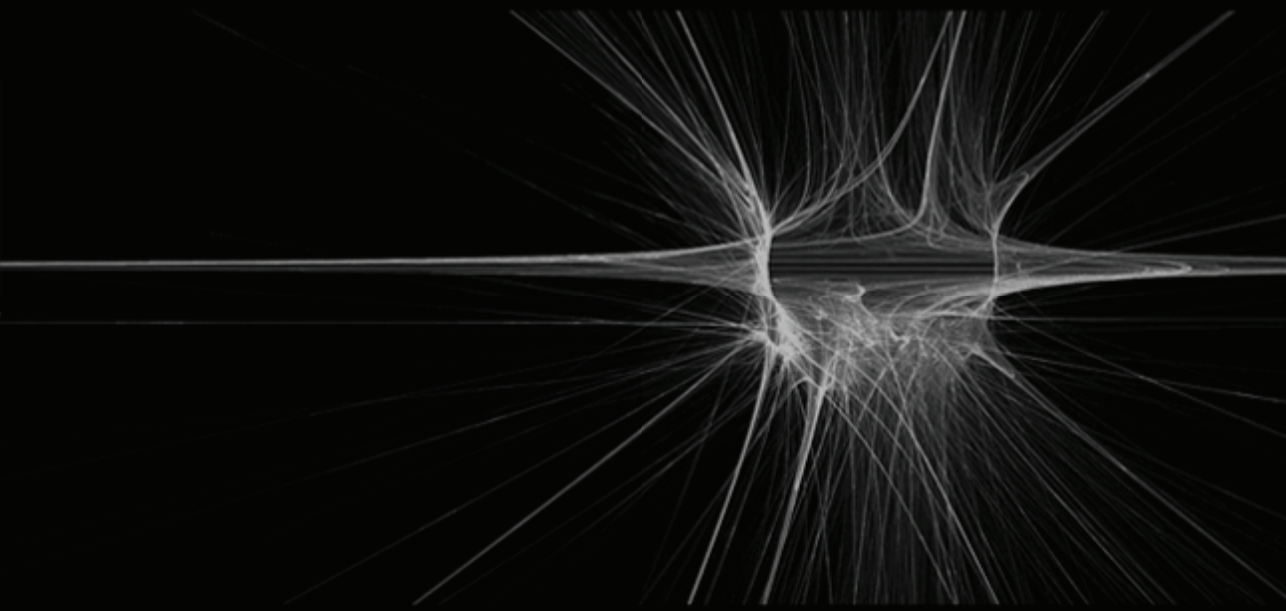

Nerea Llamosas Muñozguren

Leioa, 2015

eman ta zabal zazu

Universidad del País Vasco

Euskal Herriko Unibertsitatea

NEW INSIGHTS INTO THE TREATMENT OF DEPRESSION: ROLE OF GIRK CHANNELS AND THE GLUTAMATERGIC ANTAGONIST KETAMINE IN THE NEUROPHYSIOLOGY OF THE DORSAL RAPHE NUCLEUS

Doctoral thesis presented by Nerea Llamosas Muñozguren

Leioa, 2015

This doctoral thesis has been partially supported by the University of the Basque Country (UFI11/32), Instituto de Salud Carlos III (PI12/00613), and the Basque Government (IT747-13). N. Llamosas has held a predoctoral fellowship for the Training of Research Personnel (Formación de Personal Investigador) for the period 2011-2015.

Desde estas líneas quisiera mostrar mi agradecimiento a las personas que de un modo u otro han colaborado a que este trabajo sea posible, si bien es cierto que seguro me deje a muchas otras en el tintero ante mi interés en ser breve.

A mis directoras de tesis. A la Dra. Luisa Ugedo por haberme acogido en su laboratorio, así como por su disposición y colaboración durante estos años. A la Dra. María Torrecilla, porque su inestimable constancia, dedicación y cercanía durante estos años han colaborado enormemente a mi formación. Gracias por haberme aclarado tantas dudas y haberme hecho aprender a hacerme muchas preguntas.

To all the people I met in Portland during my pleasant stay in Williams' lab, where I learned many new things and I had an unforgettable experience. Especially to John, but also to Stephanie and Erica. Thanks so much for your willingness and attention, you made me feel like home.

A todos los miembros del laboratorio por tantos buenos ratos compartidos. Desde los "mayores" (JA, Javier, Asier y las chicas, Teresa y Cristina, siempre dispuestas a ayudar con una sonrisa y mucho humor) hasta los jóvenes (Igor, Irati, Unai y Sergio). Por supuesto, a mis dos grandes compañeras durante esta tesis, Ainhoa y Cris, vosotras ya sabéis lo mucho que me habéis ayudado, dentro y fuera del laboratorio, sé que me llevo a dos buenas amigas. Junto con Itzi formamos nuestro cuarteto de pintxo-pote ¡gracias por vuestro apoyo!

Al todo el personal del departamento por hacer de él un centro de trabajo muy agradable, además de haber compartido muchas comidas, encuentros y cafés. Especialmente a Esti, Laura, Mari, Patri, Igor e Isa.

Sin duda, sin mi ocio, disfrute y crecimiento fuera del laboratorio este trabajo hubiera sido imposible. Por eso deseo agradecer enormemente a todos

los amigos que me habéis ayudado desde fuera. Sois muchos, pero los más importantes ya sabéis quienes sois, los que día a día habéis estado ahí, escuchándome, aconsejándome y haciéndome reír. Me gustaría mencionar a mi gran amiga Julia y a Jon por su apoyo incondicional, y a Álvaro, entre otras cosas por haberme sacado mil carcajadas durante nuestras jornadas de montaña ¡mil gracias chicos!

De especial reconocimiento, a mi familia. Aita y ama, os agradezco infinitamente haberme ayudado a llegar hasta aquí, los valores que me habéis inculcado y la confianza que habéis puesto en mí. Iván, admiro tu interés y curiosidad, gracias por tantas y tantas entretenidas charlas de domingo con tu simpatía y buen humor. En especial, a mi hermana Naiara. Sister, desde que éramos pequeñitas siempre has estado ahí cuando te he necesitado y has sido mi guía y mi cómplice. Te agradezco una infinidad de cosas en diversos ámbitos, pero en especial en esta etapa tu gran compresión y cercanía. A los pequeñajos, Elaia y Anaitz, porque habéis traído aire fresco a la familia y me habéis hecho reír y distraerme incluso en los momentos menos buenos. Quisiera incidir especialmente en Elaia porque su carácter me ha aportado mucha alegría y vitalidad cuando lo necesitaba.

Por último, a toda la colonia de ratones que he criado para hacer posible este trabajo, desde los ratones “exitosos” hasta los menos afortunados, todos ellos han sido la herramienta fundamental en esta tesis.

¡Muchas gracias a todos!

INDEX

ABBREVIATION LIST

ABBREVIATION LIST

5-HT	serotonin
5-HIIA	5-hydroxyindoleacetic acid
ACSF	artificial cerebrospinal fluid
AHP	afterhyperpolarization potential
AMPA	α-amino-3-hydroxy-5-methyl-4-isoxazolepropionic acid
ANOVA	analysis of the variance
AP	action potential
ATP	adenosine triphosphate
BDNF	brain-derived neurotrophic factor
cAMP	cyclic adenosine monophosphate
CB1	cannabinoid receptor type 1
CNS	central nervous system
CRF	*corticotropin-releasing factor*
CSDS	chronic social defeat stress
CTD	cytoplasmatic domain
DAB	3,3´diaminobenzidine
DG	*dentate gyrus*
DR	*dorsal raphe nucleus*
DRd	dorsal part of the *dorsal raphe*

DRif *dorsal raphe interfascicularis*

DRv ventral part of the *dorsal raphe*

DRvl lateral portions or wings of the *dorsal raphe*

EAAT exicitatory aminoacid transporter

ED_{50} effective dose 50

eEPSC evoked excitatory postsynaptic current

eIPSC evoked inhibitory postsynaptic current

E_{max} maximum effect

FST forced swimming test

G1 slope conductance between - 70 and - 80 mV

G2 slope conductance between - 110 and - 120 mV

GABA gamma-aminobutyric acid

GCL granular cell layer

GFAP glial fibrillary acidic protein

GHB γ-hydroxybutyrate

GIRK G protein-coupled inwardly rectifying K^+

GIRK2^{wv} *weaver* mice

GIRK2$^{+/-}$ GIRK2 heterozygous

GIRK2$^{-/-}$ GIRK2 homozygous

GPCR G protein coupled receptor

GTP	guanosine triphosphate
H5	pore-forming region
HH3	phosphorylated Histone H3
HH3-IR	HH3 immunoreactiviy
HPP	*hippocampus*
i.c.v.	intracerebroventricular
i.p.	intraperitoneal
I/V	current-voltage relation
Kir	inwardly rectifying K^+
LC	*locus coeruleus*
LHb	*lateral habenula*
MDMA	3,4-methyl-enedioxymethamphetamine
ML	molecular layer
mPFC	*medial prefrontal cortex*
mRNA	messenger ribonucleic acid
mTOR	mammalian target of rapamycin
mTORC1	mammalian target of rapamycin complex 1
nAChR	nicotinic acetylcholine receptor
NCAM	neural cell adhesion molecule
NA	noradrenaline

NK1	neurokinin 1
NMDA	N-methyl-D-aspartate
NSFT	novelty suppressed feeding test
$p75^{NTR}$	nerve growth factor receptor (p75 neurotrophin receptor)
PAG	periaqueductal gray matter
PB	phosphate buffer
PCR	Polymerase Chain Reaction
PFC	*prefrontal cortex*
PIP_2	phosphatidylinositol 4,5-bisphosphate
PKA	protein kinase A
PLC	phospholipase C
RGS	regulators of G protein signaling
sEPSC	spontaneous excitatory postsynaptic current
SERT	5-HT transporter
sIPSC	spontaneous inhibitory postsynaptic current
SN	*substantia nigra*
SNX27	sorting nexin 27 protein
SVZ	subventricular zone
TM1	transmembrane domain 1
TM2	transmembrane domain 2

TMD	transmembrane domain
TrPH	tryptophan hydroxylase
TS	trizma base saline
TST	tail suspension test
VGLUT3	vesicular glutamate transporter 3
V_h	holding potential
VTA	*ventral tegmental area*
WT	wild-type
WT TPN-Q	tertiapin-Q-injected wild-type

1. INTRODUCTION

1. INTRODUCTION

Major depressive disorder is a debilitating mental illness that represents the main cause of disability throughout the world (Collins et al., 2011). In general, it is characterized by low mood, anhedonia, and loss of interest in daily activities. It is associated with severe consequences including suicide and risk of cardiovascular events (Zarate et al., 2013). Clinical depression leads to severe health and socioeconomic consequences (Kessler et al., 2003) and although its estimated lifetime prevalence in the United States is ~ 17 % (Kessler et al., 2005), its worldwide prevalence ranges depending on the country (Andrade et al., 2003; Kessler and Ustun, 2004; Kessler et al., 2010). According to the *Diagnostic and Statistical Manual of Mental Disorders,* fifth Edition (DSM-5), major depression is presented when a patient exhibits during a consecutive 2-week time frame, 5 or more symptoms including depressive mood, decreased interest (apathy) or pleasure in activity, significant weight loss, insomnia or excessive sleep, psychomotor retardation or agitation, loss of energy, feelings of inappropriate guilt and recurrent thoughts of death.

Many efforts have been made in order to understand the pathophysiology of this mental illness over the last forty years, and as a result multiple depression hypotheses have been postulated, all of which could be interrelated. The monoamine hypothesis of depression is, till date, the most established one and that in which the currently antidepressant treatments are based on. It proposes that the underlying biological or neuroanatomical basis of depression is a deficiency of central monoamine neurotransmitters noradrenaline (NA), serotonin (5-HT), and/or dopamine (Schildkraut, 1965; Delgado, 2006). The main sources of NA and 5-HT monoamines are the noradrenergic *locus coeruleus* (LC) and the serotonergic *dorsal raphe nucleus* (DR), respectively. Therefore, these brain regions have been extensively considered and studied in the research of the etiology of this psychiatric disease (Lowry et al., 2008; Itoi and Sugimoto, 2010).

Introduction

More than 20 different antidepressant medications, all of which target monoaminergic systems, are currently available (Abdallah et al., 2015). However, they are still considered a matter of debate, given the limited efficacy of these medications. A substantial proportion of patients fail to achieve a sustained remission (Rush et al., 2006) and others suffer side effects, complicating the compliance of the treatment (Racagni and Popoli, 2010). Moreover, the full clinical benefit of these traditional antidepressants is only achievable following weeks to months of treatment (Katz, 2004), although brain monoaminergic levels are rapidly restored. It has been proposed that the time needed for 5-HT_{1A} receptor desensitization may be responsible for the delay in the response to selective serotonin reuptake inhibitors (SSRIs) (Artigas et al., 1996; Blier et al., 1998), proposing 5-HT_{1A} receptors and/or their downstream effectors as candidates for the study of antidepressant treatment responses. In addition, other hypotheses involving adult neurogenesis and neurotrophic factors have emerged in order to give alternative explanations. It is proposed that chronic stress, which frequently precipitates depression, reduces adult neurogenesis in the *hippocampus* (Dranovsky and Hen, 2006; Pittenger and Duman, 2008). Moreover, antidepressant treatments increase hippocampal adult neurogenesis, and the time needed to obtain this effect is coincident with the appearance of a clinical benefit (Malberg et al., 2000), suggesting that there is a requirement of adult neurogenesis to obtain a behavioral response to antidepressants. Subsequent studies suggest that the antidepressant-induced increase in neurogenesis is mediated by 5-HT_{1A} receptors (Santarelli et al., 2003). Altogether, 5-HT_{1A} receptor-mediated signaling plays a relevant role in the etiology of depression and response to antidepressants. However, there is still a need of a better understanding of the specific mechanisms responsible for the delay in the response to antidepressants, in order to progress in the development of new faster-acting efficacious antidepressant drugs.

Nevertheless, research in the field of depression continues, and currently, targeting brain regions and neurotransmission systems other than the monoaminergic ones seems a promising field to elucidate possible unknown mechanisms and processes involved in the etiology of depression. In this sense, dysfunctional glutamatergic and gamma-aminobutyric acid (GABA) systems are also considered to play a relevant role in the pathophysiology of depression and anxiety (Luscher et al., 2011; Sanacora et al., 2012). Indeed, glutamatergic transmission currently represents a novel target for drug development and pharmacotherapy of affective disorders (Soiza-Reilly and Commons, 2011; Musazzi et al., 2013).

1.1. Serotonergic system: the *dorsal raphe nucleus*

1.1.1. Anatomy

The serotonergic system is formed by 5-HT cell clusters typically divided into nine groups (B_{1-9}) (Dahlstroem and Fuxe, 1964), known as the *raphe nuclei*. There are two anatomical regions, 1) the rostral group, including the *nucleus linearis*, the *dorsal raphe nucleus*, the *medial raphe nucleus* and the *raphe pontis*, all of them located in the *mesencephalon* and *rostral pons*; and 2) the caudal group, which comprises the *nucleus raphe magnus* and the *raphe pallidus* and *obscure*. It extends from the *caudal pons* to the caudal portion of the *medulla* (Baumgarten and Grozdanovic., 1997). The DR is the largest of the brainstem serotonergic nuclei containing about 50% of 5-HT neurons in the rat central nervous system (CNS) (Wiklund and Bjorklund, 1980; Descarries et al., 1982). In mice, it contains approximately 9000 5-HT neurons, in rats 10000-12000, representing approximately two thirds of all neurons in the nucleus (Molliver, 1987; Jacobs and Azmitia; 1992), and in humans it contains approximately about 235000 5-HT neurons (Baker et al., 1990). Rostrally, the DR is bound by the *Edingher Westphal nucleus* (III) and, caudally, it extends ventral to the confluence of the fourth ventricle and the cerebral aqueduct

(Steinbusch, 1981; Descarries et al., 1982; Imai et al., 1986; Tork, 1990; Jacobs and Azmitia, 1992). In most species, the DR is composed of several subregions distinguished by their different cell density, morphology, and projections: 1) a medial portion, subdivided in turn into dorsomedial and ventromedial components, just below the cerebral aqueduct and surrounding the *medial longitudinal fasciculi*, respectively; 2) lateral portions or wings which are in the dorsoventral portion, and 3) a caudal component (Azmitia and Gannon, 1986; Johnson and Ma, 1993) (Fig. 1.1). While the DR is not exclusively composed of 5-HT neurons, it is frequently defined anatomically by four major clusters of 5-HT cells within its borders (Diaz-Cintra et al., 1981; Steinbusch, 1981; Agnati et al., 1982; Abrams et al., 2004). Accordingly, there are dorsomedial, ventromedial, and two bilateral groupings of 5-HT cells in the lateral wings of the nucleus. Hence, there is an anatomical proximity between different 5-HT cell clusters that provides the ground for a network of interconnections of high degree cross-talk among 5-HT neurons at the somatodendritic level (Pineyro and Blier, 1999).

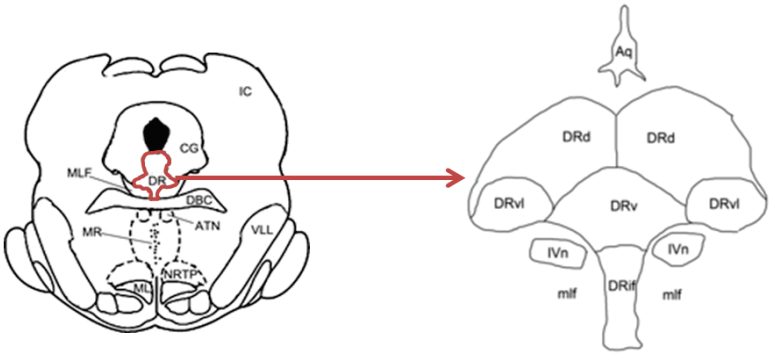

Figure 1.1. Representative picture of the *dorsal raphe* localization in a coronal section. On the left, the localization of the *dorsal raphe* (DR), ventral to the cerebral aqueduct. On the right, a magnified representation of the DR showing its different subregions. DRd: dorsal parts of the *dorsal raphe*, DRv: ventral part of the *dorsal raphe*, DRvl: lateral portions or wings of the *dorsal raphe*, DRif: caudal part of the *dorsal raphe*, *dorsal raphe* interfascicular. Taken and modified from Stopper and Floresco (2014).

1.1.2. Physiology

The DR is a nucleus of heterogeneous nature, composed by neuronal groups that differ in cellular morphology, electrophysiological properties and the expression of neurotransmitters and neuromodulators (Jacobs and Azmitia, 1992).

1.1.2.1. Serotonergic neurons

A) Localization, morphology, and electrophysiological and pharmacological properties

The 5-HT neurons are highly concentrated in the DR, at rostral levels essentially confined to the midline, at more caudal levels spreading out with two lateral wings, and a dorsal and more ventral midline nucleus, and most caudally "returning" to the midline (Fu et al., 2010) (Fig. 1.2). Most of the 5-HT neurons

are immunopositive for the 5-HT-synthesizing enzyme tryptophan hydroxylase (TrPH) (Weissmann et al., 1990). Morphologically, 5-HT neurons have fusiform, triangular or multipolar cell bodies with a diameter ranging from 15 to 35 μm. The dendrites display a poorly branched radiating pattern of arborization (Li et al., 2001).

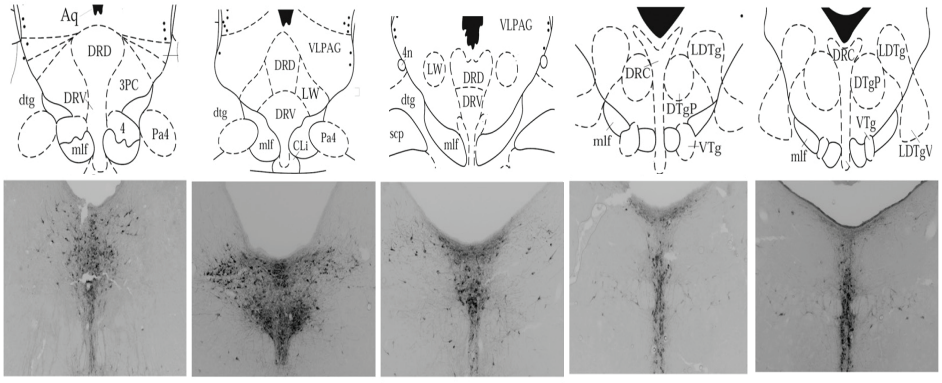

Figure 1.2. Tryptophan hydroxylase (TrPH, the enzyme responsible for serotonin production) immunostained coronal sections across the rostral (left) to caudal (right) extent of the rat *dorsal raphe*. Pictures showing the localization of TrPH immunostained neurons, corresponding to 5-HT neurons, across the sections of the *dorsal raphe* (DR). At rostral levels, 5-HT neurons are confined in the midline, spreading to the lateral parts of the DR at more caudal levels, and returning to the midline at the most caudal sections (from the left to the right).Taken and modified from Vasudeva et al. (2011).

The electrophysiological and pharmacological properties of DR 5-HT neurons have been widely characterized. *In vivo* intracellular recordings followed by neurochemical identification, found that 5-HT neurons have a slow (0.5 - 3 Hz) and rhythmic firing pattern, a large afterhyperpolarization potential (AHP), gradual interspike depolarization, and a long duration action potential (1 - 2 ms) (Aghajanian et al., 1978). Later, intracellular recordings in brain slices found that 5-HT neurons are either silence or spontaneously active with a slow,

regular firing rate (0.5 - 2.5 Hz), a high input resistance (150-400 MΩ), and have a long duration action potential (AP, approximately 1.8 ms) followed by a large and slow AHP (amplitude = 10 - 20 mV, duration = 200 - 800 ms) (Vandermaelen and Aghajanian, 1983; Burlhis and Aghajanian, 1987). Spike trains elicited by weak long depolarizing current pulses in these neurons show no adaptations of spike frequency (Li et al., 2001). In addition, pharmacologically, 5-HT neurons are hyperpolarized and their firing inhibited by stimulation of inhibitory 5-HT_{1A} receptors. It has been broadly described two different populations of 5-HT neurons (Hajos et al., 1995a; Hajos and Sharp, 1996; Hajos et al., 2007). There are single-spike neurons, which exhibit the previous electrophysiological characteristics, and also another population of 5-HT neurons of burst-firing neurons, that also show the previously mentioned properties but their firing pattern is comprised of doublets, triplets, or even quadruplets of broad spikes. Spikes within these brief bursts have a short interspike time interval (>10 ms) and diminishing spike amplitude (Hajos et al., 1995a; Hajos et al., 1995b).

B) Auto-regulation of 5-HT firing activity and release

To date, seven serotonergic receptors (5-HT_1 - 5-HT_7) with a 15 total variants have been identified and cloned (Barnes and Sharp, 1999; Hoyer et al., 2002; Kroeze et al., 2002). The 5-HT G protein coupled receptors, which are all the 5-HT receptors with the exception of the 5-HT_3 receptor that is a ligand-gated ion channel, can be divided into three major subgroups depending on which G protein signaling they activate. 5-HT_1 receptors couple mainly to the $G_{i/o}$ pathway; 5-HT_4, 5-HT_5, 5-HT_6, and 5-HT_7 receptors couple to the G_s pathway; and 5-HT_2 receptors activate the $G_{q/11}$ pathway (Maejima et al., 2013). Some of them are expressed as autoreceptors, which in the case of the 5-HT system are defined as receptors that are expressed within 5-HT neurons and provide feedback in modulating the activity of those neurons. These receptors are also expressed on non 5-HT neurons and in this case they are defined as

heteroreceptors. All members of 5-HT_1 family are expressed in 5-HT neurons and consist of 5-HT_{1A}, 5-HT_{1B}, 5-HT_{1D}, 5-HT_{1E}, and 5-HT_{1F}. They share high affinity for 5-HT, and provide negative feedback in 5-HT neuronal firing and 5-HT release (Andrade, 1998), maintaining a certain homeostatic tone in serotonergic function (McDevitt and Neumaier, 2011) (Fig. 1.3).

Auto-regulation of 5-HT neuronal firing is predominantly regulated by 5-HT_{1A} receptors located in the DR (Sprouse and Aghajanian, 1987). Also 5-HT release is under the control of 5-HT_{1A} receptors (Stamford et al., 2000). Their activation leads to inhibition of action potentials via opening G protein coupled inwardly rectifying potassium (GIRK) channels in a $G_{i/o}$-dependent manner (Aghajanian and Lakoski, 1984; Innis and Aghajanian, 1987; Bayliss et al., 1997). The opening of GIRK channels upon 5-HT_{1A} receptor stimulation results in an enhanced K^+ conductance that leads to a hyperpolarization of the membrane potential and inhibition of 5-HT action potential (VanderMaelen et al., 1986; Sprouse and Aghajanian, 1987; Sinton and Fallon, 1988). In addition, polysynaptic feedback loops through the *medial prefrontal cortex* (mPFC) also exert a control of the 5-HT firing in the DR, since 5-HT_{1A} receptors in ventral regions of the mPFC exert inhibitory and excitatory control over DR 5-HT neuronal activity (Hajos et al., 1999; Martin-Ruiz et al., 2001) by modulating glutamatergic excitatory input to DR GABAergic and 5-HT neurons (Bambico et al., 2007).

5-HT_{1A} receptors are the predominant autoreceptors in the DR. They are found on soma and dendrites of 5-HT neurons and non 5-HT cells (Sotelo et al., 1990; Miquel et al., 1992). In fact, there is also a modest expression of 5-HT_{1A} receptors in a number of GABAergic neurons throughout the rostrocaudal axis of the DR (Beck et al., 2004; Day et al., 2004). The DR, *medial raphe* and *hippocampus* are the most enriched areas with 5-HT_{1A} receptors (Pompeiano et al., 1992; Kia et al., 1996a) but they are also present in cortical areas and the *hypothalamus*, *ventral tegmental area* (VTA), *substantia nigra compacta,* and

LC (Austin et al., 1994; Azmitia et al., 1996; Kia et al., 1996a; Kia et al., 1996b).

5-HT_{1B} autoreceptors are the predominant 5-HT receptors at the presynaptic terminal. Electrophysiological experiments have shown that the 5-HT_{1B} autoreceptor inhibits 5-HT release from the axonal varicosities (Sprouse and Aghajanian, 1987; Boeijinga and Boddeke, 1993; Morikawa et al., 2000). It has also been shown that it reduces extracellular 5-HT concentrations in terminal regions, synthesis of 5-HT (Hjorth et al., 1995), and up-regulates the reuptake via the 5-HT transporter (SERT) (Xie et al., 2008; Hagan et al., 2012). Moreover, 5-HT_{1B} receptors have been shown to underlie presynaptic autoinhibition of 5-HT release in which 5-HT_{1A} receptor-mediated slow inhibitory postsynaptic currents are reduced by previous 5-HT release activating presynaptic 5-HT_{1B} receptors (Morikawa et al., 2000). It is distributed in axon varicosities and terminals but not in the soma or dendrites of 5-HT neurons (Boschert et al., 1994; Sari et al., 1999). It is also present in glutamatergic terminals as a heteroreceptor (Li and Bayliss, 1998).

5-HT_{1D} autoreceptor contributes to autoinhibition of 5-HT function at terminals and possibly dendrites (Pineyro et al., 1995; Pineyro and Blier, 1996; Trillat et al., 1997), and also controls the 5-HT release (Stamford et al., 2000). Its distribution is very similar to that of 5-HT_{1B} receptor (Bruinvels et al., 1994). Little is known about 5-HT_{1E} and 5-HT_{1F} receptors. However, it has been described the presence of 5-HT_{1E} receptors in cortical areas, *caudate putamen*, *amygdale,* and *hypothalamus* (Bruinvels et al., 1994). 5-HT_{1F} receptor has been identified in the DR (Bruinvels et al., 1994).

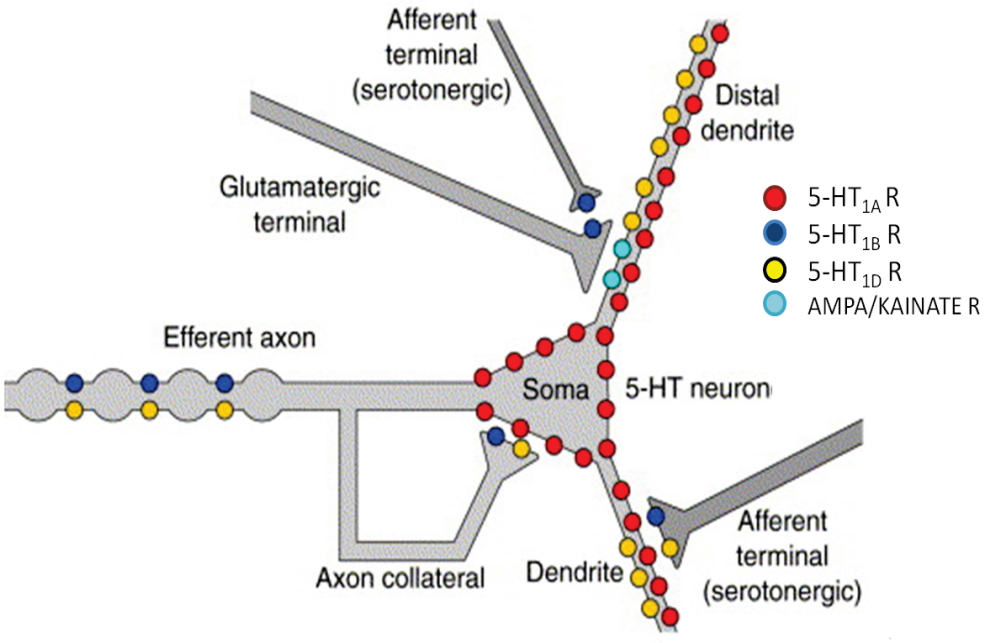

Figure 1.3. Possible location and functions of 5-HT$_1$ receptors in the *dorsal raphe*. Localization of 5-HT$_{1A}$ receptors (represented by red circles) in the 5-HT cell soma and proximal dendrites controlling 5-HT cell firing, and throughout the dendritic field, modulating the 5-HT release. 5-HT$_{1B}$ receptors (dark blue circles), which control the 5-HT release, are located on serotonergic afferents, glutamatergic terminals, and terminal portions of efferent axons. 5-HT$_{1D}$ receptors (yellow circles) are found on the dendrites and preterminal axons, modulating 5-HT release. 2-amino-3-(3-hydroxy-5-methyl-isoxazol-4-yl) propanoic acid (AMPA)/Kainate receptors location is represented by light blue circles. Taken and modified from Stamford et al. (2000).

5-HT$_2$ receptor mRNA and proteins have been identified in embryonic 5-HT neurons of the DR (Clemett et al., 2000; Wylie et al., 2010), and are also expressed on GABAergic interneurons (Liu et al., 2000; Leysen, 2004).There is no direct modulatory effect of 5-HT$_2$ receptors on 5-HT neurons, but they may increase 5-HT$_{1A}$ receptor-mediated responses in these neurons (Kidd et al., 1991).

5-HT_3 receptors enhance 5-HT release in various brain areas including the DR (Bagdy et al., 1998), but there is no direct evidence of the presence of 5-HT_3 receptors in 5-HT neurons (van Hooft and Vijverberg, 2000).

5-HT_4 receptors may be presynaptically localized since 5-HT release is modulated by 5-HT_4 agonists (Vilaro et al., 2005).

The functional role of 5-HT_5, 5-HT_6, and 5-HT_7 receptors in the modulation of 5-HT neurons is uncertain, although 5-HT_6 and 5-HT_7 receptor protein and mRNA have been detected in the DR (Ruat et al., 1993; To et al., 1995; Gustafson et al., 1996; Woolley et al., 2004).

C) Serotonin reuptake: serotonin transporter

Following release, the reuptake of 5-HT by 5-HT neurons is the principal mechanism of terminating the action of the transmitter on postsynaptic sites, and this process is carried out by the high-affinity SERT, located on the presynaptic plasma membrane (Kuhar et al., 1972; O'Reilly and Reith, 1988). It functions in series with another type of carrier, the vesicular transporter, which sequesters intracellular 5-HT within secretory vesicles (Pineyro and Blier, 1999). Two different types of SERT have been described, one is located in the CNS, and the other is peripheral. In the CNS, SERT mRNA is abundantly expressed in the DR and in 5-HT projection areas such as *frontal cortex*, *hippocampus* and *neostriatum* (Lesch et al., 1993). Disruption of the gene coding for the SERT does not alter the basal firing rate of DR 5-HT neurons (Mannoury la Cour et al., 2001).

SERT is the pharmacological target for various therapeutic and abused substances. SSRIs block 5-HT transporter increasing extracellular 5-HT, which has been considered to be the basis for their therapeutic role in depression and other psychiatric disorders (Pineyro and Blier, 1999). There is much evidence demonstrating that the acute administration of SSRIs increases 5-HT levels

preferentially in the *raphe nuclei* (Bel and Artigas, 1992; Gartside et al., 1995; Malagie et al., 1995; Hervas and Artigas, 1998). However, after sustained treatment with SSRIs 5-HT release is also increased in the forebrain (Bel and Artigas, 1992; Invernizzi et al., 1995; Le Poul et al., 1995; Hervas et al., 2001). Tricyclic antidepressants block SERT and NA transporter.

In addition to its role in the reuptake of extracellular 5-HT, SERT can promote the release of 5-HT through reversal of uptake mechanism, being the process involved in the mechanism of some drugs of abuse, such as cocaine, p-chloroamphetamine and 3,4-methyl-enedioxymethamphetamine (MDMA) (Rudnick and Wall, 1992a; Rudnick and Wall, 1992b; Adell et al., 1993).

D) Hetero-regulation and afferent pathways of *dorsal raphe*

The hetero-regulation of the 5-HT neurons involves various neurotransmitter systems since 5-HT modulates complex behaviors. Therefore, the 5-HT system receives feedback and feedfordward information from other brain areas and networks involved in regulating the different behaviors (Adell et al., 2002; Sharp et al., 2007) (Fig. 1.4). 5-HT neurons within the DR receive in particular GABAergic but also glutamatergic input. GABAergic input onto 5-HT neurons reduces the neuronal firing, and glutamatergic input increases the firing activity (Pan and Williams, 1989; Levine and Jacobs, 1992; Becquet et al., 1993a; Becquet et al., 1993b). These effects are attributed to the expression of ionotropic GABA and glutamate receptors in 5-HT neurons (Tao and Auerbach, 2000; Gartside et al., 2007).

There is a prominent GABAergic input not only from intrinsic GABAergic interneurons, but also from the periaqueductal gray, the lateral and posterior hypothalamic areas, lateral preoptic area, the *substancia nigra reticulata*, and VTA (Boschert et al., 1994; Gervasoni et al., 2000). The two main GABA receptors involved in the regulation of serotonergic transmission are the $GABA_A$ and $GABA_B$, and both types have been described in the DR

(Bowery et al., 1987; Chu et al., 1990; Bischoff et al., 1999). $GABA_A$ receptors belong to 5-HT cell bodies (Mennini et al., 1986), whereas $GABA_B$ receptors are present in 5-HT cell bodies (Innis and Aghajanian, 1987) and also in GABAergic terminals as autoreceptors (Waldmeier et al., 1988; Bowery, 1993). GABA inhibits DR 5-HT cell firing (Baraban and Aghajanian, 1980; Abellan et al., 2000a) and 5-HT release in forebrain projection areas (Gallager and Aghajanian, 1976; Gervasoni et al., 2000). However, it has been reported that it does not alter 5-HT release in the DR (Abellan et al., 2000b). The $GABA_A$ receptor antagonist, bicuculline increases 5-HT release in the DR, suggesting that GABAergic transmission exerts a tonic inhibition on 5-HT release (Tao et al., 1996). However, the fact that GABA inhibits DR cell firing but not release, suggests that at least one part of the 5-HT release does not depend on 5-HT cell firing. Regarding the $GABA_B$ receptor activity, different results have been obtained when the $GABA_B$ receptor agonist baclofen was perfused in DR neurons. In some studies baclofen increased the 5-HT release (Abellan et al., 2000a; Abellan et al., 2000b) but in others it decreased 5-HT release (Tao et al., 1996). These different results might be due to the different GABAergic tone across the sleep/wake cycle. Hence, in light conditions, in a presence of an active GABAergic input onto DR, baclofen removes the tonic $GABA_A$ input through its preferential activation of presynaptic $GABA_B$ receptors reducing 5-HT firing activity, via activation of GIRK channels (Innis and Aghajanian, 1987; Cornelisse et al., 2007). Thus, this leads to an increase in 5-HT release through a $GABA_A$ disinhibiton (Adell et al., 2002). In contrast, during darkness, the presynaptic effect of baclofen is quantitatively less important and its direct inhibitory effect on 5-HT neurons overcomes the presynaptic (indirect) effect, resulting in a reduction of 5-HT release (Tao et al., 1996). In addition, since $GABA_B$ receptor antagonists are without effect either in light or dark conditions (Tao et al., 1996; Abellan et al., 2000a) it is assumed that $GABA_B$ receptors do not tonically control the release of 5-HT in the DR.

Introduction

The sources for glutamatergic input into the DR are the *lateral habenula*, *periaqueductal gray*, *lateral hypothalamus*, mPFC, the *interpeduncular nucleus*, and medullary regions, including the *parabrachial nucleus*, (Aghajanian and Wang, 1977; Maciewicz et al., 1981; Kalen et al., 1985; Kalen et al., 1986; Marcinkiewicz et al., 1989; Behzadi et al., 1990). These diverse areas are associated with many functions. For example, hypothalamic sites are linked to endocrine and metabolic functions, the *habenula* to reward state, medullary areas to autonomic function, visceral and somatic sensation, and the mPFC with conscious perception and decision making, all of which influence mood and motivated behavior associated with 5-HT function. The glutamatergic receptors involved in the regulation of 5-HT neurons are N-methyl-D-aspartate (NMDA), 2-amino-3-(3-hydroxy-5-methyl-isoxazol-4-yl) propanoic acid (AMPA) and kainate receptor, all of which are expressed in 5-HT neurons (Wylie et al., 2010). The application of glutamate in the DR stimulates DR 5-HT cell firing, and kainate, which binds both to AMPA and kainate receptors, increases 5-HT release (Tao et al., 1997; Tao and Auerbach, 2000). Similarly, NMDA receptor agonists elicit an increase of 5-HT release (Tao and Auerbach, 2000). However, there is a low tonic influence of glutamatergic inputs into 5-HT neurons since perfusion of AMPA and kainate receptor antagonists entails a moderate reduction of 5-HT release but prevents the effect of AMPA/kainate receptor agonist on the increase in 5-HT release (Tao et al., 1997; Tao and Auerbach, 2000). The control by glutamate of 5-HT cell firing and release also involves AMPA receptors in mPFC. They mediate the activation of ascending serotonergic pathways via descending glutamatergic inputs onto the DR (Celada and Artigas, 1993). Little is known about the role of the different metabotropic glutamate receptors in the control of 5-HT activity and release within the DR so far (Maejima et al., 2013). It has been reported that administration of group II metabotropic glutamate receptors antagonist increases 5-HT neuronal activity. This seems to be an indirect effect that involves presynaptic excitatory neurons (Kawashima et al., 2005). Nicotinic

acetylcholine receptors (nAChRs) can increase 5-HT neuronal firing (Mihailescu et al., 2002) via presynaptic modulation of glutamate release (Garduno et al., 2012), or via opening of nAChR expressed in 5-HT neurons (Galindo-Charles et al., 2008; Chang et al., 2011).

There are prominent dopamine projections from the VTA, the *substantia nigra*, and the A11 cell group of the *hypothalamus* (Sakai et al., 1977; Beckstead et al., 1979; Kalen et al., 1988; Peyron et al., 1996). Dopamine increases 5-HT neuronal firing and also 5-HT release (Ferre and Artigas, 1993; Ferre et al., 1994; Matsumoto et al., 1996; Mendlin et al., 1998; Haj-Dahmane, 2001; Martin-Ruiz et al., 2001). To date, low levels of dopamine D2 and D3 receptors have been detected in the DR (Bouthenet et al., 1987; Yokoyama et al., 1994; Suzuki et al., 1998). The modulatory effects of dopamine on 5-HT neurons are mediated by direct activation of D2 receptors expressed in 5-HT neurons (Haj-Dahmane, 2001), or by activation of D1 and D2 receptors located outside the DR, possibly in the *substantia nigra* since the local perfusion of apomorphine in this region enhances the release of 5-HT in the DR (Martin-Ruiz et al., 2001).

The DR receives noradrenergic innervation from the LC and the input may vary across the sleep/wake cycle (Adell et al., 2002; Lechin et al., 2006). α_1 and α_2 adrenergic receptor mRNA and protein have been detected in the DR (Unnerstall et al., 1985; Scheinin et al., 1994; Rosin et al., 1996; Day et al., 1997; Strazielle et al., 1999). The α_1 adrenoceptor is located on 5-HT cell bodies and the endogenous tone of α_1 adrenoceptor varies across the sleep-wake (Gallager and Aghajanian, 1976). Given that α_{1B} adrenoceptor subtype predominates in the DR it seems to be the responsible for the tonic stimulatory action of noradrenaline on 5-HT neurons (Pieribone et al., 1994; Day et al., 1997). The α_2 adrenergic receptors are highly expressed in the DR and their activation by agonists of α_2 adrenergic receptors located on the soma or presynaptic terminal of 5-HT neuron reduces 5-HT neuronal firing (Hopwood

and Stamford, 2001). Likewise, α_2 adrenergic receptor antagonists increase DR 5-HT neuronal firing (Freedman and Aghajanian, 1984; Garratt et al., 1991). In addition, NA inhibits the release of 5-HT in the DR and it has been demonstrated that this effect is mediated by α_2 adrenergic receptors (Frankhuijzen et al., 1988; Bortolozzi and Artigas, 2003).

The cannabinoid CB1 receptor is expressed in serotonergic fibers (Haring et al., 2007; Ferreira et al., 2012). CB1 receptor activation in DR decreases 5-HT release in projection areas and may regulate the function and expression of 5-HT_{1A} receptors (Nakazi et al., 2000; Egashira et al., 2002; Aso et al., 2009; Moranta et al., 2009; Zavitsanou et al., 2010). Within the DR, endocannabinoids mainly act on glutamatergic terminals and probably also on GABAergic terminals (Haj-Dahmane and Shen, 2009; Mendiguren and Pineda, 2009; Tao and Ma, 2012). Their action on these terminals leads to a reduction in glutamate and GABA release onto 5-HT neurons and therefore changes in the activity of the 5-HT neurons (Maejima et al., 2013).

5-HT neurons in the DR also receive dynorphinergic, enkephalinergic, and β-endorphinergic innervation (Adell et al., 2002). Activation of μ opiod receptors in GABAergic neurons within the DR inhibits GABAergic neurons and results in an increase in 5-HT release in projection areas (Tao and Auerbach, 1994; Jolas and Aghajanian, 1997). Activation of δ and κ opioid receptors increases and decreases 5-HT release in the DR, respectively (Tao and Auerbach, 2002).

Substance P influence 5-HT transmission through neurokinin 1 (NK1) receptors, which are extensively expressed in the DR (Maeno et al., 1993; Sergeyev et al., 1999; Froger et al., 2001). NK1 receptors are found in the cytoplasm of 5-HT neurons and in dendritic membranes of GABAergic neurons and modulate 5-HT neuronal firing under certain physiological conditions (Lacoste et al., 2009). Activation of NK1 receptors in the DR increases the 5-

HT release within the DR and decreases 5-HT release in *frontal cortex* (Guiard et al., 2007).

Galanin is a peptide expressed in the DR and appears to potentiate the inhibitory effect of 5-HT on 5-HT_{1A} receptors, possibly via a galanin-5-HT_{1A} receptor interaction (Hokfelt et al., 1998; Xu et al., 1998; Razani et al., 2000).

Cholecystokinin and hypocreatin-orexin display direct excitatory actions on DR 5-HT neurons (Boden et al., 1991; Brown et al., 2001), whereas corticotropin-releasing factor (CRF) appears to be predominantly inhibitory (Kirby et al., 2000).

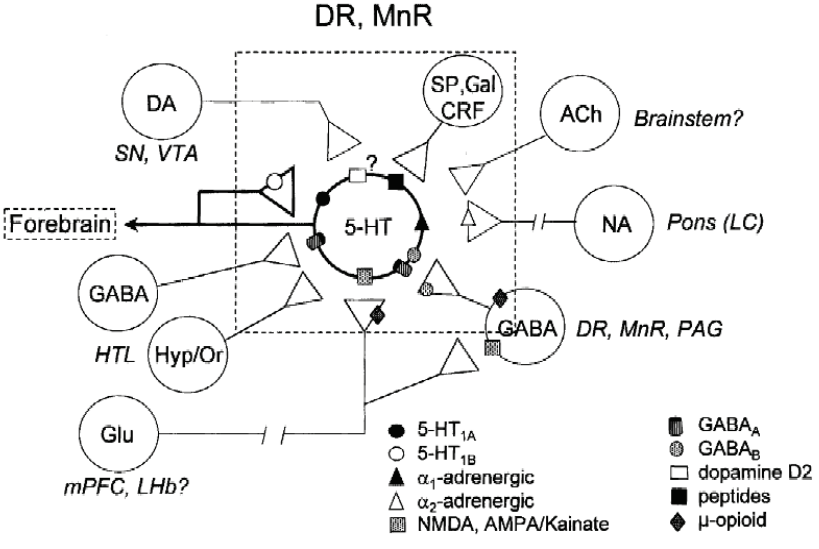

Figure 1.4. Schematic representation of the main structures involved in the regulation of 5-HT neurons. LC: *locus coeruleus*; mPFC: *medial prefrontal cortex*; LHb: *lateral habenula*; SN: *substantia nigra*; PAG: periaqueductal gray matter; HTL: *hypothalamus*; VTA: *ventral tegmental area*. Taken from Adell et al. (2002).

1.1.2.2. Non serotonergic neurons

Non 5-HT neurons are also present in the DR and occur in equal or greater number to 5-HT neurons (Descarries et al., 1982; Kohler and Steinbusch, 1982; Van Bockstaele et al., 1993; Kiss et al., 2002; Li et al., 2011). However, for any given neurotransmitter, the number of non 5-HT neurons is one third to one tenth less than the number of 5-HT neurons. These neurons are 5-HT immunonegative and produce dopamine, enkephalin, neurotensin, substance P, somatostatin, cholecystokinin, GABA or glutamate (Pineyro and Blier, 1999). In general, they present a similar morphology and size to 5-HT neurons, but in contrast rarely have dendritic spines (Li et al., 2001). GABA cell bodies, also known as GABAergic interneurons, constitute a large population of non 5HT neurons forming a GABAergic intrinsic network in the DR (Massari et al., 1976). They can be seen in the lateral wings of DR or in areas devoid of 5-HT neurons (Calizo et al., 2011). These cells are markedly smaller and fire spikes characterized by short width and high frequency (Allers and Sharp, 2003). CRF cell bodies are also present in the DR, predominantly distributed in the dorsomedial part (Allers and Sharp, 2003; Commons et al., 2003; Day et al., 2004). In addition, there are also dopamine neurons, immunopositive for tyrosine hydroxylase, which overlap in the rostral portion with 5-HT neurons (Fu et al., 2010); glutamatergic neurons expressing the vesicular glutamate transporter 3 (VGLUT3), which co-localize with 5-HT in the midline region (Commons, 2009); and nitrergic neurons (NOS-containing) which co-localize with 5-HT neurons in the dorsomedial and ventromedial part, but rarely co-localize in the lateral wings (Vasudeva et al., 2011).

Electrophysiologically, using the traditionally-defined parameters alone (large membrane resistance, large AHP, long AP duration and a hyperpolarization in response to 5-HT_{1A} receptor activation) is difficult to differentiate non 5-HT neurons from 5-HT neurons. However, in all subfields, there are some perceptible differences, though the magnitude of the differences

varies (Calizo et al., 2011). Compared to 5-HT neurons, non 5-HT neurons have a more depolarized membrane potential, a smaller amplitude and duration of AP, a faster and more irregular train of spikes in response to small depolarizing current steps, and spike trains elicited in these non 5-HT cells frequently show adaptations of spike frequency (Li et al., 2001; Calizo et al., 2011).

Pharmacologically, the 5-HT_{1A} receptor-mediated response is smaller in non 5-HT neurons, although the sensitivity to the 5-HT_{1A} agonist, 5-CT, is different among subfields regardless of cell type (Calizo et al., 2011). However, both 5-HT and non 5-HT neurons are heterogeneous with respect to their response to 5-HT, given that in both groups the majority of the neurons show an outward current in response to 5-HT but some show an inward current, which are similar in magnitude (Marinelli et al., 2004).

1.1.3. *Dorsal raphe* projections

5-HT neurons of the DR display a topographic organization with respect to efferent projections. Neurons located more rostrally project to more rostral areas of the brain than neurons located more caudally in the DR (Michelsen et al., 2007). There are three ascending pathways, the dorsal, medial and ventral ascending pathways, being the dorsal and ventral ascending pathways the two most important efferent projections of the DR. Dorsal ascending pathway innervates the *striatum*, *globus pallidus* and *nucleus accumbens*. Medial ascending pathway projects to *substantia nigra compacta* and to a lesser extent the *striatum*. Ventral ascending pathway targets *hypothalamic nuclei*, *habenula*, *septum*, *amygdala*, *cortex*, the olfactory bulb, *hippocampus*, *interpeduncular nucleus,* and geniculate body (Michelsen et al., 2007).

In addition, four descending projections leave the DR, the bulbospinal pathway, cerebellar pathway, propriobulbar pathway, and a pathway that

innervates the LC, *dorsal tegmental nucleus* and *pontine raphe nucleus* (Michelsen et al., 2007) (Fig. 1.5).

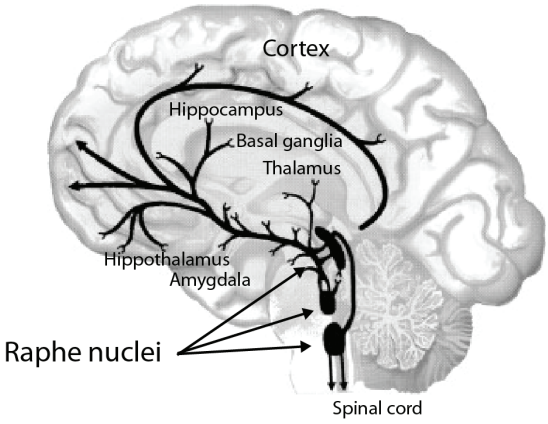

Figure 1.5. ***Dorsal raphe nucleus*** **and its major ascending and descending projections**. Schematic sagittal section of a rat brain, showing the locations of the most important groups of 5-HT neurons and the distribution of their axons and terminal buttons.

1.1.4. Serotonergic system, *dorsal raphe,* and depression

It is well-known that 5-HT is involved in many physiological aspects and behavioral processes including mood, core temperature, appetite, sleep, activity, suicide, sexual behavior, and cognition. Several clinical conditions, such as affective disorders, anxiety, obsessive-compulsive disorders, eating disorder, aggression, suicide, impulsive disorders, alcohol abuse, and premenstrual syndrome are linked to alterations in serotonergic function (Jans et al., 2007). In depression, which is one of the most intensively studied affective disorders in relation to a diminished serotonergic function, all the previously mentioned physiological and behavioral processes are affected.

Based on the physiological and behavioral evidence that relates serotonergic system and depression the DR has long received much attention in the study of depression, as it is the nucleus where the majority of the 5-HT cells are located on. In this sense, controversial results have been obtained from diverse *postmortem* studies examining the number of 5-HT cells, SERT binding sites, and functionality of 5-HT_{1A} receptors in the DR of depressed patients. While some investigations have observed a reduction in the number of neurons in the DR of depressed patients (Baumann et al., 2002), others have failed to find evidence of a variation in the neuronal number (Hendricksen et al., 2004). Regarding SERT, one study has reported a reduction in the number of SERT binding sites but another reported no changes (Bligh-Glover et al., 2000; Arango et al., 2001). In the same line, some positron emission tomography studies have observed a reduced 5-HT_{1A} receptor signaling in DR of depressed suicide victims (Drevets et al., 1999; Arango et al., 2001; Drevets et al., 2007) also observed in animals after chronic stress (Fernandes et al., 1997), while an increased 5-HT_{1A} receptor density has been reported in others (Stockmeier et al., 1998).

Introduction

Genetic and imaging studies in humans have suggested that different levels or regulation of the 5-HT_{1A} receptor are associated with anxiety, depression and the response to antidepressants (Strobel et al., 2003; Lesch and Gutknecht, 2004; Le Francois et al., 2008). An association between a C(-109)G polymorphism in the promoter region of the *Htr1a* gene and depression and response to antidepressant treatment has been reported (Lemonde et al., 2004; Le Francois et al., 2008). However, whether this polymorphism controls only autoreceptor or both auto and heteroreceptor levels remains unclear, since some studies suggest that heteroreceptor levels are not affected and others suggest that both 5-HT_{1A} auto- and heteroreceptors are affected (Lemonde et al., 2004; Parsey et al., 2006).

The *in vivo* implication of 5-HT system and DR 5-HT_{1A} autoreceptors in the response to antidepressants has been widely studied during the last years. During the 80', preclinical and clinical evidence was accumulated indicating the involvement of the 5-HT system in the therapeutic action of some antidepressant drugs (Blier and de Montigny, 1994). It was demonstrated, for example, that compounds that increase serotonergic function, such as tryptophan and lithium, potentiated the effect of antidepressant drugs (de Montigny et al., 1983). Conversely, impairment of 5-HT synthesis led to a reappearance of depressive symptoms in patients in remission obtained with various antidepressant drugs (Shopsin et al., 1975; Delgado et al., 1990). In fact, it was by that time when electrophysiological findings were obtained demonstrating that short-term administration of SSRIs and monoamine oxidase inhibitors reduces the firing activity of 5-HT and increases the 5-HT levels in the DR in the rodent brain, but also that the firing activity was recovered as the treatment was pursed. This was shown to be due to a desensitization of DR 5-HT_{1A} autoreceptors, which control their firing activity (Quinaux et al., 1982; Blier and de Montigny, 1994) and the levels of extracellular 5-HT through GIRK channel activation (VanderMaelen et al., 1986; Sprouse and Aghajanian,

1987; Sinton and Fallon, 1988). In fact, it has been reported that GIRK channels are implicated in the action of some SSRIs. Specifically, one study describes that the local administration of the SSRI citalopram into the DR produced a decrease in the extracellular 5-HT levels in DR projection areas, such as *striatum*, and this effect was prevented by a pretreatment with pertussis toxin (Romero et al., 1994), which uncouples 5-HT_{1A} receptors from GIRK channels, and prevents the inhibitory action of 5-HT on DR neurons (Innis and Aghajanian, 1987).

It is proposed that at the beginning of the antidepressant treatment, or with short-term treatments, 5-HT levels in the synaptic cleft in DR neurons increase, 5-HT couples to 5-HT_{1A} receptors and thus DR firing activity is reduced. This, in turn, prevents an increase of 5-HT extracellular levels in forebrain projection areas (Artigas, 1993). However, as the treatment continues, or with a long-term treatment, DR 5-HT_{1A} autoreceptors desensitize and firing rate completely recovers, leading to a robust increase in basal 5-HT extracellular levels in the DR and projection areas (Rutter et al., 1994; Invernizzi et al., 1995; Kreiss and Lucki, 1995) and obtaining the antidepressant effect (Fig. 1.6).

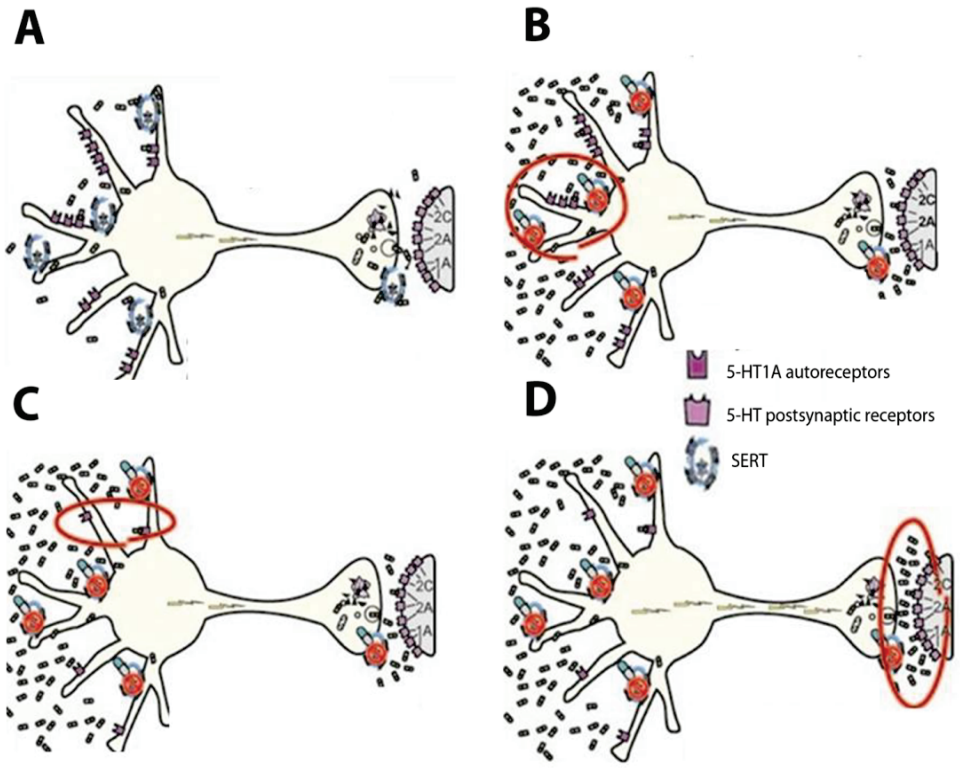

Figure 1.6. The proposed mechanism of action of SSRIs involving the 5-HT$_{1A}$ autoreceptor desensitization. (A) Representation in the depressed state, where there are low levels of 5-HT in the synaptic cleft, low 5-HT postsynaptic release and an up-regulation of 5-HT$_{1A}$ autoreceptors. (B) Antidepressant action state, beginning of an antidepressant treatment. SERT blockade produces an increase in 5-HT levels and therefore a reduction in the firing rate. (C) As the treatment continues, the increase in 5-HT levels causes the desensitization of 5-HT$_{1A}$ autoreceptors. (D) 5-HT$_{1A}$ sustained desensitization leads to a completely recovery of the firing rate and therefore 5-HT postsynaptic levels are increased obtaining the therapeutic benefit of the antidepressant treatment. Taken and modified from 'Essential Psychopharmacology' by McCarver (2011).

Thus, nowadays, it is generally accepted that DR 5-HT_{1A} autoreceptor desensitization is needed to obtain the antidepressant response, and that this desensitization is the responsible for the delay in the response to antidepressant drugs (Artigas et al., 1996; Blier et al., 1998; Berney et al., 2008). This idea of the involvement of the DR 5-HT_{1A} receptor desensitization in the antidepressant response was supported by the fact that when 5-HT_{1A} autoreceptors are blocked, the time needed to obtain the clinical improvement is shorter. In two clinical studies, the administration of the 5-HT_{1A} receptor antagonist pindolol, which blocks 5-HT_{1A} receptors (Romero et al., 1996), in combination with paroxetine accelerated the antidepressant effects in patients with major depression (Artigas et al., 1994; Blier and Bergeron, 1995).

However, despite significant interest and evidence regarding the involvement of the 5-HT_{1A} autoreceptors in the treatment and etiology of depression in humans, a direct test of their involvement has not been possible due to the lack of available techniques (Richardson-Jones et al., 2010). The 5-HT_{1A} receptor involvement in the modulation of depression related behaviors has been reported from studies in mice (Heisler et al., 1998; Klemenhagen et al., 2006), but these studies have not distinguished between auto- and heteroreceptors. In this sense, using the classic transgenic techniques, it was created the constitutive 5-HT_{1A} receptor knockout mice. This animal model typically showed an "antidepressed" phenotype but also a robust anxiety-like behavior (Heisler et al., 1998; Parks et al., 1998; Ramboz et al., 1998), making this combined phenotype difficult to interpret given the co-morbidity of anxiety and depression in humans, and therefore it has been somehow ignored. However, the development of modern techniques made possible to conditionally decrease the 5-HT_{1A} receptor expression specifically in the DR. It has been reported that the selective DR 5-HT_{1A} receptor knockdown increases the antidepressant response and 5-HT release in stressful conditions, as well as promotes an "antidepressive-like" behavior (Ferres-Coy et al., 2013) without

altering the anxiety-like behavior. In the same line, another study where mice with high and low levels of 5-HT_{1A} autoreceptors were generated reports that mice with high levels of 5-HT_{1A} autoreceptors in the DR show a blunted response to acute stress and no behavioral response to antidepressants. Moreover, it also reports that reducing the 5-HT_{1A} autoreceptor levels prior to antidepressant treatment is sufficient to convert non-responders into responders (Richardson-Jones et al., 2010). Altogether, it seems that development of new techniques, which are making possible to distinguish between auto- and heteroreceptors, is confirming the particular involvement of DR autoreceptors in the etiology and treatment of depression.

However, it cannot be ruled out the involvement of other components in this phenomenon of desensitization. In this sense, the low functionality of 5-HT_{1A} receptors could be due to reduced levels and/or function of the receptor, but also to alterations of downstream components, such as the GIRK channels.

1.2. GIRK channels

1.2.1. Overview

G protein coupled inwardly rectifying K^+ (GIRK, also known as Kir3.x) channels are members of the inwardly rectifying K^+ (Kir) channels family. Kir channels were first described in the skeletal muscle and the term "inwardly rectifying" comes from fact that Kir channels allow K^+ to move more easily into the cell, having a greater conductance, rather than out to the cell (Hibino et al., 2010). This is possible because the outward flow of K^+ ions is inhibited by the intracellular polyamines and Mg^{2+}, which block the pore in a voltage-dependent manner (Whorton and MacKinnon, 2011).

The primary sequences of the first Kir channels were elucidated in 1993, and Kir1.1 and the classical Kir2.1 (Kubo et al., 1993) were also isolated (Ho et al., 1993). To date, 15 Kir subunit genes have been identified and classified into seven subfamilies categorized into four functional groups:

1. K^+ transport channels: Kir1.x, Kir4.x, Kir5.x, and Kir7.x
2. Classical Kir channels: Kir2.x
3. G protein coupled Kir channels: Kir3.x or GIRK
4. ATP-sensitive K^+ channels: Kir6.x

Kir channels play pivotal roles in controlling insulin release, vascular tone, heart rate, neuronal signaling, and membrane excitability (Hille, 1992). All of them share the same basic topology and are activated by phosphatidylinositol 4,5-bisphosphate (PIP_2). However, GIRK channels are the unique in this family that also require G protein, in combination with PIP_2, for activation (Wickman et al., 1994; Huang et al., 1998). Intracellular Na^+ ions can also modulate certain GIRK channels (Lesage et al., 1995; Sui et al., 1996). GIRK are the downstream effectors of some G protein coupled receptors (GPCRs), such as the 5-HT_{1A} receptors, and they can be activated by direct

binding of the βγ subunit of G protein to the channels, an interaction with important physiological consequences (Wickman and Clapham, 1995; Yamada et al., 1998).

GIRK channels hyperpolarize neurons in response to activation of $G_{i/o}$ protein coupled receptors and decrease the excitability of neurons, slow synaptic potentials, and volume transmission (Krapivinsky et al., 1995; Wickman and Clapham, 1995; Luscher et al., 1997; Signorini et al., 1997; Wickman et al., 1998). Therefore, abnormal GIRK function can lead to excessive or deficient neuronal excitability, which is related to several pathologies such as epilepsy or Down's syndrome. Thus, GIRK channels are proposed as new pharmacological targets for the treatment of a plethora of illnesses.

1.2.2. Structure, composition, and localization of GIRK channels in the brain

The GIRK channel primary structure, which is common for all types of Kir channels, is that observed in a GIRK subunit. It is composed by a common motif of two putative transmembrane domains (TM1 and TM2), linked by an extracellular pore-forming region (H5), and cytoplasmic amino (NH_2-) and carboxy (COOH-) terminal domains. The H5 region serves as the "ion-selectivity filter" (Heginbotham et al., 1994) (Fig. 1.7A).

This primary structure is insufficient to form a complete ion channel, and therefore functional GIRK channels are made up of four such subunits in a tetrameric complex. These four subunits combine to form a canonical K^+ pore forming trasmembrane domain (TMD), and a large cytoplasmatic domain (CTD) (Whorton and MacKinnon, 2011) (Fig. 1.7B).

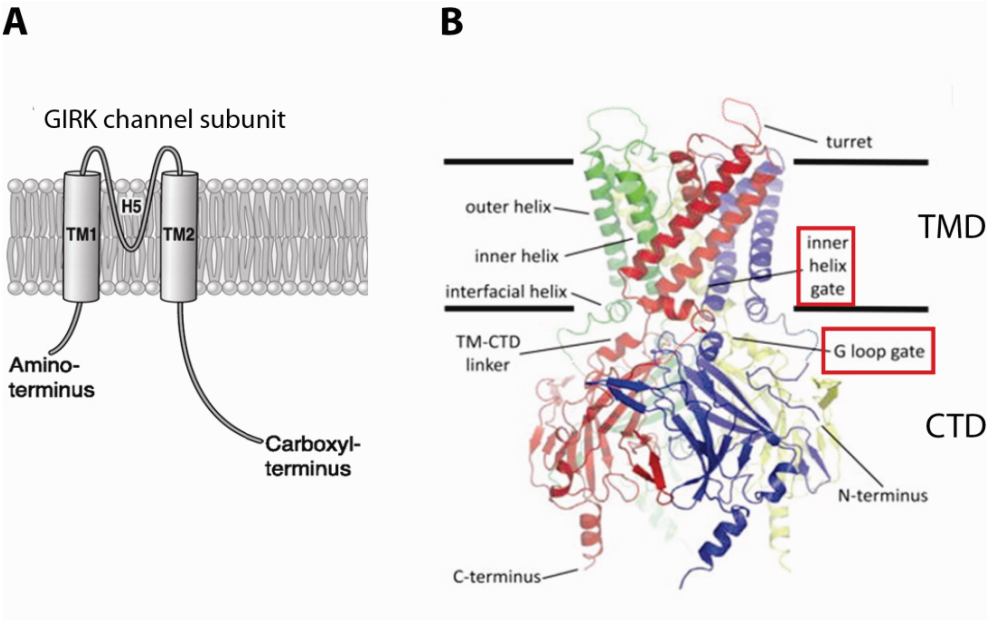

Figure 1.7. Structure of GIRK channels. (A) Primary structure of a GIRK channel subunit, which contains two transmembrane domain (TM1 and TM2) regions, a pore-forming region (H5) loop, and cytosolic NH_2 and COOH termini. (B) Cartoon diagram of a complete GIRK channel. Each subunit of the tetramer is in a different color. The approximate boundary of the phospholipid bilayer is indicated by the thick black lines separating the transmembrane domain (TMD) from the cytoplasmatic domain (CTD). The extracellular surface is on top. Taken and modified from (A) Hibino et al. (2010) and (B) Whorton and MacKinnon (2011).

In mammals, four subunits (GIRK1-4) have been cloned, which assemble into homo and heterotetrameric channels (Wickman et al., 2002). GIRK1, GIRK2, and GIRK3 are broadly expressed in many areas of the CNS, whereas GIRK4 expression is restricted to a small number of neuron populations including some specific areas of the *neocortex*, *ventromedial hypothalamic nucleus*, *laterodorsal* and *lateral posterior thalamic nuclei, insular cortex*, and Golgi cells from the *cerebellum* (Karschin et al., 1996; Wickman et al., 2000; Aguado et al., 2008). This narrow distribution effectively reduces its contribution to neuronal GIRK channel formation.

GIRK2 and GIRK4 subunits can form homomeric channels (Inanobe et al., 1999; Kobayashi et al., 1999). Although homomeric GIRK2 and GIRK4 channels have been found in native tissues, exogenously expressed homomers of these channels give very brief and poorly resolved open-time kinetics that are different from native channels (Chan et al., 1997; Corey and Clapham, 1998). Both GIRK2 and GIRK4 can recruit GIRK1, greatly increasing its surface expression and resulting in highly active channels that are indistinguishable from native channels (Krapivinsky et al., 1995; Chan et al., 1997; Woodward et al., 1997; Kennedy et al., 1999).

GIRK1 and GIRK3 subunits are unable to independently form functional channels (Chan et al., 1997; Woodward et al., 1997; Jelacic et al., 1999; Mirshahi and Logothetis, 2004). Indeed, GIRK1 requires co-expression with another GIRK subunit to achieve membrane distribution (Krapivinsky et al., 1995; Hedin et al., 1996; Kennedy et al., 1996; Ma et al., 2002). GIRK1 and GIRK2 subunits can co-assemble with GIRK3 to form GIRK1/3 and GIRK2/3. Interestingly, it has been shown that GIRK2/GIRK3 heterotetramers have some activity, but reduced $G_{\beta\gamma}$ sensitivity, compared with other heterotetramers containing GIRK1 subunits (Jelacic et al., 2000).

Most neuronal GIRK channels are thought to be heteromeric, containing GIRK1 and GIRK2 subunits (Luscher et al., 1997; Signorini et al., 1997). Indeed, GIRK1 and GIRK2 knockout mice display similar behavioral phenotypes (Pravetoni and Wickman, 2008). Interestingly, the levels of GIRK1 subunit are decreased in GIRK2$^{-/-}$ mice (Signorini et al., 1997; Torrecilla et al., 2002). However, several findings indicate that a wide array of GIRK subunit combinations may be relevant and exhibit specific functional properties. Thus, it has been shown that GIRK2/GIRK3 heterotetramers, which as previously mentioned exhibit reduced $G_{\beta\gamma}$ sensitivity, could account for the GIRK currents in GABAergic neurons from VTA (Cruz et al., 2004). Also, the opiod-induced currents in noradrenergic neurons from LC are mediated by GIRK1, GIRK2, and GIRK3 subunit-containing channels (Torrecilla et al., 2002). In the *cerebellum*, for example, there is a cell type-specific expression of GIRK channels, since there are at least seven distinct GIRK subunit expression patterns in several cell types (Aguado et al., 2008). In neurons from the *hippocampus* and spinal cord ultrastructural studies show that GIRK2, but not GIRK1, is present at post-synaptic specialization (Koyrakh et al., 2005; Marker et al., 2005). In dopamine neurons from the *substantia nigra* GIRK channels are formed by homomeric combination of splice variants of GIRK2 subunits (Inanobe et al., 1999), and in VTA the most typical combination is the assembly of distinct GIRK2 alternatively spliced isoforms with GIRK3 (Cruz et al., 2004; Labouebe et al., 2007). Three splice variants of GIRK2 (GIRK2a-c) exist in the brain, and splice variants of GIRK1 have also been reported, although its relevance is not well understood (Isomoto et al., 1996; Inanobe et al., 1999; Iwanir and Reuveny, 2008). No splice variants of GIRK3 and GIRK4 have been reported so far.

Despite its broad distribution in the CNS, the functional relevance of GIRK3 is uncertain. GIRK3 knockout mice are indistinguishable from wild-type mice in some behavioral tests (Pravetoni and Wickman, 2008), have

similar agonist-induced GIRK currents, but exhibit less severe withdrawal from sedatives and reduced cocaine-self-administration (Morgan et al., 2003; Kozell et al., 2009). Interestingly, GIRK3 subunits, together with the major splice variant of GIRK2 which is GIRK2c, have been proposed to play a key role in regulating endosomal trafficking of GIRK channels (Ma et al., 2002; Lunn et al., 2007).

In neurons, GIRK1 and GIRK2 subunits are localized at dendritic spines in the postsynaptic density, and also at presynaptic regions, whereas GIRK3 subunit has been detected in certain axons (Liao et al., 1996; Inanobe et al., 1999; Morishige et al., 1999; Grosse et al., 2003; Koyrakh et al., 2005; Kulik et al., 2006). In CA1 hippocampal pyramidal neurons GIRK channels are expressed in the soma, along the dendrites, and in dendritic spines (Chen and Johnston, 2005; Koyrakh et al., 2005; Kulik et al., 2006). In the *cortex* and *cerebellum*, they are also present at presynaptic sites in a subpopulation of excitatory axon terminals, close to $GABA_B$ receptors. Thus, GIRK channels may be involved not only in slow inhibitory postsynaptic potentials, but also in the presynaptic modulation of neuronal activity, although this idea still remains under debate.

Interestingly, differences in the subunit composition of GIRK channels have been detected between synaptic and extrasynaptic plasma membrane, suggesting that there is a compartmental molecular diversity. Only GIRK2 is detected in the spines in the postsynaptic density, whereas both GIRK1 and GIRK2 are located in the extrasynaptic membranes of the spine head, as well as in the dendritic shafts (Koyrakh et al., 2005).

1.2.3. Physiology and regulation of GIRK channels

As mentioned earlier, GIRK channels are members of the inwardly rectifying K^+ channel family. The term "inward rectification" refers to a change in the slope of the current-voltage relationship of the channel at the reversal potential. At membrane potentials well above the equilibrium potential for K^+, the channel permits the efflux of K^+, causing a very small outward current compared to the inward current caused at potentials well below equilibrium potential for K^+. This rectification is due to the occlusion of the central pore by intracellular Mg^{2+} and polyamines at potential above equilibrium potential for K^+ (Yamada et al., 1998). Under physiological conditions, the resting membrane potential of a typical neuron is positive to equilibrium potential for K^+, and the small outward current through the channels decreases the excitability of the neuron.

Postsynaptic inhibitory effects induced by activation of a wide range of pertussis toxin-sensitive G_i or G_o type couple-receptors are mediated by direct binding of the G protein subunits $G_{\beta\gamma}$ to the GIRK channel (Logothetis et al., 1988). Thus, activation of GIRK channel by the binding of $G_{\beta\gamma}$ complex permits the efflux of K^+ ions and leads the cell to more hiperpolarized membrane potentials.

GIRK channels' activity is dependent on interaction with several co-assembled protein partners. In addition, GIRK channels undergo controlled subcellular trafficking that strongly regulates the GIRK-mediated signaling and contributes to their physiological roles (Lujan et al., 2009). Dysregulation of GIRK channels may contribute to particular human diseases and disorders. Given this, and because the efficacy of many clinically relevant and abused drugs relates to their actions on $G_{i/o}$-GIRK-dependent signaling, it is important to understand the cellular, subcellular, and molecular details of how GIRK channels and GIRK signaling are organized and regulated (Lujan et al., 2014).

1.2.3.1. Regulation of ion conduction

As mentioned previously, GIRK channels are made up by four subunits which combine to form a K^+ pore-forming TMD and a large CTD (Fig. 1.7). It is thought that ion conduction may be regulated by two functional gates in series: the inner helix gate, which is formed by the inner helices of the TMD, just inside the membrane; and the other gate, the G loop gate, which is formed by the G loop at the apex of the CTD, just outside the membrane (Doyle et al., 1998; Jiang et al., 2002). For the complete activation of GIRK channels both gates have to be open (Pegan et al., 2005; Nishida et al., 2007).

There are three main ligands that interact simultaneously with GIRK channels to regulate their activation: G protein, PIP_2, and Na^+ (Whorton and MacKinnon, 2011) (Fig. 1.8). Previous electrophysiological studies suggest that G proteins and Na^+ function in a codependent manner with PIP_2 to open GIRK channels (Huang et al., 1998). Recently, in reconstitution experiments using purified components, it has been proposed that these regulators individually activate GIRK channels partially, but in combination they activate the channels to a greater extent (Whorton and MacKinnon, 2011).

- G protein: when a G protein coupled receptor is stimulated through the binding of a neurotransmitter or drug on the outside of the cell membrane, it catalyzes guanine nucleotide exchange -GTP replaces GDP on the G_α subunit- and releases G_α(GTP) and $G_{\beta\gamma}$ subunit on the cytoplasmatic side (Gilman, 1987). Then, $G_{\beta\gamma}$ subunits can activate GIRK channels. Much evidence indicates that G_α can also interact directly with GIRK channels (Huang et al., 1995; Rebois et al., 2006). It is suggested that direct binding of G_α subunit to GIRK channels is the responsible for their basal activity levels, even in the absence of receptor signaling, and that it also primes for activation by $G_{\beta\gamma}$ (Peleg et al., 2002; Clancy et al., 2005). It has been demonstrated that GDP-bound G_α can interact not only with GIRK1 and GIRK2, but also with a complex of $G_{\beta\gamma}$-GIRK channels (Slesinger et al., 1995; Peleg et al., 2002; Ivanina et al., 2004). So,

even without agonist, GIRK channels make a complex with GDP-bound G_{α} and $G_{\beta\gamma}$ called "preformed" complex (Hibino et al., 2010). It is proposed that, when the agonists bind to the receptor, G_{α} is released from the "preformed" complex and $G_{\beta\gamma}$ stimulates the channels. In this condition, $G_{\beta\gamma}$ may be always in close vicinity with GIRK channels and thus could quickly activate them. Accordingly, the formation of the "preformed" complex is suggested to be involved in rapid activation of GIRK channels in response to agonists (Slesinger et al., 1995; Peleg et al., 2002; Riven et al., 2006). Therefore, it is considered that whereas co-expression of G_{α} chelates $G_{\beta\gamma}$ and reduces the basal activity of GIRK channels, it simultaneously augments the number of "preformed" complex and increases the pool of $G_{\beta\gamma}$ available in the vicinity of the channels for their activation in response to agonists. Recently, the crystallization of a complex formed by $G_{\beta\gamma}$ and the GIRK2 homomer has elucidated that GIRK2 channels may have four binding sites for $G_{\beta\gamma}$, one per subunit. These four binding sites are found at the well-conserved cytoplasmatic interfaces between the adjacent subunits that contribute to the formation of the extended cytoplasmatic pore. $G_{\beta\gamma}$ alone only opens the G loop but not the inner helix gate of the channel, for the full gate opening PIP_2 is also required (Whorton and MacKinnon, 2011).

- PIP_2: like other Kir channels, GIRK channels also require PIP_2, which stabilizes its functional integrity, to maintain their activity (Huang et al., 1998). In experiments where PIP_2 is removed in inside-out patches, $G_{\beta\gamma}$ cannot activate GIRK channels and therefore GIRK currents are absent (Sui et al., 1998). It has been suggested that one PIP_2 lipid molecule binds to each subunit of the channels, near the TMD-CTD interface. The crystal structure of a GIRK2 channels revealed that in the presence of PIP_2, both the G loop gate and inner helix gate remain closed, and this is consistent with the observation that PIP_2 alone is insufficient to open GIRK channels in electrophysiological experiments (Whorton and MacKinnon, 2011). Accordingly, a recent study shows that, when

PIP_2 was added in bilayer membranes containing GIRK2 channel vesicles, the activity of GIRK channels was essentially unchanged, and similarly, addition of $G_{\beta\gamma}$ subunits in the absence of PIP_2 did not alter the channels activity. Only when both PIP_2 and $G_{\beta\gamma}$ were present, did they observe large K^+ currents due to robust GIRK2 channel opening (Wang et al., 2014).

As mentioned before, PIP_2 is required for a full gate opening in GIRK channels. PIP_2 alone binds but does not open either gate, and $G_{\beta\gamma}$ alone opens the G loop gate but not the inner helix gate, but $G_{\beta\gamma}$ in addition to PIP_2 open both gates. Thus, PIP_2 seems to play a facilitative role, this is, under conditions that favor channel opening, it presumably strengthens the interface between the CTD and the TMD, coupling tightly the two gates so upon G protein stimulation both gates open to activate the channel (Whorton and MacKinnon, 2011; Whorton and MacKinnon, 2013).

- Na^+: certain GIRK channels, specifically those containing GIRK2 and GIRK4 subunits, are modulated by intracellular Na^+ ions, which have their binding site near the TMD-CTD interface (Lesage et al., 1995; Sui et al., 1996; Sui et al., 1998; Ho and Murrell-Lagnado, 1999a; Ho and Murrell-Lagnado, 1999b; Whorton and MacKinnon, 2011). A recent study in bilayer membranes containing GIRK2 channels shows that GIRK channels do open in the absence of internal Na^+, but opening increases as the concentration of Na^+ is increased (Wang et al., 2014). Thus, it seems that Na^+ is not essential but augments the opening of the channels. This Na^+ activation of GIRK channels is thought to serve an important physiological function by producing negative feedback on excessive electrical excitability. During excitation, Na^+ entry elevates intracellular Na^+ concentrations above the normal range, and this activates GIRK channels and drives the membrane potential negative again (Whorton and MacKinnon, 2011).

1.2.3.2. Regulation of GIRK signaling

Besides the regulation that the previously mentioned molecules exert on ion conductance of GIRK channels, there are other regulatory proteins and molecules that modulate GIRK channel activity through different mechanisms. Some of them are shown in figure 1.8.

- Regulators of G protein signaling (RGS) proteins: GPCR-GIRK signaling is negatively modulated by RGS proteins (Hibino et al., 2010; Luscher and Slesinger, 2010). They regulate various G protein-mediated signal pathways by accelerating intrinsic GTPase hydrolysis in the Gα subunit, promoting the formation of the inactive heterotrimeric G protein (Hepler, 1999; Ross and Wilkie, 2000; Lujan et al., 2009). Accordingly, RGS proteins primarily accelerate receptor-induced GIRK current deactivation kinetics, by as much as 100-fold, among other influences (Doupnik et al., 1997). The increase in the rate of deactivation can be simply explained by the fact that activated RGS accelerate the hydrolysis of GTP on G_{α}, reduce the amount of free the $G_{\beta\gamma}$ and decrease the activity of GIRK channels (Inanobe et al., 2001; Ishii et al., 2002). Discrete protein modules confer unique functionality to specific RGS proteins, and this, together with their unique cell and/or tissue expression patterns, appears to promote different interactions with GIRK channels (Sjogren, 2011; Lujan et al., 2014). For example, there is a selective gene expression of *Rgs2* in VTA dopamine neurons that is preferentially associated with GIRK3 subunit containing channels. This association weakens the coupling between $GABA_B$ receptors and GIRK2/3 heteromers (Labouebe et al., 2007). Indeed, it has been suggested that chronic γ-hydroxybutyrate (GHB, $GABA_B$ receptor agonist) and morphine (μ-opioid receptor agonist) change the expression of *Rgs2*, leading to an alteration of the $GABA_B$-GIRK signaling and possibly contributing to the development of tolerance to GHB. Recently, it has been demonstrated a novel role of RGS7 in hippocampal synaptic plasticity and memory formation. Mice lacking RGS7, which regulates $GABA_B$-GIRK signaling in hippocampal

pyramidal neurons, exhibit deficits in learning and memory (Ostrovskaya et al., 2014). It has been proposed that RGS7, in cooperation with its binding partner, R7BP, modulates the inhibitory effects of the $GABA_B$-GIRK signaling, and that deletion of RGS7 sensitizes GIRK responses to $GABA_B$ receptor stimulation and slows channels deactivation kinetics, leading to a decreased neuronal excitability and disruption of inhibitory forms of synaptic plasticity.

- Sorting nexin 27 protein (SNX27): it is a GIRK3-interacting protein (Lunn et al., 2007) because it regulates the GIRK trafficking between the cell surface and endosome (Pfeffer, 2013). In the context of GIRK signaling, a proper function of SNX27 involves targeting GIRK3-containing channels to early endosomes, reducing the surface expression of GIRK channels and therefore enhancing the excitability of host neurons (Lunn et al., 2007; Balana et al., 2011; Balana et al., 2013). However, although GIRK2c can bind to SNX27, the surface distribution of homomeric GIRK2c channels is unaffected by SNX27 levels, suggesting that other unknown factors may influence the trafficking fates of GIRK channels (Nassirpour and Slesinger, 2007). SNX27 has been implicated in Down's syndrome and pscychostimulant addiction (Wang et al., 2013). Although an altered SNX27 expression and function impacts upon a wide array of cell signaling pathways, it has been suggested that an altered GIRK signaling may contribute to some of the cellular and behavioral deficits linked to these disorders. On one hand, in Down's syndrome, there is a loss of SNX27 and interestingly, GIRK signaling is enhanced in the *hippocampus* and *cortex* of a mouse model of Down's syndrome (Harashima et al., 2006; Best et al., 2007). Moreover, GIRK2 triploid mice display some of the neurological phenotypes associated with this syndrome (Cooper et al., 2012). On the other hand, there is an up-regulation of the b isoform of SNX27 in response to *in vivo* exposure to psychostimulants, such as cocaine and amphetamine. Interestingly, $GABA_B$-GIRK signaling in VTA dopamine and GABA neurons is weakened after acute psychostimulant exposure and also

following chronic cocaine in layer 5/6 pyramidal neurons of the *prelimbic cortex* (Arora et al., 2011; Hearing et al., 2013).

- Neural cell adhesion molecule (NCAM): it regulates the trafficking and expression of GIRK channels. Cultured hippocampal neurons from mice lacking NCAM show larger GIRK currents, probably mediated by GIRK1/2 subunit-containing GIRK channels. Co-expression of NCAM140 or NCAM180 with GIRK1/2 in *Xenopus oocytes* led to a decrease in the surface expression of the cannels. Consistently, in cultured hippocampal neurons of NCAM-null mice the cell surface expression of GIRK1/2 is augmented, and this is not observed for GIRK1/4 channels (Delling et al., 2002).

- GPCR linked to G_q-type may decrease GIRK channels activity through the activation of phospholipase C (PLC). It reduces PIP_2 membrane levels and therefore its activation may reduce GIRK channel activity (Sadja et al., 2003).

- GPCR linked to $G\alpha_s$ –type G proteins may increase GIRK channels activity, through the activation of protein kinase A (PKA). GIRK channels have a PKA phosphorylation site on the C-terminal domain that might mediate the effects of PKA on GIRK channels activity (Rusinova et al., 2009).

It is noteworthy that the last two above mentioned pathways can modulate GIRK channel activity but do not induce channel activation and/or deactivation (Raveh et al., 2009).

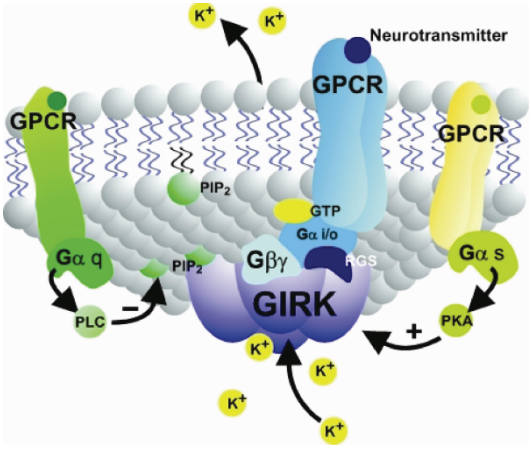

Figure 1.8. Regulating mechanisms of the GIRK signaling complex. GIRK channels are activated following the activation of GPCRs associated with PTX-sensitive G proteins ($G_{i/o}$) that release $G_{\beta\gamma}$ dimmers to couple to the channel directly (blue). PIP_2 is in close vicinity to stabilize its functional integrity. GPCRs that are associated with G_q-type G proteins (green) can reduce channel activity through activation of PLC, which breaks down PIP_2. GPCRs that are associated with $G\alpha_s$ -type G proteins (yellow) can increase channels' activity through activation of PKA. Taken from Sadja et al. (2003).

- Macromolecular organization

It is thought that GIRK channels exist in a macromolecular multiprotein complex on the plasma membrane (Fig. 1.9). This complex is postulated to contain G proteins, GPCRs, GIRK channels and regulatory proteins (Doupnik et al., 1997; Hibino et al., 2010; Luscher and Slesinger, 2010). Although few protein-protein interactions involving GIRK channels have been demonstrated using the classical biochemical approaches or native system, some evidence support this established idea. First, because GIRK channels remain open as long as $G_{\beta\gamma}$ subunits are available, Gα subunits have to remain near the channel to terminate GIRK channel activation (Luscher and Slesinger, 2010). Second, given that stimulation of GPCRs that couple to only PTX-sensitive ($G_{i/o}$ type) G

proteins activate GIRK channels (Clancy et al., 2005; Geng et al., 2009), it has been suggested that Gα may establish receptor specificity and also may associate directly with GIRK channels altering their gating (Schreibmayer et al., 1996; Peleg et al., 2002; Ivanina et al., 2004; Clancy et al., 2005). Third, spectroscopic studies using fluorescence G proteins, GPCP and RGS proteins, have provided evidence regarding a special relationship between proteins within the macromolecular complex (Lavine et al., 2002; Fowler et al., 2007).

Moreover, some studies investigating the regulation and localization of GIRK channels in their native environment confirm the existence of this complex. Limiting the movement of μ opiod receptors does not alter the rate of GIRK activation in cerebellar granule cells, revealing that these signaling proteins are localized in membrane compartments and do not diffuse in the membrane (Lober et al., 2006). In addition, in PC12 neuronal cells chronic stimulation of M_2 muscarinic receptors leads to a down-regulation of both M_2 receptors and GIRK channels (Clancy et al., 2007), suggesting that they are co-regulated in a complex. Furthermore, given that subunit 2 of the $GABA_B$ receptor dimerizes with M_2 receptors, it has been proposed the existence of a larger functional heteromeric complex (Boyer et al., 2009).

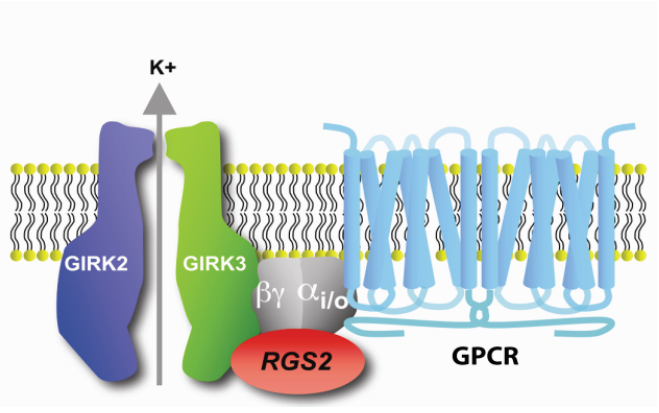

Figure 1.9. Macromolecular signaling complex containing G proteins, G protein-coupled receptors (GPCR), GIRK channels and regulatory proteins (RGS). Representation of the postulated macromolecular complex in which GIRK channels could exist. Note that RGS interacts selectively with GIRK channels whereas the heterotrimeric G protein associates directly with both GIRK and GPCR. Taken and modified from Lomazzi et al. (2008).

1.2.4. Physiological and pathophysiological aspects of GIRK channels

The physiological activation of GIRK channel can shape the neuronal network behavior at different levels. Their basal activity contributes to the resting membrane potential of neurons, shifting the membrane voltage by approximately -8 mV (Luscher et al., 1997; Torrecilla et al., 2002). In addition, receptor activation of GIRK channels provides another level of inhibition, to which three different changes in signaling can be generally ascribed: neuronal self-inhibition, neuron to neuron inhibition, and network level inhibition.

As for neuronal self-inhibition or autaptic transmission, some neurons release a neurotransmitter to activate GPCR and in turn, GIRK channels on their own dendrites causing self-inhibition (Bacci et al., 2004). This is a well-known mechanism by which the firing rate of some neurons is autoinhibited. For example, in DR neurons, 5-HT or 5-HT_{1A} receptor agonists activate 5-HT_{1A} autoreceptors. Their activation leads to inhibition of action potentials via

opening GIRK channels, resulting in an enhanced K^+ conductance that leads to a hyperpolarization of the membrane potential and inhibition of 5-HT action potential (Sprouse and Aghajanian, 1987; Sinton and Fallon, 1988).

The second case is the neuron to neuron inhibition. When a neurotransmitter is released from neighboring neurons, it may also activate postsynaptic GIRK channels. Indeed, this occurs upon activation of postsynaptic $GABA_B$ receptors, D2 receptors, and group II metabotropic glutamate receptors by transmitters released to the synaptic cleft (Newberry and Nicoll, 1985; Dutar et al., 1999; Beckstead and Williams, 2007). While GABA spontaneously released produces a fast inhibitory postsynaptic potential mediated by $GABA_A$ receptors, strong or repetitive stimulation is required to elicit the slow inhibitory potential, suggesting that GABA released into the synaptic cleft diffuses and activates perisynaptic $GABA_B$ receptors coupled to GIRK channels. In the *hippocampus* generation of the slow inhibitory postsynaptic currents is important for regulating the rhythmic activity of the network (Scanziani, 2000). In addition to postsynaptic activation, recent characterization of $GABA_B$ receptor-mediated presynaptic inhibition suggests a presynaptic role for these channels in inhibiting GABA release (Ladera et al., 2008; Michaeli and Yaka, 2010).

In the last case, the regulation of ambient levels of several endogenous G protein-coupled receptor agonists (for example, adenosine and somatostatin) may have a modulatory effect on large-scale neuronal networks through GIRK channel activation. This large-scale effect of neuromodulators is known as volume transmission. Moderate activation of GIRK channels in a population of neurons would be expected to reduce membrane excitability. For example, somatostatin acting onto somatostatin receptor subtype 5, might alter the oscillation behavior of thalamic networks through postsynaptic GIRK channel activation, together with presynaptic inhibition (Sun et al., 2002). Similarly, endogenous adenosine may suppress gamma oscillations in the *hippocampus*

(Pietersen et al., 2009), possibly owing to the selective expression of adenosine A1 receptors on pyramidal neurons, which also activate GIRK channels. All these findings suggest a role for GIRK channels in signaling pathways beyond the direct membrane hyperpolarization.

In this context, the use of GIRK mutant mice has been a key tool to study the roles of specific GIRK channel composition on neuronal physiology and animal behavior. Thus, GIRK channels functional relevance has been linked to susceptibility to seizures (Signorini et al., 1997), hyperalgesia and analgesia (Blednov et al., 2003; Marker et al., 2004; Marker et al., 2005), drug addiction, and alcohol-related behavioral effects (Kobayashi et al., 1999; Blednov et al., 2001b; Morgan et al., 2003; Cruz et al., 2008), as well as motor activity, co-ordination, and reward- and anxiety-related behaviors (Pravetoni and Wickman, 2008) (see table 1 to observe the most studied implications of GIRK mutation in physiology).

The first mutant mice regarding GIRK channels were the *weaver* mice ($GIRK^{wv}$). These mice carry an spontaneous mutation in the pore region of GIRK2 subunit ($GIRK2^{wv}$) (Patil et al., 1995), leading to a loss of K^+ selectivity and G protein insensitivity (Kofuji et al., 1996; Navarro et al., 1996; Slesinger et al., 1997). Upon receptor activation, $GIRK2^{wv}$ depolarizes rather than hyperpolarizes neurons. Homozygous mice are characteristic because they have an abnormal walk as a consequence of the lost of granular neurons in *cerebellum* (Rakic and Sidman, 1973). They also show motor hyperactivity, spontaneous temblor, ataxia, and male sterility by the degeneration of dopamine neurons of the *substantia nigra* (Lane et al., 1977; Liao et al., 1996; Roffler-Tarlov et al., 1996). In *weaver* mice it is showed an important decrease of GIRK2 subunit as well as GIRK1 subunits (Liao et al., 1996). Therefore, this mutation could have different qualitative effects in different neuronal populations depending on GIRK2 and GIRK1 expression levels.

One of the aspects in which GIRK channels might be relevant in the physiology is analgesia or pain perception.GIRK1 knockout and GIRK2 knockout mice, as well as wild-type mice given intrathecal injection of the GIRK channel blocker tertiapin-Q, exhibit thermal hyperalgesia and blunted analgesic responses to intrathecal morphine (Marker et al., 2004; Marker et al., 2005). Interestingly, GIRK channels make a dose-dependent contribution to the analgesic effect of the μ-opioid receptors agonist. In this sense, the effect of high, but not low doses of the opioid agonist, is selectively blunted after pharmacologic or genetic ablation of spinal GIRK channels. Morphine and the selective κ-opioid agonist, U-50488, which are known to activate GIRK2 containing channels through their coupling to opioid receptors, reduce pain perception in wild-type mice but not in the *weaver* mice (Ikeda et al., 2000). Moreover, in GIRK2$^{-/-}$ mice, for example, the dose–response curve for analgesia produced by morphine and clonidine (an α_2-adrenergic receptor agonist) is shifted to higher concentrations, but the maximal effect is preserved (Mitrovic et al., 2003). This finding was confirmed in a study using double knockout mice for GIRK2 and GIRK3. In LC neurons of these mice, the potency (coupling efficiency) of opioid-induced analgesia is reduced, but the efficacy (maximal response) is intact (Cruz et al., 2008). Similarly, in LC neurons from GIRK2 mutant mice opioid-induced currents were reduced in both *in vivo* and *in vitro* studies (Torrecilla et al., 2002; Torrecilla et al., 2013).

GIRK channels have also been implicated in opioid tolerance and dependence, as the channels undergo adaptive changes during chronic exposure to morphine, such as desensitization. In neurons of the LC inhibiting the signaling by both G protein coupled receptor kinase 2 and extracellular signal-regulated kinase significantly reduces the met-enkephalin-induced GIRK current desensitization that normally occurs within minutes of drug application (Dang et al., 2009). However, GIRK current desensitization may not occur when μ-opioid receptors are activated by morphine. Morphine causes less GIRK

channel desensitization *in vitro* and *in vivo* than met-enkephalin (Whistler et al., 1999). In addition, in wild-type animals strong withdrawal signs are induce by the opioid receptor antagonist, naloxone, after chronic exposure to morphine. However, mice lacking GIRK2 and GIRK3 have strongly reduced withdrawal signs, fail to display an increase in LC neuron firing rate, which is an established electrophysiological hallmark of withdrawal, and morphine-induced GIRK-dependent postsynaptic currents are absent in LC neurons in these mutant mice (Cruz et al., 2008).

Regarding drug dependence, GIRK channels are thought to have a role in the acute rewarding effects and/or the adaptation that occurs with chronic exposure to addictive drugs that work through GPCR, such as opioids, the 'club drug' GHB, and cannabinoids. The initial target for addictive drugs in reward pathway is the VTA. Based on *in vivo* and *in vitro* experiments, distinct cellular mechanisms have been proposed for different classes of drugs (Luscher and Ungless, 2006). Morphine stimulates μ-opioid receptors that are selectively expressed on GABAergic interneurons of the VTA and activates GIRK channels, reducing the firing of these cells and eventually leading to disinhibition of dopamine neurons (Johnson and North, 1992). It is suggested that GHB selectively activates GIRK currents in GABAergic interneurons, leading to desinhibition of dopamine neurons. This indirect effect is probably due to the fact that $GABA_B$ receptors in GABAergic interneurons are more efficaciously coupled to GIRK channels than those in dopamine neurons (Cruz et al., 2004). In addition, dopamine neurons in the VTA selectively express RGS proteins, and this could account for the lower sensitivity of $GABA_B$ receptors for GIRK channels in these neurons (Labouebe et al., 2007). Furthermore, chronic drug exposure can dynamically regulate the expression levels of RGS proteins. In fact, it has been demonstrated that chronic morphine or GHB enhances the coupling efficiency of $GABA_B$ receptors and GIRK channels by decreasing RGS protein levels in dopamine neurons from VTA,

and therefore low drug concentrations are sufficient to inhibit dopamine neurons, losing the rewarding properties and becoming aversive (Lomazzi et al., 2008).

GIRK channels are also involved in alcohol-induced behavior and addiction, as alcohol directly binds and activates GIRK channels (Kobayashi et al., 1999; Mullner et al., 2000; Aryal et al., 2009). Indeed, *weaver* mice lack ethanol analgesia (Kobayashi et al., 1999). In GIRK2$^{-/-}$ mice some effects induced by ethanol, as stimulation of home cage motor activity, anxiety, and handling-induced convulsions are absent (Blednov et al., 2001b). GIRK3$^{-/-}$ mice display less severe withdrawal from ethanol and barbiturates (Pravetoni and Wickman, 2008). Moreover, it has been demonstrated that ethanol increases $GABA_B$ receptor-induced GIRK currents in VTA neurons, decreasing excitability of dopamine neurons (Federici et al., 2009).

Memory and learning processes are also altered in mutant mice. Mice with low levels of GIRK1 have difficulties in learning and memory (Kourrich et al., 2003). In the same line, GIRK4$^{-/-}$ mice have difficulties with spatial learning (Wickman et al., 2000).

Regarding the implication of GIRK channels in the pathophysiology of several diseases, two broad principles should be taken into account. First, the loss of GIRK function can lead to excessive neuronal excitability, such as in epilepsy, whereas a gain of GIRK function can considerably reduce neural activity, such as is postulated to occur in Down's syndrome. Second, the loss of selectivity can cause aberrant ion fluxes across GIRK channels, such as aberrant Na^+ influx that triggers cell death, which is exemplified in a model of Parkinson's disease. In epilepsy, GIRK2$^{-/-}$ mice develop spontaneous convulsions and show a propensity for generalized seizures when injected with a pro-convulsive $GABA_A$ receptor antagonist (Signorini et al., 1997). In Down's syndrome, two mouse models have been generated that carry either a partial or

full segment duplication of the mouse chromosome 16, the orthologue of human chromosome 21 (Reeves et al., 1995; Sago et al., 1998). In both cases GIRK2 protein is up-regulated, resulting in a larger slow inhibitory postsynaptic current mediated by $GABA_B$ receptors (Siarey et al., 1999). Moreover, hippocampal long term potentiation is reduced and long-term depression is enhanced in both models, and therefore synaptic plasticity of glutamatergic transmission is altered.

Additionally, cell death is implicated in Parkinson's disease. The involvement of GIRK channels in Parkinson's disease was first inferred from the *weaver* mouse (Patil et al., 1995), in which constitutively active $GIRK2^{wv}$ channels produce chronic depolarization and cell death in a subset of neurons in the brain (Kofuji et al., 1996; Navarro et al., 1996; Slesinger et al., 1996), mimicking the neuronal degeneration observed in Parkinson's disease (Schein et al., 2005). The gain-of-function phenotype in dopamine neurons of *weaver* mice is of clinical interest owing to the progressive degeneration of dopamine neurons in the *substantia nigra*. However, other mechanisms are also implicated in Parkinson's cell death such as the nerve growth factor receptor (also known as $p75^{NTR}$). The nerve growth factor mediates the programmed cell death in *dorsal root ganglion* neurons, which represents an important step in the development of the nervous system. In this sense, it has been reported that activation of $p75^{NTR}$ increases PIP_2 plasma membrane levels, activating GIRK channels and creating a sustained K^+ efflux that stimulates programmed cell death (Coulson et al., 2008).

Moreover, although GIRK channels have a relatively well characterized role in controlling neuronal excitability by mediating the actions of inhibitory neurotransmitters in adult neurons, the role of GIRK channels before the development of mature neuronal circuitry has not been fully investigated. It has been suggested that GIRK channel action during early postnatal development regulates maturation of functional circuits at a time when activity is primarily

excitatory (Karschin et al., 1996; Sickmann and Alzheimer, 2002). In addition, it has been proposed that GIRK channels participate in the fundamental process of neuronal selection that occurs both in development and in neurodegenerative disease, as a checkpoint in the $p75^{NTR}$-mediated death pathway (Coulson et al., 2008) (Table 1.1).

Table 1.1. Physiological and pathophysiological relevance of *Girk* gene mutation on GIRK signaling. Taken and modified from Lujan et al. (2014).

	Girk gene(s)	Mutation	Phenotype	References
Nociception				
Thermal	*Girk1, Girk2*	Knockout	Hyperalgesia	Mitrovic et al., 2003 Marker et al., 2004
Mechanical	*Girk2*	Knockout	Hyperalgesia	Mitrovic et al., 2003
Chemical	*Girk2*	Knockout	Hyperalgesia	Mitrovic et al., 2003
Antinociception				
Opiod	*Girk1, Girk2*	Knockout	Decreased analgesia	Mitrovic et al., 2003 Cruz et al., 2008
	Girk3	Knockout	Decreased sensitivy	Smith et al., 2008
	GIRK2	Polymorphism	Increased dose requirement	Nishizawa et al., 2009 Lotsch et al., 2010
α_2 Adrenergic	*Girk2, Girk3*	Knockout	Decreased analgesia	Blednov et al., 2003 Mitrovic et al., 2003 Smith et al., 2008
$GABA_B$	*Girk2*	Knockout	Decreased analgesia	Blednov et al., 2003
Cholinergic	*Girk2*	Knockout	Decreased analgesia	Blednov et al., 2003
Cannabinoid	*Girk2, Girk3*	Knockout	Decreased sensitivity	Blednov et al., 2003, Smith et al., 2008
Reward				
Motor activity	*Girk1, Girk2*	Knockout	Enhanced basal and cocaine-induced	Blednov et al., 2002 Morgan et al., 2003 Arora et al., 2010
Natural rewards	*Girk2, Girk4*	Knockout	Elevated responding for food	Perry et al., 2008 Pravetoni and Wickman, 2008
	Girk2	Triploid	Enhanced sucrose intake	Cooper et al., 2012

	Girk gene(s)	Mutation	Phenotype	References
Self-administration	*Girk2, Girk3*	Knockout	Decreased (cocaine)	Morgan et al., 2003
	Girk2	Knockout	Enhanced consumption (ethanol)	Blednov et al., 2001b
Dependence/withdrawal	*Girk2/3*	Knockout	Decreased opiod withdrawal	Cruz et al., 2008
	Girk3	Knockout	Decreased sedative-hypnotic withdrawal	Kozell et al., 2009
	GIRK2	Polymorphism	Associated with ethanol intake and stress	Clarke et al., 2011
Learning and memory				
Spatial learning/memory	*Girk4*	Knockout	Decreased recall	Wickman et al., 2000
Fear conditioning	*Girk2*	Triploid	Decreased contextual recall	Cooper et al., 2012
Anxiety	*Girk2*	Knockout	Anxiolysis	Blednov et al., 2001a Pravetoni and Wickman, 2008
Schizophrenia	GIRK1	Polymorphism	Genetic association	Yamada et al., 2012
Seizure/epilepsy	*Girk2*	Knockout	Increased spontaneous and PTZ-induced	Signorini et al., 1997
Thermoregulation	*Girk2*	Knockout	Decreased drug-induced hypothermia	Costa et al., 2005
Neurodevelopment	*Girk2*	Weaver	Loss of granule and dopamine neurons	Gregerson et al., 2001

1.2.5. Pharmacology

Although GIRK channels are activated or inhibited by an array of psychoactive compounds, most of these compounds usually have other primary molecular targets (Lujan et al., 2014).

Antipsychotic drugs like tiorizadine, clozapine, pimozide, and haloperidol inhibit GIRK channels to different levels of efficacy. Risperidone has a lower inhibitory effect onto GIRK channels (Kobayashi et al., 2000; Kobayashi et al., 2004b). Antidepressants, especially those that inhibit NA or 5-HT transporter, have important implications on the efficacy of GIRK channels, although they do not represent their primary target. As an example, fluoxetine has been shown to indirectly inhibit GIRK channels when they are over-expressed on *Xenopus oocytes* (Kobayashi et al., 2003). Similarly, in studies conducted in GIRK2 *weaver* aberrant channel mutant mice, where the channels have less selectivity for K^+ ions, fluoxetine also inhibits the activity of these channels (Takahashi et al., 2006). In contrast, in native systems containing GIRK channels, antidepressants as fluoxetine are expected to indirectly increase GIRK conductance given their coupling to 5-HT_{1A} receptors. In addition, fluoxetine derivates have been also identified as selective agonists and antagonists of GIRK channels (Nishizawa et al., 2009). Tricyclic antidepressants including imipramine, desipramine, amitriptiline, nortriptiline, clomipramine, and maprotiline also inhibit over-expressed GIRK channels in *Xenopus oocytes* (Kobayashi et al., 2004a). Furthermore, it has also been described that fluoxetine and other tricyclic antidepressants are able to inhibit GIRK current induced by ethanol at clinical concentrations (Kobayashi et al., 2003; Kobayashi et al., 2004a). Moreover, antitussives including caramiphen, which in addition show antidepressant-like effect in the forced swimming test, have an inhibitory action in the activated GIRK currents (Kawaura et al., 2010). Altogether, these investigations suggest that the modulation of GIRK channels by antidepressants could contribute to some therapeutic and secondary effects.

Ethanol and methanol increase GIRK channel function. Ethanol effect is independent of G protein activation and secondary to cytolitic messengers (Kobayashi et al., 1999; Lewohl et al., 1999). Nowadays, it is well known that the activation of GIRK2 subunits-containing GIRK channels mediates the behavioral effects of the ethanol (Blednov et al., 2001b). Some other compounds, as for example halothane, isoflurane, and enfluorane, which are volatile anesthetics, or the bioflavonoid found in the grapefruit, naringin can also activate GIRK channels in a G protein-independent manner (Weigl and Schreibmayer, 2001; Yamakura et al., 2001; Yow et al., 2011). In addition, the mechanism of analgesic action of flupirtine is believed to be related to the activation of GIRK channels (Kornhuber et al., 1999).

Regarding GIRK channel inhibitors, some other drugs, such as verapamil, a Ca^{2+} channel blocker, have been described as inhibitors of the channels. However, the most selective GIRK channel blocker is tertiapin-Q (Lesage et al., 1995). This peptide obtained from the honey bee venom is a high affinity blocker for GIRK channels and it is widely used in investigations studying GIRK signaling (Jin and Lu, 1998).

The pharmacologic manipulation of GIRK channels should evoke a wide range of undesirable consequences given their broad distribution, contribution and roles in the nervous system and cardiac and endocrine physiology. In this sense, new GIRK agents or strategies associated with enhancing or inhibiting GIRK signaling are likely to achieve their full therapeutic potential if they act selectively in a specific region and/or GIRK subunit. Recently, a new class of subunit-selective, efficacious, potent, and direct-acting GIRK channel agonists and antagonists has been identified (Kaufmann et al., 2013; Ramos-Hunter et al., 2013; Wen et al., 2013). Among them, it is interesting the novel G protein-independent GIRK channel modulator, ML297, which is a potent agonist selective for GIRK1 subunit-containing channels (Kaufmann et al., 2013). This small molecule was firstly

described as being efficacious in mice in delaying seizure onset in a maximal electroshock model of epilepsy, and it is also able to prevent convulsions and lethality in a chemically induce epilepsy model (Kaufmann et al., 2013). Further behavioral investigations have revealed that, in addition to its antiseizure efficacy, ML297 also has anxiolytic effects, since it decreases the anxiety-related behavior without sedative or addictive liabilities (Wydeven et al., 2014).

The recent identification of the subunit-selective, efficacious and potent direct modulators of GIRK signaling represents a step forward in this field. These compounds, when available will greatly facilitate the efforts directed at understanding the physiological relevance of GIRK channels at the same time it will allow to reduce the use of mutant mice.

1.3. Novel antidepressant treatments: ketamine as a rapid-acting antidepressant

Depression standard of care for the last 50 years has focused on monoamine neurotransmitters, including such treatments as selective serotonin reuptake inhibitors and serotonin-noradrenaline reuptake inhibitors (Zarate et al., 2013). However, the efficacy of these medications is limited, with a substantial proportion of patients failing to achieve a sustained remission (Rush et al., 2006). In addition, the full clinical benefit of these traditional antidepressants is only achieved following weeks to months of treatment (Katz, 2004). Therefore, there is a clear need for rapid-acting antidepressants with robust efficacy. In this regard, ketamine has turned out to be the prototype for a new generation of antidepressants that rapidly alleviate depression symptoms and display efficacy in patients who are refractory to currently available treatments (Abdallah et al., 2015).

Ketamine is a non-competitive NMDA receptor antagonist that has been widely used for induction and maintenance of anesthesia. The implication of the NMDA receptor in the pathophysiology and treatment of depression was first described in 1996 by Skolnick et al. By the late-1990s, it was found that low (subanesthesic) doses of this drug administered intravenously began to reduce depression symptoms within 4 hours of administration in severely treatment-resistant depressed patients (Berman et al., 2000). The striking finding in this study was the rapid emerge and the persistence for so long of the antidepressant effects following a single dose of ketamine. The antidepressant effects tend to emerge 1-2 hours after the acute perceptual disturbances of ketamine have abated, and can persist for two weeks or longer in some patients. To date, five placebo-controlled studies have replicated the rapid antidepressant effects of ketamine in major depression and bipolar depression (Berman et al., 2000; Zarate et al., 2006; Diazgranados et al., 2010; Valentine et al., 2011; Zarate et al., 2013). In these studies, the antidepressant effects were evident within 4

hours of treatment and sustained for 3-7 days. Little is known about the long-term safety and efficacy of repeated ketamine dosing, which appears to extend the benefits of a single ketamine infusion. However, it seems that repeated ketamine infusions may safely extend the benefits for several months or even a year or more (Blier et al., 2012; Szymkowicz et al., 2013). In this line, the results of a larger controlled study of repeated ketamine administration (NCT01627782) will be published in the coming months.

Studies in animals using several behavioral models confirmed the rapid-antidepressant effect of ketamine (Maeng et al., 2008; Li et al., 2010; Koike et al., 2013). These included a significant decrease in immobility in the forced swimming test (FST), a decreased escape failure and latency to escape in the learned helplessness paradigm, and a decreased latency to feed in the novelty suppressed feeding test (NSFT). The large body of evidence highlighting the antidepressant effect of ketamine led to establish the general idea that during depression there might be alterations in the glutamatergic transmission controlling the synaptic connectivity in different brain regions such as the PFC.

Convergent evidence has highlighted the involvement of synaptic plasticity alterations in the pathophysiology and treatment of depression (Popoli et al., 2002; Duman and Aghajanian, 2012). In fact, this altered synaptic plasticity represents the link between the neurobiology of depression and the therapeutic effects of ketamine. Synaptic plasticity, which can be "local", such as long term potentiation, or "global" such as homeostatic plasticity (Turrigiano, 2012), regulates the excitability and connectivity of neuronal circuits in the context of adaptation, and it is accomplished by modulating the synaptic strength and synaptic number. This means changing the number of AMPA receptors and the synaptic and extrasynaptic number of NMDA receptors, which promote and reduce synaptic strength, respectively (Hardingham and Bading, 2010). The global synaptic plasticity is of particular

interest in depression given that clinical depression is associated with a reduced prefrontal synaptic connectivity.

Prolonged stress and depression have been associated with neuronal atrophy and overall synaptic depression or dysfunction in the PFC and the *hippocampus* (Bessa et al., 2009; Kang et al., 2012; Yuen et al., 2012). However, the *amygdala* and *nucleus accumbens* show neuronal hypertrophy and synaptic potentiation (Vyas et al., 2004; Bessa et al., 2013). These changes are thought to result from the altered glutamate release induced by prolonged stress and the astroglial loss, leading to deficits in neurotrophic factors and to a sustained increase in extracellular glutamate. In the PFC, this excess in glutamate precipitates excitotoxicity, altered synaptic strength, dendritic retraction, and reduction in spine density and branching (Popoli et al., 2011; Krystal et al., 2013), leading to a down-regulation of PFC activity. Consecutively, this reduced activity leads to a gain of function in the *amygdala*, which is negatively controlled by the PFC and associated with increased anxiety and hypothalamic-pituitary-adrenal axis reactivity (Savitz and Drevets, 2009). It has been found that the stress-related prefrontal synaptic dysfunction is precipitated by reduction in the brain-derived neurotrophic factor (BDNF) (Duman and Monteggia, 2006), and also by inhibition of the mammalian target of rapamycin complex 1 (mTORC1) (Ota et al., 2014). Data from preclinical studies and studies in animal models of depression propose that the enhancement of BDNF and mTORC1 signaling, leading to prefrontal synaptogenesis and reversal of stress and depression-induced neuronal atrophy and synaptic disconnectivity, are required for efficacious antidepressant treatment (Duman and Monteggia, 2006; Ota et al., 2014).

Although antidepressants targeting monoaminergic systems were found to increase BDNF and synaptogenesis (Duman and Monteggia, 2006; Popoli et al., 2011), these effects were evident only after chronic treatment. Therefore, a

rapid acting antidepressant should directly target the mTOR and BDNF to ultimately increase the PFC synaptogenesis.

Studies conducted in rodents have begun to elucidate the downstream effects of ketamine that may underlie the beneficial effects in depressed patients. In the cascade of effects, the first step is ketamine's antagonism of the glutamatergic NMDA receptor. Specifically, low-dose ketamine administration rapidly triggers three consecutive effects: first, a presynaptic disinhibition of glutamatergic neurons owing to a blockade of NMDA receptors on GABAergic interneurons, leading to a glutamate surge in the PFC; second, an increased activation of AMPA receptors (Maeng et al., 2008; Koike et al., 2011; Tizabi et al., 2012); and third, a postsynaptic activation of neuroplasticity-related pathways involving the mTORC1 and BDNF, resulting in synaptogenesis and synaptic potentiation (Homayoun and Moghaddam, 2007; Li et al., 2010; Autry et al., 2011). Together, these data show that these acute effects of ketamine rapidly oppose the stress- and depression-induced PFC neuronal atrophy and synaptic disconnectivity (Li et al., 2011) (Fig. 1.10).

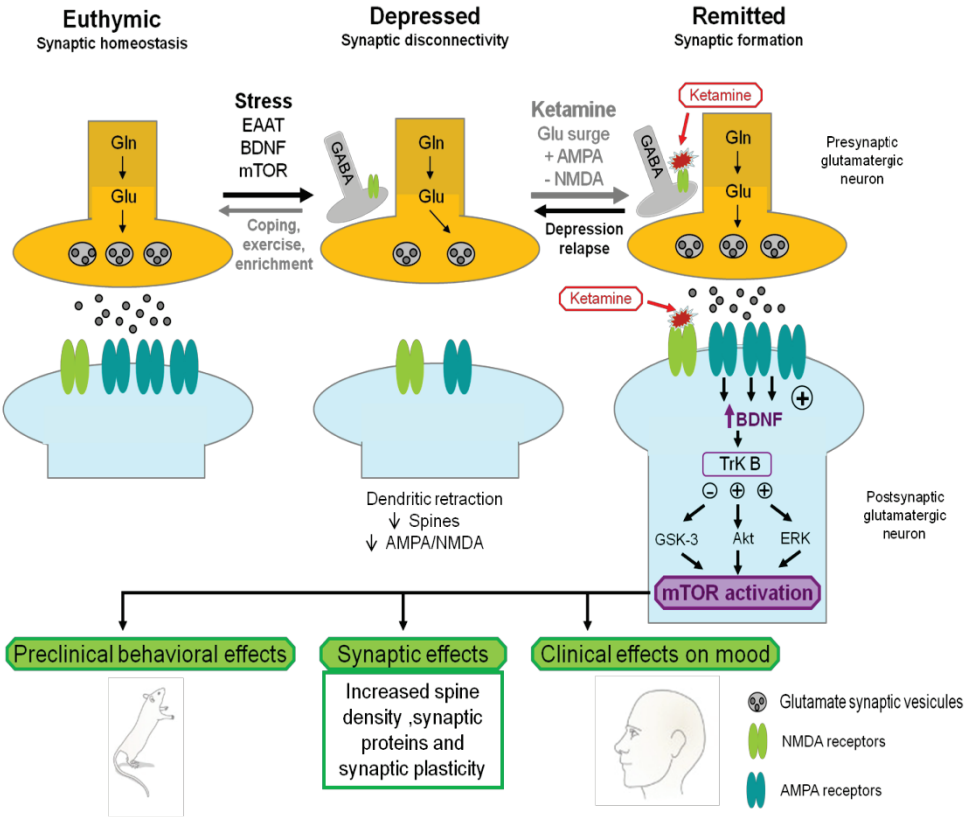

Figure 1.10. Representation of the prefrontal synaptic connectivity during normal mood, depression, and remission of depression, and the postulated mechanism of action of ketamine on the glutamatergic neurotransmission. In euthymic individuals, stimuli and activity maintain and regulate synaptic strength. Following stress or depression, a synaptic disconnectivity is observed together with a reduction in the glutamatergic transmission, excitatory aminoacid transporters (EAAT), brain-derived neurotrophic factor (BDNF), and the mammalian target of rapamycin (mTOR) signaling. Remission, characterized by synaptic formation, is believed to arise from blockade of NMDA receptors located extrasynaptially on GABAergic interneurons, leading to a glutamate surge, activation of AMPA receptors, and an increase in BDNF release and mTOR signaling. Activation of mTOR signaling, ultimately, leads to increased synaptic proteins, spine densities and synaptogenesis (Jourdi et al., 2009; Akinfiresoye and Tizabi, 2013). Taken and modified from Naughton et al. (2014) and Abdallah et al. (2015).

Similar to SSRIs, acute administration of ketamine increases 5-HT levels in the PFC (Amargos-Bosch et al., 2006) and the stimulated 5-HT efflux in the DR (Tso et al., 2004). Traditional antidepressants, including SSRIs, have been found to increase BDNF and synaptogenesis as ketamine does (Popoli et al., 2002; Duman and Monteggia, 2006). Besides this, it has been suggested that the effects of SSRIs may also involve alterations in NMDA function (Dutta et al., 2015). Therefore, it seems evident and consistent that there is an involvement of the 5-HT system in the antidepressant effect of ketamine and, obviously, as confirmed by a large body of studies, in the neurobiology of depression. Li et al. (2010) reported that a low dose of ketamine resulted in a rapid induction of spine formation in layer 5 pyramidal neurons of the PFC, which was correlated with an increase in the frequency and amplitude of 5-HT-induced excitatory postsynaptic currents (EPSCs), which in turn, indicates an increase in cortico-cortical connections. As previously indicated, ketamine produces rapid antidepressant effects in various behavioral models including the FST (Li et al., 2010). Interestingly, this effect seen in the FST was later demonstrated to be via a 5-HT-dependent mechanism, since depletion of 5-HT, using the tryptophan hydroxylase inhibitor para-chlorophenylalanine, abolished the behavioral antidepressant effect of ketamine (Gigliucci et al., 2013). Moreover, 5-HT_{1A} receptors have been also specifically involved in the antidepressant effect of ketamine in the NSFT (Fukumoto et al., 2014). In this study, pretreatment with the 5-HT_{1A} receptor antagonist, WAY100635 blocked the effect of ketamine in the NSFT, suggesting 5-HT_{1A} receptor stimulation upon the AMPA receptor-dependent 5-HT release. Recently, it has been demonstrated that ketamine induces prefrontal 5-HT release through the activation of AMPA receptors and α4β2-nicotinic acetylcholine receptors in the DR (Nishitani et al., 2014). In this study, the direct stimulation of DR AMPA receptors significantly increased the 5-HT levels in the PFC, mimicking the effect of ketamine. Also, a microinjection of the AMPA receptor antagonist, DNQX, directly into the DR, attenuated the ketamine-induced 5-HT release. In

addition, a microinjection of the α4β2-nicotinic acetylcholine receptor antagonist, DHβE, into the DR attenuated the ketamine-induced 5-HT release in the PFC. Consistently, α4β2-nicotinic acetylcholine receptor agonist increased 5-HT levels in the rat PFC. The DR is innervated by glutamatergic neurons from several brain regions including the PFC. Thus, it seems possible that indirect activation of glutamatergic neurons in the PFC might induce glutamate release in the DR leading to a 5-HT release in the PFC. It is also postulated that the resulting 5-HT release in the PFC is because ketamine may disinhibit 5-HT neurons in the DR through the blockade of NMDA receptors on GABA interneurons, which suppress 5-HT neuronal activity (Boothman et al., 2006). Altogether, it is an established factor that ketamine administration induces alterations at the 5-HT neurotransmission level and/or its major source the DR, confirmed also by behavioral studies in animal models of depression (Fukumoto et al., 2014). In spite of these reports, to our knowledge, it has not been fully investigated whether a single dose of ketamine induces alterations in the glutamatergic activity and mTOR activation within the DR, and in that case, the time duration of the effects.

2. HYPOTHESIS AND OBJECTIVES

2. HYPOTHESIS AND OBJECTIVES

Depression is a highly disabling mood disorder with a big impact on public health, social, and economic aspects. It is well known that the monoaminergic systems have long been implicated in the etiology of this pathology. In this sense, much evidence indicates that depression is related to a decreased serotonergic neurotransmission, and as a result most of the antidepressants are aimed at increasing the extracellular levels of serotonin. Thus, the serotonergic system and its main biological substrate, the DR, are considered important therapeutic targets in this disorder.

The activity of the DR is primarily controlled by 5-HT_{1A} receptors, which play a critical role in the negative feedback regulation of serotonergic neurotransmission (Barnes and Sharp, 1999; Stamford et al., 2000). In fact, the SSRIs, which nowadays are the first-line therapies in depression, activate DR 5-HT_{1A} receptors by increasing 5-HT levels (Trivedi et al., 2006; Duman and Aghajanian, 2012). Microdialysis and electrophysiological studies using chronic administrations of SSRIs have indicated that desensitization of 5-HT_{1A} receptors correlates with the delayed onset of the clinical response to these drugs, which takes several weeks to appear (Sanchez et al., 2015). In addition to the delayed response, these medications have limited efficacy (Duman, 2014).

GIRK channels are coupled to inhibitory G protein coupled receptors, such as 5-HT_{1A} receptors. It has been described that they control the electrophysiological properties of neurons and some neurotransmitter systems in different brain areas, as well as some animal behaviors (for review see Luscher et al., 2010). Specifically, the deletion of GIRK2 subunit promotes important electrophysiological and biochemical alterations in different brain regions including the noradrenergic LC (Torrecilla et al., 2013). Regarding behavior, GIRK2 deficient mice display a reduced anxiety compared to wild-type mice (Blednov et al., 2001a; Pravetoni and Wickman, 2008). Thus, the

selective manipulation of GIRK channels offers hope to treat a variety of debilitating afflictions (for review see Lujan et al., 2014).

Central serotonergic transmission is also influenced by the synaptic excitatory and inhibitory inputs to the DR (Nitz and Siegel, 1997; Gervasoni et al., 2000; Adell et al., 2002; Judge et al., 2004). In this sense, dysregulation of the GABAergic system has been considered to play a key role in the etiology of depression (Krystal et al., 2002; Sanacora et al., 2012). For example, it has been reported that SSRIs alter, ultimately, the GABAergic transmission (Zhong and Yan, 2004; Luscher et al., 2011). Likewise, alterations in the glutamatergic system have also been linked to depression. In fact, the glutamatergic antagonist ketamine produces fast antidepressant actions in depressed patients, including treatment-resistant patients (Zarate et al., 2006). The specific effects of this drug on the glutamatergic activity of the *prefrontal cortex* (PFC) have been well described (Moghaddam and Adams, 1998; Li et al., 2010; Aan Het Rot et al., 2012). However, it is likely that ketamine also has effects on glutamate synapses of other brain regions related to the pathophysiology of depression, such as the DR. In fact, some studies point out the DR and serotonergic system as key targets of the biochemical and antidepressant-like effects of ketamine in rodents (Fukumoto et al., 2014; Nishitani et al., 2014).

All this highlights that there is a major need for a better understanding and identification of novel strategies and targets for depression to develop new safer rapid acting agents with greater efficacy. Thus, we stated two hypotheses based on two alternative approaches in the field of depression therapy. First, GIRK2 subunit-containing GIRK channels are controlling the basal activity and regulation of DR neurons, and therefore restraining the serotonergic neurotransmission and impacting on depression-like behaviors and other functional aspects related to depression, such as adult neurogenesis. As a consequence, the electrophysiological, physiological and behavioral responses to serotonergic agents and antidepressants are altered in GIRK2 mutant mice

compared to wild-type mice. Secondly, the actions of ketamine related to its antidepressant effects extend to the DR, and therefore electrophysiological and biochemical alterations are observed in DR neurons of wild-type mice after ketamine administration.

The global aim of this study was to study in the DR two alternative approaches in the field of depression therapy, which are GIRK2 subunit containing GIRK channels as potential therapeutic targets, and the novel rapid-acting antidepressant ketamine. To this end, we proposed two main objectives; first, to characterize the neurophysiology of DR neurons and the behavioral response in depression-related tests of mice lacking GIRK2 subunits; and second, to characterize the effect of ketamine in the glutamatergic transmission of the DR.

The specific objectives of the present study were:

I. To investigate *in vivo* the contribution of GIRK2 subunit-containing GIRK channels to the electrophysiological properties of central serotonergic transmission. For this purpose, we measured the basal electrical activity of DR neurons and its modulation by serotonergic drugs, such as the 5-HT_{1A} receptor agonist 8-OH-DPAT, and the selective serotonin reuptake inhibitor citalopram, in GIRK2 mutant mice.

II. To study the involvement of GIRK2 subunit-containing GIRK channels in depression-related behaviors and in the behavioral response to the SSRI citalopram. For this purpose, we assessed the depression-related behavior in the tail suspension test and novelty suppressed feeding test, as well as the citalopram-induced behavioral response in the tail suspension test in GIRK2 mutant mice.

Hypothesis and objectives

III. To investigate *in vitro* the involvement of GIRK2 subunit-containing GIRK channels in the regulation of the activity of DR neurons. For this purpose, we performed patch-clamp recordings of passive and active membrane properties and 5-HT_{1A} receptor-mediated whole-cell currents, as well as of the glutamatergic and GABAergic pre- and postsynaptic transmissions in DR neurons of GIRK2 mutant mice.

IV. To study the electrophysiological and biochemical effects of ketamine on the glutamatergic transmission in the DR, as well as its impact on the mTOR activity in this brain area. To this end, we carried out *in vitro* patch-clamp recordings to investigate the acute and sustained effects of ketamine on the glutamatergic transmission in DR neurons. In addition, we measured the mTOR activation after ketamine administration in DR neurons using the western blot technique.

3. MATERIALS AND METHODS

3. MATERIALS AND METHODS

3.1. Materials

3.1.1. Animals

C57BL6/J wild-type mice (WT), GIRK2$^{+/-}$ (heterozygous), and GIRK2$^{-/-}$ (homozygous) mice derived from heterozygote crossing (Signorini et al., 1997) were used. Initial breeding pairs were kindly provided by Dr. Kevin Wickman from the University of Minnesota (Minneapolis, USA). From this initial source a stable colony of GIRK2 mutant mice was grown. Animals were maintained at 22±2 ºC in a 12-h light/dark cycle with food and water provided *ad libitum*. Mice were genotyped by PCR screening as previously described by Torrecilla et al. (2002) at the Department of Neurochemistry Research of the Basque Health Service (Zamudio, Spain). Male and female adult mice (3-4 months) were used for the behavioral tests and electrophysiological procedures (4-8 weeks old for *in vitro* recordings). Male mice were used for the immunohistochemistry, physiological tests, and western blotting experiments (3 months). Every effort was made to minimize the animals' suffering and to reduce the number of animals used to a minimum. All procedures were conducted in accordance with European Community Council Directive on 'The Protection of Animals Used for Experimental and Other Scientific Purposes' (86/609/EEC) and the Spanish Law (RD 1201/2005) for the care and use of laboratory animals. Experimental protocols were reviewed and approved by Local Committee for Animal Experimentation at the University of the Basque Country.

3.1.2. Drugs and antibodies

The drugs and antibodies used in this study are shown in table 3.1.

Table 3.1. Pharmacological activity of the drugs and antibodies used in this study

Drug	Activity	Pursached from
Baclofen (*R*)-4-Amino-3-(4-chlorophenyl)butanoic acid	$GABA_B$ receptor agonist	Sigma-Aldrich
Chloral hydrate	Anesthetic	Sigma-Aldrich
CGP55845 (2*S*)-3-[[(1*S*)-1-(3,4-Dichlorophenyl)ethyl]amino-2-hydroxypropyl](phenylmethyl)phosphinic acid hydrochloride	$GABA_B$ receptor antagonist	Tocris Bioscience
Citalopram 1-[3-(dimethylamino)propyl]-1-(4-fluorophenyl)-1,3-dihydro-5-isobenzofurancarbonitrile hydrobromide	SSRI	Tocris Bioscience
5-CT 5-Carboxamidotryptamine maleate salt	$5\text{-}HT_{1A}$ receptor agonist	Sigma-Aldrich
D-AP5 D-2-Amino-5-phosphonovaleric acid	NMDA receptor antagonist	Tocris Bioscience
DNQX 6,7-Dinitroquinoxaline-2,3-dione	Non-NMDA receptor antagonist	Abcam
GABA γ-Aminobutyric acid	Inhibitory neurotransmitter	Abcam
Isoflurane	Inhalatory anesthetic	Abbott

Drug	Activity	Pursached from
Ketamine 2-(2-Chlorophenyl)-2-(methylamino)cyclohexanone	Non-competitive NMDA receptor antagonist	Ketamidor ® Richter Pharma AG
Kynurenic acid Hydroxyquinoline-2-carboxylic acid	Excitatory amino acid antagonist	Sigma-Aldrich
MK801 (5*S*,10*R*)-(+)-5-Methyl-10,11-dihydro-5*H*-dibenzo[*a*,*d*]cyclohepten-5,10-imine maleate	NMDA receptor antagonist	Abcam
8-OH-DPAT **(±)-**8-Hydroxy-2-(dipropylamino)tetralin hydrobromide	5-HT_{1A} receptor agonist	Sigma-Aldrich
Pentobarbital 5-Ethyl-5-(1-methylbutyl)-2,4,6-trioxohexahydropyrimidine	Anesthetic	Sigma-Aldrich
Picrotoxin	$GABA_A$ receptor antagonist	Abcam
PP242 2-[4-Amino-1-(1-methylethyl)-1*H*-pyrazolo[3,4-*d*]pyrimidin-3-yl]-1*H*-indol-5-ol	mTOR inhibitor	Tocris Bioscience
Tertiapin-Q	GIRK channel blocker	Tocris Bioscience
WAY100635 N-[2-[4-(2-Methoxyphenyl)-1-piperazinyl]ethyl]-N-2-pyridinylcyclohexanecarboxamide maleate salt	5-HT_{1A} receptor antagonist	Sigma-Aldrich

The following antibodies were used in this study:

Antibody	Activity	Pursached from
Rabbit polyclonal antiserum for phosphorylated Histone H3 (HH3)	Primary antibody raised against HH3	Merck Millipore (Upstate)
Mouse monoclonal antiserum for glial fibrillary acidic protein (GFAP)	Primary antibody raised against GFAP	Sigma-Aldrich
Biotinylated donkey anti-rabbit IgG	Secondary antibody generated against rabbit IgG	Stratech Scientific
Biotinylated horse anti-mouse IgG	Secondary antibody generated against mouse IgG	Vector Laboratories
Rabbit monoclonal antibody anti-phospho-mTOR (Ser2448)	Primary antibody raised against phosphor-mTOR (Ser2448; Akt phophorylation site)	Cell signaling
Rabbit polyclonal antibody anti- phospho-mTOR (Ser2481)	Primary antibody raised against phosphor-mTOR (Ser2481; autophophorylation site)	Cell signaling
Rabbit monoclonal antibody anti-mTOR	Primary antibody raised against mTOR	Cell signaling
Rabbit monoclonal antibody anti-Raptor	Primary antibody raised against Raptor (regulatory associated protein of mTOR)	Cell signaling

Antibody	Activity	Pursached from
Rabbit monoclonal antibody anti- GβL	Primary antibody raised against GβL (mediates rictor-mTOR signaling to PKCα)	Cell signaling
Rabbit polyclonal antibody anti-actin	Primary antibody raised against β-actin	Sigma-Aldrich
Goat polyclonal anti-rabbit IgG	Secondary antibody generated against rabbit IgG	Cell signaling

For intraperitoneal administrations chloral hydrate, citalopram, 8-OH-DPAT, and WAY100635 were prepared in physiological saline (0.9% NaCl). For intracerebroventricular administrations tertiapin-Q was dissolved in artificial cerebrospinal fluid (ACSF) containing (in mM): 125 NaCl, 2.5 KCl, 1.2 $MgCl_2$, 26 NaH_2CO_3, 1.25 NaH_2PO_4, 2.4 $CaCl_2$, and 11 D-glucose (pH 7.3-7.4). With the exception of chloral hydrate, drugs were freshly prepared immediately prior to the use.

For the *in vitro* recordings drug stocks were prepared in either distilled water (baclofen, 5-CT, D-AP5, GABA, ketamine, and WAY100635) or dimethyl sulfoxide (CGP55845, DNQX, MK801, and PP242), and diluted in ACSF right before application. Kynurenic acid and picrotoxin were directly dissolved in ACSF before bath-perfusion.

3.2. Methods

3.2.1. Electrophysiological procedures

3.2.1.1. *In vivo* single-unit extracellular recordings of *dorsal raphe* neuronal activity in anesthetized mice

Preparation for electrophysiological procedures was performed as previously described (Torrecilla et al., 2013).

A) Animal preparation and surgery

Mice were anesthetized with chloral hydrate (400 mg/kg, i.p.) and placed in a sterotaxic frame. A catheter (Terumo Surflo) was inserted in the peritoneum for additional administrations of anesthetic and other systemic drugs. In order to maintain a full anesthetic state, characterized by the absence of a nociceptive reaction to a paw/tail pinch and eye blink response to pressure, supplemental doses of chloral hydrate (100 mg/kg, i.p.) were periodically administered. Body temperature was maintained at ~ 37 º C for the entire experiment by means of a heating pad. For the recordings, the head was oriented in the horizontal plane. A bur hole (3 mm diameter approximately) was drilled and an electrode was lowered into the DR (relative to bregma: AP -4.5 mm, ML -1.0 mm, DV -2.5 to -4.0 mm) (Franklin and Paxinos, 1997) with a lateral angle of 20° in order to avoid the damage of the sagital sinus.

Intracerebroventricular administrations (tertiapin-Q 100 pmol in 1μL, dissolved in ACSF; or ACSF used as a control group) were performed using a microsyringe (5μl, Hamilton, Bonaduz, Switzerland) connected to a 30-gauge stainless-steel needle that was perpendicularly inserted into the right lateral ventricle (relative to bregma: AP -0.5 mm, ML -1.0 mm, DV -2.0 mm). Intracerebroventricular administrations were performed 10 min prior to the recordings.

B) Recording and neuronal identification

For the preparation of the recording electrode, an Omegadot single barrel micropipette was stretched using an automatic vertical electrode stretcher. After that, the electrode was filled with 2 % solution of Pontamina Sky Blue in 0.5 % sodium acetate, previously filtered in a 0.22 μm pore diameter filter. The tip of the electrode was broken under microscope inspection (40X magnification) to obtain a tip diameter of 1-2 μm. The electrode was lowered into the DR (found in the above mentioned sterotaxic coordinates) by means of a hydraulic microdrive (David Kopf Instruments, California, USA).

The extracellular signal from the electrode was preamplified (10X), amplified later (10X) by means of a high-input impedance amplifier, and monitored with an oscilloscope and an audioanalyzer. The extracellular signal was bandpass-filtered at 30-5000 Hz in a second amplifier and digitalized by an interface (CED micro 1401) (Fig. 3.1). Firing patterns were analyzed off-line, using the computer software Spike2 (Cambridge Electronic Design, UK). The following parameters were calculated: firing rate, coefficient of variation, percentage of cells exhibiting burst firing, firing rate of burst firing neurons, number of burst, percentage of spikes in burst, mean spikes per burst, and response to drug administration. Only one cell was studied in each animal when any drug was administered.

Figure 3.1. Schematic illustration of extracellular electrophysiological procedure in anesthetized mice. Briefly, the extracellular signal recorded was passed through a high-input impedance amplifier, displayed in an oscilloscope, and monitored with an audioanalyzer. Individual (single-unit) neuronal spikes were isolated and analyzed by means of PC-based software Spike2.

DR neurons were identified using established criteria, which included slow (0.5-2.5 Hz) and regular firing rate, and characteristic spikes with a long-lasting and long duration (0.8-1.2 ms) positive-negative waveform. A burst was defined according to (Gartside et al., 2000), and burst-firing neurons in mice were identified as described previously (Gobbi et al., 2007), including a first interspike interval of 20 ms or less and a termination interspike interval greater than or equal to 160 ms (Fig. 3.2).

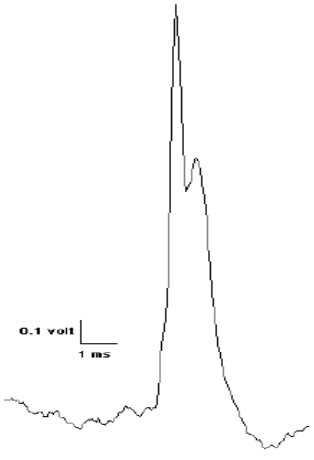

Figure 3.2. Example of a single spike from a *dorsal raphe* neuron recorded *in vivo*. Picture was taken from *Spike2* recordings. The abscise and ordinate axes represent duration (ms) and amplitude (volt) of the action potential, respectively.

C) Histological verification procedure

At the end of some experiments, a Pontamine Sky Blue mark was deposited in the recording site by passing a 5 μA cathodic current for 10 min through the recording electrode (FICTE 10, Cibertec, Spain). This procedure left a discrete spot of Pontamine Sky Blue at the recording site. Afterwards, brains were carefully dissected and sliced to visually localize the Pontamine Sky Blue mark within the DR, which was identified on the midline and ventral

to the aqueduct. Only measurements from cells within the DR were included in the analyses.

3.2.1.2. *In vitro* patch-clamp recordings of *dorsal raphe* neuronal activity in mice brain slices

Whole-cell patch-clamp recordings were performed as previously described (Torrecilla et al., 2008; Bruzos-Cidón et al., 2015).

A) Brain slice preparation

Male and female wild-type and GIRK2 mutant mice (4-8 weeks old) were anesthetized with isoflurane and killed by decapitation. Immediately afterwards, brains were removed quickly and mounted in a vibratome chamber (Leica VT 1200S or Microm HM 650V). Coronal slices (220 μm) were prepared in ice-cold artificial cerebrospinal fluid (ACSF, external bath solution) containing the following (in mM): 126 NaCl, 2.5 KCl, 1.2 $MgCl_2$, 2.6 $CaCl_2$, 1.2 NaH_2PO_4, 11 D-Glucose, and 21.4 $NaHCO_3$. ASCF was oxygenated and maintained at pH 7.4 by bubbling 95 % O_2/5 % CO_2 gas. Slices were stored in glass vials at 34ºC with oxygenated (95 % O_2 /5 % CO_2) ACSF. In order to reduce the neuronal damage, MK801 (10 μM) was included in the cutting and initial incubation solution to block NMDA receptors. To record excitatory synaptic activity, MK801 was substituted with kynurenic acid (2 mM). After an incubation period of at least 40 min, slices were transferred to the recording chamber for recording.

B) Neuronal identification and recording

The DR was located in slices that were rostral to the level where the aqueduct begins to meet the fourth ventricle and caudal to the decussation of the cerebellar peduncle. The slice containing DR was mounted on the recording chamber attached to a microscope (Eclipse FN1, Nikon), and was continuously perfused with ACSF at 1.5–3 ml/min at 32 - 34°C, maintained by an in-line solution heater (TC-324; Warner Instruments). Cells were visualized under 60X water-immersion objective with an upright microscope with infrared illumination. The image from the microscope was enhanced using a CCD camera and a camera controller (C2741-62; Hamamatsu), and ultimately displayed on a computer monitor (Fig. 3.3). DR neurons selected for recordings were located on the midline, which is identified the translucent area between the medial longitudinal fasciculus and the aqueduct, and ventral to the aqueduct. Only neurons that exhibited membrane properties typical of putative 5-HT neurons were included in this study (Haj-Dahmane and Shen, 2009; Gocho et al., 2013; Levitt et al., 2013). The recorded neurons, apart from being in the midline, had a large cell body and met the previously published properties of 5-HT cells (see results section). Schematic illustration of the patch-clamp electrophysiological procedure is shown in figure 3.4.

Figure 3.3. Microphotograph (60X magnification) illustrating a DR cell being recorded. The recording pipette patching the cell is also shown.

A visualized cell was approached with the electrode, a GΩ seal established, and the cell membrane ruptured to obtain a whole-cell recording. Patch-clamp recordings made in current or voltage-clamp mode (V_h = -70 mV) were detected with a Multiclamp 700B amplifier. Signals were then digitized by Digidata 1440A analog-to-digital converter, and data were acquired and stored on-line using pClamp 10 software (all from Molecular Devices) (sampled at 10 kHz, filtered at 5 kHz). Recording pipettes pulled from glass capillaries (1.7–3 MΩ; World Precision Instruments) were used for all the experiments.

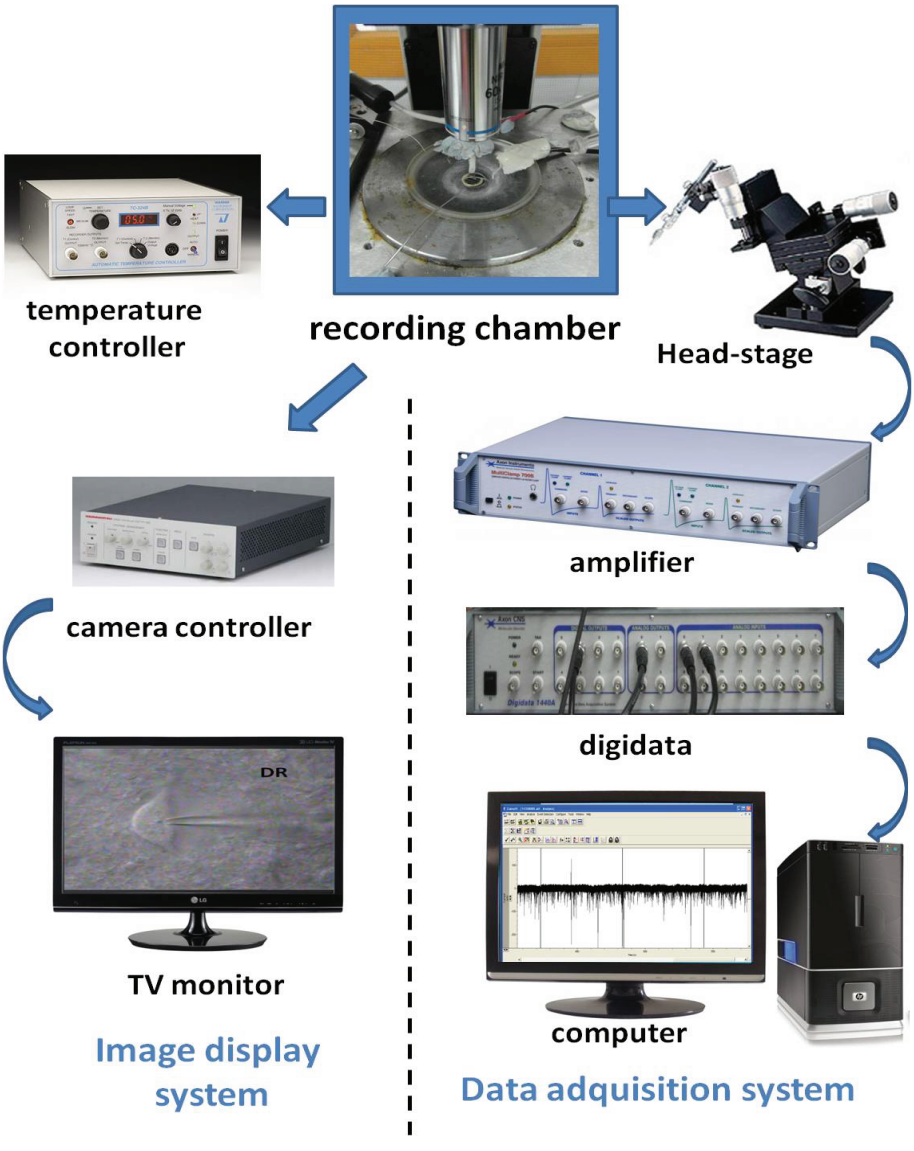

Figure 3.4. Schematic illustration of the patch-clamp procedure carried out in mouse DR slices. Briefly, data from the recordings were acquired using a Multiclamp 700B amplifier, digitized with a digidata, and stored on-line using the pClamp 10 software (all from Molecular Devices). To visualize the cells, the image from the microscope was enhanced with a CCD camera and a camera controller ,and displayed on a TV monitor.

Materials and methods

To record the electrophysiological intrinsic membrane properties, characteristics of action potentials, and 5-CT- and baclofen-induced currents recording pipettes were filled with internal solution containing the following (in mM): 130 K-Gluconate, 5 NaCl, 1 $MgCl_2$, 1 EGTA, 10 HEPES (K), 2 Mg-ATP, 0.5 Na-GTP and 10 Na_2-phosphocreatine (pH: 7.3 - 7.4, 280 mOsm). Series resistance was not compensated and was monitored with a 5 mV depolarizing steps (200 ms) given every 60 s to ensure sufficient and stable electrical access to the cell throughout the experiments (<15 MΩ for inclusion). Immediately after gaining access to the cell, membrane capacitance and input resistance were measured using the Clampex application of pClamp 10 software. In some experiments the resting membrane potential (V_m) was also recorded (I = 0). Afterwards, in current-clamp mode firing rate and active electrophysiological properties were measured by current injection (50 – 200 pA, 2 s). For current-voltage (I/V) analysis voltage steps were applied. With this protocol the presence of an inwardly rectifying potassium current was detected by a typical current-voltage relationship obtained when the membrane potential was hyperpolarized from - 60 to -140 mV in -10 mV increments (100 ms per step) (Williams et al., 1982). Activation of GIRK currents induced by 5-CT and baclofen was also detected using the I/V protocol before and during drug administration.

Junction potential between the pipette internal solution and the ACSF was ~ 15 mV and was not corrected. Slices used for recording were discarded after each experimental procedure, and no recording was performed more than 6 h after animal's decapitation.

- **Recordings of inhibitory postsynaptic currents**

In order to study the spontaneous inhibitory postsynaptic currents (sIPSCs) and the evoked inhibitory postsynaptic currents (eIPSCs) we added DNQX (10 μM) to the external solution (ACSF) to block AMPA/kainate receptors. Recording electrodes were filled with the following internal solution (in mM): 70 K-Gluconate, 70 KCl, 2 NaCl, 4 EGTA, 10 HEPES (K), 4 Mg-ATP, and 0.3 Na-GTP (pH: 7.3 - 7.4, 280 mOsm). To analyze sIPSCs, we voltage-clamped the cells at – 70 mV and the spontaneous activity of the cells was recorded for at least 3 min once the recording was steady and stable. To evoke eIPSCs,a monopolar stimulating electrode was positioned 100 - 200 μm dorsolateral to the cell being recorded and pairs of electrical stimuli (100 μs at 20 Hz, interpulse interval 100 ms, interpair interval 20 s) were delivered with an Iso-Flex stimulus isolator (A.M.P.I.). In some cells (in both spontaneous and evoked IPSC experiments), the $GABA_A$ receptor mediation of IPSC was verified at the end of the experiment with the addition of the $GABA_A$ receptor antagonist picrotoxin (100 μM).

- **Recordings of excitatory postsynaptic currents**

To isolate the spontaneous excitatory postsynaptic currents (sEPSCs) and the evoked inhibitory postsynaptic currents (eEPSCs) picrotoxin (100 μM) was added in the ACSF to block $GABA_A$ receptors. Glass pipettes were filled with an internal solution containing (in mM): 70 Cs_2SO_4, 20 CsCl, 20 NaCl, 15 $MgCl_2$, 5 HEPES (K), 1 EGTA, 2 Mg-ATP and 0.5 Na-GTP (pH: 7.3 - 7.4, 280 mOsm). To study the sEPSCs, we recorded the spontaneous activity of the cells (V_h = – 70 mV) for at least 3 min, once the recording was steady and stable. To evoke eEPSCs, holding potential was held at + 40 mV in order to evoke both AMPA receptor- and NMDA receptor- mediated eEPSCs (AMPAR-eEPSCs and NMDAR-eEPSCs, respectively). A single electrical stimulus (100 μs at 10

Hz) (Iso-Flex stimulus isolator, A.M.P.I.) was applied every 30 s using a monopolar stimulating electrode positioned 100 - 200 μm dorsolateral to the cell being recorded. Once the evoked events were stable, the NMDA receptor antagonist D-AP5 (50 μM) was applied during 5-7 min in order to isolate AMPA-eEPSCs and calculate the AMPA/NMDA ratio. In some cells (in both spontaenous and evoked EPSC experiments), the AMPA receptor mediation of EPSC was verified at the end of the experiment with the addition of the AMPA/kainate receptor antagonist DNQX (10 μM). Under these conditions, DNQX eliminated all EPSC activity (for example, see Fig. 4.21A).

3.2.2. 8-OH-DPAT-induced hypothermia

Animals were singly housed in clean cages 1 h before testing. Body temperature was assessed intrarectally, inserting a lubricated probe (BIO-BRET-3, Cibertec, Spain) approximately 2 cm and monitored with a digital thermometer (CITEC, Cibertec, Spain). Three baseline body temperature measurements were taken as a control value before drug administration. 10 min after the third baseline measurement, animals received 8-OH-DPAT (0.5 mg/kg i.p.) or 0.9% physiological saline (i.p.) in equivalent volumes, and body temperature was monitored and measured the subsequent 10, 20, 30 and 60 min.

3.2.3. Behavioral tests

All tests were performed between 9:00 and 13:00 h. Mice were transferred to a noise free and temperature-controlled testing room at least 1 h before the tests for environmental habituation. No more than one test was performed in each mouse.

3.2.3.1. Novelty suppressed feeding test

The novelty suppressed feeding test (NSFT) is a conflict test that elicits competing motivations between the drive to eat and the fear of venturing into the center of brightly lit arena. The NSFT was performed as previously

described (Santarelli et al., 2003). Briefly, animals were food-deprived 24 h prior to the test (water *ad libitum*). The testing apparatus consisted of a plastic box (45x45x20 cm) with wooden bedding covered floor (approximately 2 cm) illuminated by a 70W lamp and with a white paper platform where a food pellet was placed in the centre. Mice were tested individually, placing them in the corner of the box and a stopwatch was immediately started. The test was carried out during 10 min and the latency to eat was timed. Only one mouse was studied at each time. Afterwards, animals were transferred to their home cages and the amount of food consumed by each mouse in the subsequent 5 min was measured as a control for change in appetite as a possible confounding factor.

3.2.3.2. Tail suspension test

In the tail suspension test (TST) mice were suspended 60 cm from the surface and secured by adhesive tape placed approximately 2 cm from the tip of the tail. Animals, both acoustically and visually isolated, were monitored by video camera for subsequent blind analysis. The total duration of the test was 6 min, and mice were considered immobile when they stood completely motionless or hung passively. A decreased immobility time is considered an antidepressant-like activity according to Cryan et al. (2005). Intraperitoneal administration of citalopram (10 mg/kg) was carried out 30 min prior to the experiment in the same testing room. When the effect of citalopram was tested in a group of animals, another group of mice was injected with 0.9% saline in identical time and volume as a control group.

3.2.4. Immunohistochemistry procedures

3.2.4.1. Fixation and tissue processing

Male adult mice (n = 6 - 10/group) were anesthetized with an intraperitoneal injection of sodium pentobarbital (200 mg/kg). Animals were perfused through the aortic arch with 3.75 % acrolein (25 mL, TAAB, UK) in a

solution of 2 % paraformaldehyde and 0.1 M phosphate buffer (PB) pH 7.4, followed by 2 % paraformaldehyde (75 mL). Brains were removed and cut into coronal blocks that were post-fixed in 2 % paraformaldehyde for 24 h and kept in 0.1 M PB pH 7.4. Coronal sections were cut into 40 μm thickness using a vibrating microtome (VT1000 S, Leica, Milton Keynes, UK). Free floating sections in 0.1 M PB pH 7.4, were collected and stored in cryoprotectant solution containing 25% sucrose and 3.5% glycerol in 0.05 M PB, pH 7.4. Coronal sections at levels -1.34 mm/ -2.30 mm posterior to bregma and 1.18 mm/ 0.26 mm anterior to bregma from hippocampus (HPP) and subventricular zone (SVZ), respectively, were selected for immunohistochemistry according to the stereotaxic mouse brain atlas of Franklin and Paxinos (1997).

3.2.4.2. Antibodies

A polyclonal affinity-purified rabbit antibody raised against phosphorylated Histone H3 (HH3) and a monoclonal mouse antiserum generated against glial fibrillary acidic protein (GFAP) from pig spinal cord were used for the determination of proliferating cells and glia. We determined the number of proliferating cells by the presence of HH3 that were not co-localized with GFAP to exclude glial phenotype. A series of control experiments were previously performed to asses for the non-specific background labeling or cross reactivity between antibodies derived from different host species. Furthermore, omission of primary and/ or secondary antibodies resulted in a total absence of target labeling (Rodriguez et al., 2008; Rodriguez et al., 2009).

3.2.4.3. Immunohistochemistry

To minimize methodological variability, sections containing HPP and SVZ from both hemispheres of all animals were processed at the same time using precisely the same experimental conditions. For this procedure, as previously reported (Rodriguez et al., 2008; Rodriguez et al., 2009), the sections

were first incubated for 30 min in 30% methanol in 0.1 M PB and 30% hydrogen peroxide (H_2O_2). Sections were then rinsed with 0.1 M PB for 5 min and placed in 1% sodium borohydride for 30 min. The sections were then profusely washed with 0.1 M PB before rinsing in 0.1 M Trizma base saline (TS) for 10 min. Brain sections were then incubated in 0.5% bovine serum albumin, in 0.1 M TS and 0.25% Triton X-for 30 min. Sections were incubated for 68 h at room temperature in 0.1% bovine serum albumin, in 0.1 M TS and 0.25% Triton X-100 containing rabbit polyclonal antiserum for HH3 (1:1000) and mouse monoclonal antiserum for GFAP (1:60000). After the incubation, sections were rinsed in 0.1 M TS for 30 min. Subsequently, the HH3 and GFAP antibodies were detected in a sequential manner on the same sections. For HH3 labeling, sections were placed in 0.1 M TS and 0.25% Triton X-100 containing (1) 1:400 dilutions of biotinylated donkey anti-rabbit IgG (Jackson Immunoresearch, Stratech Scientific Ltd., Soham, UK) for 1 h at room temperature and (2) avidin-bioctin peroxidase complex for 30 min at room temperature. The peroxidase reaction product was visualized in a solution prepared from SGZ kits for 2-3 min. For GFAP labeling, sections were the rinsed again in 0.1 M TS for 30 min and incubated in 0.1 M TS and 0.25% Triton X-100 containing (1) 1:400 dilution of biotinylated horse anti-mouse IgG (Vector Laboratories, Peterborough, UK) for 1 h at room temperature and (2) avidin-biocytin peroxidase complex for 30 min at room temperature. The GFAP peroxidase reaction was visualized by incubation in a solution containing 0.022% 3,3´diaminobenzidine (DAB) and 0.003% H_2O_2 for 1-2 min. With this procedure, the GFAP labeling was seen in brown, allowing us to differentiate it from the HH3 labeled cells (blue). After stopping the reaction by rinsing the sections in 0.1 M TS for 5 min followed by 0.1 M PB for 15 min, sections were mounted onto gelatinized slides and allowed to dry overnight. Sections were then dehydrated in increasing concentrations of ethanol (50%, 70%, 80%, 90%, 95% and 100%) and finally, xylene. Coverslips were applied using Entellan and slides were left overnight before counting.

3.2.4.4. Cell quantification

The number of HH3-immunoreactive neurons and HH3/GFAP co-localized cells was determined by counting the labeled cells in both hemispheres in coronal sections taken through representative sections of *dentate gyrus* (DG) of the HPP, and of the SVZ, at levels previously mentioned. Cells were counted and images obtained using light microscopy (Nikon Eclipse 80i). The number of HH3 positive cells and the area measurements of the DG and SVZ, bounded by the lateral ventricles, *corpus callosum* and *caudate-putamen nucleus*, were determined blindly to ensure consistency and reproducibility.

3.2.5. Western Blotting

Fresh tissue samples from the DR region were collected at 30 min and 24 h after injection of the ketamine 30 mg/kg (i.p.) or vehicle (0.9% saline). All the samples were homogenized in 25 mM Tris-HCl (pH 7.4) and 0.32 M sucrose, supplemented with a phosphatase and protease inhibitor cocktails (Sigma Chemical Co., Spain). To detect the proteins in the tissue homogenates, equal amounts of protein (30 μg) were separated in SDS-PAGE gels and then transferred to a polyvinylidene difluoride membrane (BioRad Laboratories). After washing in Tris-buffered saline containing 0.1% Tween-20 (TBST), the blots were blocked with 5% bovine serum albumin (Sigma) in TBST and incubated overnight at 4°C in rabbit anti-phospho-mTOR (Ser2448), rabbit anti-phospho-mTOR (Ser2481), rabbit anti-mTOR, rabbit anti-Raptor, rabbit anti-GβL (1:1000; Cell Signaling Technology) and rabbit anti-β-actin (1:250000; Sigma-Aldrich) antibodies diluted in 5% bovine serum albumin–TBST.

After thorough washing, these primary antibodies were detected by incubating for 1h at room temperature with IRDye 800CW goat anti-rabbit secondary antibody (1:10000; LI-COR Biosciences). After three final washes with TBST, the antibody binding was detected by using a LI-COR Odyssey two-channel quantitative fluorescence imaging system (LI-COR Biosciences).

Digital images of Western blots were analyzed by densitometry using the ImageJ free access software (National Institutes of Health, Bethesda, MD). The data from immunoblottings assays were normalized against β-actin. No protein bands were detected when the primary antibody was omitted.

3.2.6. Data and statistical analysis

Statistical analyses were performed using the GraphPad Prism Software (v.5.01; GraphPad Software Inc., USA).

3.2.6.1. Analysis of the *in vivo* electrophysiological data

The analysis of the *in vivo* electrophysiological data was carried out by means of the software Spike2 (Cambridge Electronic Design, UK). The following parameters were estimated:

A. Firing rate: Defined as the number of neuronal discharges per second. Data were represented in a bar histogram that showed the mean firing rate each 10 s. Basal firing rate was recorded for 180 s and mean firing rate after drug administration for 60 - 300 s (depending on *plateau* effect for each dose of drug).

B. Coefficient of variation: This parameter is related to the interval between consecutive discharges (inter-spike interval) and gives an idea of the regularity of the firing. The representation of the inter-spike interval histogram followed by the analysis ran by Spike 2 (script meaninx.s2s) led to the numerical value. Data was represented in percentage, as the division between the standard deviation and the mean value. The recording period analyzed (3 min) was the same as that one used for the analysis of the firing rate.

C. Burst spikes: Some neurons of the DR show burst firing activity (first interspike interval $\leq$ 20 ms ; termination interspike interval $\geq$ 160 ms). In those neurons the firing rate, number of burst, percentage of spikes in burst and

mean spikes per burst was analyzed. The analysis of the burst firing was performed using the Spike 2 software (script w_burst.s2s) in the same period as the previous parameters.

D. Dose-effect curve: Dose - effect curves were analyzed for the best non-linear fit to a logistic three-parameter equation (Parker and Waud, 1971) as described previously (Miguelez et al., 2009).

The following equation was used:

$$E= E_{max} [A]^n / (ED^n_{50}+ [A]^n),$$

Where [A] is the concentration of the drug, E is the effect on the firing rate induced by A, E_{max} is the maximal effect, ED_{50} is the effective dose for eliciting 50 % of the E_{max} and n is the slope factor of the dose-response curve. Extra sum-of-squares F test (GraphPad Prism Software, San Diego, USA) was used for statistical comparison of the response to a drug in dose-response curves and for comparison of ED_{50} among groups.

Spontaneous firing rate and coefficient of variation were analyzed in selected pair comparisons using two-tailed unpaired t-test. Two-sided χ^2 analysis of contingency tables was used to evaluate differences in the percentage of neurons presenting burst firing. Other parameters derived from burst pattern were analyzed by the non-parametric Kruskal-Wallis test followed by Dunn's post-hoc test. The level of significance was considered as $p < 0.05$.

3.2.6.2. Analysis of the *in vitro* electrophysiological data

Recordings were post-hoc filtered at 1 kHz and visually inspected. Analyses were carried out off-line using Clampfit application of pClamp 10 software.

Electrophysiological intrinsic membrane properties (membrane capacitance, input resistance and resting membrane potential) were measured immediately after gaining access to the cell. A period of 1 s was taken for the analysis of the electrophysiological properties of action potentials at each current injection step (50 - 200 pA, 2 s steps). To this end a semi-automated sliding event detection procedure was used (Clampfit 10.3 software). We measured the frequency of the spikes at each current step, as well as parameters derived from the action potential (AP) waveform (AP threshold and AP amplitude) and AP kinetic parameters (AP half-width, AP rise time, and AP decay time) at the minimum depolarizing current injection (50 pA).

To calculate the effect of 5-CT, baclofen, and GABA on DR cells, the amplitude of the currents induced by these drugs was measured when the maximal effect was reached, only in those cells where there was a complete washout after drug perfusion.

One minute period was taken for off-line analysis of the spontaneous activity. Frequency, amplitude, and half-width of the events were analyzed. Single peak spontaneous synaptic currents were detected using a semi-automated sliding template detection procedure (Clampfit 10.3 software). The template was generated by averaging multiple spontaneous currents (different templates for sIPSCs and sEPSCs), and the selection was fitted to 4 threshold of the template. Each detected event was visually inspected and discarded if the amplitude was < 7 pA.

Materials and methods

Duration of synaptic events was determined by measuring the width at 50 % of the peak amplitude (half-width).

The amplitude of eIPSCs and eEPSCs was calculated by measuring the average current at the peak of each evoked event and subtracted from the current obtained during the 10 ms window taken immediately before the stimulus artifact. Other parameters such as half-width and decay time (calculated from 10 to 90 % of the decay phase) of the evoked currents were also inspected.

To analyze the eIPSCs, paired stimuli were given at 20 s intervals (interpulse interval 100 ms), and the ratios of the amplitudes of the second and the first eIPSC were averaged for at least 10 trials (200 s). By analyzing the paired pulse ratio we studied if there was a paired-pulse facilitation or depression pattern in each DR cell, which is related to changes in the probability of GABA release (Bonci and Williams, 1997). Decay time and half-width of eIPSCs were also inspected.

To analyze the eEPSCs, a total of 30 evoked synaptic currents were recorded (15 min) before the application of D-AP5 (50 μM). Glutamatergic total response and AMPA-eEPSCs were calculated from the average of 5 consecutive events. NMDA-eEPSCs was calculated by subtraction of AMPA receptors-mediated response to total eEPSCs. Peak currents of isolated AMPA- and NMDA-eEPSC were used to calculate the AMPA/NMDA ratio.

When possible, data were compared through groups by one-way analysis of variance (ANOVA) followed by Newman-Keuls post-hoc test, otherwise two-tailed t-test (paired or unpaired t-test according to the data). Repeated measures one-way ANOVA followed by Newman-Keuls post-hoc test was also used in some cases. Two-sided χ^2 analysis of contingency tables was used to evaluate differences in the percentage of neurons presenting paired-pulse facilitation. The level of significance was considered as $p < 0.05$.

3.2.6.3. Analysis of the behavioral, immunohistochemical, hypothermic response, and western blotting data

In the NSFT the latency to eat (s) was measured over a total duration of 10 min. Scoring for the measure of interest did not begin until the mouse reached for the food with its forepaws and began eating. Afterwards, the amount of food consumed (g) during 5 min was measured.

In the TST the immobility time (s) was measured over a 6 min period. To investigate the effect induced by citalopram on the immobility time we calculated the immobility time reduction. Data was presented in percentage, as the division between the immobility time after citalopram injection for each individual mouse and the mean basal immobility time value obtained in its group.

Data compiled from the TST, immunohistochemical and western blotting experiments were compared through groups by one-way ANOVA followed by Newman-Keuls post-hoc test. For the analysis of the latency to eat obtained from the NSFT Kruskal-Wallis nonparametric test followed by Dunn's post-hoc test was used. For the 8-OH-DPAT hypothermic response analysis, two-way ANOVA followed by Bonferroni post-hoc test was used for statistical comparison among genotypes. The level of significance was considered as $p < 0.05$.

4. RESULTS

4.1. STUDY I: Deletion of GIRK2 subunit of GIRK channels alters the 5-HT_{1A} receptor-mediated signaling and results in a depression- resistant behavior

4. RESULTS

4.1. STUDY I: Deletion of GIRK2 subunit of GIRK channels alters the 5-HT_{1A} receptor-mediated signaling and results in a depression-resistant behavior

4.1.1. Electrophysiological properties of *dorsal raphe* neurons of GIRK2 mutant mice

To examine the contribution of GIRK2 subunit-containing GIRK channels to the spontaneous activity of *dorsal raphe* (DR) neurons, the firing pattern in GIRK2 mutant mice was studied (firing rate, coefficient of variation and burst activity).

All neurons recorded from wild-type (WT n = 86), GIRK2 heterozygous ($GIRK2^{+/-}$ n = 79), and GIRK2 homozygous mice ($GIRK2^{-/-}$ n = 45) fitted the standard criteria previously mentioned (see methods section 3.2.1.1.).

Spontaneous firing rate of DR neurons in $GIRK2^{-/-}$ mice was higher than in wild-type (1.99 ± 0.15 Hz, n = 45; 1.68 ± 0.08 Hz, n = 86; for $GIRK2^{-/-}$ and WT mice, respectively. $p < 0.05$, unpaired two-tailed t-test). No changes were seen either in the coefficient of variation or in the burst activity among the groups (Table 4.1). A more extended study of the burst pattern done by analyzing the mean firing rate, number of bursts, the percentage of spikes firing in bursts, and mean spikes in burst showed no differences among groups.

Next, the effect of the high affinity GIRK channel blocker, tertiapin-Q (100 pmol, i.c.v.) (Jin and Lu, 1998; Kanjhan et al., 2005) on the electrophysiological properties of DR neurons was assessed. The firing rate of DR neurons in tertiapin-Q-injected wild-type mice (WT TPN-Q) was statistically higher (38 %) than in wild-type group (WT TPN-Q: 2.32 ± 0.27 Hz, n = 15 and WT: 1.68 ± 0.08 Hz, n = 86. $p < 0.001$, unpaired two-tailed t-test).

Results

However, no significant changes were seen either in the coefficient of variation or in any of the burst parameters, compared to wild-type mice. In order to clarify if the intracerebroventricular injection was producing an effect by itself, an intracerebroventricular ACSF-injected WT group was added as a control. No differences were observed in firing rate (1.80 ± 0.27 Hz, $n = 7$), coefficient of variation (35.13 ± 4.42 %, $n = 7$) or number of burst firing neurons (14 %) in this group compared to wild-type (data not shown).

Table 4.1. *In vivo* electrophysiological properties of *dorsal raphe* neurons recorded under basal conditions in wild-type and GIRK2 mutant mice

	WT (*n*=86)	GIRK2$^{+/-}$ (*n*=79)	GIRK2$^{-/-}$ (*n*=45)	WT TPN-Q (*n*=15)
Firing rate (Hz)	1.68±0.08	1.88±0.09	1.99±0.15*	2.33±0.27**
Coefficient of variation (%)	37.64±1.21	36.57±1.21	35.21±1.54	40.38±3.25
Burst firing neurons (%)	7	5	2	13
- Firing rate (Hz)	2.22±0.36	2.01±0.37	4.03	1.49±0.38
- Number of burst	1.33±0.21	4.33±1.85	1.00	2.5±1.50
- Spikes in burst (%)	1.15±0.46	1.01±0.87	0.41	2.8±1.32
- Mean spikes per burst	3.00±0.81	2.00	2.00	3.50±0.50

Each cell was recorded for at least 3 min (180 seconds were taken for subsequent analysis). All data are presented as the mean ± S.E.M of *n* experiments. WT: wild-type; GIRK2$^{+/-}$: GIRK2 heterozygous mice; GIRK2$^{-/-}$: GIRK2 homozygous mice. WT TPN-Q: tertiapin-Q-injected WT mice. $^{*}p < 0.05$ and $^{**}p < 0.01$ *vs* WT, unpaired two-tailed t-test.

4.1.2. Effect of *Girk2* gene deletion on the 5-HT_{1A} receptor-mediated inhibition of *dorsal raphe* neuronal activity

To investigate the role of GIRK2 subunit in the 5-HT_{1A} receptor-mediated signaling, we compared the inhibitory effect of cumulative increasing doses of the 5-HT_{1A} receptor agonist, 8-OH-DPAT (12.5 - 300 µg/kg, i.p.) onto firing rate of DR neurons of wild-type and GIRK2 mutant mice. In all the groups, 8-OH-DPAT caused a progressive and dose-dependent inhibition of the firing rate (Fig. 4.1A, B). In $GIRK2^{+/-}$ mice, the dose-response curve was shifted to the right, so that the ED_{50} mean value was significantly higher than the one obtained in wild-type mice (ED_{50}: 42.15 ± 2.89 µg/kg, n = 8; ED_{50}: 34.93 ± 3.41 µg/kg, n = 15, for $GIRK2^{+/-}$ mice and WT, respectively. $p < 0.05$, nonlinear fit analysis, extra sum-of-squares F test). In $GIRK2^{-/-}$ mice, the shift in the dose-response curve was even greater and so ED_{50} mean value increased 2-fold compared to wild-type mice ($ED_{50:}$ 69.50 ± 8.57 µg/kg, n = 5. $p < 0.01$, nonlinear fit analysis, extra sum-of-squares F test) (Fig. 4.1C). The following administration of the 5-HT_{1A} receptor antagonist, WAY100635 (1 - 1.5 mg/kg, i.p.), completely recovered the firing activity in the three groups (WT: 86.22 ± 7.04 %, n = 13; $GIRK2^{+/-}$: 92.54 ± 12.98 %, n = 6; $GIRK2^{-/-}$: 122.20 ± 23.27 %, n = 3). No significant differences were found among the groups.

Next, the sensitivity of the 5-HT_{1A} receptor to the SSRI citalopram (0.5-3 mg/kg, i.p.), in GIRK2 mutant groups was evaluated. For this purpose, citalopram dose-response curves obtained from GIRK2 mutant mice were compared to those obtained in wild-type mice. In all the groups, cumulative doses of citalopram caused a progressive and dose-dependent inhibition of the firing rate. However, citalopram showed less potency inhibiting DR neurons in $GIRK2^{-/-}$ mice, so that ED_{50} mean value for this group was significantly greater than the values obtained for $GIRK2^{+/-}$ and wild-type mice (ED_{50}: 1.36 ± 0.04 mg/kg, n = 6; ED_{50}: 1.04 ± 0.04 mg/kg, n = 7; ED_{50}: 0.97 ± 0.03 mg/kg, n = 13,

for GIRK2$^{-/-}$, GIRK2$^{+/-}$, and WT mice, respectively. $p < 0.0001$, nonlinear fit analysis, extra sum-of-squares F test) (Fig. 4.1D).

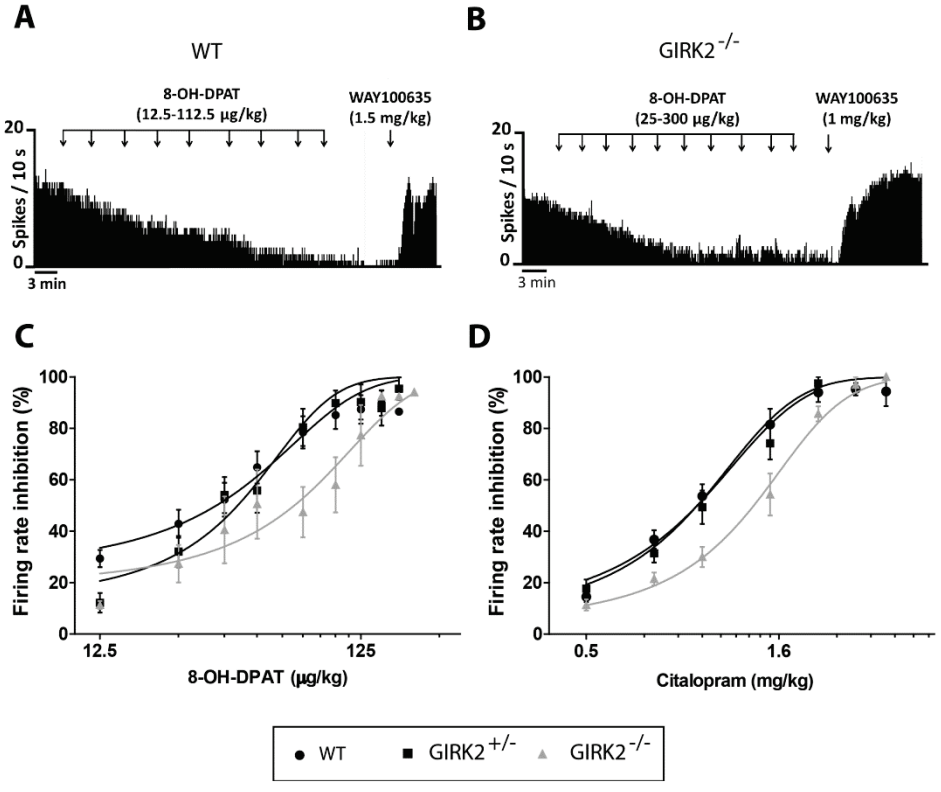

Figure 4.1. The inhibitory effect of 8-OH-DPAT and citalopram on the firing rate of *dorsal raphe* neurons in wild-type and GIRK2 mutant mice. (A) Representative firing rate histograms illustrate the inhibitory effect of 8-OH-DPAT (12.5 - 300 µg/kg, i.p.) on *dorsal raphe* (DR) basal activity in wild-type (WT) and (B) GIRK2$^{-/-}$ mice. Following adminitration of the 5-HT$_{1A}$ receptor antagonist WAY100635 (1-1.5 mg/kg, i.p.) completely reversed the 8-OH-DPAT-induced inhibitory effect. (C) Dose-response curves for 8-OHDPAT and (D) citalopram (0.5 - 3 mg/kg, i.p.) on DR firing rate in WT, GIRK2$^{+/-}$ and GIRK2$^{-/-}$ mice. Each point represents the mean ± S.E.M. of *n* experiments (*n* = 5 - 15 mice/group).

4.1.3. Effect of WAY100635 on the citalopram inhibitory effect in *dorsal raphe* neurons of wild-type and GIRK2$^{+/-}$ mice

In addition, we wanted to assess if the inhibitory effect of citalopram was mediated through 5-HT$_{1A}$ receptors. For this purpose, we performed experiments where we first blocked the 5-HT$_{1A}$ receptor with the 5-HT$_{1A}$ receptor antagonist WAY100635 (25 μg/kg, i.p.), and recorded the firing rate for 10 min to observe whether the antagonist was altering the firing rate of DR neurons. After this, the inhibitory effect of two different doses of citalopram was studied in wild-type and GIRK2$^{+/-}$ mice. The doses were those corresponding to the ED$_{50}$ and Emax mean values previously obtained for each group.

First, we observed that the administration of WAY100635 did not alter the firing rate of DR neurons in wild-type (Before WAY: 2.83 ± 0.41 Hz; After WAY: 3.26 ± 0.59 Hz, n = 7) or in GIRK2$^{+/-}$ mice (Before WAY: 2.60 ± 0.27 Hz; After WAY: 2.44 ± 0.36 Hz, n = 10) (Fig. 4.2A). Additionally, WAY100635 attenuated the inhibitory effect produced by citalopram on the firing rate of DR neurons in both groups (Fig. 4.2B). In wild-type mice in the presence of WAY100635, the inhibitory effect of citalopram (1 mg/kg, i.p.; ED$_{50}$ value for this group) was significantly smaller (11.84 ± 1.99 %, n = 5) than that obtained in the absence of WAY100635 (53.63 ± 4.67 %, n = 10) (p < 0.0001, unpaired two-tailed t-test). Similarly, in GIRK2$^{+/-}$ mice in the presence of WAY100635, the inhibitory effect of citalopram (1 mg/kg, i.p.; ED$_{50}$ value for this group) was statistically smaller (15.97 ± 5.94 % n = 7) than that obtained in the absence of WAY100635 (49.36 ± 6.50 %, n = 5) (p < 0.01, unpaired two-tailed t-test). However, in wild-type the firing rate inhibition obtained with the E$_{max}$ dose (1.5 mg/kg, i.p.) in the presence of WAY100635 (74.86 ± 11.75 %, n = 7) was smaller, but not statistically different, than that obtained in the absence of WAY100635 (81.51 ± 6.15 %, n = 11). In GIRK2$^{+/-}$ mice the firing rate inhibition obtained with the dose of citalopram

corresponding to the E_{max} value for this group (2 mg/kg, i.p.) was statistically smaller in the presence of WAY100635 (53.24 ±7.82 %, n = 7) than that obtained in the absence of WAY100635 (97.16 ± 2.54 %, n = 3) ($p < 0.01$, unpaired two-tailed t-test).

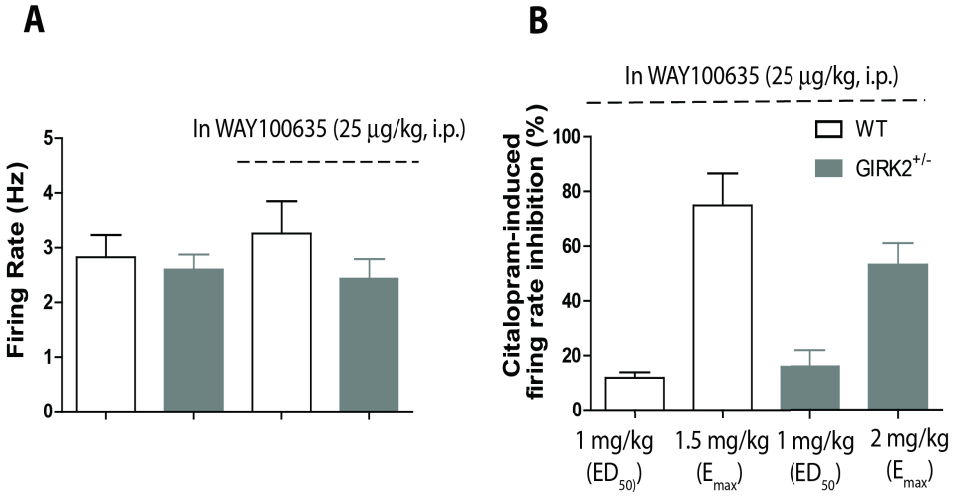

Figure 4.2. Effect of WAY100635 on the firing rate and citalopram-induced inhibitory effect of *dorsal raphe* neurons in wild-type and GIRK2$^{+/-}$ mice. (A) Bar graphs showing that WAY100635 (25 µg/kg, i.p.) had no effect in the firing rate of *dorsal raphe* neurons in wild-type (WT) and GIRK2$^{+/-}$ mice. (B). Bar graphs showing that the blockade of the 5-HT_{1A} receptor with WAY100635 decreased the inhibitory effect of the of citalopram in both groups. Bars represent means ± S.E.M. of n expermiments (n = 10 - 3 cells/group).

4.1.4. Effect of pharmacological blockade of GIRK channels on the citalopram-induced inhibition of *dorsal raphe* neuronal activity

To further investigate the 5-HT_{1A}-GIRK signaling pathway, we performed a pharmacological blockade of GIRK channels with tertiapin-Q and the sensitivity of the 5-HT_{1A} receptor to the effect of citalopram was evaluated in this group. For this purpose, we studied the inhibitory effect of citalopram on WT TPN-Q mice and also on the wild-type control group (ACSF-injected group, WT control). In both groups, citalopram (0.5-3 mg/kg, i.p) caused a progressive and dose-dependent inhibition of the firing rate (Fig. 4.3A, B), but showed less potency inhibiting DR neurons in WT TPN-Q so that ED_{50} mean value for this group was significantly greater than the value obtained for WT control (ED_{50}: 1.25 ± 0.04 mg/kg, n = 5; ED_{50}: 0.99 ± 0.06 mg/kg, n = 4 for WT TPN-Q and WT control, respectively. $p < 0.0001$, nonlinear fit analysis, extra sum-of-squares F test) (Fig. 4.3C). Interestingly, ED_{50} mean values were similar between $GIRK2^{-/-}$ mice and WT TPN-Q, indicating that citalopram had the same potency in both groups (ED_{50}: 1.25 ± 0.04 mg/kg, n = 5; ED_{50}: 1.36 ± 0.04 mg/kg, n = 6; for WT TPN-Q and $GIRK2^{-/-}$ mice, respectively). As expected, WT control showed similar ED_{50} values to the WT group.

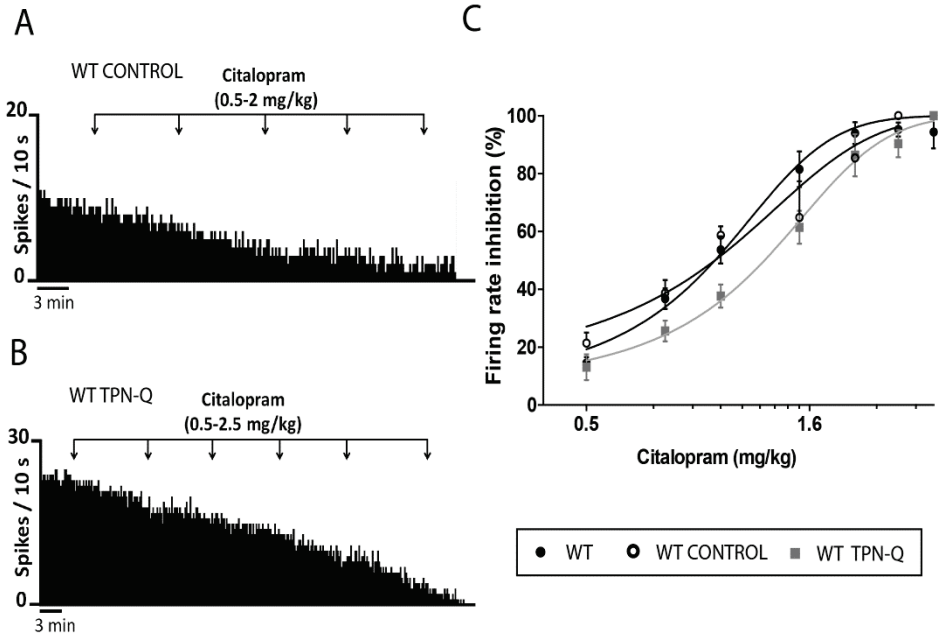

Figure 4.3. The inhibitory effect of citalopram on the firing rate of *dorsal raphe* neurons in wild-type and tertiapin-Q injected mice. (A) Representative firing rate histograms illustrate the inhibitory effect of citalopram (0.5 - 2.5 mg/kg, i.p.) on *dorsal raphe* (DR) basal activity in artificial cerebrospinal fluid-injected mice (WT control, i.c.v.) and (B) tertiapin-Q injected mice (WT TPN-Q, 100 pmol, i.c.v.). (C) Dose-response curves for citalopram (0.5 - 3 mg/kg, i.p.) on DR firing rate in wild-type (WT), WT control, and WT TPN-Q. Each point represents the mean ± S.E.M. of *n* experiments (*n* = 4 - 5 mice/group).

4.1.5. Characterization of 8-OH-DPAT-induced hypothermia in GIRK2 mutant mice

To further study the functional status of 5-HT_{1A} receptors in GIRK2 mutant mice, we evaluated the 8-OH-DPAT-induced hypothermic response. In all the groups, 8-OH-DPAT (0.5 mg/kg, i.p.) caused a decrease in temperature (n = 6-7 per group). $GIRK2^{-/-}$ mice showed a reduced 8-OH-DPAT-induced hypothermia in every different time point, compared to wild-type mice. A two-way ANOVA revealed that in the minute 30, the temperature decrease induced by 8-OH-DPAT was significantly smaller in $GIRK2^{-/-}$ mice compared to wild-type ([$F(2,68) = 10.30$, $p < 0.05$]) (Fig. 4.4). In addition, another three groups of $GIRK2^{+/-}$, $GIRK2^{-/-}$, and wild-type mice were injected with 0.9% saline (saline groups, i.p.), in order to check if the manipulation of the animals or the intraperitoneal injection were causing an effect on the response. No significant changes in the temperature were observed in these groups.

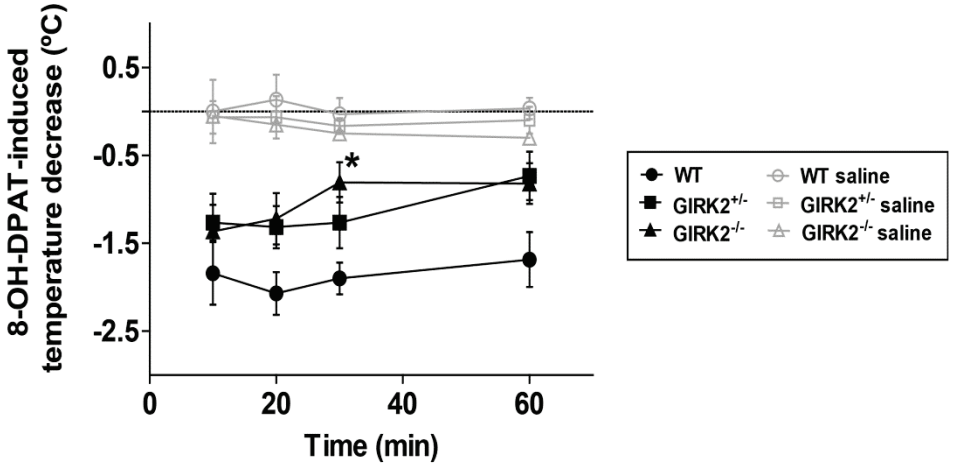

Figure 4.4. The hypothermic response induced by 8-OH-DPAT in wild-type and GIRK2 mutant mice. The temperature decrease induced by 8-OH-DPAT (0.5 mg/kg, i.p.) was significantly lower in GIRK2$^{-/-}$ mice relative to wild-type (WT) in minute 30. Mice of each genotype injected with 0.9% saline (saline groups) were used as controls. Each point represents the mean ± S.E.M of *n* animals (*n* = 6 - 7 mice/group; $^{*}p < 0.05$ *vs* WT, two-way ANOVA followed by Bonferroni post-hoc test).

4.1.6. Behavioral characterization of GIRK2 mutant mice and the response to citalopram

To evaluate whether GIRK2 subunit ablation impacts on depressive-related behavior, GIRK2 mutant mice were evaluated using two well-established behavioral models of antidepressant activity, the NSFT and TST (Santarelli et al., 2003; Cryan et al., 2005; Heurteaux et al., 2006).

In the NSFT, both GIRK2$^{-/-}$ and GIRK2$^{+/-}$ mice showed a decreased latency to eat, compared to wild-type mice (GIRK2$^{-/-}$: 145.60 ± 19.63 s, n = 9; GIRK2$^{+/-}$: 154.60 ± 14.30 s, n = 20; WT: 212.00 ± 14.85 s, n = 22. $p < 0.05$, Kruskal-Wallis nonparametric test following Dunn's post-hoc test) (Fig. 4.5A). This decrease in the latency to eat observed in the mutant groups was not due to an increased appetite (Fig. 4.5B).

When evaluating the behavioral characteristics in the TST, GIRK2$^{-/-}$ mice showed a lower immobility time than GIRK2$^{+/-}$ and wild-type mice (GIRK2$^{-/-}$: 115.10 ± 9.08 s, n = 16; GIRK2$^{+/-}$: 189.10 ± 3.24 s, n = 16; WT: 191.80 ± 8.87 s, n = 14. $p < 0.0001$, one-way ANOVA following Newman-Keuls test) (Fig. 4.5C). Next, we examined the effect of citalopram on the immobility time in the TST. In all the groups, the administration of citalopram (10 mg/kg, i.p.) 30 min prior to the test caused a reduction of the immobility time (Fig. 4.5D). However, in GIRK2$^{-/-}$ and GIRK2$^{+/-}$ mice this reduction was significantly lower than that observed in wild-type mice (GIRK2$^{-/-}$: 53.2 ± 9.5 %, n = 7; GIRK2$^{+/-}$: 50.5 ± 5.9 %, n = 7; WT: 79.2 ± 5.1 %, n = 10. $p < 0.05$, one-way ANOVA following Newman-Keuls post-hoc test).

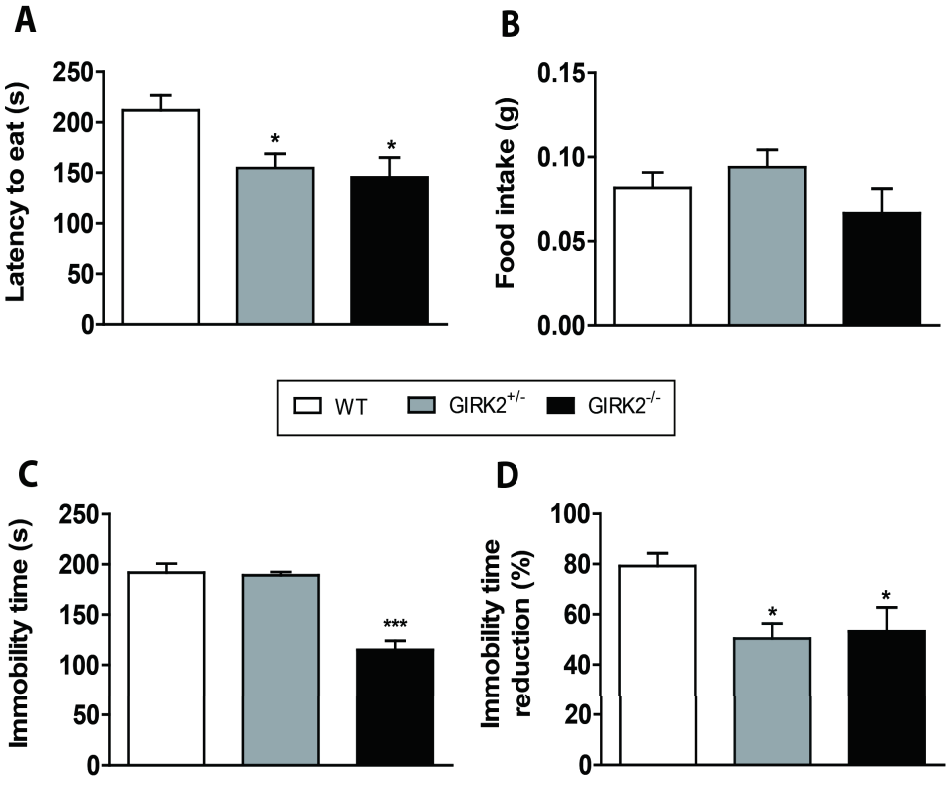

Figure 4.5. Behavioral characterization of GIRK2 mutant mice. (A) In the novelty suppressed feeding test (NSFT), both GIRK2$^{+/-}$ and GIRK2$^{-/-}$ mice displayed a lower latency to eat compared to wild-type (WT) mice (n = 9 - 22 mice/group; $^{*}p < 0.05$ *vs* WT, Kruskal-Wallis nonparametric test following Dunn's post-hoc test). (B) No changes among groups in the amount of food consumed after the NSFT (n = 9 - 22 mice/group). (C) In the tail suspension test (TST), GIRK2$^{-/-}$ mice displayed a lower immobility time compared to GIRK2$^{+/-}$ mice and WT (n = 14 - 16 mice/group; $^{***}p < 0.001$ *vs* WT, one-way ANOVA followed by Newman-Keuls post-hoc test). (D) In the TST, 30 min after the citalopram injection (10 mg/kg, i.p.), both GIRK2$^{+/-}$ and GIRK2$^{-/-}$ mice showed a lower reduction of the immobility time compared to WT (n = 7 - 10 mice/group; $^{*}p < 0.05$ *vs* WT, one-way ANOVA followed by Newman-Keuls post-hoc test). Bars represent means ± S.E.M. of n animals.

4.1.7. Basal neurogenesis in GIRK2 mutant mice

We next investigated whether GIRK2 subunit is involved in basal adult neurogenesis measuring the area density (#cells/mm^2, Sv) of new proliferating cells in the DG of the HPP and in the SVZ of GIRK2 mutant mice compared to wild-type mice.

In the DG of the HPP and SVZ of all the groups newly generated cells were visualized, as indicated by HH3 immunoreactiviy (HH3-IR). GFAP immunoreactivity was detected throughout both areas, but less than 2% of HH3-IR cells expressed GFAP. Quantitative analysis of the Sv of HH3-IR cells showed no differences among genotypes either in the DG (WT: 17.18 ± 1.89, GIRK2$^{+/-}$: 16.69 ± 1.36, and GIRK2$^{-/-}$: 14.71 ± 1.51. (Fig. 4.6A, B, C) or in the SVZ (WT: 152.43 ± 8.81; GIRK2$^{+/-}$: 154.34 ± 6.10; GIRK2$^{-/-}$: 139.99 ± 16) (Fig. 4.6D).

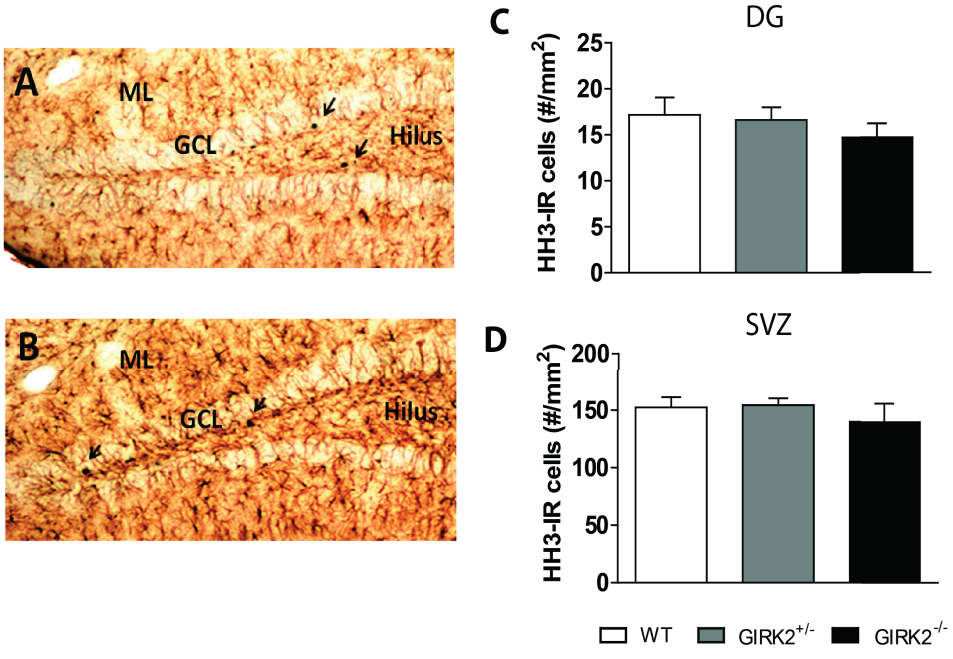

Figure 4.6. Brightfield micrographs showing phosphorilated Histone H3 (HH3, a proliferating mitotic marker) labelled cells within the *dentate gyrus* and subventricular zone of wild-type and GIRK2 mutant mice. (A - B) Dual labeling of HH3 positive cells (arrows) and glial cells (GFAP, brown) in the hippocampal *dentate gyrus* (DG) of (A) wild-type (WT) and (B) GIRK2$^{-/-}$ mice. Bar graphs showing no differences among groups in the area density of HH3 positive cells within (C) the DG (all layers included) and (D) the subventricular zone (SVZ) of WT and GIRK2 mutant mice. Bars represent means ± S.E.M. of *n* animals (*n* = 6 - 10 mice/group). GCL: Granular Cell Layer, ML: Molecular Layer.

4.2. STUDY II: Altered inhibitory pre- and postsynaptic activity in *dorsal raphe* neurons of GIRK2 mutant mice

4.2. STUDY II: Altered inhibitory pre- and postsynaptic activity in *dorsal raphe* neurons of GIRK2 mutant mice

4.2.1. *In vitro* electrophysiological properties of *dorsal raphe* neurons of GIRK2 mutant mice

DR neurons were found ventral to the aqueduct in slices that were rostral to the level where the aqueduct begins to meet the fourth ventricle and caudal to the decussation of the cerebellar peduncle. Whole-cell recordings were carried out in voltage- (V_h = -70 mV) or current-clamp mode from preumed 5-HT DR neurons. These cells were confined and densely present within the midline DR, which is an area where non serotonergic cells are hardly observed (Gocho et al., 2013). Putative 5-HT neurons were initially identified by midline location and large cell body. Moreover, the electrophysiological properties of the recorded neurons from wild-type mice in this study were similar and consistent with previously reported of tryptophan hydroxylase positive, non-GABAergic median *dorsal raphe* neurons from mice (Gocho et al., 2013; Levitt et al., 2013).

Thus, we analyzed the intrinsic membrane properties of DR neurons from wild-type, GIRK2$^{+/-}$, and GIRK2$^{-/-}$ mice. Membrane capacitance and resting membrane potential of DR neurons did not change among genotypes. However, input resistance values obtained in GIRK2$^{-/-}$ mice were statistically higher than those in GIRK2$^{+/-}$ and wild-type mice ($p < 0.05$ and $p < 0.01$ *vs* GIRK2$^{+/-}$ and WT mice, respectively, one-way ANOVA followed by Newman-Keuls post-hoc test) (Table 4.2).

Table 4.2. Electrophysiological intrinsic membrane properties of *dorsal raphe* neurons of wild-type and GIRK2 mutant mice.

	WT	GIRK2$^{+/-}$	GIRK2$^{-/-}$
Membrane capacitance (pF)	52.29 ± 2.24 (23)	51.55 ± 3.18 (17)	52.33±2.37 (38)
Input resistance (MΩ)	479.40±31.07 (24)	448.70±38.93 (16)	667.00±55.25$^{\#**}$ (35)
Resting membrane potential (mV)	-57.71±0.73 (56)	-54.48±1.50 (29)	-55.58± 1.19 (43)

Values represent the mean ± S.E.M of (*n*) cells. WT: wild-type; GIRK2$^{+/-}$: GIRK2 heterozygous mice; GIRK2$^{-/-}$: GIRK2 homozygous mice. $^{\#}p < 0.05$ and $^{**}p < 0.01$ *vs* GIRK2$^{+/-}$ and WT mice, respectively. One-way ANOVA followed by Newman-Keuls.

Since the differences in the electrophysiological properties were found between wild-type and GIRK2$^{-/-}$ mice, posterior analyses of the action potential (AP) characteristics were performed in these two genotypes.

In current-clamp mode, DR neurons were sometimes active (50 % of the total number of neurons recorded in wild-type and 58 % in GIRK2$^{-/-}$ mice), and injection of current (50 – 200 pA) produced slow, regular firing of long-duration action potentials (AP half-width) that increased in frequency with larger current injections (WT 50 pA = 9.63 ± 0.49 Hz; 100 pA = 15.13 ± 0.68 Hz ; 150 pA = 19.57 ± 0.88 Hz; 200 pA = 23.71 ± 1.14 Hz; $n = 24$. GIRK2$^{-/-}$ 50 pA = 10.32 ± 0.58 Hz; 100 pA = 16.32 ± 0.79 Hz; 150 pA = 21.28 ± 1.03 Hz; 200 pA = 24.97 ± 1.2 Hz; $n = 35$) (Fig. 4.7A, B, C). In this sense, neurons from

GIRK2$^{-/-}$ and wild-type mice had a similar sensitivity to injected currents (Fig. 4.7C).

Then, we analyzed the AP properties in each group. As shown in figure 4.7D, GIRK2$^{-/-}$ cells had similar AP amplitudes and threshold compared to those of wild-type cells. Regarding AP kinetics, such as half-width, rise time, and decay time, GIRK2$^{-/-}$ neurons had significantly narrower AP compared to wild-type neurons (Table 4.3), shown by a shorter AP half-width and decay time ($p < 0.05$, unpaired two-tailed t-test).

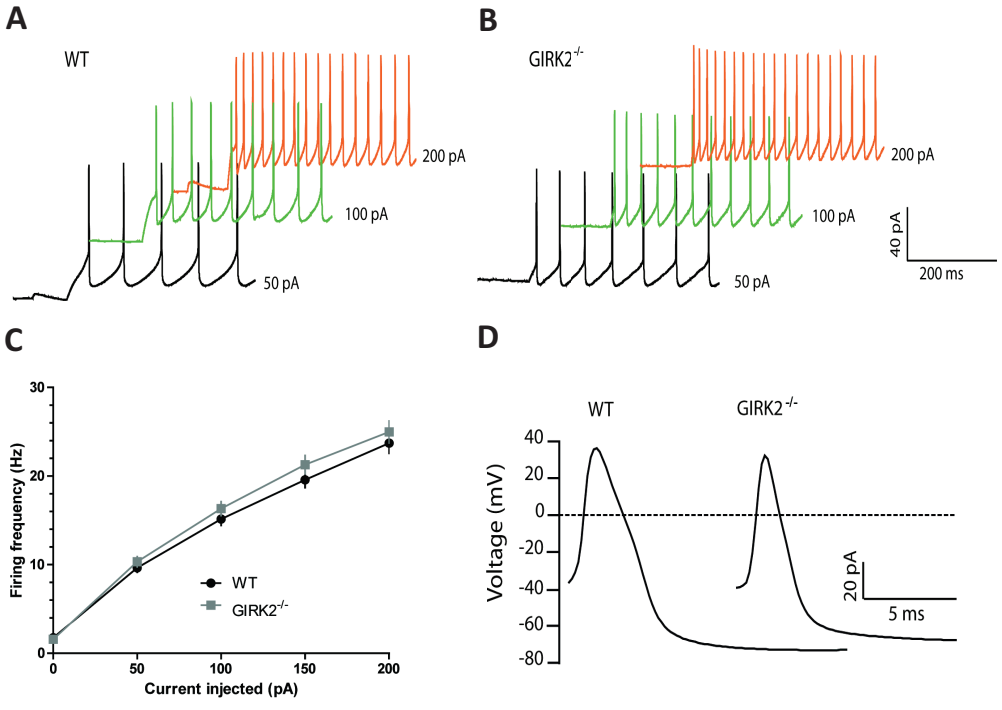

Figure 4.7. Electrophysiological properties of action potentials of *dorsal raphe* neurons of wild-type and GIRK2$^{-/-}$ mice. (A and B) Action potential (AP) waveforms of *dorsal raphe* (DR) neurons from wild-type (WT) and GIRK2$^{-/-}$ mice elicited by current injections of 50, 100 and 200 pA (black, green and orange, respectively). (C) Input-output relationship curves of DR neurons from WT (n = 24) and GIRK2$^{-/-}$ mice (n = 35). Means ± S.E.M. To calculate the firing frequency, APs were elicited by application of current steps from 0 to 200 pA in 50 pA increments (2 seconds per step). (D) Representative AP waveforms of DR neurons in WT and GIRK2$^{-/-}$ mice elicited with the minimum depolarizing current injection.

Table 4.3. Electrophysiological properties of action potentials of *dorsal raphe* neurons of wild-type and GIRK2 mutant mice

	WT	GIRK2$^{-/-}$
AP threshold (mV)	-32.26 ± 1.94 (16)	-35.73 ± 0.97 (35)
AP amplitude (mV)	71.48 ± 1.09 (17)	72.70 ± 1.06 (35)
AP half-width (ms)	1.55 ± 0.08 (17)	1.33 ± 0.05 *(36)
Rise time 10 – 90 % (ms)	0.55 ± 0.03 (14)	0.62 ± 0.03 (25)
Decay time 10 – 90 % (ms)	1.42 ± 0.08 (17)	1.16 ± 0.06 *(36)

Values represent the means ± S.E.M of (*n*) cells. WT: wild-type; GIRK2$^{-/-}$: GIRK2 homozygous mice. $^{*}p < 0.05$, unpaired two-tailed t-test.

4.2.2. Role of GIRK2 subunit-containing GIRK channels in 5-HT_{1A}- and $GABA_B$ receptor-mediated whole currents in *dorsal raphe* neurons

We studied the role of GIRK2 subunit-containing GIRK channels in mediating the postsynaptic actions of 5-HT and GABA through the activation of 5-HT_{1A} and $GABA_B$ receptors, respectively.

In the first series of experiments, in order to evaluate the 5-HT_{1A} receptor-mediated postsynaptic transmission on DR neurons of GIRK2 mutant mice, we examined the action of 5-CT, a high-affinity full agonist of 5-HT_{1A} receptors on the holding current of DR cells. Whole-cell voltage-clamp recordings performed in wild-type mice revealed that the application of 5-CT (100 nM) elicited an outward current that reached the steady-state in 1 - 2 min and slowly returned to baseline as the compound was washed from the slice (Fig. 4.8A). The amplitude of the 5-CT induced current ranged from 15.70 to 104.00 pA (mean = 54.21 ± 7.23 pA, n = 13). Voltage steps (-60 to -140 mV, 100 ms) were applied to determine the identity of the 5-CT induced-outward current before and during drug application. For this purpose, the current produced by 5-CT at each voltage was determined by subtracting the corresponding control current at baseline conditions, before the perfusion of 5-CT. The 5-CT-induced current displayed inward rectification shown as a change in the slope of the current-voltage relationship, being more pronounced at more hyperpolarized potentials (Fig. 4.8B), and reversed at the potassium equilibrium potential. This is consistent with the activation of GIRK channels. In this sense, in wild-type animals the slope conductance between - 70 and - 80 mV (G1) was 5.44 ± 0.43 nS, and statistically increased to 8.79 ± 0.41 nS (n = 9) when measured between - 110 and - 120 mV (G2) ($p < 0.01$, paired two-tailed t-test) (Fig. 4.8D). Thus, in wild-type mice, 5-CT activated 5-HT_{1A} somatodendritic receptors resulting in an increase in GIRK conductance in DR neurons. In line with this, the 5-CT-induced current was reduced in DR neurons of $GIRK2^{+/-}$ mice (34.18 %), and even more in $GIRK^{-/-}$ mice (68.75 %) compared that in

wild-type mice. In GIRK2$^{+/-}$ DR neurons, the amplitude of the outward current ranged from 12.10 to 67.90 pA (mean = 35.68 ± 3.84 pA, n = 18), and from 2.90 to 59.60 pA (mean = 16.94 ± 5.28 pA, n = 12) in GIRK2$^{-/-}$ DR neurons (Fig. 4.8C). Therefore, mean amplitudes of the 5-CT-induced currents in GIRK2$^{+/-}$ and GIRK2$^{-/-}$ mice were statistically smaller than in wild-type mice ($p < 0.05$ and $p < 0.001$ for GIRK2$^{+/-}$ and GIRK2$^{-/-}$ mice, respectively. One-way ANOVA followed by Newman-Keuls post-hoc test). Voltage steps were also performed in GIRK2 mutant mice before and after 5-CT application. In GIRK2$^{+/-}$ mice current-voltage analysis of the 5-CT induced currents showed inward rectification revealing activation of GIRK channels (GIRK2$^{+/-}$ G1 = 5.09 ± 0.43 nS; GIRK2$^{+/-}$ G2 = 6.38 ± 0.68 nS, n = 10. $p < 0.05$, paired two-tailed t-test). However, no inward rectification was displayed in GIRK2$^{-/-}$ mice (GIRK2$^{-/-}$ G1= 2.58 ± 0.24 nS; GIRK2$^{-/-}$ G2 = 3.03 ± 0.56 nS, n = 7) (Fig. 4.8D). Values obtained for G1 and G2 in GIRK2$^{-/-}$ were statistically different to those obtained for G1 and G2 in wild-type mice ($p < 0.05$ and $p < 0.0001$ for G1 and G2 in GIRK2$^{-/-}$ mice *vs* G1 and G2 in WT mice, respectively. One-way ANOVA followed by Newman-Keuls post-hoc test). These results suggest a lack of function of GIRK channels in GIRK2$^{-/-}$ DR neurons.

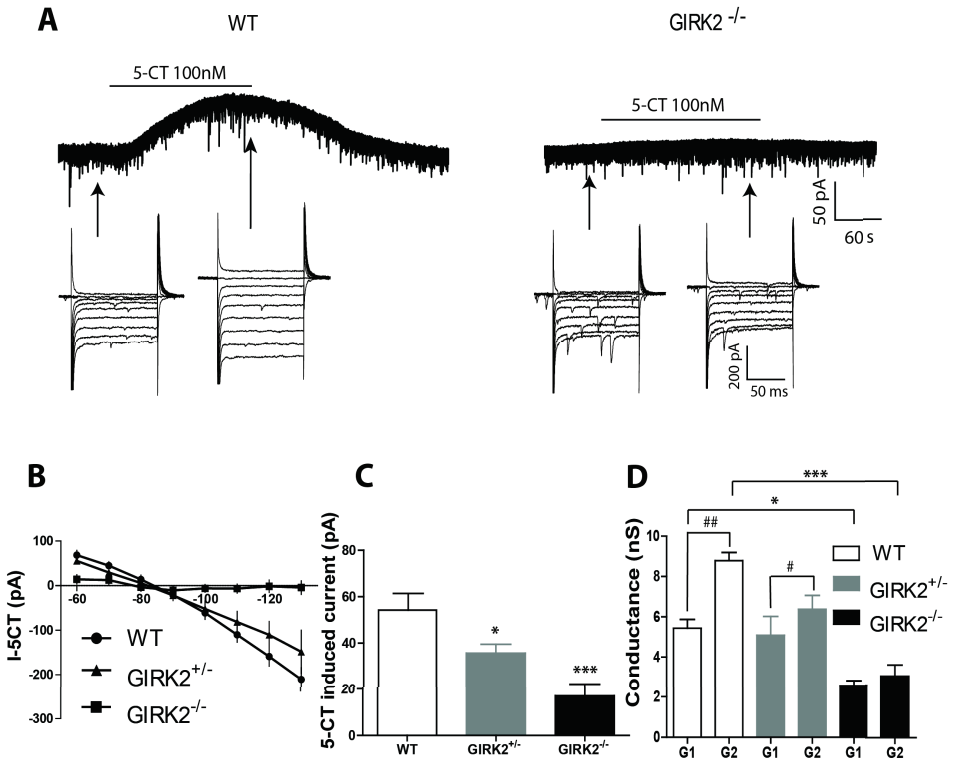

Figure 4.8. 5-CT-induced outward currents in *dorsal raphe* neurons of wild-type and GIRK2 mutant mice. (A) Representative whole-cell recordings illustrating the outward current induced by 5-CT (100 nM) in *dorsal raphe* (DR) neurons of wild-type (WT) mice, and the diminished 5-CT-induced outward current in GIRK2$^{-/-}$ mice. Voltage steps (-60 to -140 mV) were performed before and during 5-CT perfusion. (B) Summary graph of 5-CT induced current (pA) *vs* potential (mV) in DR neurons of WT, GIRK2$^{+/-}$ and GIRK2$^{-/-}$ mice. Note that 5-CT-induced currents showed inward rectification in DR neurons of WT and GIRK2$^{+/-}$ mice but not in GIRK2$^{-/-}$ mice. (C) Summary bar graph showing the amplitudes of the 5-CT-induced outward currents in WT, GIRK2$^{+/-}$ and GIRK2$^{-/-}$ mice. (D) Summary bar graphs showing the conductance between – 70 to – 80 mV (G1) and -110 to – 120 mV (G2) in DR neurons of the three groups. Bars represent the means ± S.E.M. of *n* experiments (n = 13 for WT; n = 18 for GIRK2$^{+/-}$; and n = 12 for GIRK2$^{-/-}$ mice). $^{*}p < 0.05$ and $^{***}p < 0.001$ *vs* WT, one-way ANOVA followed by Newman-Keuls post-hoc test. $^{\#}p < 0.05$ and $^{\#\#}p < 0.01$, paired two-tailed t-test.

Besides to 5-HT_{1A} receptors, GIRK channels are coupled to $GABA_B$ receptors in the DR. Thus, in the second set of experiments, we studied the $GABA_B$ receptor-mediated postsynaptic transmission on DR neurons of GIRK2 mutant mice. Figure 4.9A shows that the application of the selective $GABA_B$ agonist baclofen (30 μM), which activates GIRK channels (Andrade et al., 1986; Thompson and Gahwiler, 1992), elicited an outward current that was reduced in $GIRK2^{+/-}$ (40 %) and in $GIRK2^{-/-}$ (78 %) compared to wild-type mice. The mean amplitudes of the baclofen-induced currents were statistically smaller in GIRK2 mutant mice compared to wild-type mice (WT = 34.97 ± 5.79 pA, n = 11; $GIRK2^{+/-}$ = 21.15 ± 2.39 pA, n = 11; and $GIRK2^{-/-}$ = 7.60 ± 0.79 pA, n = 13. $p < 0.0001$ and $p < 0.001$ for $GIRK2^{+/-}$ and $GIRK2^{-/-}$ mice respectively. One-way ANOVA followed by Newman-Keuls post-hoc test) (Fig. 4.9B). Current-voltage analysis derived from voltage steps made before and during baclofen perfusion revealed that in wild-type and $GIRK2^{+/-}$ mice baclofen induced an inward rectification consistent with GIRK channels activation, although $GIRK2^{-/-}$ mice did not display inward rectification (data not shown).

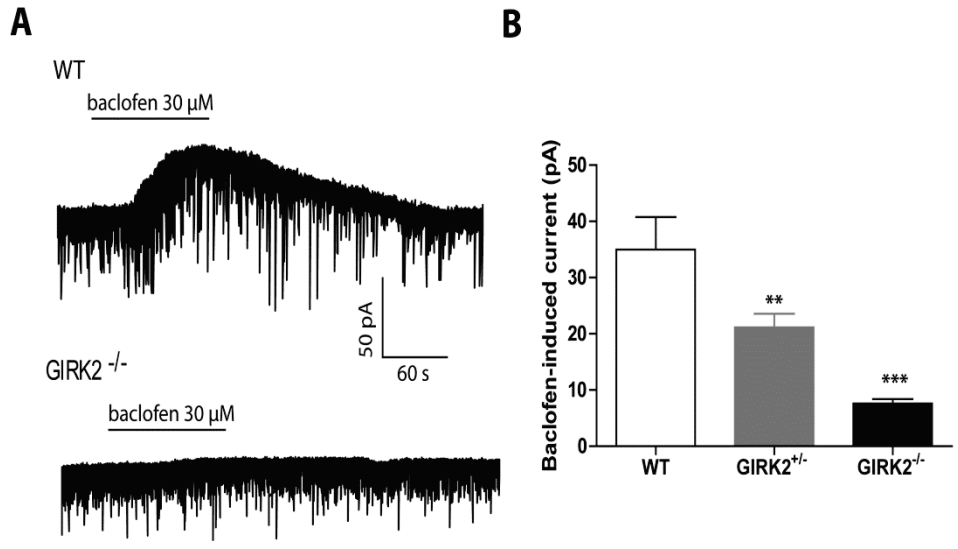

Figure 4.9. Baclofen-induced outward currents in *dorsal raphe* neurons of wild-type and GIRK2 mutant mice. (A) Representative whole-cell recordings in *dorsal raphe* (DR) neurons illustrating the outward current induced by the bath perfusion of baclofen (30 µM) in wild-type (WT), and the diminished baclofen-induced outward current in GIRK2$^{-/-}$ mice. (B) Summary bar graph showing the amplitudes of the baclofen-induced outward currents in DR neurons of WT, GIRK2$^{+/-}$ and GIRK2$^{-/-}$ mice. Bars represent means ± S.E.M. of *n* experiments (n = 11 for WT; n = 11 for GIRK2$^{+/-}$; and n = 13 for GIRK2$^{-/-}$ mice). $^{**}p < 0.001$ and $^{***}p < 0.0001$ *vs* WT, one-way ANOVA followed by Newman-Keuls post-hoc test.

4.2.3. Role of GIRK2 subunit-containing GIRK channels in the GABAergic synaptic activity in *dorsal raphe* neurons

To study the fast GABAergic synaptic activity we first blocked the glutamatergic transmission and isolated the $GABA_A$ activity by adding the AMPA/kainate receptor antagonist, DNQX (10 μM), to the external solution. We investigated the spontaneous and evoked GABAergic presynaptic activity, as well as the GABA-induced postsynaptic currents in GIRK2 mutant mice.

First, we evaluated if *Girk2* gene mutation alters the GABAergic synaptic activity by studying the spontaneous and evoked inhibitory postsynaptic currents (sIPSCs and eIPSCs, respectively). Regarding sIPSCs, GIRK2 mutant mice displayed a statistically significant reduction, compared to those in wild-type, in both the mean frequency ($GIRK2^{+/-}$ = 2.01 ± 0.14 Hz, n = 32; $GIRK2^{-/-}$ = 2.55 ± 0.20 Hz, n = 44; and WT = 3.56 ± 0.31 Hz, n = 31. $p <$ 0.0001 for $GIRK2^{+/-}$ and $p < 0.001$ for $GIRK2^{-/-}$ *vs* WT. One-way ANOVA followed by Newman-Keuls post-hoc test) (Fig. 4.10A, C), and the mean amplitude of the events ($GIRK2^{+/-}$ = 33.63 ± 2.55 pA, n = 32; $GIRK2^{-/-}$ = 34.88 ± 2.04 pA, n = 41; and WT = 49.66 ± 3.51 pA, n = 31. $p < 0.0001$ for $GIRK2^{+/-}$ and $GIRK2^{-/-}$ *vs* WT. One-way ANOVA followed by Newman-Keuls post-hoc test) (Fig. 4.10B, C). However, no differences were found in the mean duration of the sIPSC (sIPSCs half-width) among genotypes ($GIRK2^{+/-}$ = 3.04 ± 0.09 ms, n = 32; $GIRK2^{-/-}$ = 3.07 ± 0.08 ms, n = 41; and WT = 2.89 ± 0.09 ms, n = 31) (Fig. 4.10C).

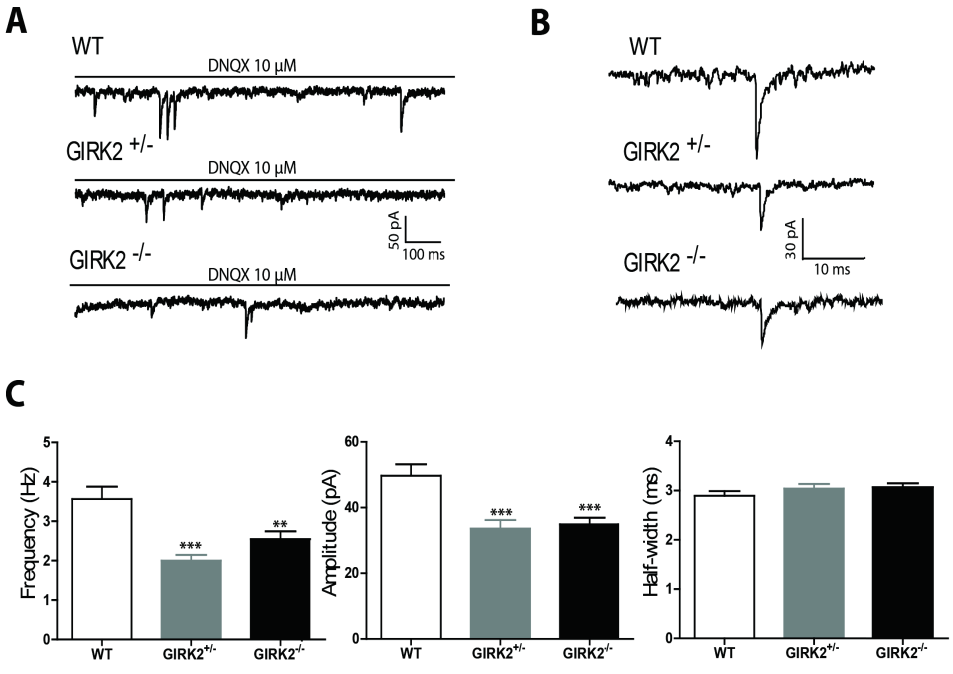

Figure 4.10. Spontaneous GABAergic synaptic activity in *dorsal raphe* neurons of wild-type and GIRK2 mutant mice. (A) Representative current traces showing spontaneous inhibitory postsynaptic currents (sIPSCs) in *dorsal raphe* (DR) neurons of wild-type (WT), GIRK2$^{+/-}$ and GIRK2$^{-/-}$ mice. (B) Representative magnified sIPSCs in DR neurons illustrating the amplitudes of the sIPSCs in WT, GIRK2$^{+/-}$ and GIRK$^{-/-}$ mice. (C) Summary bar graph showing the frequency, amplitude, and half-width of sIPSCs in DR neurons of WT, GIRK2$^{+/-}$ and GIRK2$^{-/-}$ mice. Bars represent the means ± S.E.M. of *n* experiments (n = 31 for WT; n = 32 for GIRK2$^{+/-}$; and n = 41 - 44 for GIRK2$^{-/-}$ mice). $^{**}p < 0.001$ and $^{***}p < 0.0001$ *vs* WT, one-way ANOVA following Newman-Keuls post-hoc test.

Then, we evaluated the role of GIRK2 subunit-containing GIRK channels in the presynaptic inhibition of GABA release. For this purpose, GABA release was evoked by pairs of electrical stimuli (paired-pulse stimulation, 100 μs at 20 Hz) every 20 seconds (Fig. 4.11A). In wild-type mice, a 22% of the DR neurons showed paired-pulse facilitation, being the mean amplitude of the peak 1 855.50 ± 89.59 pA, and the mean amplitude of peak 2 766.80 ± 80.10 pA (n = 17). Thus, the paired-pulse ratio, which is the ratio of the amplitudes between peak 2 and peak 1, was 0.89 ± 0.04 (n = 17). Compared to wild-type, GIRK2$^{+/-}$ mice showed a similar number of cells displaying paired-pulse facilitation (30 %) and no significant changes were found either in the mean values of the amplitude of peak 1 and peak 2 (654.60 ± 94.90 pA, and 567.70 ± 71.80 pA, respectively. n = 19), or in the paired-pulse ratio (0.94 ± 0.03, n = 19). However, GIRK2$^{-/-}$ mice displayed a statistically significant increase in the number of cells that showed paired-pulse facilitation (59 %) ($p <$ 0.0001 *vs* WT, chi-square test). In addition, the mean amplitude of the peak 1 was statistically smaller than in wild-type (534.00 ± 72.77 pA, n = 18) ($p <$ 0.05, one-way ANOVA followed by Newman-Keuls post-hoc test). No changes were found in the mean amplitude of peak 2 (555.90 ± 71.60 pA, n = 18) compared to wild-type mice. Paired-pulse ratio was statistically greater in DR neurons of GIRK2$^{-/-}$ mice (1.05 ± 0.05, n = 17) compared to that obtained for DR neurons in wild-type mice ($p <$ 0.05, one-way ANOVA followed by Newman-Keuls post-hoc test) (Fig. 4.11B, C, D).

Other kinetic parameters such as half-width and decay time of the peak 1 (Fig. 4.11E) were also analyzed and were similar among genotypes (WT peak 1 mean half-width: 5.04 ± 0.43 ms, n = 14, and WT peak 1 mean decay time: 16.29 ± 1.14 ms, n = 18; GIRK2$^{+/-}$ peak 1 mean half-width: 5.75 ± 0.73 ms, n = 14, and GIRK2$^{+/-}$ peak 1 mean decay time: 20.58 ± 2.32 ms, n = 19; GIRK2$^{-/-}$ peak 1 mean half-width: 5.60 ± 0.54 ms, n = 15, and GIRK2$^{-/-}$ peak 1 mean decay time: 18.88 ± 2.39 ms, n = 15).

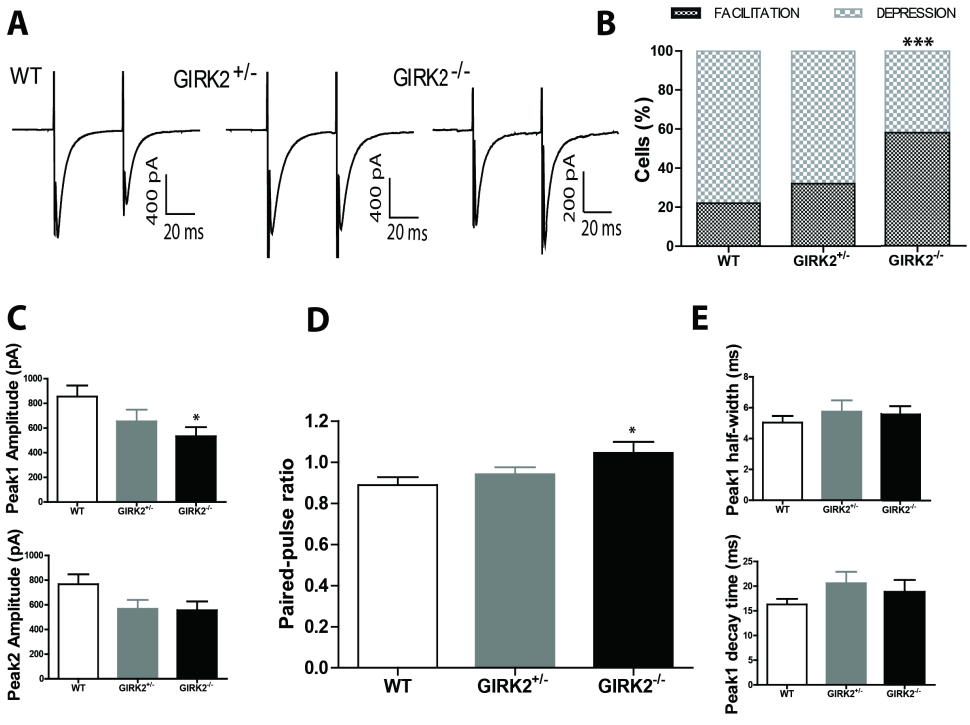

Figure 4.11. Electrophysiological parameters of evoked inhibitory postsynaptic currents in *dorsal raphe* neurons of wild-type and GIRK2 mutant mice. (A) Representative traces of the recordings of evoked inhibitory postsynaptic currents (eIPSCs) in *dorsal raphe* (DR) neurons of wild-type (WT), GIRK2$^{+/-}$, and GIRK2$^{-/-}$ mice, showing a different pattern in the response to the paired-pulse stimulation in DR neurons of GIRK2 mutant mice compared to WT. (B) Summary bar graph comparing percent of DR neurons that display paired-pulse facilitation in WT, GIRK2$^{+/-}$, and GIRK2$^{-/-}$ mice. (C) Summary bar graphs showing the mean amplitudes of the peak 1 (top), and peak 2 (bottom) of eIPSCs in DR neurons of WT GIRK2$^{+/-}$ and GIRK2$^{-/-}$ mice. (D) Paired-pulse mean ratios of DR neurons in WT, GIRK2$^{+/-}$, and GIRK2$^{-/-}$ mice summarized in a bar graph. (E) Summary bar graphs showing half-width (top) and decay time (bottom) of the peak 1 of eIPSCs in DR neurons of WT, GIRK2$^{+/,-}$ and GIRK2$^{-/-}$ mice. Bars represent the means ± S.E.M. of *n* experiments (*n* = 17 - 18 for WT; *n* = 19 - 20 for GIRK2$^{+/-}$; and *n* = 17 - 18 for GIRK2$^{-/-}$ mice). $^{*}p < 0.05$ *vs* WT, one-way ANOVA followed by Newman-Keuls post-hoc test. $^{***}p < 0.0001$ *vs* WT, chi-square test.

- **Control of the GABAergic presynaptic activity by 5-HT_{1A} and $GABA_B$ presynaptic receptors in GIRK2 mutant mice**

Once having detected that *Girk2* gene mutation promotes alterations in the GABAergic activity at the presynaptic level, we studied whether the control that 5-HT_{1A} and $GABA_B$ receptors exert on the GABAergic presynaptic activity was normal in GIRK2 mutant mice.

In the first set of experiments we evaluated the control of the GABAergic presynaptic activity exerted by presynaptic 5-HT_{1A} receptors in DR neurons of GIRK2 mutant mice. For this purpose, we recorded the sIPSCs in basal and stable conditions, when the frequency and amplitude of the events and the holding current remained steady. Then, the 5-HT_{1A} receptor antagonist, WAY100635 (10 nM and 1 μM), was perfused during 5 min, and frequency and amplitude of the sIPSCs were analyzed before and after drug perfusion (Fig. 4.12A).

In DR neurons of wild-type mice, WAY100635 10 nM and 1 μM caused a significant increase (50 % and 47 %, respectively) in sIPSCs frequency that was similar at both concentrations (WT WAY 10 nM ratio: 1.50 ± 0.25, n = 6; WT WAY 1 μM ratio: 1.47 ± 0.18, n = 9). However, in $GIRK2^{-/-}$ mice, WAY100635 10 nM and 1 μM caused only a slight increase (10% and 5%, respectively) in the frequency of sIPSCs ($GIRK2^{-/-}$ WAY 10 nM ratio: 1.10 ± 0.09, n = 8; $GIRK2^{-/-}$ WAY 1 μM ratio: 1.05 ± 0.08, n = 9) that was statistically smaller at the higher concentration compared to that in wild-type ($p < 0.05$, unpaired two-tailed t-test) (Fig. 4.12A, B).

Regarding the effect of WAY100635 on the amplitude of sIPSCs, no statistical changes were seen either in wild-type (WT WAY 10 nM ratio: 1.06 ± 0.08, n = 6; WT WAY 1 μM ratio: 1.19 ± 0.15, n = 8) or in $GIRK2^{-/-}$ mice ($GIRK2^{-/-}$ WAY 10 nM ratio: 1.24 ± 0.21, n = 6; $GIRK2^{-/-}$ WAY 1 μM ratio: 1.60 ± 0.27, n = 7) after perfusion of WAY100635 (Fig. 4.12C).

In addition, no statistical differences were found in the effect of WAY100635 on the amplitude of the sIPSCs between genotypes.

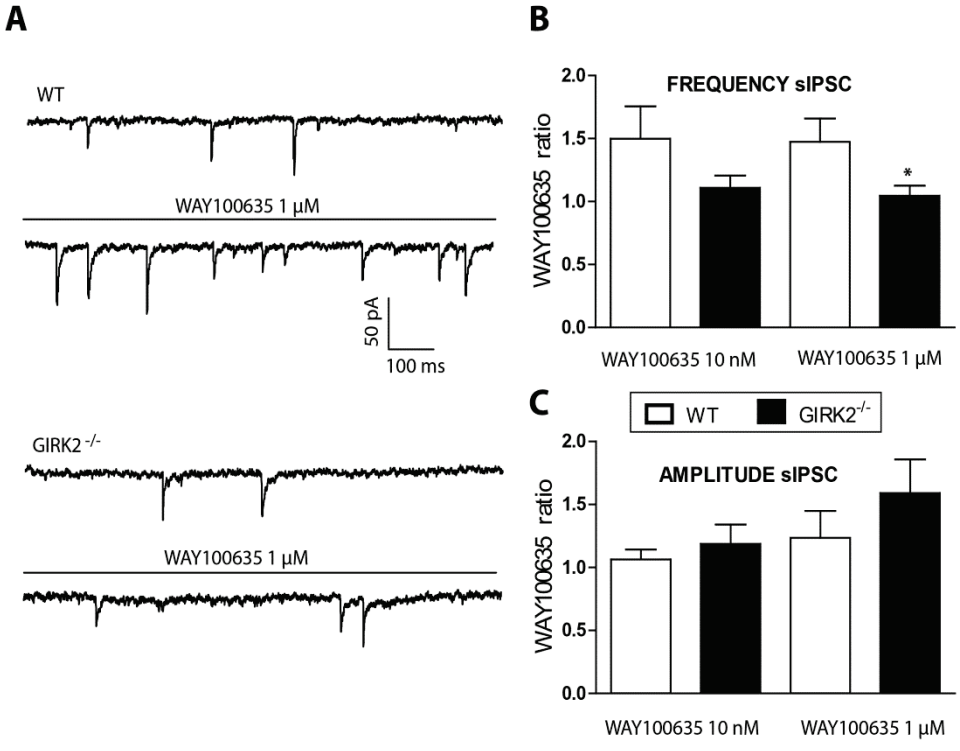

Figure 4.12. Effect of the 5-HT$_{1A}$ receptor antagonist, WAY100635, on the spontaneous GABAergic presynaptic activity in *dorsal raphe* neurons of wild-type and GIRK2 mutant mice. (A) Representative current traces showing spontaneous inhibitory postsynaptic currents (sIPSCs), before and after WAY100635 (1 µM) perfusion, in *dorsal raphe* (DR) neurons of wild-type (WT) and GIRK2$^{-/-}$ mice. (B) Summary bar graph showing the effect of WAY100635 (10 nM and 1 µM) on the frequency of the sIPSCs, normalized to basal values, in DR neurons of WT and GIRK2$^{-/-}$ mice. (C) Summary bar graph showing the effect of WAY100635 (10 nM and 1 µM) on the amplitude of the sIPSCs, normalized to basal values, in DR neurons of WT and GIRK2$^{-/-}$ mice. Bars represent the means ± S.E.M. of *n* experiments (*n* = 6 - 9 for WT, *n* = 8 - 9 for GIRK2$^{-/-}$ mice). $^{*}p < 0.05$ *vs* WT WAY 1 µM, unpaired two-tailed t-test.

In the second group of experiments, the control of the GABAergic presynaptic activity by presynaptic $GABA_B$ receptors in DR neurons was studied. For this purpose, we recorded the sIPSCs in basal conditions and then we applied the $GABA_B$ receptor antagonist, CGP55845 (1 μM) during 5 min (Fig. 4.13A). Frequency and amplitude of the sIPSCs were analyzed before and after drug perfusion. In wild-type mice, CGP55845 caused a significant increase (81 %) in the frequency of sIPSCs compared to basal frequency (WT CGP ratio: 1.81 ± 0.21, $n = 12$). However, in $GIRK2^{-/-}$ mice, CGP55845 perfusion caused a slight increase (24 %) in the frequency ($GIRK2^{-/-}$ CGP ratio: 1.24 ± 0.09, $n = 9$), and this increment in the frequency was statistically smaller than that produced by CGP55845 in DR neurons of wild-type mice (Fig. 4.13A, B) ($p < 0.05$, unpaired two-tailed t-test). Perfusion of CGP55845 did not change the amplitude of the sIPSCs either in wild-type mice (WT CGP ratio: 1.11 ± 0.09, $n = 11$) or in $GIRK2^{-/-}$ mice ($GIRK2^{-/-}$ CGP ratio: 1.17 ± 0.08, $n = 8$) and therefore no differences were obtained between genotypes (Fig. 4.13C).

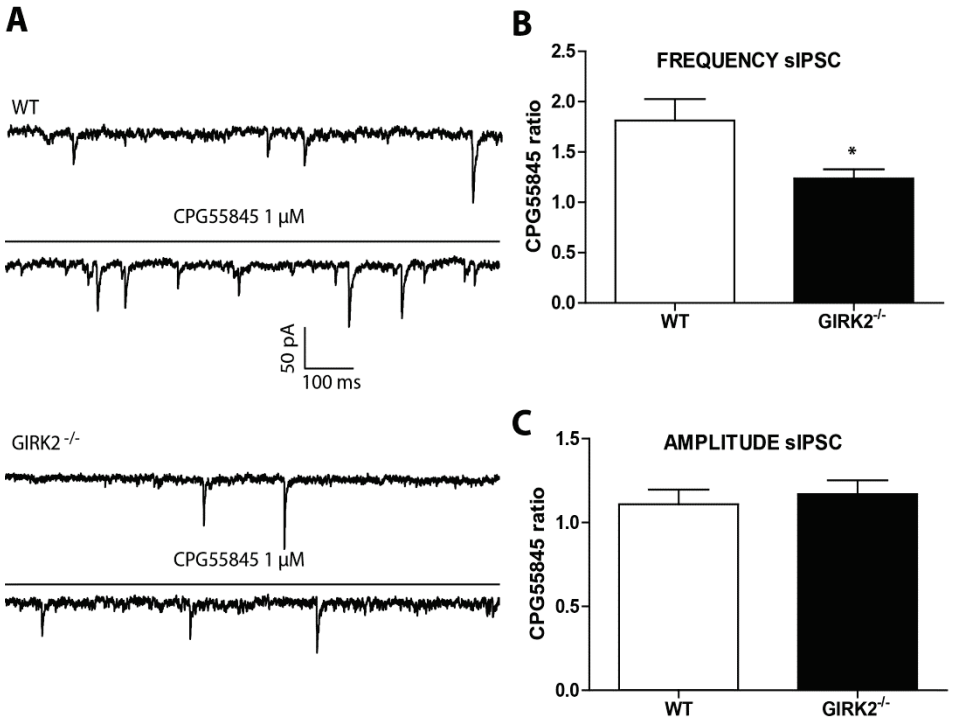

Figure 4.13. Effect of the $GABA_B$ receptor antagonist, CGP55845, on the spontaneous GABAergic presynaptic activity in *dorsal raphe* neurons of wild-type and GIRK2 mutant mice. (A) Representative current traces showing spontaneous inhibitory postsynaptic currents (sIPSCs) before and after CGP55845 (1 µM) perfusion in *dorsal raphe* (DR) neurons of wild-type (WT) and GIRK2$^{-/-}$ mice. (B) Summary bar graph showing the effect of CGP55845 on the frequency of the sIPSCs, normalized to basal values, in DR neurons of WT and GIRK2$^{-/-}$ mice. (C) Summary bar graph showing the effect of CGP55845 on the amplitude of the sIPSCs, normalized to baseline values, in DR neurons of WT and GIRK2$^{-/-}$ mice. Bars represent the means ± S.E.M. of *n* experiments (*n* = 11 - 12 for WT; and *n* = 8 - 9 for GIRK2$^{-/-}$ mice). $^{*}p < 0.05$, unpaired two-tailed t-test.

Additionally, we investigated whether GIRK2 subunit ablation could cause alterations in the GABAergic postsynaptic activity. Whole-cell currents of DR neurons induced by two different concentrations of the neurotransmitter GABA (100 and 300 μM) were recorded at a holding potential of -70 mV. In both wild-type and GIRK2$^{-/-}$ DR neurons, GABA elicited fast onset inward currents in a concentration dependent manner ([$F(1,64) = 15{,}75$, $p < 0.001$]. Two-way ANOVA followed by Bonferroni post-hoc test) that reached the steady-state in 1-2 min and slowly returned to baseline as the compound was washed from the slice (Fig. 4.14A). However, in GIRK2$^{-/-}$ mice the amplitude of the inward currents induced by GABA 100 μM (58.81 ± 9.21 pA, $n = 18$) was statistically smaller than in wild-type (106.30 ± 18.65 pA, $n = 17$) ($p < 0.05$, unpaired two-tailed t-test). Similarly, in GIRK2$^{-/-}$, the perfusion of GABA 300 μM induced an inward current (137.80 ± 21.53 pA, $n = 15$) that was statistically smaller that the GABA-induced current in wild-type mice (331.20 ± 59.62 pA, $n = 16$) ($p < 0.01$, unpaired two-tailed t-test) (Fig. 4.14A, B).

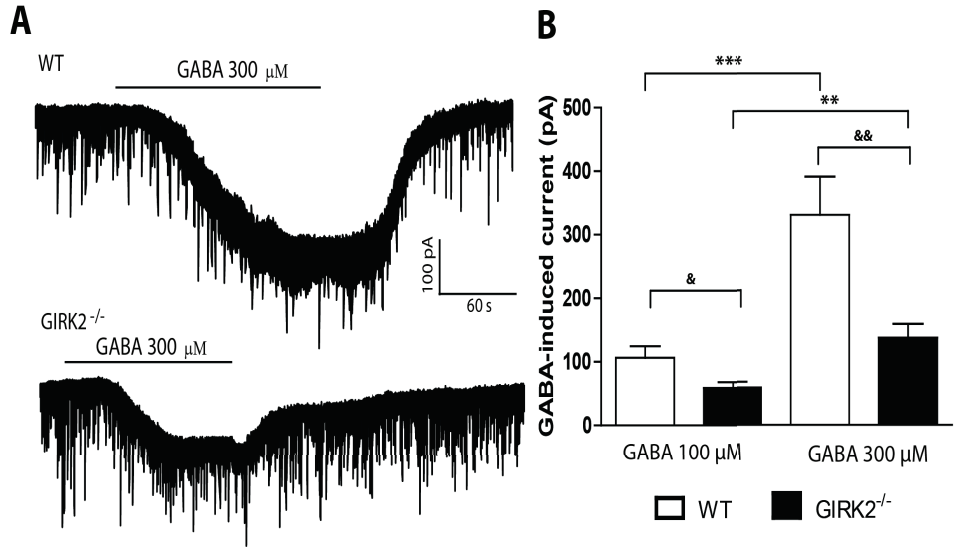

Figure 4.14. GABA-induced inward currents in *dorsal raphe* neurons of wild-type and GIRK2 mutant mice. (A) Representative whole-cell recordings illustrating the inward currents induced by the bath perfusion of GABA (300 μM) in *dorsal raphe* (DR) neurons of wild-type (WT) and the diminished GABA-induced inward current in DR neurons of GIRK2$^{-/-}$ mice. (B) Summary bar graph showing the amplitudes of the GABA-induced inward currents (100 and 300 μM) in DR neurons of WT and GIRK2$^{-/-}$ mice. Note that GABA induced inward currents in a concentration dependent manner in WT and GIRK2$^{-/-}$ mice. $^{***}p < 0.0001$, $^{**}p < 0.001$, $^{\&}p < 0.05$, and $^{\&\&}p < 0.01$, unpaired two-tailed t-test. Bars represent the means ± S.E.M. of *n* experiments (n = 16 - 17 for WT; n = 15 - 18 for GIRK2$^{-/-}$ mice).

4.2.4. Role of GIRK2 subunit-containing GIRK channels in the glutamatergic synaptic activity in *dorsal raphe* neurons

To evaluate the role of GIRK2 subunit in the control of the glutamatergic presynaptic activity in DR neurons, we studied the spontaneous and evoked excitatory postsynaptic currents (sEPSCs and eEPSCs, respectively) in GIRK2 mutant mice. To ensure the blockade of $GABA_A$ transmission we continuously bath perfused picrotoxin (100 μM) during the experiments.

Regarding the sEPSCs, compared to those in wild-type, no differences were observed in GIRK2$^{-/-}$ mice either in the mean frequency (GIRK2$^{-/-}$ = 4.77 ± 0.45 Hz, *n* = 28 and WT = 5.86 ± 0.46 Hz, *n* = 38) (Fig. 4.15A, C) or in the mean amplitude of the events (GIRK2$^{-/-}$ = 22.43 ± 1.53 pA, *n* = 28; and WT = 24.56 ± 1.18 pA, *n* = 32) (Fig. 4.15B, C). In addition, the kinetic of the sEPSCs remained similar since the mean duration of the events (sEPSCs half-width) in GIRK2$^{-/-}$ mice was similar to that obtained in the wild-type group (GIRK2$^{-/-}$ = 1.16 ± 0.04 ms, *n* = 28; and WT = 1.17 ± 0.04 ms, *n* = 32) (Fig. 4.15C).

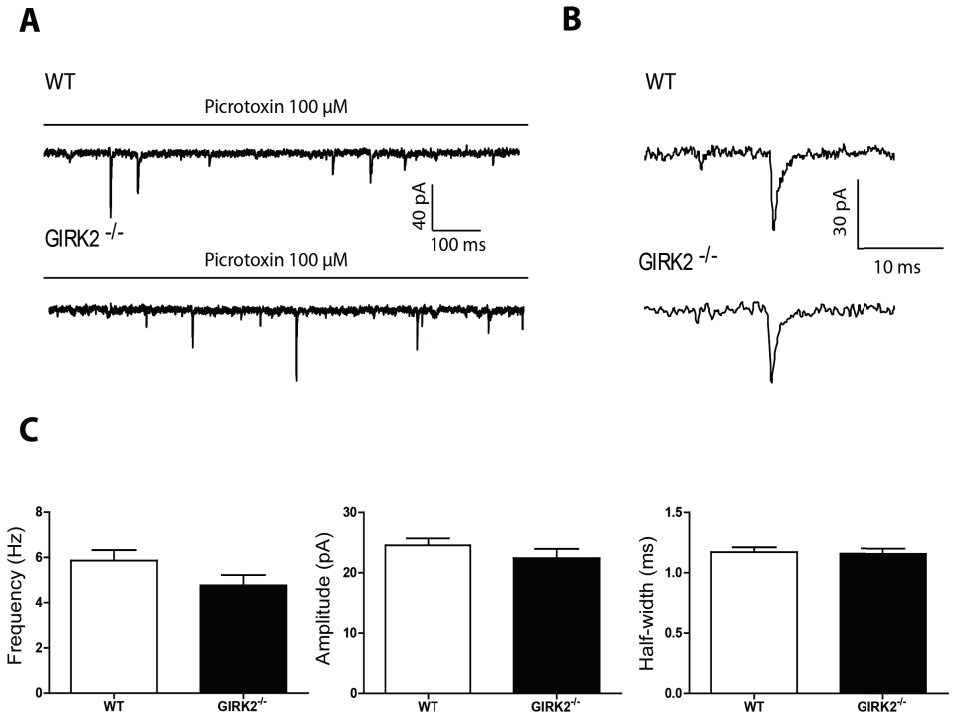

Figure 4.15. Spontaneous glutamatergic synaptic activity in *dorsal raphe* neurons of wild-type and GIRK2 mutant mice. (A) Representative current traces showing spontaneous excitatory postsynaptic currents (sEPSCs) of *dorsal raphe* (DR) neurons from wild-type mice (WT), and GIRK2$^{-/-}$ mice. (B) Representative magnified sEPSCs of DR neurons illustrating the amplitudes of the sEPSCs in DR neurons of WT and GIRK2$^{-/-}$ mice. (C) Summary bar graph showing the frequency, amplitude, and half-width of sEPSCs in DR neurons of WT and GIRK2$^{-/-}$ mice. Bars represent the means ± S.E.M. of *n* experiments (*n* = 32 – 38 for WT and *n* = 28 for GIRK2$^{-/-}$ mice).

Next, glutamate release was evoked by a single electrical stimulus (100 μs at 10 Hz) every 30 seconds at a holding potential of +40 mV in order to trigger simultaneously both AMPA and NMDA receptor-dependent eEPSCs (Fig 4.16A). No differences were observed between genotypes either in the mean amplitude of the eEPSCs ($GIRK2^{-/-}$ = 450.90 ± 92.46 pA, *n* = 14; and WT = 460.10 ± 87.64 pA, *n* = 24) or in the mean half-width ($GIRK2^{-/-}$ = 2.24 ± 0.26 ms, *n* = 12; and WT = 3.08 ± 0.34 ms, *n* = 21). We further studied possible differences in the balance of AMPA/NMDA mediation of eEPSCs. In order to do this, 5 min after evoking the first eEPSC, we bath-perfused the NMDA receptor antagonist, D-AP5 (50 μM) to block NMDA receptor dependent eEPSCs. No differences were observed between groups either in the mean amplitude of the AMPA-eEPSCs ($GIRK2^{-/-}$ = 345.80 ± 79.85 pA, *n* = 14; and WT = 327.70 ± 50.29 pA, *n* = 24) or in the mean amplitude of the NMDA-eEPSCs ($GIRK2^{-/-}$ = 141.40 ± 30.16 pA, *n* = 14; and WT = 126.60 ± 32.47 pA, *n* = 24). Therefore, no differences were found in the AMPA/NMDA mean ratio of the amplitude between groups ($GIRK2^{-/-}$ = 3.84 ± 1.11, *n* = 14; and WT = 4.37 ± 1.23, *n* = 24) (Fig. 4.16A, B).

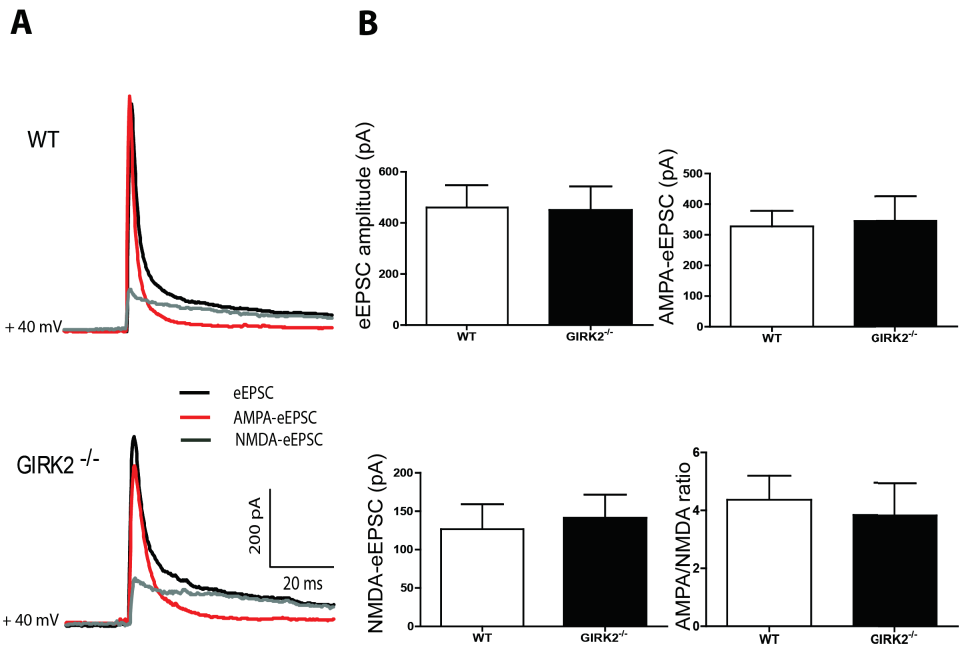

Figure 4.16. Electrophysiological parameters of evoked excitatory postsynaptic currents in *dorsal raphe* neurons of wild-type and GIRK2 mutant mice. (A) Representative traces of the recordings of evoked excitatory postsynaptic currents (eEPSCs) in *dorsal raphe* (DR) neurons of wild-type (WT) and GIRK2$^{-/-}$ mice. The relative contribution of AMPA- and NMDA-eEPSCs is also shown. (B) Summary bar graph showing the eEPSCs amplitude, AMPA-eEPSCs amplitude, NMDA-eEPSCs amplitude and AMPA/NMDA ratio of the amplitude in DR neurons of WT and GIRK2$^{-/-}$ mice. Bars represent the means ± S.E.M. of *n* experiments (*n* = 21 - 24 for WT, *n* = 12 - 14 for GIRK2$^{-/-}$ mice).

4.3. SUDY III: Ketamine promotes electrophysiological and biochemical alterations in the glutamatergic transmission in the *dorsal raphe*

4.3. SUDY III: Ketamine promotes electrophysiological and biochemical alterations in the glutamatergic transmission in the *dorsal raphe*

4.3.1. Behavioral effect of ketamine in the tail suspension test

To evaluate whether ketamine promotes an antidepressed-like behavior, we performed the TST, a well recognized animal model for assessing the antidepressant activity (Cryan et al., 2005). For this purpose, wild-type animals were acutely treated with ketamine (30 mg/kg, i.p.), 30 min or 24 h prior to the test. Injections of 0.9% saline were carried out in the control group in order to work in the same conditions in all the groups.

Ketamine administered 30 min prior to the test (ket 30 min) significantly reduced the immobility time in the TST (control: 195.10 ± 7.49 s, n = 18; ket 30 min: 84.30 ± 6.64 s, n = 10. $p < 0.0001$, one-way ANOVA following Newman-Keuls post-hoc test) (Fig. 4.17). Interestingly, this antidepressant-like effect was maintained when ketamine was administered 24 h before the TST (ket 24 h). Thus, the immobility time was statistically smaller in ket 24 h (ket 24 h: 152.10 ± 9.50 s, n = 10) compared to that in control group ($p < 0.0001$, one-way ANOVA followed by Newman-Keuls post-hoc test), although the antidepressant-like effect was more pronounced when ketamine was administered 30 min prior to the test than 24 h before the test ($p < 0.001$, one-way ANOVA followed by Newman-Keuls post-hoc test).

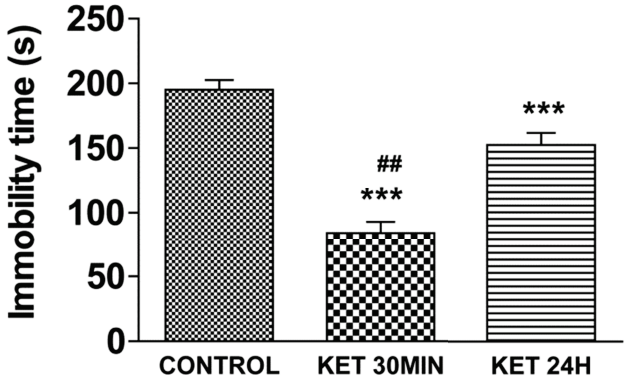

Figure 4.17. Effect of ketamine on the immobility time in the tail suspension test. Summary bar graph showing the effect of ketamine (30 mg/kg i.p.) on the immobility time of wild-type mice in the tail suspension test. The administration of ketamine 30 min (ket 30min) prior to the test significantly decreased the immobility time compared to control group. $^{***}p < 0.0001$, one-way ANOVA followed by Newman-Keuls post-hoc test. In the same line, ketamine (30 mg/kg, i.p.) administered 24 hours (ket 24h) prior to the test significantly reduced the immobility time compared to control group. $^{***}p < 0.0001$, one-way ANOVA followed by Newman-Keuls post-hoc test. The immobility time reduction was significantly more pronounced in the ket 30min group than in the ket 24h group. $^{\#\#}p < 0.001$ *vs* ket 24h, one-way ANOVA followed by Newman-Keuls post-hoc test. Bars represent mean ± S.E.M. of *n* experiments ($n = 10$ - 18 mice/group).

4.3.2. *In vitro* electrophysiological effects of ketamine administration 24 hours prior to the recordings on the glutamatergic synaptic activity in *dorsal raphe* neurons

In order to study if ketamine could produced sustained alterations on excitatory synaptic activity of DR neurons, we examined whether a single injection of ketamine 24 hours prior to the recordings (ket 24h, 30 mg/kg, i.p.), could have any effect on the sEPSCs and eEPSCs of DR neurons. For these recordings, picrotoxin (100 μM) was added to the external solution to block $GABA_A$ receptors.

First, we examined the sEPSCs of DR neurons in control mice and in mice treated with ketamine 24 hours prior to the recordings (Fig. 4.18A, B). For this purpose, sEPSCs were recorded during at least 3 min and the frequency and amplitude of the events were evaluated. Ketamine injection produced no alterations either in the frequency (ket 24 h: 6.05 ± 0.61 Hz, n = 13) or in the amplitude (ket 24 h: 25.15 ± 1.64 pA, n = 13) of the events, compared to those obtained in the control group (control sEPSC frequency: 5.86 ± 0.46 Hz, n = 38; control sEPSC amplitude: 24.42 ± 1.00 pA, n = 38) (Fig. 4.18C, D).

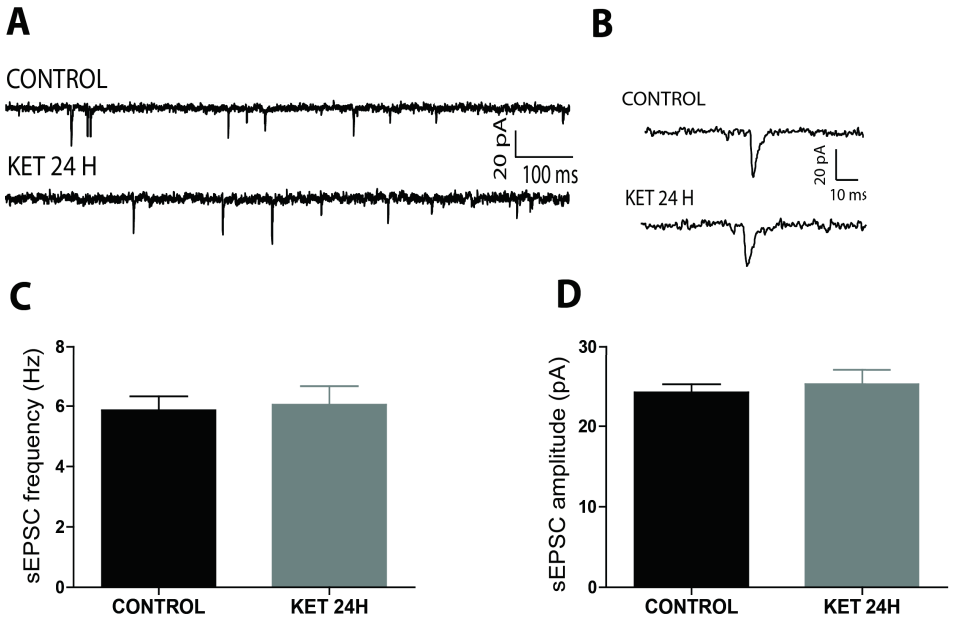

Figure 4.18. Effect of ketamine on spontaneous excitatory postsynaptic currents in *dorsal raphe* neurons. (A) Representative current traces showing sEPSCs in *dorsal raphe* (DR) neurons of control mice (control) and mice treated with ketamine (30 mg/kg, i.p.) 24 hours prior to the recordings (ket 24h). (B) Representative magnified sEPSCs of DR neurons illustrating similar amplitudes in control and ket 24h mice. (C) Summary bar graph showing similar sEPSC frequency and (D) amplitude between control and ket 24h mice. Bars represent mean ± S.E.M. of *n* experiments (*n* = 38 cells for control group; *n* = 13 for ket 24h group).

Then, we studied the specific mediation of the sEPSCs by AMPA receptors of DR neurons. For this purpose, in these experiments the selective NMDA receptor antagonist, D-AP5 (50 μM), was added to block excitatory transmission via NMDA receptors (Fig. 4.19A, B). On one hand, in control animals, D-AP5 produced no changes either in the sEPSCs frequency (control basal: 6.79 ± 0.52 Hz, n = 6; control D-AP5: 5.74 ± 1.05 Hz, n = 6) (Fig. 4.19C) or in the sEPSCs amplitude (control basal: 22.31 ± 0.67 pA, n = 6; control D-AP5: 20.66 ± 1.30 pA, n = 6) (Fig. 4.19D), demonstrating that sEPSCs in DR neurons are predominantly mediated by AMPA receptors in control animals. On the other hand, in mice treated with ketamine, the perfusion of D-AP5 did not alter the sEPSCs frequency (ket 24 h basal: 6.87 ± 0.88 Hz, n = 13; ket 24 h D-AP5: 6.09 ± 0.55 Hz, n = 13) or amplitude (ket 24 h basal: 25.55 ± 1.72 pA, n = 13; ket 24 h D-AP5: 23.14 ± 1.86 pA, n = 13).Therefore, the injection of ketamine 24 hours prior to the recordings did not alter the AMPA receptor-mediation of the frequency of the sEPSCs (control D-AP5: 5.74 ± 1.05 Hz, n = 6; ket 24 h D-AP5: 6.09 ± 0.55 Hz, n = 13. p = 0.7846, unpaired two-tailed t-test) (Fig. 4.19C, D).

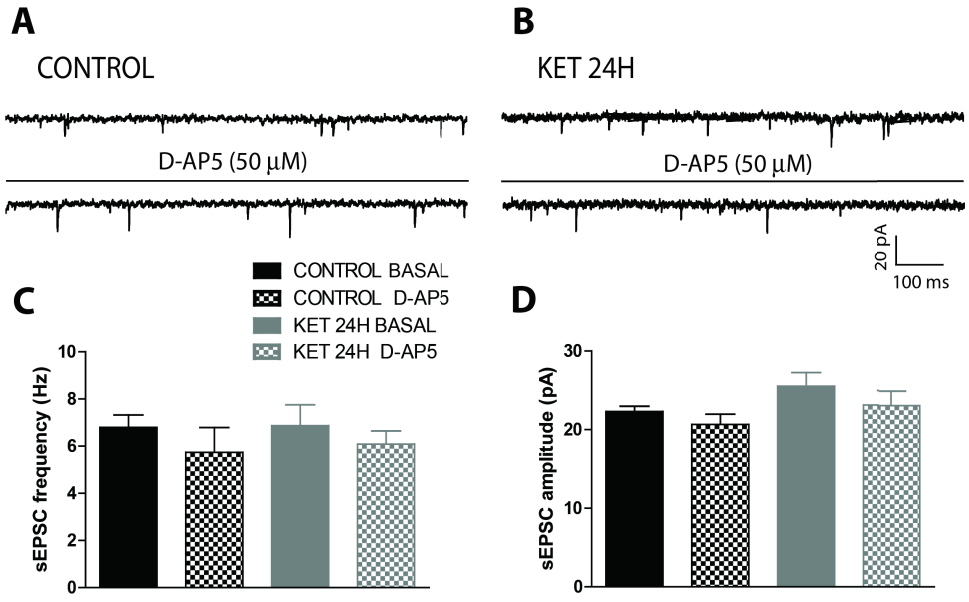

Figure 4.19. Effect of D-AP5 on spontaneous excitatory postsynaptic currents in *dorsal raphe* neurons of control mice and mice treated with ketamine. (A) Representative current traces showing sEPSCs, before and after D-AP5 perfusion (50 µM), in *dorsal raphe* (DR) neurons of control mice (control) and in (B) mice treated with ketamine (30 mg/kg, i.p.) 24 hours prior to the recordings (ket 24h). (C) Summary bar graph showing similar sEPSCs frequency and (D) amplitude before (control basal and ket 24h basal), and after D-AP5 perfusion (control D-AP5 and ket 24h D-AP5). Bars represent mean ± S.E.M. of *n* experiments (*n* = 6 for control groups; *n* = 13 for ket 24h groups).

Next, we assessed if ketamine was producing any effect on the eEPSCs of DR neurons. For this purpose, glutamate release was electrically evoked by a single-stimulus (100 μs at 10 Hz) application every 30 seconds at a holding potential of +40 mV in order to trigger simultaneously both AMPA and NMDA receptor-dependent eEPSCs (Fig. 4.20A). No differences were observed in the eEPSCs amplitude between groups (control: 460.10 ± 87.64 pA, n = 24; ket 24h: 415.10 ± 46.54 pA, n = 25). To further study whether ketamine was producing any alteration in the balance of AMPA/NMDA mediation of eEPSC, we studied the AMPA and NMDA receptor-dependent-eEPSCs separately in both groups (AMPA-eEPSCs and NMDA-eEPSCs). In order to do this, 15 min after evoking the first eEPSC, we bath-perfused the NMDA receptor antagonist, D-AP5 (50 μM), to block NMDA receptor dependent eEPSCs. No differences were observed between groups either in the AMPA-eEPSC amplitude (control: 332.3 ± 49.45 pA, n = 24; ket 24h: 296.00 ± 30.46 pA, n = 25) or in the NMDA-eEPSC amplitude (control: 101.51 ± 17.43 pA, n = 24; ket 24h: 132.82 ± 19.51 pA, n = 25). Therefore, no differences were found in the AMPA/NMDA ratio of the amplitude between groups (control: 3.86 ± 0.72, n = 24; ket 24h: 2.81 ± 0.36, n = 25) (Fig. 4.20B).

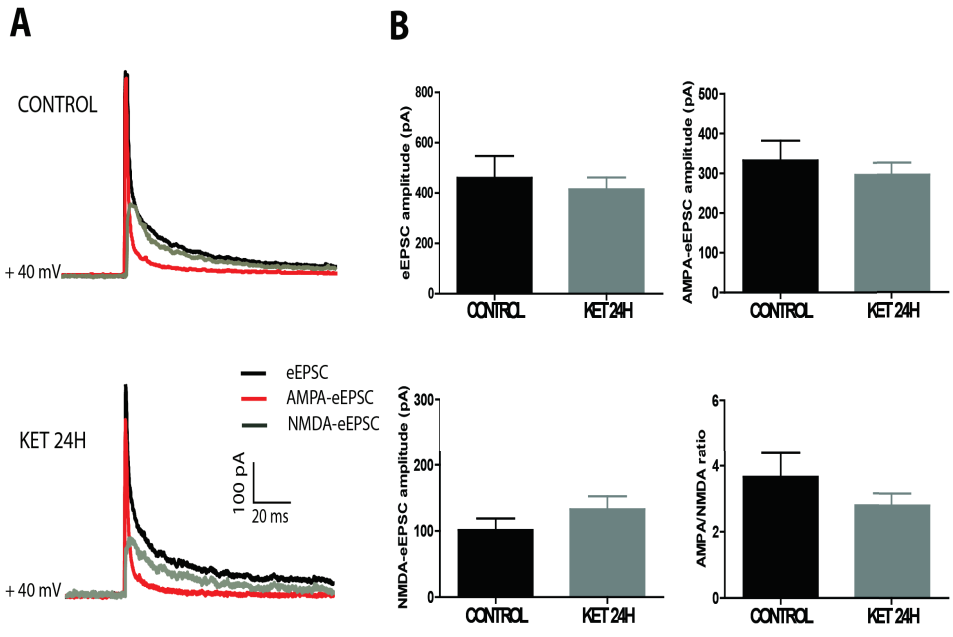

Figure 4.20. Effect of ketamine on the electrically-evoked excitatory postsynaptic currents in *dorsal raphe* neurons. (A) Representative recordings of eEPSCs in *dorsal raphe* (DR) neurons of control mice (control) and mice treated with ketamine (30 mg/kg, i.p.) 24 hours prior to the recordings (ket 24 h). The relative contribution of AMPA- and NMDA-eEPSCs is also shown. (B) Summary bar graph showing the eEPSCs amplitude, AMPA-eEPSCs amplitude, NMDA-eEPSCs amplitude, and AMPA/NMDA ratio of the amplitude in DR neurons of control (n = 24) and ket 24 h (n = 25) groups. Bars represent the means ± S.E.M. of n experiments.

4.3.3. *In vitro* electrophysiological acute effects of ketamine on the glutamatergic synaptic activity in *dorsal raphe* neurons

Next, we investigated if ketamine perfusion could alter the excitatory synaptic transmission of DR neurons. Thus, we bath-perfused ketamine (50 μM) during 10 min and examined the sEPSCs and eEPSCs in DR slices.

Regarding the sEPSCs of DR neurons, perfusion of ketamine during 10 min produced a statistically significant increase in the sEPSCs frequency at minute 5 (ket 5 min: 7.38 ± 0.97 Hz, $n = 8$) and at minute 10 (ket 10 min: 8.34 ± 1.69 Hz, $n = 8$), compared to the sEPSCs frequency prior to the ketamine perfusion (basal: 5.43 ± 1.08 Hz, $n = 8$. $p < 0.001$ for ket 5 min and $p < 0.0001$ for ket 10 min *vs* basal, repeated measures one-way ANOVA following Newman-Keuls post-hoc test) (Fig. 4.21A, C). Moreover, at minute 10, this increase in the frequency was significantly greater than the increase at minute 5 ($p < 0.001$, repeated measures one-way ANOVA following Newman-Keuls post-hoc test). Ketamine perfusion produced no changes in the sEPSCs amplitude either at minute 5 (ket 5 min: 16.83 ± 1.67 pA, $n = 8$) or at minute 10 (ket 10 min: 15.07 ± 1.34 pA, $n = 8$) compared to the sEPSC amplitude prior to the ketamine perfusion (basal: 15.98 ± 1.66 pA, $n = 8$) (Fig. 4.21B, D).

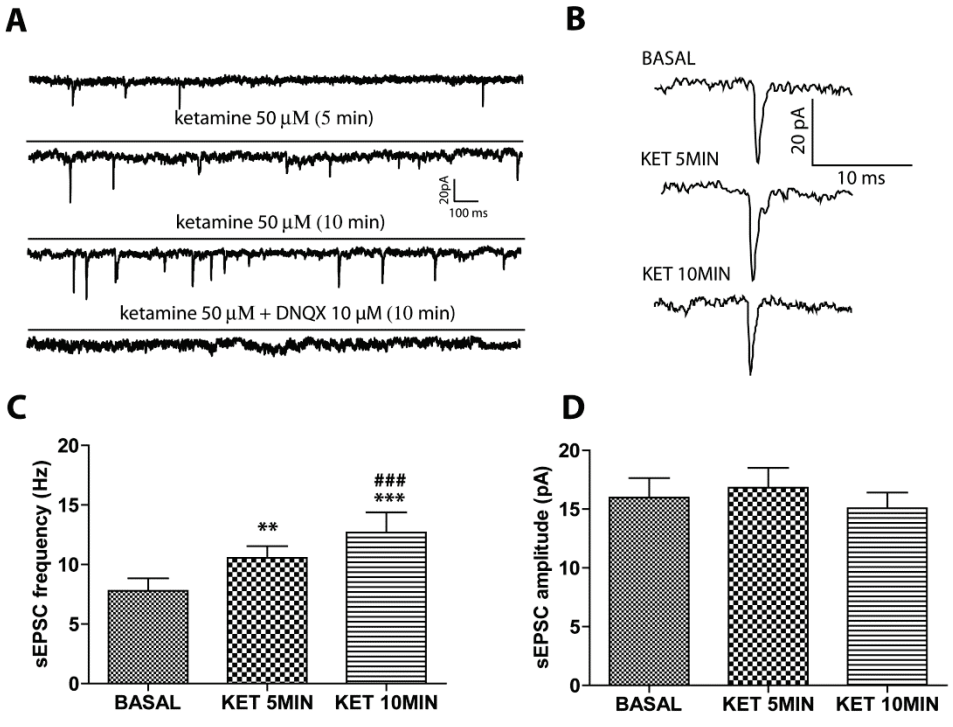

Figure 4.21. Effect of ketamine on spontaneous excitatory postsynaptic currents in *dorsal raphe* neurons. (A) Representative current traces showing sEPSCs, before (basal) and after 5 min (ket 5 min) and 10 min (ket 10 min) of ketamine perfusion (50 µM) in *dorsal raphe* (DR) neurons. The blockade of sEPSCs after ketamine perfusion by DNQX (10 µM) is also shown. (B) Representative magnified sEPSCs of DR neurons illustrating similar amplitudes in basal, ket 5 min and ket 10 min groups. (C) Summary bar graph showing the sEPSC frequency in basal, ket 5 min and ket 10 min groups. (D) Summary bar graph showing the sEPSC amplitude in basal, ket 5 min, and ket 10 min groups. Bars represent mean ± S.E.M. of *n* experiments (n = 8 for all the groups). $^{**}p <$ 0.001 and $^{***}p < 0.0001$ *vs* basal. $^{###}p < 0.001$ *vs* ket 5 min, repeated measures one-way ANOVA following Newman-Keuls post-hoc test.

Moreover, by comparison of the effect of ketamine to the previously described effect of D-AP5 on sEPSCs frequency, we could rule out the NMDA receptor antagonism as the mechanism by which ketamine is increasing glutamate release. In this sense, D-AP5 perfusion did not produce any change in sEPSCs frequency and amplitude, but the perfusion of ketamine did increase the sEPSCs, suggesting that ketamine is producing an increase in the excitatory synaptic through a NMDA-receptor independent mechanism (Fig. 4.19C and 4.21C). Moreover, the effect of ketamine perfusion on sEPSCs was completely blocked by the AMPA receptor antagonist DNQX (10 μM), demonstrating that the ketamine-induced effect increasing glutamate release is mediated by AMPA receptors (Fig. 4.21A).

Additionally, we assessed if ketamine could produce any effect on the eEPSC of DR neurons. Given that ketamine acts as an NMDA antagonist we did not measure the NMDA receptor-dependent eEPSCs. No changes were found in the AMPA-eEPSCs amplitude at minute 10 (ket 10 min: 330.3 ± 93.41 pA, n = 8) compared to control group (control: 332.2 ± 49.45 pA, n = 24) (Fig. 4.22).

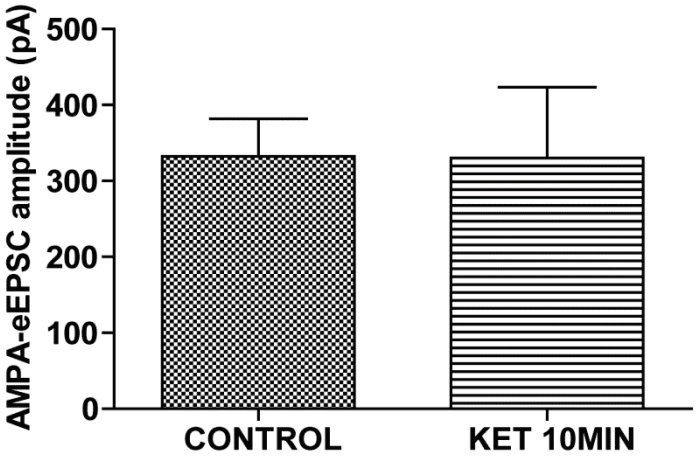

Figure 4.22. Effect of ketamine on the electrically-evoked excitatory postsynaptic currents in *dorsal raphe* neurons. Summary bar graph showing the AMPA receptor-mediated eEPSCs amplitude in *dorsal raphe* (DR) neurons in the absence of ketamine (control), and 10 min after ketamine perfusion (50 μM) (ket 10 min). Bars represent means ± S.E.M. of *n* experiments (*n* = 24 for control group and *n* = 8 for ket 10 min group).

4.3.4. *In vitro* electrophysiological effects of the mTOR inhibitor, PP242, on the glutamatergic synaptic activity in *dorsal raphe* neurons. Partial blockade by PP242 of the ketamine-induced effects on the spontaneous excitatory postsynaptic currents

It has been suggested that mammalian target of rapamycin (mTOR) activation positively regulates excitatory synaptic function (Schratt et al., 2004; Jaworski et al., 2005; Kumar et al., 2005), although mTOR activation has also been linked to depression of excitatory synaptic function (Hou and Klann, 2004). In addition, it has been also reported that ketamine produces some of its effects, including the antidepressant effects, by activation of the mTOR pathway (Li et al., 2010). Therefore, our aims were to evaluate the effect of the selective active-site mTOR inhibitor PP242 (Apsel et al., 2008; Choo and Blenis, 2009; Feldman et al., 2009; Dowling et al., 2010; Janes et al., 2010) on the glutamatergic synaptic activity of DR neurons, as well as to investigate if the observed increased sEPSCs frequency produced by ketamine was due to an activation of the mTOR in DR neurons.

4.3.4.1. Effect of PP242 on the glutamatergic synaptic activity in *dorsal raphe* neurons

We first incubated DR slices for at least 45 min with the mTOR inhibitor PP242 (2.5 μM) and examined the frequency and amplitude of sEPSCs. In the presence of PP242, frequency of sEPSCs in DR neurons remained unaltered compared to the frequency of sEPSCs in control animals (PP242: 7.98 ± 1.14 Hz, $n = 17$; control: 8.80 ± 1.14 Hz, $n = 5$) (Fig. 4.23A, C). However, the amplitude of sEPSCs in the presence of PP242 was statistically smaller than that in control animals (PP242: 20.99 ± 2.49 pA, $n = 17$; control: 34.07 ± 5.38 pA, $n = 5$. $p < 0.05$, unpaired two-tailed t-test) (Fig. 4.23B, D).

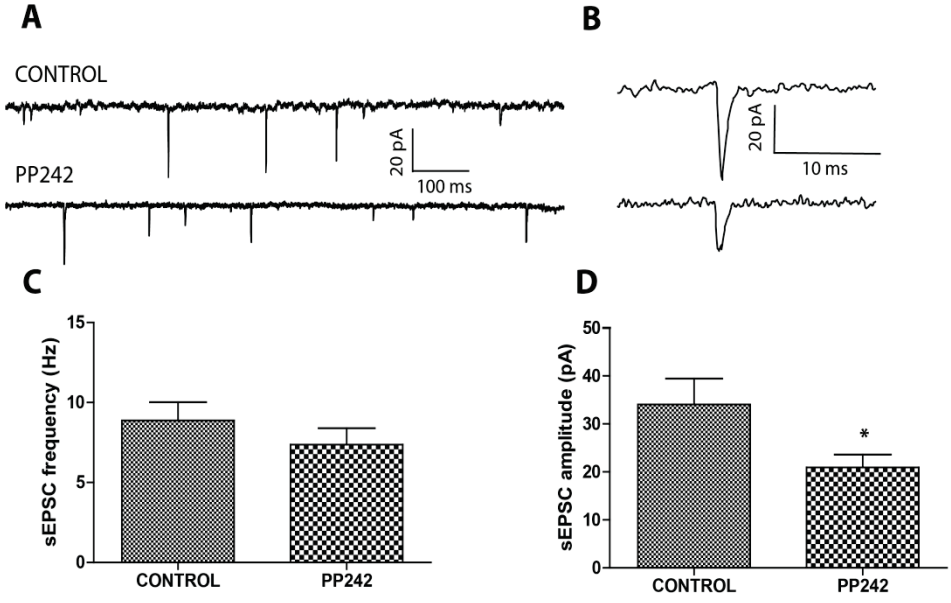

Figure 4.23. Effect of the mTOR inhibitor, PP242, on spontaneous excitatory postsynaptic currents in *dorsal raphe* neurons. (A) Representative current traces showing sEPSCs in *dorsal raphe* (DR) neurons of control mice (control) and DR slices incubated with the mTOR inhibitor PP242 (2.5 μM). (B) Representative magnified sEPSCs of DR neurons illustrating sEPSCs amplitude in control and PP242 groups. (C) Summary bar graph showing sEPSCs frequency in control and PP242 groups. (D) Summary bar graph showing sEPSCs amplitude in control and PP242 mice. Bars represent means ± S.E.M. of *n* experiments (n = 5 cells for control group and n = 17 for PP242 group). $^{*}p < 0.05$, unpaired two-tailed t-test.

4.3.4.2. Effect of PP242 on the ketamine-induced increase in the frequency of spontaneous excitatory postsynaptic currents in *dorsal raphe* neurons

Then, we studied the effect of PP242 on the increase in sEPSCs frequency induced by ketamine perfusion. For this purpose, we incubated DR slices with PP242 (2.5 μM) for at least 45 min, and recorded the spontaneous excitatory activity in DR neurons for at least 3 min. Then, we bath perfused ketamine (50 μM) for 10 min and examined the frequency and amplitude of sEPSCs in DR neurons. The perfusion of ketamine in the presence of PP242 did not significantly increase the sEPSCs frequency at minute 5 (PP242 + ket 5 min: 7.591 ± 0.88 Hz, n = 14) or at minute 10 (PP242 + ket 10 min: 8.338 ± 1.06 Hz, n = 14) compared to the sEPSC frequency prior to the ketamine perfusion (PP242 basal: 6.891 ± 1.17 Hz, n = 14) (Fig. 4.24A, B). Neither the sEPSC amplitude was different with the perfusion of ketamine at minute 5 (PP242 + ket 5 min: 27.41 ± 2.64 pA, n = 14) or at minute 10 (PP242 + ket 10 min: 25.44 ± 2.40 pA, n = 14), compared to the sEPSC amplitude prior to the ketamine perfusion (PP242 basal: 33.00 ± 3.64 pA, n = 14) (Fig. 4.24C). Taking into account the ketamine-induced increase in sEPSC frequency observed in control conditions (see section 4.3.3), and comparing it to the effect in the presence of PP242 (Fig. 4.24D), it seems that the mTOR activation mediates, at least in part, the effect of ketamine on glutamatergic synaptic activity of DR neurons.

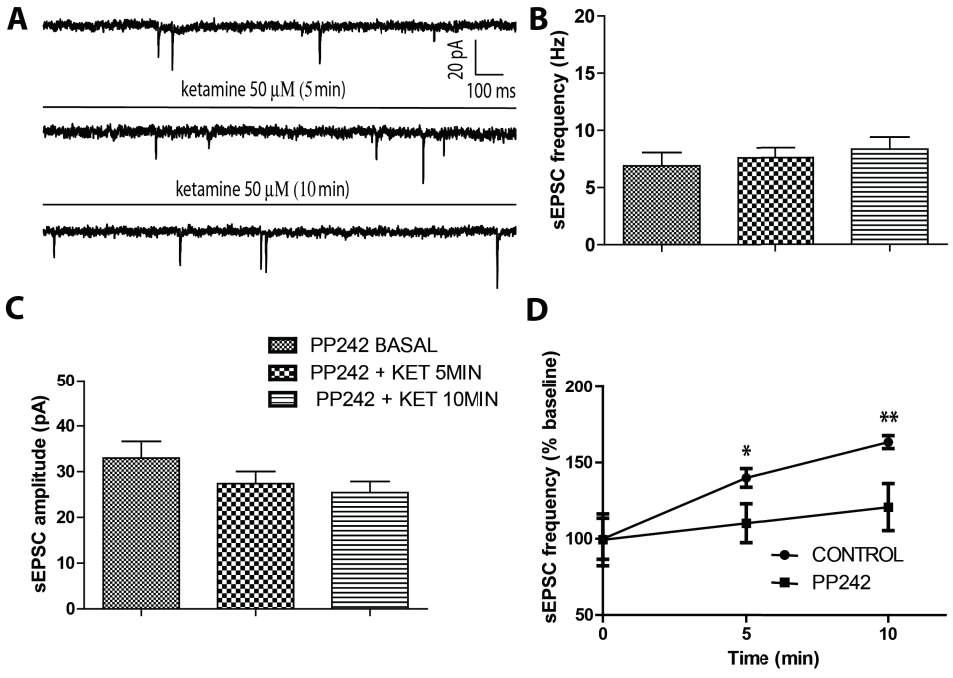

Figure 4.24. Effect of the mTOR inhibitor, PP242, on the ketamine-induced increase in frequency of spontaneous excitatory postsynaptic currents in *dorsal raphe* neurons. (A) Representative current traces showing sEPSCs before (PP242 basal), after 5 min (PP242 + ket 5 min), and after 10 min (PP242 + ket 10 min) of ketamine perfusion (50 µM) in *dorsal raphe* (DR) slices incubated with PP242 (2.5 µM). (B) Summary bar graph showing the sEPSC frequency in PP242 basal, PP242 + ket 5 min, and PP242 + ket 10 min mice. (C) Summary bar graph showing the sEPSCs amplitude in PP242 basal, PP242 + ket 5 min, and PP242 + ket 10 min mice. (D) Summary sEPSCs frequency-time plots normalized to basal values for the control group (ketamine perfusion without PP242, see section 4.3.3) and PP242 group, showing the effect of the perfusion of ketamine in both groups. Bars and dots represent mean ± S.E.M. of *n* experiments (*n* = 14 cells for PP242 basal, PP242 + ket 5 min, and PP242 + ket 10 min groups; *n* = 8 for control group). $^{*}p < 0.05$ and $^{**}p < 0.01$ *vs* control at min 0, repeated measures one-way ANOVA following Newman-Keuls post-hoc test.

4.3.5. Effect of ketamine administration on phospho-mTOR levels in the *dorsal raphe*

Finally, we investigated whether a single injection of ketamine (30 mg/kg; i.p.) produces acute and/or sustained effects on the mTOR pathway in the DR. For this purpose we studied the Ser 2448 (phospho-mTOR 2448) and Ser 2481 (phosphor-mTOR 2481) phophorylation sites of the mTOR, which are the Akt phophorylation site and the autophophorylation site of mTOR, respectively (Peterson et al., 2000; Hay and Sonenberg, 2004). In addition, we assessed the GβL expression, a protein that stimulates the mTOR kinase activity (Kim et al., 2003), mTOR expression, and Raptor expression, in mice injected with ketamine or with physiological saline (0.9 % NaCl, control mice).

Ketamine administration produced an increase in the expression of phospho-mTOR 2448 in the DR, being the expression levels 24 hours after the injection significantly higher than the levels obtained in control mice (ket 24 h: 0.6945 ± 0.05915, $n = 7$; ket 30 min: 0.6089 ± 0.03973, $n = 7$; control: 0.5180 ± 0.01971, $n = 7$. $p < 0.05$, one-way ANOVA followed by Newman-Keuls post-hoc test) (Fig. 4.25A). In addition, this increase was not due to a ketamine-induced increase in the expression of phospho-mTOR 2481 (autophophorylation site) or in the expression of no phosphorilated mTOR (Fig. 4.25B, E), suggesting that ketamine administration produced an activation of the Akt/mTOR pathway in the DR.

When examining the expression levels of the rest of the proteins studied, we showed that ketamine did not change the expression levels of any of them either 30 min or 24 hours after the injection (Fig. 4.25C, D, E).

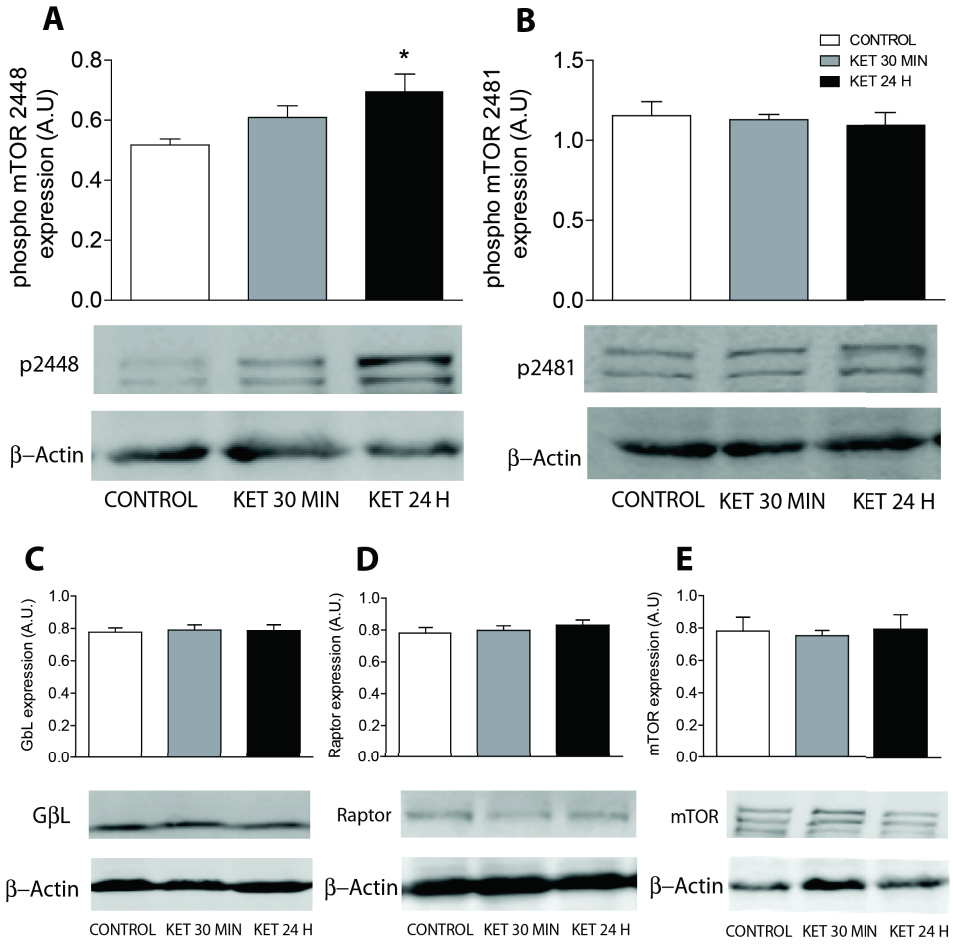

Figure 4.25. Effect of ketamine on phospho-mTOR 2448, phospho-mTOR 2481, GβL, raptor, and mTOR expression in the *dorsal raphe*. (A) Ketamine produced a statistically significant increase in the phospho mTOR 2448 levels in *dorsal raphe* (DR) 24 h after the injection. (B-E) Ketamine did not produce significant alterations in the expression levels of (B) phospho-mTOR 2481, (C) GβL, (D) raptor, and (E) mTOR in DR neurons, either 30 min or 24 h after the injection. Below the graphs are images of the blots showing phospho-mTOR 2448 (289 kDa), phosphor-mTOR 2481 (289 kDa), GβL (37 kDa), raptor (150 kDa), mTOR (289 kDa), and β-actin (42 kDa) expression from each experimental group. Bars represent mean ± SEM of *n* animals (*n* = 7 mice/group). $^{*}p < 0.05$ *vs* control group, one-way ANOVA following Newman-Keuls post-hoc test.

5. DISCUSSION

5. DISCUSSION

5.1. Deletion of GIRK2 subunit of GIRK channels alters 5-HT_{1A} receptor-mediated signaling and results in a depression-resistant behavior

The goal of our study was to determine the role that GIRK2 subunit-containing GIRK channels play in depression-related behaviors as well as in the control of 5-HT_{1A}-mediated inhibitory effects. We found that mice lacking GIRK2 subunits of GIRK channels display a depression-resistant phenotype combined with a reduced behavioral response to citalopram, an increase in the firing rate of DR neurons and a reduction of 5-HT_{1A} receptor-mediated responses. In addition, GIRK2 subunit deletion does not affect basal adult neurogenesis.

Our findings suggest that *Girk2* gene deletion promotes a depression-resistant behavior and determines the response to the antidepressant citalopram. Thus, $GIRK2^{-/-}$ mice showed a marked decrease in the immobility time in the tail suspension test (TST), and both $GIRK2^{+/-}$ and $GIRK2^{-/-}$ mice presented a lower latency to eat in the novelty suppressed feeding test (NSFT), that was not correlated with an increase in appetite. It is important to remark that general locomotor activity status is a confusing factor in these tests (Blednov et al., 2001a). Previous studies showed that $GIRK2^{-/-}$ mice, but not $GIRK2^{+/-}$ mice, have signs of hyperactivity (Blednov et al., 2001a; Cruz et al., 2008; Arora et al., 2010) that has been attributed to D1 receptor activation (Blednov et al., 2002). Given that $GIRK2^{+/-}$ mice do not have hyperactivity but showed depression-resistant phenotype in the NSFT, these results might be due to a less depressive-like behavior rather than to a more active state. We suggest that the 5-HT_{1A}-GIRK signaling may be mediating this depression-resistant phenotype: first, studies in 5-HT_{1A} receptor knockout mice show that they display an antidepressant-like phenotype under baseline conditions (Heisler et al., 1998; Mayorga et al., 2001), as we observed in GIRK2 mutant mice. Secondly, here citalopram was less potent in reducing the immobility in the TST. Similarly, it

has been reported that the expression of the antidepressant-like behavioral response of SSRIs in the TST requires the presence of functional 5-HT_{1A} receptors (Mayorga et al., 2001). Additionally, our observations are in line with those showing that chronic administration of fluoxetine exerts a beneficial influence on a rodent model of depression through suppression of GIRK-dependent signaling in the DR (Cornelisse et al., 2007). Interestingly, the depression-resistant phenotype that we observed here is combined with the previously reported reduced anxiety-like behavior that GIRK2 mutant mice display (Blednov et al., 2001a; Pravetoni and Wickman, 2008). Therefore, this phenotype represents a great advance over the classic antidepressed-like phenotype of 5-HT_{1A} knockout mice, since they display a robust anxiety-like behavior (Heisler et al., 1998; Parks et al., 1998; Ramboz et al., 1998). Given the constitutive and global nature of the *Girk2* gene deletion, it is not possible to completely identify the circuit(s) or neurotransmitter system(s) that explain this "antidepressive" phenotype. However, we can rule out the involvement of the $GABA_B$-GIRK2 signaling, since $GABA_B$ mutant mice showed elevated anxiety-related behaviors (Mombereau et al., 2004).

The implication of GIRK2 subunit-containing GIRK channels in the 5-HT_{1A} receptor-mediated neurotransmission is also supported by our *in vivo* electrophysiological findings. First, we observed that the lack of GIRK2 subunits induces an increase in the firing rate of DR neurons. This increase was also observed by the total blocking of GIRK channels with tertiapin-Q. On one hand, these results suggest that the intrinsic activity of GIRK2 subunit-containing GIRK channels controls the transmission in the DR. Similar findings have been obtained in LC neurons, where it has been observed that GIRK2 subunit-containing GIRK channels regulate the tonic activity of LC neurons *in vivo* (Torrecilla et al., 2013). *In vitro* studies have reported that dopamine neurons in $GIRK2^{-/-}$ mice exhibit a reduced firing rate (Arora et al., 2010), and in $GIRK2/3^{-/-}$ mice LC neurons show an increased firing rate (Cruz et al., 2008).

In addition, the contribution of GIRK2 subunits to the resting membrane potential has been reported in different type of neurons, including LC and HPP neurons (Luscher et al., 1997; Torrecilla et al., 2002; Chen and Johnston, 2005). Nevertheless, in layer 5/6 pyramidal neurons of the prelimbic cortex of GIRK2$^{-/-}$ mice, intrinsic electrophysiological properties remained unaltered compared to WT mice (Hearing et al., 2013). Taken all together, the contribution of GIRK2 subunits to neuronal excitability seems to vary across cell types and brain regions. On the other hand, the complete blockade of GIRK channels with tertiapin-Q results in a similar increase in the firing rate of DR neurons to that observed in GIRK2$^{-/-}$ mice. This suggests that GIRK2 subunits, though their expression is low in the DR (Saenz del Burgo et al., 2008), are forming important populations of GIRK channels, which are involved in the control of neuronal tonic activity. Given that GIRK1 subunits are almost absent when deleting GIRK2 subunits (Signorini et al., 1997), both GIRK1 and GIRK2 subunits might be forming functional GIRK channels that control the tonic 5-HT activity of the DR. Alternatively, alterations in neurotransmitter levels could also affect the firing pattern of DR neurons in GIRK2 mutant mice, since there are decreased and increased levels of 5-HT and 5-HIAA, respectively (Torrecilla et al., 2013). Secondly, our study also reveals that DR 5-HT$_{1A}$ receptors, both endogenously and exogenously activated, are affected by the deletion of GIRK2 subunits, which is shown by reduced receptor functionality. Similar results were observed in an *in vivo* electrophysiological study in LC neurons in GIRK2 mutant mice, showing that μ and α2 receptors were desensitized (Torrecilla et al., 2013). Our results agree with this study, indicating that in the DR, ablation of the *Girk2* gene produces loss of function of the 5-HT$_{1A}$-GIRK signaling pathway. It is important to remark that the reduced function of 5-HT$_{1A}$ and α_2 autoreceptors has been proposed as a key consequence of chronic antidepressant treatments, which would explain the delayed onset effect of antidepressants (McMillen et al., 1980; Lacroix et al., 1991; Artigas et al., 1996; Szabo et al., 2000; Invernizzi et al., 2001). In fact,

new pharmacological or genetic strategies to faster desensitize 5-HT_{1A} and α_2 autoreceptors have been of great interest in the study of depression treatment (Sanacora et al., 2004; Richardson-Jones et al., 2010; Portella et al., 2011). The observation that 8-OH-DPAT and citalopram preserved their maximal inhibitory efficacy is consistent with other studies. In LC neurons in GIRK2 mutant mice, the potency of morphine and clonidine was reduced, yet the inhibitory efficacy remained unaltered *in vivo* (Torrecilla et al., 2013). In hippocampal neurons in $GIRK2^{-/-}$ mice, *in vitro* postsynaptic GIRK currents induced by stimulation of the 5-HT_{1A} receptor were markedly reduced but not absent (Luscher et al., 1997). Studies conducted to determine the analgesic properties of morphine showed that while the potency of morphine was reduced, its efficacy was preserved in $GIRK2^{-/-}$ and $GIRK2/3^{-/-}$ mice (Mitrovic et al., 2003; Cruz et al., 2008). Also the pharmacological blockade of GIRK channels caused a reduction in the potency but not in the inhibitory efficacy of citalopram, supporting the role of GIRK2 subunit-containing GIRK channels in the inhibitory response of 5-HT_{1A} receptors. The dose of tertiapin-Q used was selected according to a previous study, where doses higher than 100 pmol caused dangerous effects (Marker et al., 2004). By testing the 8-OH-DPAT-induced hypothermia, which reflects the sensitivity of 5-HT_{1A} autoreceptors in mice (Goodwin et al., 1985; Richardson-Jones et al., 2011), we confirmed that GIRK2 subunits regulate the functionality of 5-HT_{1A} autoreceptors, as previously reported (Costa et al., 2005). Overall, all the functional findings in our work indicate that in the DR GIRK2 subunits may be forming important GIRK channel populations, in charge of controlling the tonic electrical activity and mediating of 5-HT_{1A} receptor-mediated signaling.

In addition, in adult hippocampal neurogenesis, the fate of neural progenitors is substantially conditioned by the emotional state, which is demonstrated by the fact that in enriched environments hippocampal stem cells give rise to more neurons and fewer stem cells than in impoverished

environments (Dranovsky et al., 2011). Specifically, it has also been confirmed that depressive behavior and stress responses are buffered by adult hippocampal neurogenesis (Snyder et al., 2011). Our findings show that in basal conditions, *Girk2* gene ablation promotes a depression-resistant phenotype without modifying adult neurogenesis in the DG of the HPP or in the SVZ. In line with this, it has also been observed that deletion of the background potassium channel TREK-1 results in a depression-resistant phenotype while the adult neurogenesis is unaltered (Heurteaux et al., 2006). It is worth mentioning that there is a very abundant expression of GIRK2 protein in the HPP and in the SVZ (Saenz del Burgo et al., 2008), and GIRK2 subunit-containing GIRK channels are also coupled to postsynaptic 5-HT_{1A} receptors (Luscher et al., 1997). Taking into consideration the presence and function of GIRK2 subunit-containing GIRK channels in the HPP, we suggest that the absence of changes in basal neurogenesis observed in GIRK2 mutant mice may be ascribed to the probable requirement of 5-HT_{1A} receptor stimulation to promote neurogenesis (Santarelli et al., 2003).

In conclusion, our results show the specific role of GIRK2 subunit-containing GIRK channels in the promotion of a depression-resistant phenotype, as well as their control of the tonic neuronal activity and mediation of the 5-HT_{1A} receptor inhibitory responses. New strategies targeting the 5-HT_{1A}-GIRK2 pathway could be of great therapeutic interest for the study of pathologies related to an altered 5-HT transmission, such as depression, and development of alternative treatments.

5.2. Altered inhibitory pre- and postsynaptic activity of *dorsal raphe* neurons in GIRK2 mutant mice

The goal of this study was, on one hand, to characterize the contribution of GIRK2 subunit-containing GIRK channels to the electrophysiological properties of DR neurons and, on the other hand, to determine the role that GIRK2 subunits play in the 5-HT, GABAergic and glutamatergic presynaptic and postsynaptic activity *in vitro,* when the majority of the projections to the DR are disrupted. The present work shows that GIRK2 subunits of GIRK channels contribute to some of the passive and active electrophysiological properties of DR neurons, and play a pivotal role in the control of 5-HT_{1A} and $GABA_B$ receptor-mediated postsynaptic currents. Moreover, also the inhibitory GABAergic pre- and postsynaptic activity is affected when deleting the GIRK2 subunit, whereas the excitatory glutamatergic synaptic activity remains unaltered.

The deletion of GIRK2 subunit increased the membrane input resistance of DR neurons, without altering the resting membrane potential. Given that changes in input resistance could be due to presence/absence or opening/closing of ion channels, such as K^+ and/or Cl^-, it is conceivable that the lack of GIRK channels increases the membrane input resistance of DR cells. In fact, in dorsal CA1 neurons, a higher adenosine A1 receptor-mediated GIRK channel activity has been demonstrated to be responsible of some differences in intrinsic membrane properties found between dorsal and ventral *hippocampus*, including the lower input resistance that dorsal CA1 neurons show (Kim and Johnston, 2015). Alternatively, and given that GIRK2 mutation also affects GABAergic transmission (see results section 4.2.3.), the observed increase in input resistance could be due to changes in $GABA_A$ receptors. In addition, the kinetic of action potentials in $GIRK2^{-/-}$ mice was faster, shown as a shorter half-width and decay time of the spikes.

However, no changes were observed in the *in vitro* stimulated 5-HT neuronal firing in GIRK2$^{-/-}$ mice compared to wild-type, although it was increased *in vivo* (see previous section). Therefore, once having detected that GIRK2$^{-/-}$ mice have a dysfunctional GABAergic activity, we suggest that the decreased GABAergic inhibition in DR could account for the increased 5-HT neuronal firing that GIRK2 mutant mice show. Some *in vitro* studies show that GIRK2 subunit-containing GIRK channels contribute to the electrophysiological properties of neurons from different brain regions, mainly hyperpolarizing the membrane potential (Luscher et al., 1997; Torrecilla et al., 2002). However, others provide opposite results in Layer 5/6 *prelimbic cortex* (Hearing et al., 2013). From our results we suggest that in DR the tonic activity of GIRK2 subunit-containing GIRK channels contribute to some of the passive and active electrophysiogical properties of DR neurons, without impacting on the excitability of the membrane *in vitro*.

In addition, here we showed that 5-CT-induced whole-cell postsynaptic currents were greatly reduced in DR neurons of GIRK2 mutant mice. Similarly, baclofen-induced whole-cell postsynaptic currents were also markedly diminished when deleting the GIRK2 subunit, suggesting that GIRK channels formed by GIRK2 subunits mediate the inhibitory actions of 5-HT$_{1A}$ and GABA$_B$ receptors. Collectively, these results indicate that there is a postsynaptic expression of GIRK2 subunits forming GIRK channels coupled to 5-HT$_{1A}$ and GABA$_B$ receptors in DR neurons, and importantly, GIRK2 subunits are the main responsible for the control of both 5-HT$_{1A}$ and GABA$_B$ receptor-mediated postsynaptic transmissions. It has been previously reported that in the DR both GABA$_B$ and 5-HT$_{1A}$ receptors are coupled to a common pool of GIRK channels (Mannoury la Cour et al., 2004), which mediate their inhibitory actions. In this study we further demonstrate that the specific ablation of GIRK2 subunits affects to the same extent 5-HT$_{1A}$ and GABA$_B$ receptor-mediated postsynaptic currents in DR neurons. Although not studied in the DR till date,

the involvement of specific GIRK subunits in the whole-cell currents induced by stimulation of different GPCRs has been demonstrated in different brain areas. In CA1 pyramidal cells from the *hippocampus*, baclofen-, adenosine-, and 5-HT-induced postsynaptic currents were essentially absent in GIRK2$^{-/-}$ mice (Luscher et al., 1997). In the same way, in mice lacking GIRK2 subunit-containing GIRK channels a great reduction of the baclofen-induced currents was shown in VTA dopamine neurons compared to those in wild-type mice (Arora et al., 2010). In addition, another study in LC neurons of GIRK2 mutant mice showed that met-enkephalin-induced whole-cell currents were markedly reduced (Torrecilla et al., 2002). Similar results were obtained studying the morphine-induced postsynaptic currents in these mice in LC neurons (Cruz et al., 2008). Altogether, the contribution of GIRK2 subunits to the postsynaptic currents induced by agonists of inhibitory GPCR seems to be consistent in different regions. Interestingly, in our work it was still visible a small residual current, also seen in LC neurons of GIRK2/3 double knockout mice (Torrecilla et al., 2002). The modest presence of other GIRK subunits in the DR, such as GIRK1 and/or GIRK3 (Saenz del Burgo et al., 2008) could account for this small current. However, given that GIRK1 subunits are almost absent when deleting GIRK2 subunits (Signorini et al., 1997; Torrecilla et al., 2002), it seems unlikely that this subunit is mediating the residual current. Alternatively, another possible explanation is the involvement of GIRK-independent mechanisms. In this sense, it has been demonstrated that baclofen-induced currents in VTA neurons were greatly reduced in GIRK2$^{-/-}$ mice, and the small residual current was Ba^{2+} insensitive, which is a K^+ channels blocker, demonstrating its GIRK-independent nature. Given that it was inhibited by a cAMP analog, the involvement of the two-pore K^+ channel family was suggested (Cruz et al., 2004).

The current study indicates that GABAergic synaptic transmission is impaired in the DR of GIRK2 mutant mice. Regarding the GABAergic

presynaptic activity, the frequency of sIPSCs in DR neurons in GIRK2 mutant mice was reduced compared to that in wild-type mice, suggesting that probability of release of GABA in these mutant mice is diminished compared to wild-type. In addition, from the evoked synaptic activity we observed that the amplitude of the peak1 of the eIPSC was decreased in GIRK2$^{-/-}$ mice compared to wild-type mice and it was accompanied by a greater paired-pulse ratio. All of these effects are associated with a decrease in neurotransmitter release (Bonci and Williams, 1997; Dobrunz and Stevens, 1997; Melis et al., 2002; Kirby et al., 2008). Thus, these results suggest that in the DR GIRK2 subunits are expressed presynaptically and control the release of GABA. In the DR presynaptic $GABA_B$ receptors are expressed in both 5-HT and GABA cells (Innis and Aghajanian, 1987; Waldmeier et al., 1988; Bowery, 1993) and they exert an inhibitory control over GABA release (Brenowitz et al., 1998; Waldmeier et al., 2008; Kobayashi et al., 2012). Accordingly, when deleting the GIRK2 subunit there would be a loss of functionality of the GIRK channel that could limit the $GABA_B$ receptor-mediated GABA release. Our results indicate that the deletion of GIRK2 subunit diminishes the release of GABA, which is contrary to the expected effect given the inhibitory nature of GIRK channels. Therefore, it is likely that other mechanisms impacted by the mutation would be affecting the release of GABA.

Regarding the presynaptic role of GIRK channels observed in this study, it has been repeatedly reported the presynaptic labeling of GIRK channels in the proximity of active zone with a potential role in the regulation of neurotransmitter release (Ponce et al., 1996; Drake et al., 1997; Grosse et al., 2003; Koyrakh et al., 2005; Aguado et al., 2008). In addition, it has been reported that Ba^{2+} can block the $GABA_B$ receptor-mediated presynaptic inhibition in the *hippocampus* (Misgeld et al., 1989; Thompson and Gahwiler, 1992). Characterizations of $GABA_B$ receptor-mediated presynaptic inhibition in *Xenopus oocytes* have revealed a component that is sensitive to the GIRK-

specific channel blocker tertiapin-Q (Jin and Lu, 1998). Indeed, in VTA dopamine neurons it has been demonstrated that the inhibition of $GABA_A$ receptor-mediated eIPSC occurs via activation of presynaptic GIRK channels (Michaeli and Yaka, 2010). In the same line, it has been described that in the rat *cerebral cortex* the presynaptic actions of $GABA_B$ receptors involve GIRK channel activation (Ladera et al., 2008). Altogether, our results, which are in line with these results, indicate that there is a presynaptic expression of GIRK2 subunit-containing GIRK channels in DR neurons, which play a key role in the control of GABA release. Nevertheless, there are other studies that suggest that GIRK channels are not implicated in the presynaptic actions mediated by different receptors, and therefore, these observations are still a matter of debate. As an example, it has been demonstrated that in *ventrolateral periaqueductal gray* neurons, GIRK channels underlie postsynaptic but not presynaptic $GABA_B$ receptor-mediated inhibition (Liu et al., 2012). In hippocampal cells, when evaluating the presynaptic inhibition induced by different GPCR agonists, no impairments were seen in $GIRK2^{-/-}$ mice compared to wild-type mice, even though postsynaptic actions of the different agonists were reduced (Luscher et al., 1997). It was then suggested that in hippocampal cells, GPCRs in response to agonists exert a presynaptic depression by a GIRK-independent signaling mechanisms, such as the inhibition of Ca^{2+} channels or an interaction with the release machinery. Overall, this suggests that the presynaptic contribution of GIRK channels to the neurotransmitter release could be depending on their subunit composition, cell type-specific expression, and cellular localization among brain areas.

To further study the difference in GABA release found between genotypes, we perfused antagonists of 5-HT_{1A} and $GABA_B$ receptors onto DR slices. In wild-type animals, antagonists of both receptors induced an increase in the frequency, but not amplitude, of sIPSCs, but this effect was not seen in $GIRK2^{-/-}$ mice. First, this indicates that in normal conditions, as observed in

wild-type mice, presynaptic 5-HT_{1A} ad $GABA_B$ receptors exert a tonic inhibitory control over GABA release in DR neurons, possibly through a 5-HT-mediated indirect effect and a GABA direct effect over GABA release. It has been shown that $GABA_{A/B}$ and 5-$HT1_{A/B}$ agonists decrease 5-HT and GABA release in rat *raphe nuclei* (Bagdy et al., 2000), so it is conceivable that antagonist of these receptors would increase the release of GABA, as seen in this study. Secondly, since antagonists of 5-HT_{1A} and $GABA_B$ receptors had no effect on $GIRK2^{-/-}$ mice, these results further support the idea that in DR neurons, GIRK2 subunit-containing GIRK channels are coupled to these presynaptic receptors and more importantly, they regulate the roles of $GABA_B$ receptors on GABA release.

Two main observations in this study make us to come to the idea that GIRK2 subunit deletion alters the fast GABAergic postsynaptic activity. First, the amplitude of sIPSCs is reduced in GIRK2 mutant mice, indicating that postsynaptic factors could be altered. Secondly, unexpectedly, GABA-induced fast inward currents were markedly reduced in $GIRK2^{-/-}$ mice, suggesting that the functionality of postsynaptic $GABA_A$ receptors is under the control of GIRK2 channels and/or 5-HT_{1A} and $GABA_B$ receptors in the DR. Similarly, the inactivation of 5-HT_{1A} receptors in mice has revealed that expression of certain $GABA_A$ receptor subunits as well as the whole receptor functionality are under the control of 5-HT_{1A} receptors in the *hippocampus* and other brain regions (Sibille et al., 2000). In fact, one possible explanation for this GABA regulation by 5-HT_{1A} receptors in the *hippocampu*s is that due to their coupling to GIRK channels, genetic inactivation of the receptor could alter the membrane potential, frequency and duration of electrical impulses (Aghajanian and Lakoski, 1984; Corradetti et al., 1996) leading to a depolarization and increase in depolarization-evoked Ca^{2+} influx. Alternatively, chronic lack of GABA in the DR of these GIRK2 mutant mice could also lead to compensative or adaptative mechanisms regarding the functionality of postsynaptic GABA

receptors. Nevertheless, further studies will be needed to reveal how GIRK2 subunit-containing GIRK channels are controlling the $GABA_A$ receptor-mediated transmission in the DR.

Taking these results beyond their physiological meaning, and linking the observed GABAergic dysfunction to the depression-resistant phenotype that GIRK2 mutant mice display, it is important to indicate that much evidence identifies a GABAergic dysfunction in mood disorders. It has been described a GABAergic deficit in prefrontal regions of unmedicated depressed patients, and also in the PFC in animal models of depression (induced by chronic social defeat stress, CSDS) (Hasler et al., 2007; Venzala et al., 2013). On the contrary, GABA levels in the DR are not altered in mice subjected to CSDS (Venzala et al., 2013). It has been shown that chronic treatment with the SSRI fluoxetine, which is known to desensitize $5\text{-}HT_{1A}$ receptors, reduces GABAergic transmission in the *visual cortex* (Maya Vetencourt et al., 2008), and reduces eIPSCs in the PFC of normal rats (Zhong and Yan, 2004). In addition, the repeated administration of imipramine, which is a tricyclic antidepressant, markedly reduces the GABAergic transmission in healthy rats, as frequency of sIPSCs in layer 2/3 pyramidal neurons was decreased (Wabno and Hess, 2013).

In this sense, from our studies we observe that mice lacking GIRK2 subunits show desensitized $5\text{-}HT_{1A}$ receptors and also a reduced frequency of sIPSCs, mimicking the effects of repeated antidepressant administrations on 5-HT and GABAergic transmissions. It is also important to mention that Challis et al. (2013) showed that social defeat stress, which results in long-lasting social avoidance and is sensitive to the effects of antidepressants (Berton et al., 2006; Tsankova et al., 2006), suppresses the 5-HT neuronal firing through increased activity of GABA interneurons in the DR.

Furthermore, decreasing GABA activity dishinibited 5-HT cells and promoted a "resilient" phenotype in mice exposed to social defeat (Challis et al., 2013). It is interesting that in our study GIRK2$^{-/-}$ mice show a depression-resistant phenotype and an increased 5-HT neuronal firing combined with a decreased GABA transmission in the DR. Therefore, further investigations in GIRK2$^{-/-}$ mice aimed at studying other physiological changes that occur during depression and antidepressant treatments might elucidate if these mutant mice could be regarded as an "antidepressant" model or as an animal model of repeated antidepressant administration.

Regarding the glutamatergic neurotransmission in the DR, it is intact in GIRK2$^{-/-}$ mice, since no alterations are displayed on properties of sEPSCs and eEPSCs compared to those in wild-type mice. The involvement of GIRK2 subunit-containing GIRK channels in the glutamatergic neurotransmission has been reported the rat cerebral *cortex*. In this case, $GABA_B$ receptors reduce glutamate release via P/Q-type Ca^{2+} channels, and this response is reversed by the GIRK channel blocker tertiapin-Q (Ladera et al., 2008). In addition, dopamine neurons from the VTA GIRK2$^{-/-}$ showed an elevated glutamatergic neurotransmission (Arora et al., 2010). However, given that this effect was paralleled by increased synaptic levels of AMPA receptors, it is likely that GIRK2 subunit deletion affects glutamatergic neurotransmission involving secondary adaptations facilitating glutamatergic signaling in the mesolimbic reward system. Despite lacking data regarding the synaptic levels of AMPA and NMDA receptors in the DR, in the present study we separately evaluated AMPA- and NMDA-mediated eEPSCs and we did not observe differences between the AMPA/NMDA ratio in DR neurons of GIRK2 mutant mice and wild-type mice. This suggests that GIRK2 subunit deletion does not affect the AMPA and NMDA receptors synaptic levels, although further studies aimed at quantifying AMPA and NMDA synaptic levels could directly confirm it.

Altogether, our data indicate that the 5-HT and GABAergic systems are affected by the deletion of GIRK2 subunits. Thus, both intrinsic and extrinsic inhibitory mechanisms are diminished in DR neurons of GIRK2 mutant mice. In addition, the dysregulation of the GABAergic transmission could disrupt the balance between the glutamatergic and GABAergic systems, which is an important factor in the pathophysiology and treatment of mood disorders, including depression (Krystal, 2007).

5.3. Ketamine promotes electrophysiological and biochemical alterations in the glutamatergic transmission in the *dorsal raphe*

In this study we used electrophysiological and biochemical approaches to determine whether ketamine is altering the glutamatergic transmission and the mTOR pathway in the DR, besides exerting rapid antidepressant actions. In this way, we replicated the clinical and preclinical findings of ketamine in humans and in mice, showing that ketamine has acute and sustained antidepressant-like effects in behavioral models. Electrophysiological analysis revealed that the acute administration of ketamine increased the frequency of sEPSCs in DR neurons, which was attenuated by the pre-incubation of the slices with the mTOR inhibitor PP242. However, when ketamine was administered 24 hours prior to the recordings it produced no effects either in sEPSCs or eEPSCs, pointing out a functional difference between the acute and sustained effects of ketamine in the DR. The differential functional effects between the acute and sustained actions of ketamine extend to the intracellular mTOR signaling. In this sense, we found that ketamine administered 30 min before the experiments did not induce the phosphorylation of mTOR in the DR, whereas 24 hours after the administration of ketamine, it increased the levels of the phosphorylated and active form of mTOR in the DR. Collectively, these results identify functional actions of ketamine on the glutamatergic transmission in the DR, and also reveal that the electrophysiological "rapid onset effects", which may trigger other functional/cellular effects, are not maintained 24 hours after the ketamine administration.

The administration of some glutamatergic antagonists in humans, and specifically a single intravenous infusion of ketamine, has demonstrated that these compounds can alleviate depressive symptoms in patients within hours of administration (Berman et al., 2000; Zarate et al., 2006). These effects in humans have been widely mimicked in animal models of depression (Maeng et al., 2008; Li et al., 2010; Gigliucci et al., 2013; Koike et al., 2013). In this

study, we replicated these reported acute and sustained antidepressant-like effects of ketamine (30 mg/kg, i.p.), using the TST 30 minutes and 24 hours after the ketamine injection. The dose used was selected based on previous literature where ketamine doses lower than 50 mg/kg (i.p.) had significant antidepressant-like effects without impacting on locomotor activity, ataxia, and stereotypy (Popik et al., 2008; Li et al., 2010; Koike et al., 2011; Koike et al., 2013).

It has also been reported that ketamine exerts the antidepressant-like effects via activation of the mTOR and the mTOR-dependent synapse formation, given that local infusions of the mTOR inhibitor, ramapycin in the PFC blocked the acute behavioral effect of ketamine and the formation of spines (Li et al., 2010; Li et al., 2011). In this sense, we found that 24 hours after ketamine administration mTOR signaling was also activated in the DR, but only a slight tendency to be increased was seen 30 minutes after the injection. On one hand, this may suggest that the acute antidepressant effects of ketamine do not involve mTOR signaling activation, whereas the sustained effects do involve an activation of the mTOR pathway in the DR. In this sense, another study reports that the upstream components of the mTOR pathway, BDNF/TrK, are not involved in the acute behavioral effects of ketamine but they play an important role in the sustained antidepressant-like effects (Koike et al., 2013). On the other hand, Li et al. (2010) showed that in the mPFC mTOR signaling was highly activated 30 minutes after the injection, and this activation returned to baseline levels 2 hours after the injection, even though the antidepressant-like effect persists for at least 24 hours. Thus, another possible explanation may be that ketamine is first activating the mTOR pathway in PFC and then, through the prominent projections to the DR (Aghajanian and Wang, 1977; Takagishi and Chiba, 1991; Hajos et al., 1998; Peyron et al., 1998; Celada et al., 2001), indirectly acting on the mTOR pathway in the DR. Thus, the time required to obtain this latter indirect effect in the DR might explain the absence of changes

in mTOR phosphorylation levels 30 minutes after the ketamine injection. From a behavioral point of view, the fact that ketamine induced an activation of the mTOR pathway in both the PFC and DR may be important, given that it has been recently shown that selective activation of mPFC cells projecting to the DR induces a profound and rapid effect on selection of the active behavioral state in the forced swim test in freely moving rats (Warden et al., 2012).

Ketamine perfusion onto DR slices induced an increase in the frequency of sEPSCs in the DR neurons, but no other changes were found regarding the amplitude of sEPSCs, amplitude of eEPSCs, and AMPA/NMDA ratio. The observed increase in sEPSC frequency can be attributed to an increase in presynaptic glutamate release probability and/or an increase in excitatory synapse density. However, to observe the latter effect more time would be required, given that it has been shown that ketamine increases spine density in the PFC 24 hours after treatment (Li et al., 2010). This suggests that it is likely that ketamine is inducing a presynaptic glutamate release in DR neurons. Although several studies have shown that systemically administered NMDA receptor antagonists increase glutamate release in the mPFC (Adams Moghaddam et al., 1997; Moghaddam and Adams, 1998; and Moghaddam, 2001), another study in the *striatum* provides different results (Yamamoto et al., 1999). The mechanism that we propone here is that, as occurs in mPFC, ketamine may produce disinhibition of GABAergic inputs within the DR, which are abundant, to the glutamate-containing neurons thereby enhancing the glutamate release. It has been repeatedly reported that ketamine requires AMPA receptors to exert antidepressant actions (Li et al., 2010; Koike et al., 2011; Maeng et al., 2008; Tizabi et al., 2012). Thus, we asked if the observed ketamine-induced increase in sIPSCs was mediated by AMPA receptors. For this purpose, we tested D-AP5, which is an NMDA receptor antagonist, and it did not mimic ketamine's effect. Moreover, DNQX, which is an AMPA receptor antagonist, completely blocked it, suggesting that the ketamine-induced

increase in sEPSCs frequency observed in our work may be mediated by DR AMPA receptors. In fact, Nishitani et al. (2014) also showed the involvement of DR AMPA receptors in ketamine-induced effects. Here, we examined the effect of ketamine 50 μM, which it is a concentration below the anesthetic range (McCardle and Gartside, 2012) and that would correspond to the brain levels reached after an intraperitoneal injection of 30 mg/kg, given that ketamine brain levels in mice after 100 mg/kg (i.p.) have been reported to be approximately 180 μM (Irifune et al., 1992; Petrenko et al., 2004).

It has been reported that the electrophysiological effects induced by ketamine in the PFC are blocked by the local infusion of the mTOR inhibitor rapamycin (Li et al., 2010). Similarly, in our study we show the pre-incubation of DR slices with the potent and selective active-site mTOR inhibitor, PP242 attenuated the increase in sEPSC frequency shown after perfusion of ketamine, suggesting that in the DR mTOR pathway may play a key role in the ketamine-induced glutamate release. In this sense, it has been previously reported that mTOR activation positively regulates excitatory synaptic function (Schratt et al., 2004; Jaworski et al., 2005; Kumar et al., 2005).

Regarding the electrophysiological effects of ketamine 24 hours after the injection, we found that neither the sEPSCs nor the eEPSCs were changed. In contrast, the electrophysiological effects of ketamine in 5-HT-induced EPSCs in the PFC are maintained 24 hours after the injection (Li et al., 2010) suggesting that the duration of the ketamine-induced electrophysiological changes could be depending on the brain region, being more prolonged in the PFC than in the DR.

The DR has received much attention in the study of the pathophysiology of depression, and ketamine effects have been well described in the PFC. Given the prominent connections between these regions, and the evidence regarding the involvement of PFC-DR projections in behavioral responses related to depressive states, we believe that this study provides relevant data suggesting that also the DR may play a key role in the effects of the new-type fast-acting glutamatergic antidepressants.

6. CONCLUSIONS

6. CONCLUSIONS

1. GIRK2 subunits control the DR tonic activity *in vivo,* since DR neurons from GIRK2$^{-/-}$ mice show an increased firing rate compared to wild-type mice. Moreover, the blockade of GIRK channels with tertiapin-Q results in a similar increase in the firing rate of DR neurons to that observed in GIRK2$^{-/-}$ mice, indicating that GIRK2 subunits are the main subunits in those GIRK channel populations that control DR activity in a constitutive manner.

2. *In vivo,* the inhibitory effect induced by the stimulation of 5-HT$_{1A}$ autoreceptors is regulated by GIRK2 subunit-containing GIRK channels. Since the inhibitory potency of the 5-HT$_{1A}$ receptor agonist 8-OH-DPAT, and the selective serotonin reupake inhibitor, citalopram is diminished compared to that in wild-type, this result suggests that 5-HT$_{1A}$ autoreceptors are desensitized in GIRK2$^{-/-}$ mice.

3. GIRK2 subunit-containing GIRK channels contribute to the occurrence of depression-related behaviors. This is supported by our results showing that GIRK2 mutant mice show depression-resistant behaviors in the tail suspension test and novelty suppressed feeding test.

4. 5-HT$_{1A}$-GIRK2 signaling pathway mediates, at least in part, the behavioral response to citalopram, since in GIRK2 mutant mice citalopram causes a lower antidepressant effect compared to that in wild-type mice.

5. GIRK2 subunit-containing channels are not essential for adult neurogenesis**,** since basal levels of proliferating cells in the *dentate gyrus* and subventricular zone are unaltered in GIRK2 mutant mice compared to those in wild-type mice.

Conclusions

6. *In vitro*, membrane intrinsic characteristics of DR neurons are controlled by GIRK2 subunit-containing GIRK channels, since DR neurons of GIRK2$^{-/-}$ mice have a higher input resistance compared to wild-type mice.

7. GIRK2 subunit-containing GIRK channels in the DR are expressed postsynaptically and play a pivotal role in the *in vitro* outward currents induced by activation of 5-HT$_{1A}$ and GABA$_B$ receptors. This is supported by the almost absent 5-CT- and baclofen-induced currents in DR neurons of GIRK2$^{-/-}$ mice observed in this study.

8. GIRK channels formed by GIRK2 subunits are expressed at the presynaptic level where they exert a robust control over GABA release. This is demonstrated by our *in vitro* results showing that deletion of GIRK2 subunit causes a reduction in the frequency of sIPSCs, a decrease in the amplitude of eIPSCs, and an increase in the paired-pulse ratio.

9. The inhibition of GABA release by presynaptic 5-HT$_{1A}$ and GABA$_B$ receptors is limited by GIRK2 subunit-containing GIRK channels. This is confirmed by the *in vitro* results showing that, contrary to wild-type mice, the perfusion of 5-HT$_{1A}$ and GABA$_B$ receptor antagonists do not increase the frequency or amplitude of sIPSCs in DR neurons in GIRK2$^{-/-}$ mice.

10. The fast GABAergic postsynaptic activity in the DR is critically controlled by GIRK2 subunit containing GIRK channels, as it is demonstrated by our *in vitro* results showing a decreased amplitude of sIPSCs and diminished GABA$_A$ receptor-mediated inward currents in GIRK2$^{-/-}$ mice compared to those in wild-type mice.

11. On the contrary, GIRK channels containing GIRK2 subunit do not control the glutamatergic input in the DR, since no alterations are observed either in the sEPSCs or in the eEPSCs in DR neurons of GIRK2$^{-/-}$ mice compared to wild-type mice.

12. The electrophysiological effects of ketamine related to its antidepressant-like actions extend to the DR and involve AMPA receptors, since acute ketamine selectively increases the frequency of AMPA-sEPSCs. Moreover, since another NMDA antagonist, D-AP5, fails to mimic this effect these results indicate that ketamine is increasing the glutamatergic synaptic activity through a NMDA-independent mechanism.

13. mTOR activation in the DR is necessary for the acute electrophysiological effects of ketamine in this area, and it is involved its sustained antidepressant-like behavioral effects. This is demonstrated by the fact that pre-incubation with the mTOR inhibitor, PP242 partially blocks the ketamine-induced increase in the frequency of AMPA-sEPSCs, and additionally, 24 hours after ketamine injection mice show a marked antidepressant-like behavior together with mTOR activation in the DR.

In conclusion, approaches directed towards the pharmacological blockade or genetic removal of the GIRK2 subunit could limit the occurrence of depression-related behaviors, and specifically addressing GIRK2 subunits in the DR could give rise to faster acting therapies in depression. Furthermore, the DR constitutes a target for new strategies aimed at improving the current scenario of depression treatment. In this sense, in the DR ketamine promotes the “glutamate surge” and the accompanying AMPA activation, which are proposed requirements for generating the antidepressant-like response of ketamine.

7. REFERENCES

A

Aan Het Rot, M., Zarate, C.A.,Jr, Charney, D.S., Mathew, S.J., 2012. Ketamine for depression: where do we go from here? Biol. Psychiatry 72, 537-547.

Abdallah, C.G., Sanacora, G., Duman, R.S., Krystal, J.H., 2015. Ketamine and rapid-acting antidepressants: a window into a new neurobiology for mood disorder therapeutics. Annu. Rev. Med. 66, 509-523.

Abellan, M.T., Adell, A., Honrubia, M.A., Mengod, G., Artigas, F., 2000a. GABAB-RI receptors in serotonergic neurons: effects of baclofen on 5-HT output in rat brain. Neuroreport 11, 941-945.

Abellan, M.T., Jolas, T., Aghajanian, G.K., Artigas, F., 2000b. Dual control of dorsal raphe serotonergic neurons by GABA(B) receptors. Electrophysiological and microdialysis studies. Synapse 36, 21-34.

Abrams, J.K., Johnson, P.L., Hollis, J.H., Lowry, C.A., 2004. Anatomic and functional topography of the dorsal raphe nucleus. Ann. N. Y. Acad. Sci. 1018, 46-57.

Adams, B.W., Moghaddam, B., 2001. Effect of clozapine, haloperidol, or M100907 on phencyclidine-activated glutamate efflux in the prefrontal cortex. Biol. Psychiatry 50, 750-757.

Adell, A., Carceller, A., Artigas, F., 1993. In vivo brain dialysis study of the somatodendritic release of serotonin in the Raphe nuclei of the rat: effects of 8-hydroxy-2-(di-n-propylamino)tetralin. J. Neurochem. 60, 1673-1681.

Adell, A., Celada, P., Abellan, M.T., Artigas, F., 2002. Origin and functional role of the extracellular serotonin in the midbrain raphe nuclei. Brain Res. Brain Res. Rev. 39, 154-180.

References

Aghajanian, G.K., Lakoski, J.M., 1984. Hyperpolarization of serotonergic neurons by serotonin and LSD: studies in brain slices showing increased K+ conductance. Brain Res. 305, 181-185.

Aghajanian, G.K., Wang, R.Y., 1977. Habenular and other midbrain raphe afferents demonstrated by a modified retrograde tracing technique. Brain Res. 122, 229-242.

Aghajanian, G.K., Wang, R.Y., Baraban, J., 1978. Serotonergic and non-serotonergic neurons of the dorsal raphe: reciprocal changes in firing induced by peripheral nerve stimulation. Brain Res. 153, 169-175.

Agnati, L.F., Fuxe, K., Hokfelt, T., Benfenati, F., Calza, L., Johansson, O., De Mey, J., 1982. Morphometric characterization of transmitter-identified nerve cell groups: analysis of mesencephalic 5-HT nerve cell bodies. Brain Res. Bull. 9, 45-51.

Aguado, C., Colon, J., Ciruela, F., Schlaudraff, F., Cabanero, M.J., Perry, C., Watanabe, M., Liss, B., Wickman, K., Lujan, R., 2008. Cell type-specific subunit composition of G protein-gated potassium channels in the cerebellum. J. Neurochem. 105, 497-511.

Akinfiresoye, L., Tizabi, Y., 2013. Antidepressant effects of AMPA and ketamine combination: role of hippocampal BDNF, synapsin, and mTOR. Psychopharmacology (Berl) 230, 291-298.

Allers, K.A., Sharp, T., 2003. Neurochemical and anatomical identification of fast- and slow-firing neurones in the rat dorsal raphe nucleus using juxtacellular labelling methods in vivo. Neuroscience 122, 193-204.

Amargos-Bosch, M., Lopez-Gil, X., Artigas, F., Adell, A., 2006. Clozapine and olanzapine, but not haloperidol, suppress serotonin efflux in the medial

prefrontal cortex elicited by phencyclidine and ketamine. Int. J. Neuropsychopharmacol. 9, 565-573.

Andrade, L., Caraveo-Anduaga, J.J., Berglund, P., Bijl, R.V., De Graaf, R., Vollebergh, W., Dragomirecka, E., Kohn, R., Keller, M., Kessler, R.C., Kawakami, N., Kilic, C., Offord, D., Ustun, T.B., Wittchen, H.U., 2003. The epidemiology of major depressive episodes: results from the International Consortium of Psychiatric Epidemiology (ICPE) Surveys. Int. J. Methods Psychiatr. Res. 12, 3-21.

Andrade, R., 1998. Regulation of membrane excitability in the central nervous system by serotonin receptor subtypes. Ann. N. Y. Acad. Sci. 861, 190-203.

Andrade, R., Malenka, R.C., Nicoll, R.A., 1986. A G protein couples serotonin and GABAB receptors to the same channels in hippocampus. Science 234, 1261-1265.

Apsel, B., Blair, J.A., Gonzalez, B., Nazif, T.M., Feldman, M.E., Aizenstein, B., Hoffman, R., Williams, R.L., Shokat, K.M., Knight, Z.A., 2008. Targeted polypharmacology: discovery of dual inhibitors of tyrosine and phosphoinositide kinases. Nat. Chem. Biol. 4, 691-699.

Arango, V., Underwood, M.D., Boldrini, M., Tamir, H., Kassir, S.A., Hsiung, S., Chen, J.J., Mann, J.J., 2001. Serotonin 1A receptors, serotonin transporter binding and serotonin transporter mRNA expression in the brainstem of depressed suicide victims. Neuropsychopharmacology 25, 892-903.

Arora, D., Haluk, D.M., Kourrich, S., Pravetoni, M., Fernandez-Alacid, L., Nicolau, J.C., Lujan, R., Wickman, K., 2010. Altered neurotransmission

in the mesolimbic reward system of Girk mice. J. Neurochem. 114, 1487-1497.

Arora, D., Hearing, M., Haluk, D.M., Mirkovic, K., Fajardo-Serrano, A., Wessendorf, M.W., Watanabe, M., Lujan, R., Wickman, K., 2011. Acute cocaine exposure weakens GABA(B) receptor-dependent G-protein-gated inwardly rectifying K+ signaling in dopamine neurons of the ventral tegmental area. J. Neurosci. 31, 12251-12257.

Artigas, F., 1993. 5-HT and antidepressants: new views from microdialysis studies. Trends Pharmacol. Sci. 14, 262.

Artigas, F., Bel, N., Casanovas, J.M., Romero, L., 1996. Adaptative changes of the serotonergic system after antidepressant treatments. Adv. Exp. Med. Biol. 398, 51-59.

Artigas, F., Perez, V., Alvarez, E., 1994. Pindolol induces a rapid improvement of depressed patients treated with serotonin reuptake inhibitors. Arch. Gen. Psychiatry 51, 248-251.

Aryal, P., Dvir, H., Choe, S., Slesinger, P.A., 2009. A discrete alcohol pocket involved in GIRK channel activation. Nat. Neurosci. 12, 988-995.

Aso, E., Renoir, T., Mengod, G., Ledent, C., Hamon, M., Maldonado, R., Lanfumey, L., Valverde, O., 2009. Lack of CB1 receptor activity impairs serotonergic negative feedback. J. Neurochem. 109, 935-944.

Austin, M.C., Weikel, J.A., Arango, V., Mann, J.J., 1994. Localization of serotonin 5-HT1A receptor mRNA in neurons of the human brainstem. Synapse 18, 276-279.

Autry, A.E., Adachi, M., Nosyreva, E., Na, E.S., Los, M.F., Cheng, P.F., Kavalali, E.T., Monteggia, L.M., 2011. NMDA receptor blockade at rest triggers rapid behavioural antidepressant responses. Nature 475, 91-95.

Azmitia, E.C., Gannon, P.J., 1986. The primate serotonergic system: a review of human and animal studies and a report on Macaca fascicularis. Adv. Neurol. 43, 407-468.

Azmitia, E.C., Gannon, P.J., Kheck, N.M., Whitaker-Azmitia, P.M., 1996. Cellular localization of the 5-HT1A receptor in primate brain neurons and glial cells. Neuropsychopharmacology 14, 35-46.

B

Bacci, A., Huguenard, J.R., Prince, D.A., 2004. Long-lasting self-inhibition of neocortical interneurons mediated by endocannabinoids. Nature 431, 312-316.

Bagdy, E., Kiraly, I., Harsing, L.G.,Jr, 2000. Reciprocal innervation between serotonergic and GABAergic neurons in raphe nuclei of the rat. Neurochem. Res. 25, 1465-1473.

Bagdy, E., Solyom, S., Harsing, L.G.,Jr, 1998. Feedback stimulation of somatodendritic serotonin release: a 5-HT3 receptor-mediated effect in the raphe nuclei of the rat. Brain Res. Bull. 45, 203-208.

Baker, K.G., Halliday, G.M., Tork, I., 1990. Cytoarchitecture of the human dorsal raphe nucleus. J. Comp. Neurol. 301, 147-161.

Balana, B., Bahima, L., Bodhinathan, K., Taura, J.J., Taylor, N.M., Nettleton, M.Y., Ciruela, F., Slesinger, P.A., 2013. Ras-association domain of

sorting Nexin 27 is critical for regulating expression of GIRK potassium channels. PLoS One 8, e59800.

Balana, B., Maslennikov, I., Kwiatkowski, W., Stern, K.M., Bahima, L., Choe, S., Slesinger, P.A., 2011. Mechanism underlying selective regulation of G protein-gated inwardly rectifying potassium channels by the psychostimulant-sensitive sorting nexin 27. Proc. Natl. Acad. Sci. U. S. A. 108, 5831-5836.

Bambico, F.R., Katz, N., Debonnel, G., Gobbi, G., 2007. Cannabinoids elicit antidepressant-like behavior and activate serotonergic neurons through the medial prefrontal cortex. J. Neurosci. 27, 11700-11711.

Baraban, J.M., Aghajanian, G.K., 1980. Suppression of firing activity of 5-HT neurons in the dorsal raphe by alpha-adrenoceptor antagonists. Neuropharmacology 19, 355-363.

Barnes, N.M., Sharp, T., 1999. A review of central 5-HT receptors and their function. Neuropharmacology 38, 1083-1152.

Baumann, B., Bielau, H., Krell, D., Agelink, M.W., Diekmann, S., Wurthmann, C., Trubner, K., Bernstein, H.G., Danos, P., Bogerts, B., 2002. Circumscribed numerical deficit of dorsal raphe neurons in mood disorders. Psychol. Med. 32, 93-103.

Baumgarten, H.G., Grozdanovic, Z., 1997. Anatomy of Central Serotonergic Projection Systems. In: Baumgartem H.G., Bothert M. (Ed) Serotonergic neurons and 5-HT receptors in the DNS. Handb. Exp. Pharmacol. Springer, Vol. 129 (Berlin) p. 41

Bayliss, D.A., Li, Y.W., Talley, E.M., 1997. Effects of serotonin on caudal raphe neurons: activation of an inwardly rectifying potassium conductance. J. Neurophysiol. 77, 1349-1361.

Beck, S.G., Pan, Y.Z., Akanwa, A.C., Kirby, L.G., 2004. Median and dorsal raphe neurons are not electrophysiologically identical. J. Neurophysiol. 91, 994-1005.

Beckstead, M.J., Williams, J.T., 2007. Long-term depression of a dopamine IPSC. J. Neurosci. 27, 2074-2080.

Beckstead, R.M., Domesick, V.B., Nauta, W.J., 1979. Efferent connections of the substantia nigra and ventral tegmental area in the rat. Brain Res. 175, 191-217.

Becquet, D., Hery, M., Deprez, P., Faudon, M., Fache, M.P., Giraud, P., Hery, F., 1993a. N-methyl-D-aspartic acid/glycine interactions on the control of 5-hydroxytryptamine release in raphe primary cultures. J. Neurochem. 61, 1692-1697.

Becquet, D., Hery, M., Francois-Bellan, A.M., Giraud, P., Deprez, P., Faudon, M., Fache, M.P., Hery, F., 1993b. Glutamate, GABA, glycine and taurine modulate serotonin synthesis and release in rostral and caudal rhombencephalic raphe cells in primary cultures. Neurochem. Int. 23, 269-283.

Behzadi, G., Kalen, P., Parvopassu, F., Wiklund, L., 1990. Afferents to the median raphe nucleus of the rat: retrograde cholera toxin and wheat germ conjugated horseradish peroxidase tracing, and selective D-[3H]aspartate labelling of possible excitatory amino acid inputs. Neuroscience 37, 77-100.

References

Bel, N., Artigas, F., 1992. Fluvoxamine preferentially increases extracellular 5-hydroxytryptamine in the raphe nuclei: an in vivo microdialysis study. Eur. J. Pharmacol. 229, 101-103.

Berman, R.M., Cappiello, A., Anand, A., Oren, D.A., Heninger, G.R., Charney, D.S., Krystal, J.H., 2000. Antidepressant effects of ketamine in depressed patients. Biol. Psychiatry 47, 351-354.

Berney, A., Nishikawa, M., Benkelfat, C., Debonnel, G., Gobbi, G., Diksic, M., 2008. An index of 5-HT synthesis changes during early antidepressant treatment: alpha-[11C]methyl-L-tryptophan PET study. Neurochem. Int. 52, 701-708.

Berton, O., McClung, C.A., Dileone, R.J., Krishnan, V., Renthal, W., Russo, S.J., Graham, D., Tsankova, N.M., Bolanos, C.A., Rios, M., Monteggia, L.M., Self, D.W., Nestler, E.J., 2006. Essential role of BDNF in the mesolimbic dopamine pathway in social defeat stress. Science 311, 864-868.

Bessa, J.M., Ferreira, D., Melo, I., Marques, F., Cerqueira, J.J., Palha, J.A., Almeida, O.F., Sousa, N., 2009. The mood-improving actions of antidepressants do not depend on neurogenesis but are associated with neuronal remodeling. Mol. Psychiatry 14, 764-73, 739.

Bessa, J.M., Morais, M., Marques, F., Pinto, L., Palha, J.A., Almeida, O.F., Sousa, N., 2013. Stress-induced anhedonia is associated with hypertrophy of medium spiny neurons of the nucleus accumbens. Transl. Psychiatry. 3, e266.

Best, T.K., Siarey, R.J., Galdzicki, Z., 2007. Ts65Dn, a mouse model of Down syndrome, exhibits increased GABAB-induced potassium current. J. Neurophysiol. 97, 892-900.

Bischoff, S., Leonhard, S., Reymann, N., Schuler, V., Shigemoto, R., Kaupmann, K., Bettler, B., 1999. Spatial distribution of GABA(B)R1 receptor mRNA and binding sites in the rat brain. J. Comp. Neurol. 412, 1-16.

Blednov, Y.A., Stoffel, M., Alva, H., Harris, R.A., 2003. A pervasive mechanism for analgesia: activation of GIRK2 channels. Proc. Natl. Acad. Sci. U. S. A. 100, 277-282.

Blednov, Y.A., Stoffel, M., Chang, S.R., Harris, R.A., 2001a. GIRK2 deficient mice. Evidence for hyperactivity and reduced anxiety. Physiol. Behav. 74, 109-117.

Blednov, Y.A., Stoffel, M., Chang, S.R., Harris, R.A., 2001b. Potassium channels as targets for ethanol: studies of G-protein-coupled inwardly rectifying potassium channel 2 (GIRK2) null mutant mice. J. Pharmacol. Exp. Ther. 298, 521-530.

Blednov, Y.A., Stoffel, M., Cooper, R., Wallace, D., Mane, N., Harris, R.A., 2002. Hyperactivity and dopamine D1 receptor activation in mice lacking girk2 channels. Psychopharmacology (Berl) 159, 370-378.

Blier, P., Bergeron, R., 1995. Effectiveness of pindolol with selected antidepressant drugs in the treatment of major depression. J. Clin. Psychopharmacol. 15, 217-222.

Blier, P., de Montigny, C., 1994. Current advances and trends in the treatment of depression. Trends Pharmacol. Sci. 15, 220-226.

Blier, P., Pineyro, G., el Mansari, M., Bergeron, R., de Montigny, C., 1998. Role of somatodendritic 5-HT autoreceptors in modulating 5-HT neurotransmission. Ann. N. Y. Acad. Sci. 861, 204-216.

Blier, P., Zigman, D., Blier, J., 2012. On the safety and benefits of repeated intravenous injections of ketamine for depression. Biol. Psychiatry 72, e11-2.

Bligh-Glover, W., Kolli, T.N., Shapiro-Kulnane, L., Dilley, G.E., Friedman, L., Balraj, E., Rajkowska, G., Stockmeier, C.A., 2000. The serotonin transporter in the midbrain of suicide victims with major depression. Biol. Psychiatry 47, 1015-1024.

Boden, P.R., Woodruff, G.N., Pinnock, R.D., 1991. Pharmacology of a cholecystokinin receptor on 5-hydroxytryptamine neurones in the dorsal raphe of the rat brain. Br. J. Pharmacol. 102, 635-638.

Boeijinga, P.H., Boddeke, H.W., 1993. Serotonergic modulation of neurotransmission in the rat subicular cortex in vitro: a role for 5-HT1B receptors. Naunyn Schmiedebergs Arch. Pharmacol. 348, 553-557.

Bonci, A., Williams, J.T., 1997. Increased probability of GABA release during withdrawal from morphine. J. Neurosci. 17, 796-803.

Boothman, L., Raley, J., Denk, F., Hirani, E., Sharp, T., 2006. In vivo evidence that 5-HT(2C) receptors inhibit 5-HT neuronal activity via a GABAergic mechanism. Br. J. Pharmacol. 149, 861-869.

Bortolozzi, A., Artigas, F., 2003. Control of 5-hydroxytryptamine release in the dorsal raphe nucleus by the noradrenergic system in rat brain. Role of alpha-adrenoceptors. Neuropsychopharmacology 28, 421-434.

Boschert, U., Amara, D.A., Segu, L., Hen, R., 1994. The mouse 5-hydroxytryptamine1B receptor is localized predominantly on axon terminals. Neuroscience 58, 167-182.

Bouthenet, M.L., Martres, M.P., Sales, N., Schwartz, J.C., 1987. A detailed mapping of dopamine D-2 receptors in rat central nervous system by autoradiography with [125I]iodosulpride. Neuroscience 20, 117-155.

Bowery, N.G., 1993. GABAB receptor pharmacology. Annu. Rev. Pharmacol. Toxicol. 33, 109-147.

Bowery, N.G., Hudson, A.L., Price, G.W., 1987. GABAA and GABAB receptor site distribution in the rat central nervous system. Neuroscience 20, 365-383.

Boyer, S.B., Clancy, S.M., Terunuma, M., Revilla-Sanchez, R., Thomas, S.M., Moss, S.J., Slesinger, P.A., 2009. Direct interaction of GABAB receptors with M2 muscarinic receptors enhances muscarinic signaling. J. Neurosci. 29, 15796-15809.

Brenowitz, S., David, J., Trussell, L., 1998. Enhancement of synaptic efficacy by presynaptic GABA(B) receptors. Neuron 20, 135-141.

Brown, R.E., Sergeeva, O., Eriksson, K.S., Haas, H.L., 2001. Orexin A excites serotonergic neurons in the dorsal raphe nucleus of the rat. Neuropharmacology 40, 457-459.

Bruinvels, A.T., Landwehrmeyer, B., Gustafson, E.L., Durkin, M.M., Mengod, G., Branchek, T.A., Hoyer, D., Palacios, J.M., 1994. Localization of 5-HT1B, 5-HT1D alpha, 5-HT1E and 5-HT1F receptor messenger RNA in rodent and primate brain. Neuropharmacology 33, 367-386.

Bruzos-Cidon, C., Llamosas, N., Ugedo, L., Torrecilla, M., 2015. Dysfunctional inhibitory mechanisms in locus coeruleus neurons of the Wistar Kyoto rat. Int. J. Neuropsychopharmacol.

Burlhis, T.M., Aghajanian, G.K., 1987. Pacemaker potentials of serotonergic dorsal raphe neurons: contribution of a low-threshold Ca2+ conductance. Synapse 1, 582-588.

C

Calizo, L.H., Akanwa, A., Ma, X., Pan, Y.Z., Lemos, J.C., Craige, C., Heemstra, L.A., Beck, S.G., 2011. Raphe serotonin neurons are not homogenous: electrophysiological, morphological and neurochemical evidence. Neuropharmacology 61, 524-543.

Celada, P., Artigas, F., 1993. Monoamine oxidase inhibitors increase preferentially extracellular 5-hydroxytryptamine in the midbrain raphe nuclei. A brain microdialysis study in the awake rat. Naunyn Schmiedebergs Arch. Pharmacol. 347, 583-590.

Celada, P., Puig, M.V., Casanovas, J.M., Guillazo, G., Artigas, F., 2001. Control of dorsal raphe serotonergic neurons by the medial prefrontal cortex: Involvement of serotonin-1A, GABA(A), and glutamate receptors. J. Neurosci. 21, 9917-9929.

Challis, C., Boulden, J., Veerakumar, A., Espallergues, J., Vassoler, F.M., Pierce, R.C., Beck, S.G., Berton, O., 2013. Raphe GABAergic neurons mediate the acquisition of avoidance after social defeat. J. Neurosci. 33, 13978-88, 13988a.

Chan, K.W., Sui, J.L., Vivaudou, M., Logothetis, D.E., 1997. Specific regions of heteromeric subunits involved in enhancement of G protein-gated K+ channel activity. J. Biol. Chem. 272, 6548-6555.

Chang, B., Daniele, C.A., Gallagher, K., Madonia, M., Mitchum, R.D., Barrett, L., Vezina, P., McGehee, D.S., 2011. Nicotinic excitation of serotonergic projections from dorsal raphe to the nucleus accumbens. J. Neurophysiol. 106, 801-808.

Chen, X., Johnston, D., 2005. Constitutively active G-protein-gated inwardly rectifying K+ channels in dendrites of hippocampal CA1 pyramidal neurons. J. Neurosci. 25, 3787-3792.

Choo, A.Y., Blenis, J., 2009. Not all substrates are treated equally: implications for mTOR, rapamycin-resistance and cancer therapy. Cell. Cycle 8, 567-572.

Chu, D.C., Albin, R.L., Young, A.B., Penney, J.B., 1990. Distribution and kinetics of GABAB binding sites in rat central nervous system: a quantitative autoradiographic study. Neuroscience 34, 341-357.

Clancy, S.M., Boyer, S.B., Slesinger, P.A., 2007. Coregulation of natively expressed pertussis toxin-sensitive muscarinic receptors with G-protein-activated potassium channels. J. Neurosci. 27, 6388-6399.

Clancy, S.M., Fowler, C.E., Finley, M., Suen, K.F., Arrabit, C., Berton, F., Kosaza, T., Casey, P.J., Slesinger, P.A., 2005. Pertussis-toxin-sensitive Galpha subunits selectively bind to C-terminal domain of neuronal GIRK channels: evidence for a heterotrimeric G-protein-channel complex. Mol. Cell. Neurosci. 28, 375-389.

Clarke, T.K., Laucht, M., Ridinger, M., Wodarz, N., Rietschel, M., Maier, W., Lathrop, M., Lourdusamy, A., Zimmermann, U.S., Desrivieres, S., Schumann, G., 2011. KCNJ6 is associated with adult alcohol dependence and involved in gene x early life stress interactions in adolescent alcohol drinking. Neuropsychopharmacology 36, 1142-1148.

References

Clemett, D.A., Punhani, T., Duxon, M.S., Blackburn, T.P., Fone, K.C., 2000. Immunohistochemical localisation of the 5-HT2C receptor protein in the rat CNS. Neuropharmacology 39, 123-132.

Collins, P.Y., Patel, V., Joestl, S.S., March, D., Insel, T.R., Daar, A.S., Scientific Advisory Board and the Executive Committee of the Grand Challenges on Global Mental Health, Anderson, W., Dhansay, M.A., Phillips, A., Shurin, S., Walport, M., Ewart, W., Savill, S.J., Bordin, I.A., Costello, E.J., Durkin, M., Fairburn, C., Glass, R.I., Hall, W., Huang, Y., Hyman, S.E., Jamison, K., Kaaya, S., Kapur, S., Kleinman, A., Ogunniyi, A., Otero-Ojeda, A., Poo, M.M., Ravindranath, V., Sahakian, B.J., Saxena, S., Singer, P.A., Stein, D.J., 2011. Grand challenges in global mental health. Nature 475, 27-30.

Commons, K.G., 2009. Locally collateralizing glutamate neurons in the dorsal raphe nucleus responsive to substance P contain vesicular glutamate transporter 3 (VGLUT3). J. Chem. Neuroanat. 38, 273-281.

Commons, K.G., Connolley, K.R., Valentino, R.J., 2003. A neurochemically distinct dorsal raphe-limbic circuit with a potential role in affective disorders. Neuropsychopharmacology 28, 206-215.

Cooper, A., Grigoryan, G., Guy-David, L., Tsoory, M.M., Chen, A., Reuveny, E., 2012. Trisomy of the G protein-coupled K+ channel gene, Kcnj6, affects reward mechanisms, cognitive functions, and synaptic plasticity in mice. Proc. Natl. Acad. Sci. U. S. A. 109, 2642-2647.

Corey, S., Clapham, D.E., 1998. Identification of native atrial G-protein-regulated inwardly rectifying K+ (GIRK4) channel homomultimers. J. Biol. Chem. 273, 27499-27504.

Cornelisse, L.N., Van der Harst, J.E., Lodder, J.C., Baarendse, P.J., Timmerman, A.J., Mansvelder, H.D., Spruijt, B.M., Brussaard, A.B., 2007. Reduced 5-HT1A- and GABAB receptor function in dorsal raphe neurons upon chronic fluoxetine treatment of socially stressed rats. J. Neurophysiol. 98, 196-204.

Corradetti, R., Le Poul, E., Laaris, N., Hamon, M., Lanfumey, L., 1996. Electrophysiological effects of N-(2-(4-(2-methoxyphenyl)-1-piperazinyl)ethyl)-N-(2-pyridinyl) cyclohexane carboxamide (WAY 100635) on dorsal raphe serotonergic neurons and CA1 hippocampal pyramidal cells in vitro. J. Pharmacol. Exp. Ther. 278, 679-688.

Costa, A.C., Stasko, M.R., Stoffel, M., Scott-McKean, J.J., 2005. G-protein-gated potassium (GIRK) channels containing the GIRK2 subunit are control hubs for pharmacologically induced hypothermic responses. J. Neurosci. 25, 7801-7804.

Coulson, E.J., May, L.M., Osborne, S.L., Reid, K., Underwood, C.K., Meunier, F.A., Bartlett, P.F., Sah, P., 2008. p75 neurotrophin receptor mediates neuronal cell death by activating GIRK channels through phosphatidylinositol 4,5-bisphosphate. J. Neurosci. 28, 315-324.

Cruz, H.G., Berton, F., Sollini, M., Blanchet, C., Pravetoni, M., Wickman, K., Luscher, C., 2008. Absence and rescue of morphine withdrawal in GIRK/Kir3 knock-out mice. J. Neurosci. 28, 4069-4077.

Cruz, H.G., Ivanova, T., Lunn, M.L., Stoffel, M., Slesinger, P.A., Luscher, C., 2004. Bi-directional effects of GABA(B) receptor agonists on the mesolimbic dopamine system. Nat. Neurosci. 7, 153-159.

Cryan, J.F., Mombereau, C., Vassout, A., 2005. The tail suspension test as a model for assessing antidepressant activity: review of pharmacological and genetic studies in mice. Neurosci. Biobehav. Rev. 29, 571-625.

D

Dahlstroem, A., Fuxe, K., 1964. Evidence for the Existence of Monoamine-Containing Neurons in the Central Nervous System. I. Demonstration of Monoamines in the Cell Bodies of Brain Stem Neurons. Acta Physiol. Scand. Suppl. , SUPPL 232:1-55.

Dang, V.C., Napier, I.A., Christie, M.J., 2009. Two distinct mechanisms mediate acute mu-opioid receptor desensitization in native neurons. J. Neurosci. 29, 3322-3327.

Day, H.E., Campeau, S., Watson, S.J.,Jr, Akil, H., 1997. Distribution of alpha 1a-, alpha 1b- and alpha 1d-adrenergic receptor mRNA in the rat brain and spinal cord. J. Chem. Neuroanat. 13, 115-139.

Day, H.E., Greenwood, B.N., Hammack, S.E., Watkins, L.R., Fleshner, M., Maier, S.F., Campeau, S., 2004. Differential expression of 5HT-1A, alpha 1b adrenergic, CRF-R1, and CRF-R2 receptor mRNA in serotonergic, gamma-aminobutyric acidergic, and catecholaminergic cells of the rat dorsal raphe nucleus. J. Comp. Neurol. 474, 364-378.

de Montigny, C., Cournoyer, G., Morissette, R., Langlois, R., Caille, G., 1983. Lithium carbonate addition in tricyclic antidepressant-resistant unipolar depression. Correlations with the neurobiologic actions of tricyclic antidepressant drugs and lithium ion on the serotonin system. Arch. Gen. Psychiatry 40, 1327-1334.

Delgado, P.L., 2006. Monoamine depletion studies: implications for antidepressant discontinuation syndrome. J. Clin. Psychiatry 67 Suppl 4, 22-26.

Delgado, P.L., Charney, D.S., Price, L.H., Aghajanian, G.K., Landis, H., Heninger, G.R., 1990. Serotonin function and the mechanism of antidepressant action. Reversal of antidepressant-induced remission by rapid depletion of plasma tryptophan. Arch. Gen. Psychiatry 47, 411-418.

Delling, M., Wischmeyer, E., Dityatev, A., Sytnyk, V., Veh, R.W., Karschin, A., Schachner, M., 2002. The neural cell adhesion molecule regulates cell-surface delivery of G-protein-activated inwardly rectifying potassium channels via lipid rafts. J. Neurosci. 22, 7154-7164.

Descarries, L., Watkins, K.C., Garcia, S., Beaudet, A., 1982. The serotonin neurons in nucleus raphe dorsalis of adult rat: a light and electron microscope radioautographic study. J. Comp. Neurol. 207, 239-254.

Diaz-Cintra, S., Cintra, L., Kemper, T., Resnick, O., Morgane, P.J., 1981. Nucleus raphe dorsalis: a morphometric Golgi study in rats of three age groups. Brain Res. 207, 1-16.

Diazgranados, N., Ibrahim, L., Brutsche, N.E., Newberg, A., Kronstein, P., Khalife, S., Kammerer, W.A., Quezado, Z., Luckenbaugh, D.A., Salvadore, G., Machado-Vieira, R., Manji, H.K., Zarate, C.A.,Jr, 2010. A randomized add-on trial of an N-methyl-D-aspartate antagonist in treatment-resistant bipolar depression. Arch. Gen. Psychiatry 67, 793-802.

Dobrunz, L.E., Stevens, C.F., 1997. Heterogeneity of release probability, facilitation, and depletion at central synapses. Neuron 18, 995-1008.

References

Doupnik, C.A., Davidson, N., Lester, H.A., Kofuji, P., 1997. RGS proteins reconstitute the rapid gating kinetics of gbetagamma-activated inwardly rectifying K+ channels. Proc. Natl. Acad. Sci. U. S. A. 94, 10461-10466.

Dowling, R.J., Topisirovic, I., Alain, T., Bidinosti, M., Fonseca, B.D., Petroulakis, E., Wang, X., Larsson, O., Selvaraj, A., Liu, Y., Kozma, S.C., Thomas, G., Sonenberg, N., 2010. mTORC1-mediated cell proliferation, but not cell growth, controlled by the 4E-BPs. Science 328, 1172-1176.

Doyle, D.A., Morais Cabral, J., Pfuetzner, R.A., Kuo, A., Gulbis, J.M., Cohen, S.L., Chait, B.T., MacKinnon, R., 1998. The structure of the potassium channel: molecular basis of K+ conduction and selectivity. Science 280, 69-77.

Drake, C.T., Bausch, S.B., Milner, T.A., Chavkin, C., 1997. GIRK1 immunoreactivity is present predominantly in dendrites, dendritic spines, and somata in the CA1 region of the hippocampus. Proc. Natl. Acad. Sci. U. S. A. 94, 1007-1012.

Dranovsky, A., Hen, R., 2006. Hippocampal neurogenesis: regulation by stress and antidepressants. Biol. Psychiatry 59, 1136-1143.

Dranovsky, A., Picchini, A.M., Moadel, T., Sisti, A.C., Yamada, A., Kimura, S., Leonardo, E.D., Hen, R., 2011. Experience dictates stem cell fate in the adult hippocampus. Neuron 70, 908-923.

Drevets, W.C., Frank, E., Price, J.C., Kupfer, D.J., Holt, D., Greer, P.J., Huang, Y., Gautier, C., Mathis, C., 1999. PET imaging of serotonin 1A receptor binding in depression. Biol. Psychiatry 46, 1375-1387.

Drevets, W.C., Thase, M.E., Moses-Kolko, E.L., Price, J., Frank, E., Kupfer, D.J., Mathis, C., 2007. Serotonin-1A receptor imaging in recurrent depression: replication and literature review. Nucl. Med. Biol. 34, 865-877.

Duman, R.S., 2014. Neurobiology of stress, depression, and rapid acting antidepressants: remodeling synaptic connections. Depress. Anxiety 31, 291-296.

Duman, R.S., Aghajanian, G.K., 2012. Synaptic dysfunction in depression: potential therapeutic targets. Science 338, 68-72.

Duman, R.S., Monteggia, L.M., 2006. A neurotrophic model for stress-related mood disorders. Biol. Psychiatry 59, 1116-1127.

Dutar, P., Vu, H.M., Perkel, D.J., 1999. Pharmacological characterization of an unusual mGluR-evoked neuronal hyperpolarization mediated by activation of GIRK channels. Neuropharmacology 38, 467-475.

Dutta, A., McKie, S., Deakin, J.F., 2015. Ketamine and other potential glutamate antidepressants. Psychiatry Res. 225, 1-13.

E

Egashira, N., Mishima, K., Katsurabayashi, S., Yoshitake, T., Matsumoto, Y., Ishida, J., Yamaguchi, M., Iwasaki, K., Fujiwara, M., 2002. Involvement of 5-hydroxytryptamine neuronal system in Delta(9)-tetrahydrocannabinol-induced impairment of spatial memory. Eur. J. Pharmacol. 445, 221-229.

F

Federici, M., Nistico, R., Giustizieri, M., Bernardi, G., Mercuri, N.B., 2009. Ethanol enhances GABAB-mediated inhibitory postsynaptic transmission on rat midbrain dopaminergic neurons by facilitating GIRK currents. Eur. J. Neurosci. 29, 1369-1377.

Feldman, M.E., Apsel, B., Uotila, A., Loewith, R., Knight, Z.A., Ruggero, D., Shokat, K.M., 2009. Active-site inhibitors of mTOR target rapamycin-resistant outputs of mTORC1 and mTORC2. PLoS Biol. 7, e38.

Fernandes, C., McKittrick, C.R., File, S.E., McEwen, B.S., 1997. Decreased 5-HT1A and increased 5-HT2A receptor binding after chronic corticosterone associated with a behavioural indication of depression but not anxiety. Psychoneuroendocrinology 22, 477-491.

Ferre, S., Artigas, F., 1993. Dopamine D2 receptor-mediated regulation of serotonin extracellular concentration in the dorsal raphe nucleus of freely moving rats. J. Neurochem. 61, 772-775.

Ferre, S., Cortes, R., Artigas, F., 1994. Dopaminergic regulation of the serotonergic raphe-striatal pathway: microdialysis studies in freely moving rats. J. Neurosci. 14, 4839-4846.

Ferreira, S.G., Teixeira, F.M., Garcao, P., Agostinho, P., Ledent, C., Cortes, L., Mackie, K., Kofalvi, A., 2012. Presynaptic CB(1) cannabinoid receptors control frontocortical serotonin and glutamate release--species differences. Neurochem. Int. 61, 219-226.

Ferres-Coy, A., Santana, N., Castane, A., Cortes, R., Carmona, M.C., Toth, M., Montefeltro, A., Artigas, F., Bortolozzi, A., 2013. Acute 5-HT(1)A

autoreceptor knockdown increases antidepressant responses and serotonin release in stressful conditions. Psychopharmacology (Berl) 225, 61-74.

Fowler, C.E., Aryal, P., Suen, K.F., Slesinger, P.A., 2007. Evidence for association of GABA(B) receptors with Kir3 channels and regulators of G protein signalling (RGS4) proteins. J. Physiol. 580, 51-65.

Frankhuijzen, A.L., Wardeh, G., Hogenboom, F., Mulder, A.H., 1988. Alpha 2-adrenoceptor mediated inhibition of the release of radiolabelled 5-hydroxytryptamine and noradrenaline from slices of the dorsal region of the rat brain. Naunyn Schmiedebergs Arch. Pharmacol. 337, 255-260.

Franklin KBJ, Paxinos G., 1997. The Mouse Brain in Stereotaxic Coordinates. Academic Press Inc., San Diego, CA, USA.

Freedman, J.E., Aghajanian, G.K., 1984. Idazoxan (RX 781094) selectively antagonizes alpha 2-adrenoceptors on rat central neurons. Eur. J. Pharmacol. 105, 265-272.

Froger, N., Gardier, A.M., Moratalla, R., Alberti, I., Lena, I., Boni, C., De Felipe, C., Rupniak, N.M., Hunt, S.P., Jacquot, C., Hamon, M., Lanfumey, L., 2001. 5-hydroxytryptamine (5-HT)1A autoreceptor adaptive changes in substance P (neurokinin 1) receptor knock-out mice mimic antidepressant-induced desensitization. J. Neurosci. 21, 8188-8197.

Fu, W., Le Maitre, E., Fabre, V., Bernard, J.F., David Xu, Z.Q., Hokfelt, T., 2010. Chemical neuroanatomy of the dorsal raphe nucleus and adjacent structures of the mouse brain. J. Comp. Neurol. 518, 3464-3494.

Fukumoto, K., Iijima, M., Chaki, S., 2014. Serotonin-1A receptor stimulation mediates effects of a metabotropic glutamate 2/3 receptor antagonist, 2S-

2-amino-2-(1S,2S-2-carboxycycloprop-1-yl)-3-(xanth-9-yl)propanoic acid (LY341495), and an N-methyl-D-aspartate receptor antagonist, ketamine, in the novelty-suppressed feeding test. Psychopharmacology (Berl) 231, 2291-2298.

G

Galindo-Charles, L., Hernandez-Lopez, S., Galarraga, E., Tapia, D., Bargas, J., Garduno, J., Frias-Dominguez, C., Drucker-Colin, R., Mihailescu, S., 2008. Serotoninergic dorsal raphe neurons possess functional postsynaptic nicotinic acetylcholine receptors. Synapse 62, 601-615.

Gallager, D.W., Aghajanian, G.K., 1976. Effect of antipsychotic drugs on the firing of dorsal raphe cells. II. Reversal by picrotoxin. Eur. J. Pharmacol. 39, 357-364.

Garduno, J., Galindo-Charles, L., Jimenez-Rodriguez, J., Galarraga, E., Tapia, D., Mihailescu, S., Hernandez-Lopez, S., 2012. Presynaptic alpha4beta2 nicotinic acetylcholine receptors increase glutamate release and serotonin neuron excitability in the dorsal raphe nucleus. J. Neurosci. 32, 15148-15157.

Garratt, J.C., Crespi, F., Mason, R., Marsden, C.A., 1991. Effects of idazoxan on dorsal raphe 5-hydroxytryptamine neuronal function. Eur. J. Pharmacol. 193, 87-93.

Gartside, S.E., Cole, A.J., Williams, A.P., McQuade, R., Judge, S.J., 2007. AMPA and NMDA receptor regulation of firing activity in 5-HT neurons of the dorsal and median raphe nuclei. Eur. J. Neurosci. 25, 3001-3008.

Gartside, S.E., Hajos-Korcsok, E., Bagdy, E., Harsing, L.G.,Jr, Sharp, T., Hajos, M., 2000. Neurochemical and electrophysiological studies on the functional significance of burst firing in serotonergic neurons. Neuroscience 98, 295-300.

Gartside, S.E., Umbers, V., Hajos, M., Sharp, T., 1995. Interaction between a selective 5-HT1A receptor antagonist and an SSRI in vivo: effects on 5-HT cell firing and extracellular 5-HT. Br. J. Pharmacol. 115, 1064-1070.

Geng, X., Du, X.N., Rusinova, R., Liu, B.Y., Li, F., Zhang, X., Chen, X.J., Logothetis, D.E., Zhang, H.L., 2009. Specificity of Gbetagamma signaling depends on Galpha subunit coupling with G-protein-sensitive K(+) channels. Pharmacology 84, 82-90.

Gervasoni, D., Peyron, C., Rampon, C., Barbagli, B., Chouvet, G., Urbain, N., Fort, P., Luppi, P.H., 2000. Role and origin of the GABAergic innervation of dorsal raphe serotonergic neurons. J. Neurosci. 20, 4217-4225.

Gigliucci, V., O'Dowd, G., Casey, S., Egan, D., Gibney, S., Harkin, A., 2013. Ketamine elicits sustained antidepressant-like activity via a serotonin-dependent mechanism. Psychopharmacology (Berl) 228, 157-166.

Gilman, A.G., 1987. G proteins: transducers of receptor-generated signals. Annu. Rev. Biochem. 56, 615-649.

Gobbi, G., Cassano, T., Radja, F., Morgese, M.G., Cuomo, V., Santarelli, L., Hen, R., Blier, P., 2007. Neurokinin 1 receptor antagonism requires norepinephrine to increase serotonin function. Eur. Neuropsychopharmacol. 17, 328-338.

References

Gocho, Y., Sakai, A., Yanagawa, Y., Suzuki, H., Saitow, F., 2013. Electrophysiological and pharmacological properties of GABAergic cells in the dorsal raphe nucleus. J. Physiol. Sci. 63, 147-154.

Goodwin, G.M., De Souza, R.J., Green, A.R., 1985. The pharmacology of the hypothermic response in mice to 8-hydroxy-2-(di-n-propylamino)tetralin (8-OH-DPAT). A model of presynaptic 5-HT1 function. Neuropharmacology 24, 1187-1194.

Gregerson, K.A., Flagg, T.P., O'Neill, T.J., Anderson, M., Lauring, O., Horel, J.S., Welling, P.A., 2001. Identification of G protein-coupled, inward rectifier potassium channel gene products from the rat anterior pituitary gland. Endocrinology 142, 2820-2832.

Grosse, G., Eulitz, D., Thiele, T., Pahner, I., Schroter, S., Takamori, S., Grosse, J., Wickman, K., Tapp, R., Veh, R.W., Ottersen, O.P., Ahnert-Hilger, G., 2003. Axonal sorting of Kir3.3 defines a GABA-containing neuron in the CA3 region of rodent hippocampus. Mol. Cell. Neurosci. 24, 709-724.

Guiard, B.P., Guilloux, J.P., Reperant, C., Hunt, S.P., Toth, M., Gardier, A.M., 2007. Substance P neurokinin 1 receptor activation within the dorsal raphe nucleus controls serotonin release in the mouse frontal cortex. Mol. Pharmacol. 72, 1411-1418.

Gustafson, E.L., Durkin, M.M., Bard, J.A., Zgombick, J., Branchek, T.A., 1996. A receptor autoradiographic and in situ hybridization analysis of the distribution of the 5-ht7 receptor in rat brain. Br. J. Pharmacol. 117, 657-666.

H

Hagan, C.E., McDevitt, R.A., Liu, Y., Furay, A.R., Neumaier, J.F., 2012. 5-HT(1B) autoreceptor regulation of serotonin transporter activity in synaptosomes. Synapse 66, 1024-1034.

Haj-Dahmane, S., 2001. D2-like dopamine receptor activation excites rat dorsal raphe 5-HT neurons in vitro. Eur. J. Neurosci. 14, 125-134.

Haj-Dahmane, S., Shen, R.Y., 2009. Endocannabinoids suppress excitatory synaptic transmission to dorsal raphe serotonin neurons through the activation of presynaptic CB1 receptors. J. Pharmacol. Exp. Ther. 331, 186-196.

Hajos, M., Allers, K.A., Jennings, K., Sharp, T., Charette, G., Sik, A., Kocsis, B., 2007. Neurochemical identification of stereotypic burst-firing neurons in the rat dorsal raphe nucleus using juxtacellular labelling methods. Eur. J. Neurosci. 25, 119-126.

Hajos, M., Gartside, S.E., Sharp, T., 1995a. Inhibition of median and dorsal raphe neurones following administration of the selective serotonin reuptake inhibitor paroxetine. Naunyn Schmiedebergs Arch. Pharmacol. 351, 624-629.

Hajos, M., Gartside, S.E., Villa, A.E., Sharp, T., 1995b. Evidence for a repetitive (burst) firing pattern in a sub-population of 5-hydroxytryptamine neurons in the dorsal and median raphe nuclei of the rat. Neuroscience 69, 189-197.

References

Hajos, M., Hajos-Korcsok, E., Sharp, T., 1999. Role of the medial prefrontal cortex in 5-HT1A receptor-induced inhibition of 5-HT neuronal activity in the rat. Br. J. Pharmacol. 126, 1741-1750.

Hajos, M., Richards, C.D., Szekely, A.D., Sharp, T., 1998. An electrophysiological and neuroanatomical study of the medial prefrontal cortical projection to the midbrain raphe nuclei in the rat. Neuroscience 87, 95-108.

Hajos, M., Sharp, T., 1996. Burst-firing activity of presumed 5-HT neurones of the rat dorsal raphe nucleus: electrophysiological analysis by antidromic stimulation. Brain Res. 740, 162-168.

Harashima, C., Jacobowitz, D.M., Stoffel, M., Chakrabarti, L., Haydar, T.F., Siarey, R.J., Galdzicki, Z., 2006. Elevated expression of the G-protein-activated inwardly rectifying potassium channel 2 (GIRK2) in cerebellar unipolar brush cells of a Down syndrome mouse model. Cell. Mol. Neurobiol. 26, 719-734.

Hardingham, G.E., Bading, H., 2010. Synaptic versus extrasynaptic NMDA receptor signalling: implications for neurodegenerative disorders. Nat. Rev. Neurosci. 11, 682-696.

Haring, M., Marsicano, G., Lutz, B., Monory, K., 2007. Identification of the cannabinoid receptor type 1 in serotonergic cells of raphe nuclei in mice. Neuroscience 146, 1212-1219.

Hasler, G., van der Veen, J.W., Tumonis, T., Meyers, N., Shen, J., Drevets, W.C., 2007. Reduced prefrontal glutamate/glutamine and gamma-aminobutyric acid levels in major depression determined using proton magnetic resonance spectroscopy. Arch. Gen. Psychiatry 64, 193-200.

Hay, N., Sonenberg, N., 2004. Upstream and downstream of mTOR. Genes Dev. 18, 1926-1945.

Hearing, M., Kotecki, L., Marron Fernandez de Velasco, E., Fajardo-Serrano, A., Chung, H.J., Lujan, R., Wickman, K., 2013. Repeated cocaine weakens GABA(B)-Girk signaling in layer 5/6 pyramidal neurons in the prelimbic cortex. Neuron 80, 159-170.

Hedin, K.E., Lim, N.F., Clapham, D.E., 1996. Cloning of a Xenopus laevis inwardly rectifying K+ channel subunit that permits GIRK1 expression of IKACh currents in oocytes. Neuron 16, 423-429.

Heginbotham, L., Lu, Z., Abramson, T., MacKinnon, R., 1994. Mutations in the K+ channel signature sequence. Biophys. J. 66, 1061-1067.

Heisler, L.K., Chu, H.M., Brennan, T.J., Danao, J.A., Bajwa, P., Parsons, L.H., Tecott, L.H., 1998. Elevated anxiety and antidepressant-like responses in serotonin 5-HT1A receptor mutant mice. Proc. Natl. Acad. Sci. U. S. A. 95, 15049-15054.

Hendricksen, M., Thomas, A.J., Ferrier, I.N., Ince, P., O'Brien, J.T., 2004. Neuropathological study of the dorsal raphe nuclei in late-life depression and Alzheimer's disease with and without depression. Am. J. Psychiatry 161, 1096-1102.

Hepler, J.R., 1999. Emerging roles for RGS proteins in cell signalling. Trends Pharmacol. Sci. 20, 376-382.

Hervas, I., Artigas, F., 1998. Effect of fluoxetine on extracellular 5-hydroxytryptamine in rat brain. Role of 5-HT autoreceptors. Eur. J. Pharmacol. 358, 9-18.

Hervas, I., Vilaro, M.T., Romero, L., Scorza, M.C., Mengod, G., Artigas, F., 2001. Desensitization of 5-HT(1A) autoreceptors by a low chronic fluoxetine dose effect of the concurrent administration of WAY-100635. Neuropsychopharmacology 24, 11-20.

Heurteaux, C., Lucas, G., Guy, N., El Yacoubi, M., Thummler, S., Peng, X.D., Noble, F., Blondeau, N., Widmann, C., Borsotto, M., Gobbi, G., Vaugeois, J.M., Debonnel, G., Lazdunski, M., 2006. Deletion of the background potassium channel TREK-1 results in a depression-resistant phenotype. Nat. Neurosci. 9, 1134-1141.

Hibino, H., Inanobe, A., Furutani, K., Murakami, S., Findlay, I., Kurachi, Y., 2010. Inwardly rectifying potassium channels: their structure, function, and physiological roles. Physiol. Rev. 90, 291-366.

Hille, B., 1992. G protein-coupled mechanisms and nervous signaling. Neuron 9, 187-195.

Hjorth, S., Suchowski, C.S., Galloway, M.P., 1995. Evidence for 5-HT autoreceptor-mediated, nerve impulse-independent, control of 5-HT synthesis in the rat brain. Synapse 19, 170-176.

Ho, I.H., Murrell-Lagnado, R.D., 1999a. Molecular determinants for sodium-dependent activation of G protein-gated K+ channels. J. Biol. Chem. 274, 8639-8648.

Ho, I.H., Murrell-Lagnado, R.D., 1999b. Molecular mechanism for sodium-dependent activation of G protein-gated K+ channels. J. Physiol. 520 Pt 3, 645-651.

Ho, K., Nichols, C.G., Lederer, W.J., Lytton, J., Vassilev, P.M., Kanazirska, M.V., Hebert, S.C., 1993. Cloning and expression of an inwardly rectifying ATP-regulated potassium channel. Nature 362, 31-38.

Hokfelt, T., Xu, Z.Q., Shi, T.J., Holmberg, K., Zhang, X., 1998. Galanin in ascending systems. Focus on coexistence with 5-hydroxytryptamine and noradrenaline. Ann. N. Y. Acad. Sci. 863, 252-263.

Homayoun, H., Moghaddam, B., 2007. NMDA receptor hypofunction produces opposite effects on prefrontal cortex interneurons and pyramidal neurons. J. Neurosci. 27, 11496-11500.

Hopwood, S.E., Stamford, J.A., 2001. Noradrenergic modulation of serotonin release in rat dorsal and median raphe nuclei via alpha(1) and alpha(2A) adrenoceptors. Neuropharmacology 41, 433-442.

Hou, L., Klann, E., 2004. Activation of the phosphoinositide 3-kinase-Akt-mammalian target of rapamycin signaling pathway is required for metabotropic glutamate receptor-dependent long-term depression. J. Neurosci. 24, 6352-6361.

Hoyer, D., Hannon, J.P., Martin, G.R., 2002. Molecular, pharmacological and functional diversity of 5-HT receptors. Pharmacol. Biochem. Behav. 71, 533-554.

Huang, C.L., Feng, S., Hilgemann, D.W., 1998. Direct activation of inward rectifier potassium channels by PIP2 and its stabilization by Gbetagamma. Nature 391, 803-806.

Huang, C.L., Slesinger, P.A., Casey, P.J., Jan, Y.N., Jan, L.Y., 1995. Evidence that direct binding of G beta gamma to the GIRK1 G protein-gated

inwardly rectifying K+ channel is important for channel activation. Neuron 15, 1133-1143.

I

Ikeda, K., Kobayashi, T., Kumanishi, T., Niki, H., Yano, R., 2000. Involvement of G-protein-activated inwardly rectifying K (GIRK) channels in opioid-induced analgesia. Neurosci. Res. 38, 113-116.

Imai, H., Steindler, D.A., Kitai, S.T., 1986. The organization of divergent axonal projections from the midbrain raphe nuclei in the rat. J. Comp. Neurol. 243, 363-380.

Inanobe, A., Fujita, S., Makino, Y., Matsushita, K., Ishii, M., Chachin, M., Kurachi, Y., 2001. Interaction between the RGS domain of RGS4 with G protein alpha subunits mediates the voltage-dependent relaxation of the G protein-gated potassium channel. J. Physiol. 535, 133-143.

Inanobe, A., Yoshimoto, Y., Horio, Y., Morishige, K.I., Hibino, H., Matsumoto, S., Tokunaga, Y., Maeda, T., Hata, Y., Takai, Y., Kurachi, Y., 1999. Characterization of G-protein-gated K+ channels composed of Kir3.2 subunits in dopaminergic neurons of the substantia nigra. J. Neurosci. 19, 1006-1017.

Innis, R.B., Aghajanian, G.K., 1987. Pertussis toxin blocks 5-HT1A and GABAB receptor-mediated inhibition of serotonergic neurons. Eur. J. Pharmacol. 143, 195-204.

Invernizzi, R., Bramante, M., Samanin, R., 1995. Extracellular concentrations of serotonin in the dorsal hippocampus after acute and chronic treatment with citalopram. Brain Res. 696, 62-66.

Invernizzi, R.W., Parini, S., Sacchetti, G., Fracasso, C., Caccia, S., Annoni, K., Samanin, R., 2001. Chronic treatment with reboxetine by osmotic pumps facilitates its effect on extracellular noradrenaline and may desensitize alpha(2)-adrenoceptors in the prefrontal cortex. Br. J. Pharmacol. 132, 183-188.

Irifune, M., Shimizu, T., Nomoto, M., Fukuda, T., 1992. Ketamine-induced anesthesia involves the N-methyl-D-aspartate receptor-channel complex in mice. Brain Res. 596, 1-9.

Ishii, M., Inanobe, A., Kurachi, Y., 2002. PIP3 inhibition of RGS protein and its reversal by Ca2+/calmodulin mediate voltage-dependent control of the G protein cycle in a cardiac K+ channel. Proc. Natl. Acad. Sci. U. S. A. 99, 4325-4330.

Isomoto, S., Kondo, C., Takahashi, N., Matsumoto, S., Yamada, M., Takumi, T., Horio, Y., Kurachi, Y., 1996. A novel ubiquitously distributed isoform of GIRK2 (GIRK2B) enhances GIRK1 expression of the G-protein-gated K+ current in Xenopus oocytes. Biochem. Biophys. Res. Commun. 218, 286-291.

Itoi, K., Sugimoto, N., 2010. The brainstem noradrenergic systems in stress, anxiety and depression. J. Neuroendocrinol. 22, 355-361.

Ivanina, T., Varon, D., Peleg, S., Rishal, I., Porozov, Y., Dessauer, C.W., Keren-Raifman, T., Dascal, N., 2004. Galphai1 and Galphai3 differentially interact with, and regulate, the G protein-activated K+ channel. J. Biol. Chem. 279, 17260-17268.

Iwanir, S., Reuveny, E., 2008. Adrenaline-induced hyperpolarization of mouse pancreatic islet cells is mediated by G protein-gated inwardly rectifying potassium (GIRK) channels. Pflugers Arch. 456, 1097-1108.

J

Jacobs, B.L., Azmitia, E.C., 1992. Structure and function of the brain serotonin system. Physiol. Rev. 72, 165-229.

Janes, M.R., Limon, J.J., So, L., Chen, J., Lim, R.J., Chavez, M.A., Vu, C., Lilly, M.B., Mallya, S., Ong, S.T., Konopleva, M., Martin, M.B., Ren, P., Liu, Y., Rommel, C., Fruman, D.A., 2010. Effective and selective targeting of leukemia cells using a TORC1/2 kinase inhibitor. Nat. Med. 16, 205-213.

Jans, L.A., Riedel, W.J., Markus, C.R., Blokland, A., 2007. Serotonergic vulnerability and depression: assumptions, experimental evidence and implications. Mol. Psychiatry 12, 522-543.

Jaworski, J., Spangler, S., Seeburg, D.P., Hoogenraad, C.C., Sheng, M., 2005. Control of dendritic arborization by the phosphoinositide-3'-kinase-Akt-mammalian target of rapamycin pathway. J. Neurosci. 25, 11300-11312.

Jelacic, T.M., Kennedy, M.E., Wickman, K., Clapham, D.E., 2000. Functional and biochemical evidence for G-protein-gated inwardly rectifying K+ (GIRK) channels composed of GIRK2 and GIRK3. J. Biol. Chem. 275, 36211-36216.

Jelacic, T.M., Sims, S.M., Clapham, D.E., 1999. Functional expression and characterization of G-protein-gated inwardly rectifying K+ channels containing GIRK3. J. Membr. Biol. 169, 123-129.

Jiang, C., Qu, Z., Xu, H., 2002. Gating of inward rectifier K(+) channels by proton-mediated interactions of intracellular protein domains. Trends Cardiovasc. Med. 12, 5-13.

Jin, W., Lu, Z., 1998. A novel high-affinity inhibitor for inward-rectifier K+ channels. Biochemistry 37, 13291-13299.

Johnson, M.D., Ma, P.M., 1993. Localization of NADPH diaphorase activity in monoaminergic neurons of the rat brain. J. Comp. Neurol. 332, 391-406.

Johnson, S.W., Mercuri, N.B., North, R.A., 1992. 5-hydroxytryptamine1B receptors block the GABAB synaptic potential in rat dopamine neurons. J. Neurosci. 12, 2000-2006.

Jolas, T., Aghajanian, G.K., 1997. Opioids suppress spontaneous and NMDA-induced inhibitory postsynaptic currents in the dorsal raphe nucleus of the rat in vitro. Brain Res. 755, 229-245.

Jourdi, H., Hsu, Y.T., Zhou, M., Qin, Q., Bi, X., Baudry, M., 2009. Positive AMPA receptor modulation rapidly stimulates BDNF release and increases dendritic mRNA translation. J. Neurosci. 29, 8688-8697.

Judge, S.J., Ingram, C.D., Gartside, S.E., 2004. GABA receptor modulation of 5-HT neuronal firing: characterization and effect of moderate in vivo variations in glucocorticoid levels. Neurochem. Int. 45, 1057-1065.

K

Kalen, P., Karlson, M., Wiklund, L., 1985. Possible excitatory amino acid afferents to nucleus raphe dorsalis of the rat investigated with retrograde wheat germ agglutinin and D-[3H]aspartate tracing. Brain Res. 360, 285-297.

Kalen, P., Pritzel, M., Nieoullon, A., Wiklund, L., 1986. Further evidence for excitatory amino acid transmission in the lateral habenular projection to

the rostral raphe nuclei: lesion-induced decrease of high affinity glutamate uptake. Neurosci. Lett. 68, 35-40.

Kalen, P., Skagerberg, G., Lindvall, O., 1988. Projections from the ventral tegmental area and mesencephalic raphe to the dorsal raphe nucleus in the rat. Evidence for a minor dopaminergic component. Exp. Brain Res. 73, 69-77.

Kang, H.J., Voleti, B., Hajszan, T., Rajkowska, G., Stockmeier, C.A., Licznerski, P., Lepack, A., Majik, M.S., Jeong, L.S., Banasr, M., Son, H., Duman, R.S., 2012. Decreased expression of synapse-related genes and loss of synapses in major depressive disorder. Nat. Med. 18, 1413-1417.

Kanjhan, R., Coulson, E.J., Adams, D.J., Bellingham, M.C., 2005. Tertiapin-Q blocks recombinant and native large conductance K+ channels in a use-dependent manner. J. Pharmacol. Exp. Ther. 314, 1353-1361.

Karschin, C., Dissmann, E., Stuhmer, W., Karschin, A., 1996. IRK(1-3) and GIRK(1-4) inwardly rectifying K+ channel mRNAs are differentially expressed in the adult rat brain. J. Neurosci. 16, 3559-3570.

Katz, I.R., 2004. Depression and frailty: the need for multidisciplinary research. Am. J. Geriatr. Psychiatry 12, 1-6.

Kaufmann, K., Romaine, I., Days, E., Pascual, C., Malik, A., Yang, L., Zou, B., Du, Y., Sliwoski, G., Morrison, R.D., Denton, J., Niswender, C.M., Daniels, J.S., Sulikowski, G.A., Xie, X.S., Lindsley, C.W., Weaver, C.D., 2013. ML297 (VU0456810), the first potent and selective activator of the GIRK potassium channel, displays antiepileptic properties in mice. ACS Chem. Neurosci. 4, 1278-1286.

Kawashima, N., Karasawa, J., Shimazaki, T., Chaki, S., Okuyama, S., Yasuhara, A., Nakazato, A., 2005. Neuropharmacological profiles of antagonists of group II metabotropic glutamate receptors. Neurosci. Lett. 378, 131-134.

Kawaura, K., Miki, R., Shima, E., Honda, S., Soeda, F., Shirasaki, T., Takahama, K., 2010. Antidepressant-like effect of centrally acting non-narcotic antitussive caramiphen in a forced swimming test. Neurosci. Lett. 481, 188-190.

Kennedy, M.E., Nemec, J., Clapham, D.E., 1996. Localization and interaction of epitope-tagged GIRK1 and CIR inward rectifier K+ channel subunits. Neuropharmacology 35, 831-839.

Kennedy, M.E., Nemec, J., Corey, S., Wickman, K., Clapham, D.E., 1999. GIRK4 confers appropriate processing and cell surface localization to G-protein-gated potassium channels. J. Biol. Chem. 274, 2571-2582.

Kessler, R.C., Berglund, P., Demler, O., Jin, R., Koretz, D., Merikangas, K.R., Rush, A.J., Walters, E.E., Wang, P.S., National Comorbidity Survey Replication, 2003. The epidemiology of major depressive disorder: results from the National Comorbidity Survey Replication (NCS-R). JAMA 289, 3095-3105.

Kessler, R.C., Berglund, P., Demler, O., Jin, R., Merikangas, K.R., Walters, E.E., 2005. Lifetime prevalence and age-of-onset distributions of DSM-IV disorders in the National Comorbidity Survey Replication. Arch. Gen. Psychiatry 62, 593-602.

Kessler, R.C., Birnbaum, H.G., Shahly, V., Bromet, E., Hwang, I., McLaughlin, K.A., Sampson, N., Andrade, L.H., de Girolamo, G., Demyttenaere, K., Haro, J.M., Karam, A.N., Kostyuchenko, S., Kovess, V., Lara, C.,

Levinson, D., Matschinger, H., Nakane, Y., Browne, M.O., Ormel, J., Posada-Villa, J., Sagar, R., Stein, D.J., 2010. Age differences in the prevalence and co-morbidity of DSM-IV major depressive episodes: results from the WHO World Mental Health Survey Initiative. Depress. Anxiety 27, 351-364.

Kessler, R.C., Ustun, T.B., 2004. The World Mental Health (WMH) Survey Initiative Version of the World Health Organization (WHO) Composite International Diagnostic Interview (CIDI). Int. J. Methods Psychiatr. Res. 13, 93-121.

Kia, H.K., Brisorgueil, M.J., Hamon, M., Calas, A., Verge, D., 1996a. Ultrastructural localization of 5-hydroxytryptamine1A receptors in the rat brain. J. Neurosci. Res. 46, 697-708.

Kia, H.K., Miquel, M.C., Brisorgueil, M.J., Daval, G., Riad, M., El Mestikawy, S., Hamon, M., Verge, D., 1996b. Immunocytochemical localization of serotonin1A receptors in the rat central nervous system. J. Comp. Neurol. 365, 289-305.

Kidd, E.J., Garratt, J.C., Marsden, C.A., 1991. Effects of repeated treatment with 1-(2,5-dimethoxy-4-iodophenyl)-2-aminopropane (DOI) on the autoregulatory control of dorsal raphe 5-HT neuronal firing and cortical 5-HT release. Eur. J. Pharmacol. 200, 131-139.

Kim, C.S., Johnston, D., 2015. A1 adenosine receptor-mediated GIRK channels contributes to the resting conductance of CA1 neurons in the dorsal hippocampus. J. Neurophysiol. , jn.00951.2014.

Kim, D.H., Sarbassov, D.D., Ali, S.M., Latek, R.R., Guntur, K.V., Erdjument-Bromage, H., Tempst, P., Sabatini, D.M., 2003. GbetaL, a positive

regulator of the rapamycin-sensitive pathway required for the nutrient-sensitive interaction between raptor and mTOR. Mol. Cell 11, 895-904.

Kirby, L.G., Freeman-Daniels, E., Lemos, J.C., Nunan, J.D., Lamy, C., Akanwa, A., Beck, S.G., 2008. Corticotropin-releasing factor increases GABA synaptic activity and induces inward current in 5-hydroxytryptamine dorsal raphe neurons. J. Neurosci. 28, 12927-12937.

Kirby, L.G., Rice, K.C., Valentino, R.J., 2000. Effects of corticotropin-releasing factor on neuronal activity in the serotonergic dorsal raphe nucleus. Neuropsychopharmacology 22, 148-162.

Kiss, J., Csaki, A., Bokor, H., Kocsis, K., Kocsis, B., 2002. Possible glutamatergic/aspartatergic projections to the supramammillary nucleus and their origins in the rat studied by selective [(3)H]D-aspartate labelling and immunocytochemistry. Neuroscience 111, 671-691.

Klemenhagen, K.C., Gordon, J.A., David, D.J., Hen, R., Gross, C.T., 2006. Increased fear response to contextual cues in mice lacking the 5-HT1A receptor. Neuropsychopharmacology 31, 101-111.

Kobayashi, M., Takei, H., Yamamoto, K., Hatanaka, H., Koshikawa, N., 2012. Kinetics of GABAB autoreceptor-mediated suppression of GABA release in rat insular cortex. J. Neurophysiol. 107, 1431-1442.

Kobayashi, T., Ikeda, K., Kojima, H., Niki, H., Yano, R., Yoshioka, T., Kumanishi, T., 1999. Ethanol opens G-protein-activated inwardly rectifying K+ channels. Nat. Neurosci. 2, 1091-1097.

Kobayashi, T., Ikeda, K., Kumanishi, T., 2000. Inhibition by various antipsychotic drugs of the G-protein-activated inwardly rectifying K(+)

(GIRK) channels expressed in xenopus oocytes. Br. J. Pharmacol. 129, 1716-1722.

Kobayashi, T., Washiyama, K., Ikeda, K., 2004a. Inhibition of G protein-activated inwardly rectifying K+ channels by various antidepressant drugs. Neuropsychopharmacology 29, 1841-1851.

Kobayashi, T., Washiyama, K., Ikeda, K., 2004b. Modulators of G protein-activated inwardly rectifying K+ channels: potentially therapeutic agents for addictive drug users. Ann. N. Y. Acad. Sci. 1025, 590-594.

Kobayashi, T., Washiyama, K., Ikeda, K., 2003. Inhibition of G protein-activated inwardly rectifying K+ channels by fluoxetine (Prozac). Br. J. Pharmacol. 138, 1119-1128.

Kofuji, P., Hofer, M., Millen, K.J., Millonig, J.H., Davidson, N., Lester, H.A., Hatten, M.E., 1996. Functional analysis of the weaver mutant GIRK2 K+ channel and rescue of weaver granule cells. Neuron 16, 941-952.

Kohler, C., Steinbusch, H., 1982. Identification of serotonin and non-serotonin-containing neurons of the mid-brain raphe projecting to the entorhinal area and the hippocampal formation. A combined immunohistochemical and fluorescent retrograde tracing study in the rat brain. Neuroscience 7, 951-975.

Koike, H., Fukumoto, K., Iijima, M., Chaki, S., 2013. Role of BDNF/TrkB signaling in antidepressant-like effects of a group II metabotropic glutamate receptor antagonist in animal models of depression. Behav. Brain Res. 238, 48-52.

Koike, H., Iijima, M., Chaki, S., 2011. Involvement of AMPA receptor in both the rapid and sustained antidepressant-like effects of ketamine in animal models of depression. Behav. Brain Res. 224, 107-111.

Kornhuber, J., Bleich, S., Wiltfang, J., Maler, M., Parsons, C.G., 1999. Flupirtine shows functional NMDA receptor antagonism by enhancing Mg2+ block via activation of voltage independent potassium channels. Rapid communication. J. Neural Transm. 106, 857-867.

Kourrich, S., Masmejean, F., Martin-Eauclaire, M.F., Soumireu-Mourat, B., Mourre, C., 2003. Inwardly rectifying Kir3.1 subunit knockdown impairs learning and memory in an olfactory associative task in rat. Brain Res. Mol. Brain Res. 113, 97-106.

Koyrakh, L., Lujan, R., Colon, J., Karschin, C., Kurachi, Y., Karschin, A., Wickman, K., 2005. Molecular and cellular diversity of neuronal G-protein-gated potassium channels. J. Neurosci. 25, 11468-11478.

Kozell, L.B., Walter, N.A., Milner, L.C., Wickman, K., Buck, K.J., 2009. Mapping a barbiturate withdrawal locus to a 0.44 Mb interval and analysis of a novel null mutant identify a role for Kcnj9 (GIRK3) in withdrawal from pentobarbital, zolpidem, and ethanol. J. Neurosci. 29, 11662-11673.

Krapivinsky, G., Krapivinsky, L., Wickman, K., Clapham, D.E., 1995. G beta gamma binds directly to the G protein-gated K+ channel, IKACh. J. Biol. Chem. 270, 29059-29062.

Kreiss, D.S., Lucki, I., 1995. Effects of acute and repeated administration of antidepressant drugs on extracellular levels of 5-hydroxytryptamine measured in vivo. J. Pharmacol. Exp. Ther. 274, 866-876.

Kroeze, W.K., Kristiansen, K., Roth, B.L., 2002. Molecular biology of serotonin receptors structure and function at the molecular level. Curr. Top. Med. Chem. 2, 507-528.

Krystal, J.H., 2007. Ketamine and the potential role for rapid-acting antidepressant medications. Swiss Med. Wkly. 137, 215-216.

Krystal, J.H., Sanacora, G., Blumberg, H., Anand, A., Charney, D.S., Marek, G., Epperson, C.N., Goddard, A., Mason, G.F., 2002. Glutamate and GABA systems as targets for novel antidepressant and mood-stabilizing treatments. Mol. Psychiatry 7 Suppl 1, S71-80.

Krystal, J.H., Sanacora, G., Duman, R.S., 2013. Rapid-acting glutamatergic antidepressants: the path to ketamine and beyond. Biol. Psychiatry 73, 1133-1141.

Kubo, Y., Baldwin, T.J., Jan, Y.N., Jan, L.Y., 1993. Primary structure and functional expression of a mouse inward rectifier potassium channel. Nature 362, 127-133.

Kuhar, M.J., Roth, R.H., Aghajanian, G.K., 1972. Synaptosomes from forebrains of rats with midbrain raphe lesions: selective reduction of serotonin uptake. J. Pharmacol. Exp. Ther. 181, 36-45.

Kulik, A., Vida, I., Fukazawa, Y., Guetg, N., Kasugai, Y., Marker, C.L., Rigato, F., Bettler, B., Wickman, K., Frotscher, M., Shigemoto, R., 2006. Compartment-dependent colocalization of Kir3.2-containing K+ channels and GABAB receptors in hippocampal pyramidal cells. J. Neurosci. 26, 4289-4297.

Kumar, V., Zhang, M.X., Swank, M.W., Kunz, J., Wu, G.Y., 2005. Regulation of dendritic morphogenesis by Ras-PI3K-Akt-mTOR and Ras-MAPK signaling pathways. J. Neurosci. 25, 11288-11299.

L

Labouebe, G., Lomazzi, M., Cruz, H.G., Creton, C., Lujan, R., Li, M., Yanagawa, Y., Obata, K., Watanabe, M., Wickman, K., Boyer, S.B., Slesinger, P.A., Luscher, C., 2007. RGS2 modulates coupling between GABAB receptors and GIRK channels in dopamine neurons of the ventral tegmental area. Nat. Neurosci. 10, 1559-1568.

Lacoste, B., Riad, M., Ratte, M.O., Boye, S.M., Levesque, D., Descarries, L., 2009. Trafficking of neurokinin-1 receptors in serotonin neurons is controlled by substance P within the rat dorsal raphe nucleus. Eur. J. Neurosci. 29, 2303-2314.

Lacroix, D., Blier, P., Curet, O., de Montigny, C., 1991. Effects of long-term desipramine administration on noradrenergic neurotransmission: electrophysiological studies in the rat brain. J. Pharmacol. Exp. Ther. 257, 1081-1090.

Ladera, C., del Carmen Godino, M., Jose Cabanero, M., Torres, M., Watanabe, M., Lujan, R., Sanchez-Prieto, J., 2008. Pre-synaptic GABA receptors inhibit glutamate release through GIRK channels in rat cerebral cortex. J. Neurochem. 107, 1506-1517.

Lane, J.D., Nadi, N.S., McBride, W.J., Aprison, M.H., Kusano, K., 1977. Contents of serotonin, norepinephrine and dopamine in the cerebrum of the "staggerer", "weaver" and "nervous" neurologically mutant mice. J. Neurochem. 29, 349-350.

Lavine, N., Ethier, N., Oak, J.N., Pei, L., Liu, F., Trieu, P., Rebois, R.V., Bouvier, M., Hebert, T.E., Van Tol, H.H., 2002. G protein-coupled receptors form stable complexes with inwardly rectifying potassium channels and adenylyl cyclase. J. Biol. Chem. 277, 46010-46019.

Le Francois, B., Czesak, M., Steubl, D., Albert, P.R., 2008. Transcriptional regulation at a HTR1A polymorphism associated with mental illness. Neuropharmacology 55, 977-985.

Le Poul, E., Laaris, N., Doucet, E., Laporte, A.M., Hamon, M., Lanfumey, L., 1995. Early desensitization of somato-dendritic 5-HT1A autoreceptors in rats treated with fluoxetine or paroxetine. Naunyn Schmiedebergs Arch. Pharmacol. 352, 141-148.

Lechin, F., van der Dijs, B., Hernandez-Adrian, G., 2006. Dorsal raphe vs. median raphe serotonergic antagonism. Anatomical, physiological, behavioral, neuroendocrinological, neuropharmacological and clinical evidences: relevance for neuropharmacological therapy. Prog. Neuropsychopharmacol. Biol. Psychiatry 30, 565-585.

Lemonde, S., Du, L., Bakish, D., Hrdina, P., Albert, P.R., 2004. Association of the C(-1019)G 5-HT1A functional promoter polymorphism with antidepressant response. Int. J. Neuropsychopharmacol. 7, 501-506.

Lesage, F., Guillemare, E., Fink, M., Duprat, F., Heurteaux, C., Fosset, M., Romey, G., Barhanin, J., Lazdunski, M., 1995. Molecular properties of neuronal G-protein-activated inwardly rectifying K+ channels. J. Biol. Chem. 270, 28660-28667.

Lesch, K.P., Aulakh, C.S., Wolozin, B.L., Tolliver, T.J., Hill, J.L., Murphy, D.L., 1993. Regional brain expression of serotonin transporter mRNA

and its regulation by reuptake inhibiting antidepressants. Brain Res. Mol. Brain Res. 17, 31-35.

Lesch, K.P., Gutknecht, L., 2004. Focus on The 5-HT1A receptor: emerging role of a gene regulatory variant in psychopathology and pharmacogenetics. Int. J. Neuropsychopharmacol. 7, 381-385.

Levine, E.S., Jacobs, B.L., 1992. Neurochemical afferents controlling the activity of serotonergic neurons in the dorsal raphe nucleus: microiontophoretic studies in the awake cat. J. Neurosci. 12, 4037-4044.

Levitt, E.S., Hunnicutt, B.J., Knopp, S.J., Williams, J.T., Bissonnette, J.M., 2013. A selective 5-HT1a receptor agonist improves respiration in a mouse model of Rett syndrome. J. Appl. Physiol. (1985) 115, 1626-1633.

Lewohl, J.M., Wilson, W.R., Mayfield, R.D., Brozowski, S.J., Morrisett, R.A., Harris, R.A., 1999. G-protein-coupled inwardly rectifying potassium channels are targets of alcohol action. Nat. Neurosci. 2, 1084-1090.

Leysen, J.E., 2004. 5-HT2 receptors. Curr. Drug Targets CNS Neurol. Disord. 3, 11-26.

Li, N., Lee, B., Liu, R.J., Banasr, M., Dwyer, J.M., Iwata, M., Li, X.Y., Aghajanian, G., Duman, R.S., 2010. mTOR-dependent synapse formation underlies the rapid antidepressant effects of NMDA antagonists. Science 329, 959-964.

Li, N., Liu, R.J., Dwyer, J.M., Banasr, M., Lee, B., Son, H., Li, X.Y., Aghajanian, G., Duman, R.S., 2011. Glutamate N-methyl-D-aspartate receptor antagonists rapidly reverse behavioral and synaptic deficits caused by chronic stress exposure. Biol. Psychiatry 69, 754-761.

References

Li, Y.Q., Li, H., Kaneko, T., Mizuno, N., 2001. Morphological features and electrophysiological properties of serotonergic and non-serotonergic projection neurons in the dorsal raphe nucleus. An intracellular recording and labeling study in rat brain slices. Brain Res. 900, 110-118.

Li, Y.W., Bayliss, D.A., 1998. Presynaptic inhibition by 5-HT1B receptors of glutamatergic synaptic inputs onto serotonergic caudal raphe neurones in rat. J. Physiol. 510 (Pt 1), 121-134.

Liao, Y.J., Jan, Y.N., Jan, L.Y., 1996. Heteromultimerization of G-protein-gated inwardly rectifying K+ channel proteins GIRK1 and GIRK2 and their altered expression in weaver brain. J. Neurosci. 16, 7137-7150.

Liu, R., Jolas, T., Aghajanian, G., 2000. Serotonin 5-HT(2) receptors activate local GABA inhibitory inputs to serotonergic neurons of the dorsal raphe nucleus. Brain Res. 873, 34-45.

Liu, Z.L., Ma, H., Xu, R.X., Dai, Y.W., Zhang, H.T., Yao, X.Q., Yang, K., 2012. Potassium channels underlie postsynaptic but not presynaptic GABAB receptor-mediated inhibition on ventrolateral periaqueductal gray neurons. Brain Res. Bull. 88, 529-533.

Lober, R.M., Pereira, M.A., Lambert, N.A., 2006. Rapid activation of inwardly rectifying potassium channels by immobile G-protein-coupled receptors. J. Neurosci. 26, 12602-12608.

Logothetis, D.E., Kim, D.H., Northup, J.K., Neer, E.J., Clapham, D.E., 1988. Specificity of action of guanine nucleotide-binding regulatory protein subunits on the cardiac muscarinic K+ channel. Proc. Natl. Acad. Sci. U. S. A. 85, 5814-5818.

Lomazzi, M., Slesinger, P.A., Luscher, C., 2008. Addictive drugs modulate GIRK-channel signaling by regulating RGS proteins. Trends Pharmacol. Sci. 29, 544-549.

Lotsch, J., Pruss, H., Veh, R.W., Doehring, A., 2010. A KCNJ6 (Kir3.2, GIRK2) gene polymorphism modulates opioid effects on analgesia and addiction but not on pupil size. Pharmacogenet Genomics 20, 291-297.

Lowry, C.A., Hale, M.W., Evans, A.K., Heerkens, J., Staub, D.R., Gasser, P.J., Shekhar, A., 2008. Serotonergic systems, anxiety, and affective disorder: focus on the dorsomedial part of the dorsal raphe nucleus. Ann. N. Y. Acad. Sci. 1148, 86-94.

Lujan, R., Marron Fernandez de Velasco, E., Aguado, C., Wickman, K., 2014. New insights into the therapeutic potential of Girk channels. Trends Neurosci. 37, 20-29.

Lujan, R., Maylie, J., Adelman, J.P., 2009. New sites of action for GIRK and SK channels. Nat. Rev. Neurosci. 10, 475-480.

Lunn, M.L., Nassirpour, R., Arrabit, C., Tan, J., McLeod, I., Arias, C.M., Sawchenko, P.E., Yates, J.R.,3rd, Slesinger, P.A., 2007. A unique sorting nexin regulates trafficking of potassium channels via a PDZ domain interaction. Nat. Neurosci. 10, 1249-1259.

Luscher, B., Shen, Q., Sahir, N., 2011. The GABAergic deficit hypothesis of major depressive disorder. Mol. Psychiatry 16, 383-406.

Luscher, C., Jan, L.Y., Stoffel, M., Malenka, R.C., Nicoll, R.A., 1997. G protein-coupled inwardly rectifying K+ channels (GIRKs) mediate postsynaptic but not presynaptic transmitter actions in hippocampal neurons. Neuron 19, 687-695.

Luscher, C., Slesinger, P.A., 2010. Emerging roles for G protein-gated inwardly rectifying potassium (GIRK) channels in health and disease. Nat. Rev. Neurosci. 11, 301-315.

Luscher, C., Ungless, M.A., 2006. The mechanistic classification of addictive drugs. PLoS Med. 3, e437.

M

Ma, D., Zerangue, N., Raab-Graham, K., Fried, S.R., Jan, Y.N., Jan, L.Y., 2002. Diverse trafficking patterns due to multiple traffic motifs in G protein-activated inwardly rectifying potassium channels from brain and heart. Neuron 33, 715-729.

Maciewicz, R., Foote, W.E., Bry, J., 1981. Excitatory projection from the interpeduncular nucleus to central superior raphe neurons. Brain Res. 225, 179-183.

Maejima, T., Masseck, O.A., Mark, M.D., Herlitze, S., 2013. Modulation of firing and synaptic transmission of serotonergic neurons by intrinsic G protein-coupled receptors and ion channels. Front. Integr. Neurosci. 7, 40.

Maeng, S., Zarate, C.A.,Jr, Du, J., Schloesser, R.J., McCammon, J., Chen, G., Manji, H.K., 2008. Cellular mechanisms underlying the antidepressant effects of ketamine: role of alpha-amino-3-hydroxy-5-methylisoxazole-4-propionic acid receptors. Biol. Psychiatry 63, 349-352.

Maeno, H., Kiyama, H., Tohyama, M., 1993. Distribution of the substance P receptor (NK-1 receptor) in the central nervous system. Brain Res. Mol. Brain Res. 18, 43-58.

Malagie, I., Trillat, A.C., Jacquot, C., Gardier, A.M., 1995. Effects of acute fluoxetine on extracellular serotonin levels in the raphe: an in vivo microdialysis study. Eur. J. Pharmacol. 286, 213-217.

Malberg, J.E., Eisch, A.J., Nestler, E.J., Duman, R.S., 2000. Chronic antidepressant treatment increases neurogenesis in adult rat hippocampus. J. Neurosci. 20, 9104-9110.

Mannoury la Cour, C., Boni, C., Hanoun, N., Lesch, K.P., Hamon, M., Lanfumey, L., 2001. Functional consequences of 5-HT transporter gene disruption on 5-HT(1a) receptor-mediated regulation of dorsal raphe and hippocampal cell activity. J. Neurosci. 21, 2178-2185.

Mannoury la Cour, C., Hanoun, N., Melfort, M., Hen, R., Lesch, K.P., Hamon, M., Lanfumey, L., 2004. GABA(B) receptors in 5-HT transporter- and 5-HT1A receptor-knock-out mice: further evidence of a transduction pathway shared with 5-HT1A receptors. J. Neurochem. 89, 886-896.

Marcinkiewicz, M., Morcos, R., Chretien, M., 1989. CNS connections with the median raphe nucleus: retrograde tracing with WGA-apoHRP-Gold complex in the rat. J. Comp. Neurol. 289, 11-35.

Marinelli, S., Schnell, S.A., Hack, S.P., Christie, M.J., Wessendorf, M.W., Vaughan, C.W., 2004. Serotonergic and nonserotonergic dorsal raphe neurons are pharmacologically and electrophysiologically heterogeneous. J. Neurophysiol. 92, 3532-3537.

Marker, C.L., Lujan, R., Loh, H.H., Wickman, K., 2005. Spinal G-protein-gated potassium channels contribute in a dose-dependent manner to the analgesic effect of mu- and delta- but not kappa-opioids. J. Neurosci. 25, 3551-3559.

Marker, C.L., Stoffel, M., Wickman, K., 2004. Spinal G-protein-gated K+ channels formed by GIRK1 and GIRK2 subunits modulate thermal nociception and contribute to morphine analgesia. J. Neurosci. 24, 2806-2812.

Martin-Ruiz, R., Ugedo, L., Honrubia, M.A., Mengod, G., Artigas, F., 2001. Control of serotonergic neurons in rat brain by dopaminergic receptors outside the dorsal raphe nucleus. J. Neurochem. 77, 762-775.

Massari, V.J., Gottesfeld, Z., Jacobowitz, D.M., 1976. Distribution of glutamic acid decarboxylase in certain rhombenecephalic and thalamic nuclei of the rat. Brain Res. 118, 147-151.

Matsumoto, M., Yoshioka, M., Togashi, H., Ikeda, T., Saito, H., 1996. Functional regulation by dopamine receptors of serotonin release from the rat hippocampus: in vivo microdialysis study. Naunyn Schmiedebergs Arch. Pharmacol. 353, 621-629.

Maya Vetencourt, J.F., Sale, A., Viegi, A., Baroncelli, L., De Pasquale, R., O'Leary, O.F., Castren, E., Maffei, L., 2008. The antidepressant fluoxetine restores plasticity in the adult visual cortex. Science 320, 385-388.

Mayorga, A.J., Dalvi, A., Page, M.E., Zimov-Levinson, S., Hen, R., Lucki, I., 2001. Antidepressant-like behavioral effects in 5-hydroxytryptamine(1A) and 5-hydroxytryptamine(1B) receptor mutant mice. J. Pharmacol. Exp. Ther. 298, 1101-1107.

McCardle, C.E., Gartside, S.E., 2012. Effects of general anaesthetics on 5-HT neuronal activity in the dorsal raphe nucleus. Neuropharmacology 62, 1787-1796.

McCarver, B.M., 2001. Essential Psychopharmacology: Neuroscientific Basis and Practical Applications, 2nd ed. Prim. Care. Companion J. Clin. Psychiatry. 3, 269.

McDevitt, R.A., Neumaier, J.F., 2011. Regulation of dorsal raphe nucleus function by serotonin autoreceptors: a behavioral perspective. J. Chem. Neuroanat. 41, 234-246.

McMillen, B.A., Warnack, W., German, D.C., Shore, P.A., 1980. Effects of chronic desipramine treatment on rat brain noradrenergic responses to alpha-adrenergic drugs. Eur. J. Pharmacol. 61, 239-246.

Melis, M., Camarini, R., Ungless, M.A., Bonci, A., 2002. Long-lasting potentiation of GABAergic synapses in dopamine neurons after a single in vivo ethanol exposure. J. Neurosci. 22, 2074-2082.

Mendiguren, A., Pineda, J., 2009. Effect of the CB(1) receptor antagonists rimonabant and AM251 on the firing rate of dorsal raphe nucleus neurons in rat brain slices. Br. J. Pharmacol. 158, 1579-1587.

Mendlin, A., Martin, F.J., Jacobs, B.L., 1998. Involvement of dopamine D2 receptors in apomorphine-induced facilitation of forebrain serotonin output. Eur. J. Pharmacol. 351, 291-298.

Mennini, T., Gobbi, M., Romandini, S., 1986. Localization of GABAA and GABAB receptor subtypes on serotonergic neurons. Brain Res. 371, 372-375.

Michaeli, A., Yaka, R., 2010. Dopamine inhibits GABA(A) currents in ventral tegmental area dopamine neurons via activation of presynaptic G-protein coupled inwardly-rectifying potassium channels. Neuroscience 165, 1159-1169.

Michelsen, K.A., Schmitz, C., Steinbusch, H.W., 2007. The dorsal raphe nucleus--from silver stainings to a role in depression. Brain Res. Rev. 55, 329-342.

Miguelez, C., Fernandez-Aedo, I., Torrecilla, M., Grandoso, L., Ugedo, L., 2009. alpha(2)-Adrenoceptors mediate the acute inhibitory effect of fluoxetine on locus coeruleus noradrenergic neurons. Neuropharmacology 56, 1068-1073.

Mihailescu, S., Guzman-Marin, R., Dominguez Mdel, C., Drucker-Colin, R., 2002. Mechanisms of nicotine actions on dorsal raphe serotoninergic neurons. Eur. J. Pharmacol. 452, 77-82.

Miquel, M.C., Doucet, E., Riad, M., Adrien, J., Verge, D., Hamon, M., 1992. Effect of the selective lesion of serotoninergic neurons on the regional distribution of 5-HT1A receptor mRNA in the rat brain. Brain Res. Mol. Brain Res. 14, 357-362.

Mirshahi, T., Logothetis, D.E., 2004. Molecular determinants responsible for differential cellular distribution of G protein-gated inwardly rectifying K+ channels. J. Biol. Chem. 279, 11890-11897.

Misgeld, U., Muller, W., Brunner, H., 1989. Effects of (-)baclofen on inhibitory neurons in the guinea pig hippocampal slice. Pflugers Arch. 414, 139-144.

Mitrovic, I., Margeta-Mitrovic, M., Bader, S., Stoffel, M., Jan, L.Y., Basbaum, A.I., 2003. Contribution of GIRK2-mediated postsynaptic signaling to opiate and alpha 2-adrenergic analgesia and analgesic sex differences. Proc. Natl. Acad. Sci. U. S. A. 100, 271-276.

Moghaddam, B., Adams, B., Verma, A., Daly, D., 1997. Activation of glutamatergic neurotransmission by ketamine: a novel step in the pathway from NMDA receptor blockade to dopaminergic and cognitive disruptions associated with the prefrontal cortex. J. Neurosci. 17, 2921-2927.

Moghaddam, B., Adams, B.W., 1998. Reversal of phencyclidine effects by a group II metabotropic glutamate receptor agonist in rats. Science 281, 1349-1352.

Molliver, M.E., 1987. Serotonergic neuronal systems: what their anatomic organization tells us about function. J. Clin. Psychopharmacol. 7, 3S-23S.

Mombereau, C., Kaupmann, K., van der Putten, H., Cryan, J.F., 2004. Altered response to benzodiazepine anxiolytics in mice lacking GABA B(1) receptors. Eur. J. Pharmacol. 497, 119-120.

Moranta, D., Esteban, S., Garcia-Sevilla, J.A., 2009. Chronic treatment and withdrawal of the cannabinoid agonist WIN 55,212-2 modulate the sensitivity of presynaptic receptors involved in the regulation of monoamine syntheses in rat brain. Naunyn Schmiedebergs Arch. Pharmacol. 379, 61-72.

Morgan, A.D., Carroll, M.E., Loth, A.K., Stoffel, M., Wickman, K., 2003a. Decreased cocaine self-administration in Kir3 potassium channel subunit knockout mice. Neuropsychopharmacology 28, 932-938.

Morikawa, H., Manzoni, O.J., Crabbe, J.C., Williams, J.T., 2000. Regulation of central synaptic transmission by 5-HT(1B) auto- and heteroreceptors. Mol. Pharmacol. 58, 1271-1278.

Morishige, K., Inanobe, A., Yoshimoto, Y., Kurachi, H., Murata, Y., Tokunaga, Y., Maeda, T., Maruyama, Y., Kurachi, Y., 1999. Secretagogue-induced exocytosis recruits G protein-gated K+ channels to plasma membrane in endocrine cells. J. Biol. Chem. 274, 7969-7974.

Mullner, C., Vorobiov, D., Bera, A.K., Uezono, Y., Yakubovich, D., Frohnwieser-Steinecker, B., Dascal, N., Schreibmayer, W., 2000. Heterologous facilitation of G protein-activated K(+) channels by beta-adrenergic stimulation via cAMP-dependent protein kinase. J. Gen. Physiol. 115, 547-558.

Musazzi, L., Treccani, G., Mallei, A., Popoli, M., 2013. The action of antidepressants on the glutamate system: regulation of glutamate release and glutamate receptors. Biol. Psychiatry 73, 1180-1188.

N

Nakazi, M., Bauer, U., Nickel, T., Kathmann, M., Schlicker, E., 2000. Inhibition of serotonin release in the mouse brain via presynaptic cannabinoid CB1 receptors. Naunyn Schmiedebergs Arch. Pharmacol. 361, 19-24.

Nassirpour, R., Slesinger, P.A., 2007. Subunit-specific regulation of Kir3 channels by sorting nexin 27. Channels (Austin) 1, 331-333.

Naughton, M., Clarke, G., O'Leary, O.F., Cryan, J.F., Dinan, T.G., 2014. A review of ketamine in affective disorders: current evidence of clinical efficacy, limitations of use and pre-clinical evidence on proposed mechanisms of action. J. Affect. Disord. 156, 24-35.

Navarro, B., Kennedy, M.E., Velimirovic, B., Bhat, D., Peterson, A.S., Clapham, D.E., 1996. Nonselective and G betagamma-insensitive weaver K+ channels. Science 272, 1950-1953.

Newberry, N.R., Nicoll, R.A., 1985. Comparison of the action of baclofen with gamma-aminobutyric acid on rat hippocampal pyramidal cells in vitro. J. Physiol. 360, 161-185.

Nishida, M., Cadene, M., Chait, B.T., MacKinnon, R., 2007. Crystal structure of a Kir3.1-prokaryotic Kir channel chimera. EMBO J. 26, 4005-4015.

Nishitani, N., Nagayasu, K., Asaoka, N., Yamashiro, M., Shirakawa, H., Nakagawa, T., Kaneko, S., 2014. Raphe AMPA receptors and nicotinic acetylcholine receptors mediate ketamine-induced serotonin release in the rat prefrontal cortex. Int. J. Neuropsychopharmacol. 17, 1321-1326.

Nishizawa, D., Nagashima, M., Katoh, R., Satoh, Y., Tagami, M., Kasai, S., Ogai, Y., Han, W., Hasegawa, J., Shimoyama, N., Sora, I., Hayashida, M., Ikeda, K., 2009. Association between KCNJ6 (GIRK2) gene polymorphisms and postoperative analgesic requirements after major abdominal surgery. PLoS One 4, e7060.

Nitz, D., Siegel, J., 1997. GABA release in the dorsal raphe nucleus: role in the control of REM sleep. Am. J. Physiol. 273, R451-5.

O

O'Reilly, C.A., Reith, M.E., 1988. Uptake of [3H]serotonin into plasma membrane vesicles from mouse cerebral cortex. J. Biol. Chem. 263, 6115-6121.

Ostrovskaya, O., Xie, K., Masuho, I., Fajardo-Serrano, A., Lujan, R., Wickman, K., Martemyanov, K.A., 2014. RGS7/Gbeta5/R7BP complex regulates synaptic plasticity and memory by modulating hippocampal GABABR-GIRK signaling. Elife 3, e02053.

Ota, K.T., Liu, R.J., Voleti, B., Maldonado-Aviles, J.G., Duric, V., Iwata, M., Dutheil, S., Duman, C., Boikess, S., Lewis, D.A., Stockmeier, C.A., DiLeone, R.J., Rex, C., Aghajanian, G.K., Duman, R.S., 2014. REDD1 is essential for stress-induced synaptic loss and depressive behavior. Nat. Med. 20, 531-535.

P

Pan, Z.Z., Williams, J.T., 1989. GABA- and glutamate-mediated synaptic potentials in rat dorsal raphe neurons in vitro. J. Neurophysiol. 61, 719-726.

Parker, R.B., Waud, D.R., 1971. Pharmacological estimation of drug-receptor dissociation constants. Statistical evaluation. I. Agonists. J. Pharmacol. Exp. Ther. 177, 1-12.

Parks, C.L., Robinson, P.S., Sibille, E., Shenk, T., Toth, M., 1998. Increased anxiety of mice lacking the serotonin1A receptor. Proc. Natl. Acad. Sci. U. S. A. 95, 10734-10739.

Parsey, R.V., Oquendo, M.A., Ogden, R.T., Olvet, D.M., Simpson, N., Huang, Y.Y., Van Heertum, R.L., Arango, V., Mann, J.J., 2006. Altered serotonin 1A binding in major depression: a [carbonyl-C-11]WAY100635 positron emission tomography study. Biol. Psychiatry 59, 106-113.

Patil, N., Cox, D.R., Bhat, D., Faham, M., Myers, R.M., Peterson, A.S., 1995. A potassium channel mutation in weaver mice implicates membrane excitability in granule cell differentiation. Nat. Genet. 11, 126-129.

Pegan, S., Arrabit, C., Zhou, W., Kwiatkowski, W., Collins, A., Slesinger, P.A., Choe, S., 2005. Cytoplasmic domain structures of Kir2.1 and Kir3.1 show sites for modulating gating and rectification. Nat. Neurosci. 8, 279-287.

Peleg, S., Varon, D., Ivanina, T., Dessauer, C.W., Dascal, N., 2002. G(alpha)(i) controls the gating of the G protein-activated K(+) channel, GIRK. Neuron 33, 87-99.

Perry, C.A., Pravetoni, M., Teske, J.A., Aguado, C., Erickson, D.J., Medrano, J.F., Lujan, R., Kotz, C.M., Wickman, K., 2008. Predisposition to late-onset obesity in GIRK4 knockout mice. Proc. Natl. Acad. Sci. U. S. A. 105, 8148-8153.

Peterson, R.T., Beal, P.A., Comb, M.J., Schreiber, S.L., 2000. FKBP12-rapamycin-associated protein (FRAP) autophosphorylates at serine 2481 under translationally repressive conditions. J. Biol. Chem. 275, 7416-7423.

Petrenko, A.B., Yamakura, T., Fujiwara, N., Askalany, A.R., Baba, H., Sakimura, K., 2004. Reduced sensitivity to ketamine and pentobarbital in mice lacking the N-methyl-D-aspartate receptor GluRepsilon1 subunit. Anesth. Analg. 99, 1136-40, table of contents.

Peyron, C., Luppi, P.H., Fort, P., Rampon, C., Jouvet, M., 1996. Lower brainstem catecholamine afferents to the rat dorsal raphe nucleus. J. Comp. Neurol. 364, 402-413.

Peyron, C., Petit, J.M., Rampon, C., Jouvet, M., Luppi, P.H., 1998. Forebrain afferents to the rat dorsal raphe nucleus demonstrated by retrograde and anterograde tracing methods. Neuroscience 82, 443-468.

Pfeffer, S.R., 2013. A nexus for receptor recycling. Nat. Cell Biol. 15, 446-448.

Pieribone, V.A., Nicholas, A.P., Dagerlind, A., Hokfelt, T., 1994. Distribution of alpha 1 adrenoceptors in rat brain revealed by in situ hybridization experiments utilizing subtype-specific probes. J. Neurosci. 14, 4252-4268.

Pietersen, A.N., Lancaster, D.M., Patel, N., Hamilton, J.B., Vreugdenhil, M., 2009. Modulation of gamma oscillations by endogenous adenosine through A1 and A2A receptors in the mouse hippocampus. Neuropharmacology 56, 481-492.

Pineyro, G., Blier, P., 1999. Autoregulation of serotonin neurons: role in antidepressant drug action. Pharmacol. Rev. 51, 533-591.

Pineyro, G., Blier, P., 1996. Regulation of 5-hydroxytryptamine release from rat midbrain raphe nuclei by 5-hydroxytryptamine1D receptors: effect of tetrodotoxin, G protein inactivation and long-term antidepressant administration. J. Pharmacol. Exp. Ther. 276, 697-707.

Pineyro, G., Castanon, N., Hen, R., Blier, P., 1995. Regulation of [3H]5-HT release in raphe, frontal cortex and hippocampus of 5-HT1B knock-out mice. Neuroreport 7, 353-359.

Pittenger, C., Duman, R.S., 2008. Stress, depression, and neuroplasticity: a convergence of mechanisms. Neuropsychopharmacology 33, 88-109.

Pompeiano, M., Palacios, J.M., Mengod, G., 1992. Distribution and cellular localization of mRNA coding for 5-HT1A receptor in the rat brain: correlation with receptor binding. J. Neurosci. 12, 440-453.

Ponce, A., Bueno, E., Kentros, C., Vega-Saenz de Miera, E., Chow, A., Hillman, D., Chen, S., Zhu, L., Wu, M.B., Wu, X., Rudy, B., Thornhill, W.B., 1996. G-protein-gated inward rectifier K+ channel proteins (GIRK1) are present in the soma and dendrites as well as in nerve terminals of specific neurons in the brain. J. Neurosci. 16, 1990-2001.

Popik, P., Kos, T., Sowa-Kucma, M., Nowak, G., 2008. Lack of persistent effects of ketamine in rodent models of depression. Psychopharmacology (Berl) 198, 421-430.

Popoli, M., Gennarelli, M., Racagni, G., 2002. Modulation of synaptic plasticity by stress and antidepressants. Bipolar Disord. 4, 166-182.

Popoli, M., Yan, Z., McEwen, B.S., Sanacora, G., 2011. The stressed synapse: the impact of stress and glucocorticoids on glutamate transmission. Nat. Rev. Neurosci. 13, 22-37.

Portella, M.J., de Diego-Adelino, J., Ballesteros, J., Puigdemont, D., Oller, S., Santos, B., Alvarez, E., Artigas, F., Perez, V., 2011. Can we really accelerate and enhance the selective serotonin reuptake inhibitor antidepressant effect? A randomized clinical trial and a meta-analysis of pindolol in nonresistant depression. J. Clin. Psychiatry 72, 962-969.

Pravetoni, M., Wickman, K., 2008. Behavioral characterization of mice lacking GIRK/Kir3 channel subunits. Genes Brain Behav. 7, 523-531.

Q

Quinaux, N., Scuvee-Moreau, J., Dresse, A., 1982. Inhibition of in vitro and ex vivo uptake of noradrenaline and 5-hydroxytryptamine by five antidepressants; correlation with reduction of spontaneous firing rate of central monoaminergic neurones. Naunyn Schmiedebergs Arch. Pharmacol. 319, 66-70.

R

Racagni, G., Popoli, M., 2010. The pharmacological properties of antidepressants. Int. Clin. Psychopharmacol. 25, 117-131.

Rakic, P., Sidman, R.L., 1973. Sequence of developmental abnormalities leading to granule cell deficit in cerebellar cortex of weaver mutant mice. J. Comp. Neurol. 152, 103-132.

Ramboz, S., Oosting, R., Amara, D.A., Kung, H.F., Blier, P., Mendelsohn, M., Mann, J.J., Brunner, D., Hen, R., 1998. Serotonin receptor 1A knockout: an animal model of anxiety-related disorder. Proc. Natl. Acad. Sci. U. S. A. 95, 14476-14481.

Ramos-Hunter, S.J., Engers, D.W., Kaufmann, K., Du, Y., Lindsley, C.W., Weaver, C.D., Sulikowski, G.A., 2013. Discovery and SAR of a novel series of GIRK1/2 and GIRK1/4 activators. Bioorg. Med. Chem. Lett. 23, 5195-5198.

Raveh, A., Riven, I., Reuveny, E., 2009. Elucidation of the gating of the GIRK channel using a spectroscopic approach. J. Physiol. 587, 5331-5335.

Razani, H., Diaz-Cabiale, Z., Fuxe, K., Ogren, S.O., 2000. Intraventricular galanin produces a time-dependent modulation of 5-HT1A receptors in the dorsal raphe of the rat. Neuroreport 11, 3943-3948.

Rebois, R.V., Robitaille, M., Gales, C., Dupre, D.J., Baragli, A., Trieu, P., Ethier, N., Bouvier, M., Hebert, T.E., 2006. Heterotrimeric G proteins form stable complexes with adenylyl cyclase and Kir3.1 channels in living cells. J. Cell. Sci. 119, 2807-2818.

Reeves, R.H., Irving, N.G., Moran, T.H., Wohn, A., Kitt, C., Sisodia, S.S., Schmidt, C., Bronson, R.T., Davisson, M.T., 1995. A mouse model for Down syndrome exhibits learning and behaviour deficits. Nat. Genet. 11, 177-184.

Richardson-Jones, J.W., Craige, C.P., Guiard, B.P., Stephen, A., Metzger, K.L., Kung, H.F., Gardier, A.M., Dranovsky, A., David, D.J., Beck, S.G., Hen, R., Leonardo, E.D., 2010. 5-HT1A autoreceptor levels determine vulnerability to stress and response to antidepressants. Neuron 65, 40-52.

Richardson-Jones, J.W., Craige, C.P., Nguyen, T.H., Kung, H.F., Gardier, A.M., Dranovsky, A., David, D.J., Guiard, B.P., Beck, S.G., Hen, R., Leonardo, E.D., 2011. Serotonin-1A autoreceptors are necessary and sufficient for the normal formation of circuits underlying innate anxiety. J. Neurosci. 31, 6008-6018.

Riven, I., Iwanir, S., Reuveny, E., 2006. GIRK channel activation involves a local rearrangement of a preformed G protein channel complex. Neuron 51, 561-573.

Rodriguez, J.J., Jones, V.C., Tabuchi, M., Allan, S.M., Knight, E.M., LaFerla, F.M., Oddo, S., Verkhratsky, A., 2008. Impaired adult neurogenesis in

the dentate gyrus of a triple transgenic mouse model of Alzheimer's disease. PLoS One 3, e2935.

Rodriguez, J.J., Jones, V.C., Verkhratsky, A., 2009. Impaired cell proliferation in the subventricular zone in an Alzheimer's disease model. Neuroreport 20, 907-912.

Roffler-Tarlov, S., Martin, B., Graybiel, A.M., Kauer, J.S., 1996. Cell death in the midbrain of the murine mutation weaver. J. Neurosci. 16, 1819-1826.

Romero, L., Bel, N., Artigas, F., de Montigny, C., Blier, P., 1996. Effect of pindolol on the function of pre- and postsynaptic 5-HT1A receptors: in vivo microdialysis and electrophysiological studies in the rat brain. Neuropsychopharmacology 15, 349-360.

Romero, L., Celada, P., Artigas, F., 1994. Reduction of in vivo striatal 5-hydroxytryptamine release by 8-OH-DPAT after inactivation of Gi/G(o) proteins in dorsal raphe nucleus. Eur. J. Pharmacol. 265, 103-106.

Rosin, D.L., Talley, E.M., Lee, A., Stornetta, R.L., Gaylinn, B.D., Guyenet, P.G., Lynch, K.R., 1996. Distribution of alpha 2C-adrenergic receptor-like immunoreactivity in the rat central nervous system. J. Comp. Neurol. 372, 135-165.

Ross, E.M., Wilkie, T.M., 2000. GTPase-activating proteins for heterotrimeric G proteins: regulators of G protein signaling (RGS) and RGS-like proteins. Annu. Rev. Biochem. 69, 795-827.

Ruat, M., Traiffort, E., Leurs, R., Tardivel-Lacombe, J., Diaz, J., Arrang, J.M., Schwartz, J.C., 1993. Molecular cloning, characterization, and localization of a high-affinity serotonin receptor (5-HT7) activating cAMP formation. Proc. Natl. Acad. Sci. U. S. A. 90, 8547-8551.

Rudnick, G., Wall, S.C., 1992a. The molecular mechanism of "ecstasy" [3,4-methylenedioxy-methamphetamine (MDMA)]: serotonin transporters are targets for MDMA-induced serotonin release. Proc. Natl. Acad. Sci. U. S. A. 89, 1817-1821.

Rudnick, G., Wall, S.C., 1992b. The platelet plasma membrane serotonin transporter catalyzes exchange between neurotoxic amphetamines and serotonin. Ann. N. Y. Acad. Sci. 648, 345-347.

Rush, A.J., Trivedi, M.H., Wisniewski, S.R., Nierenberg, A.A., Stewart, J.W., Warden, D., Niederehe, G., Thase, M.E., Lavori, P.W., Lebowitz, B.D., McGrath, P.J., Rosenbaum, J.F., Sackeim, H.A., Kupfer, D.J., Luther, J., Fava, M., 2006. Acute and longer-term outcomes in depressed outpatients requiring one or several treatment steps: a STAR*D report. Am. J. Psychiatry 163, 1905-1917.

Rusinova, R., Shen, Y.M., Dolios, G., Padovan, J., Yang, H., Kirchberger, M., Wang, R., Logothetis, D.E., 2009. Mass spectrometric analysis reveals a functionally important PKA phosphorylation site in a Kir3 channel subunit. Pflugers Arch. 458, 303-314.

Rutter, J.J., Gundlah, C., Auerbach, S.B., 1994. Increase in extracellular serotonin produced by uptake inhibitors is enhanced after chronic treatment with fluoxetine. Neurosci. Lett. 171, 183-186.

S

Sadja, R., Alagem, N., Reuveny, E., 2003. Gating of GIRK channels: details of an intricate, membrane-delimited signaling complex. Neuron 39, 9-12.

References

Saenz del Burgo, L., Cortes, R., Mengod, G., Zarate, J., Echevarria, E., Salles, J., 2008. Distribution and neurochemical characterization of neurons expressing GIRK channels in the rat brain. J. Comp. Neurol. 510, 581-606.

Sago, H., Carlson, E.J., Smith, D.J., Kilbridge, J., Rubin, E.M., Mobley, W.C., Epstein, C.J., Huang, T.T., 1998. Ts1Cje, a partial trisomy 16 mouse model for Down syndrome, exhibits learning and behavioral abnormalities. Proc. Natl. Acad. Sci. U. S. A. 95, 6256-6261.

Sakai, K., Salvert, D., Touret, M., Jouvet, M., 1977. Afferent connections of the nucleus raphe dorsalis in the cat as visualized by the horseradish peroxidase technique. Brain Res. 137, 11-35.

Sanacora, G., Berman, R.M., Cappiello, A., Oren, D.A., Kugaya, A., Liu, N., Gueorguieva, R., Fasula, D., Charney, D.S., 2004. Addition of the alpha2-antagonist yohimbine to fluoxetine: effects on rate of antidepressant response. Neuropsychopharmacology 29, 1166-1171.

Sanacora, G., Treccani, G., Popoli, M., 2012. Towards a glutamate hypothesis of depression: an emerging frontier of neuropsychopharmacology for mood disorders. Neuropharmacology 62, 63-77.

Sanchez, C., Asin, K.E., Artigas, F., 2015. Vortioxetine, a novel antidepressant with multimodal activity: review of preclinical and clinical data. Pharmacol. Ther. 145, 43-57.

Santarelli, L., Saxe, M., Gross, C., Surget, A., Battaglia, F., Dulawa, S., Weisstaub, N., Lee, J., Duman, R., Arancio, O., Belzung, C., Hen, R., 2003. Requirement of hippocampal neurogenesis for the behavioral effects of antidepressants. Science 301, 805-809.

Sari, Y., Miquel, M.C., Brisorgueil, M.J., Ruiz, G., Doucet, E., Hamon, M., Verge, D., 1999. Cellular and subcellular localization of 5-hydroxytryptamine1B receptors in the rat central nervous system: immunocytochemical, autoradiographic and lesion studies. Neuroscience 88, 899-915.

Savitz, J., Drevets, W.C., 2009. Bipolar and major depressive disorder: neuroimaging the developmental-degenerative divide. Neurosci. Biobehav. Rev. 33, 699-771.

Scanziani, M., 2000. GABA spillover activates postsynaptic GABA(B) receptors to control rhythmic hippocampal activity. Neuron 25, 673-681.

Schein, J.C., Wang, J.K., Roffler-Tarlov, S.K., 2005. The effect of GIRK2(wv) on neurite growth, protein expression, and viability in the CNS-derived neuronal cell line, CATH.A-differentiated. Neuroscience 134, 21-32.

Scheinin, M., Lomasney, J.W., Hayden-Hixson, D.M., Schambra, U.B., Caron, M.G., Lefkowitz, R.J., Fremeau, R.T.,Jr, 1994. Distribution of alpha 2-adrenergic receptor subtype gene expression in rat brain. Brain Res. Mol. Brain Res. 21, 133-149.

Schildkraut, J.J., 1965. The catecholamine hypothesis of affective disorders: a review of supporting evidence. Am. J. Psychiatry 122, 509-522.

Schratt, G.M., Nigh, E.A., Chen, W.G., Hu, L., Greenberg, M.E., 2004. BDNF regulates the translation of a select group of mRNAs by a mammalian

target of rapamycin-phosphatidylinositol 3-kinase-dependent pathway during neuronal development. J. Neurosci. 24, 7366-7377.

Schreibmayer, W., Dessauer, C.W., Vorobiov, D., Gilman, A.G., Lester, H.A., Davidson, N., Dascal, N., 1996. Inhibition of an inwardly rectifying K+ channel by G-protein alpha-subunits. Nature 380, 624-627.

Sergeyev, V., Hokfelt, T., Hurd, Y., 1999. Serotonin and substance P co-exist in dorsal raphe neurons of the human brain. Neuroreport 10, 3967-3970.

Sharp, T., Boothman, L., Raley, J., Queree, P., 2007. Important messages in the 'post': recent discoveries in 5-HT neurone feedback control. Trends Pharmacol. Sci. 28, 629-636.

Shopsin, B., Gershon, S., Goldstein, M., Friedman, E., Wilk, S., 1975. Use of synthesis inhibitors in defining a role for biogenic amines during imipramine treatment in depressed patients. Psychopharmacol. Commun. 1, 239-249.

Siarey, R.J., Carlson, E.J., Epstein, C.J., Balbo, A., Rapoport, S.I., Galdzicki, Z., 1999. Increased synaptic depression in the Ts65Dn mouse, a model for mental retardation in Down syndrome. Neuropharmacology 38, 1917-1920.

Sibille, E., Pavlides, C., Benke, D., Toth, M., 2000. Genetic inactivation of the Serotonin(1A) receptor in mice results in downregulation of major GABA(A) receptor alpha subunits, reduction of GABA(A) receptor binding, and benzodiazepine-resistant anxiety. J. Neurosci. 20, 2758-2765.

Sickmann, T., Alzheimer, C., 2002. Agonist-specific maturation of GIRK current responses in acutely isolated pyramidal neurons of rat neocortex. Brain Res. 929, 166-174.

Signorini, S., Liao, Y.J., Duncan, S.A., Jan, L.Y., Stoffel, M., 1997. Normal cerebellar development but susceptibility to seizures in mice lacking G protein-coupled, inwardly rectifying K+ channel GIRK2. Proc. Natl. Acad. Sci. U. S. A. 94, 923-927.

Sinton, C.M., Fallon, S.L., 1988. Electrophysiological evidence for a functional differentiation between subtypes of the 5-HT1 receptor. Eur. J. Pharmacol. 157, 173-181.

Sjogren, B., 2011. Regulator of G protein signaling proteins as drug targets: current state and future possibilities. Adv. Pharmacol. 62, 315-347.

Skolnick, P., Layer, R.T., Popik, P., Nowak, G., Paul, I.A., Trullas, R., 1996. Adaptation of N-methyl-D-aspartate (NMDA) receptors following antidepressant treatment: implications for the pharmacotherapy of depression. Pharmacopsychiatry 29, 23-26.

Slesinger, P.A., Patil, N., Liao, Y.J., Jan, Y.N., Jan, L.Y., Cox, D.R., 1996. Functional effects of the mouse weaver mutation on G protein-gated inwardly rectifying K+ channels. Neuron 16, 321-331.

Slesinger, P.A., Reuveny, E., Jan, Y.N., Jan, L.Y., 1995. Identification of structural elements involved in G protein gating of the GIRK1 potassium channel. Neuron 15, 1145-1156.

Slesinger, P.A., Stoffel, M., Jan, Y.N., Jan, L.Y., 1997. Defective gamma-aminobutyric acid type B receptor-activated inwardly rectifying K+

currents in cerebellar granule cells isolated from weaver and Girk2 null mutant mice. Proc. Natl. Acad. Sci. U. S. A. 94, 12210-12217.

Smith, S.B., Marker, C.L., Perry, C., Liao, G., Sotocinal, S.G., Austin, J.S., Melmed, K., Clark, J.D., Peltz, G., Wickman, K., Mogil, J.S., 2008. Quantitative trait locus and computational mapping identifies Kcnj9 (GIRK3) as a candidate gene affecting analgesia from multiple drug classes. Pharmacogenet Genomics 18, 231-241.

Snyder, J.S., Soumier, A., Brewer, M., Pickel, J., Cameron, H.A., 2011. Adult hippocampal neurogenesis buffers stress responses and depressive behaviour. Nature 476, 458-461.

Soiza-Reilly, M., Commons, K.G., 2011. Glutamatergic drive of the dorsal raphe nucleus. J. Chem. Neuroanat. 41, 247-255.

Sotelo, C., Cholley, B., El Mestikawy, S., Gozlan, H., Hamon, M., 1990. Direct Immunohistochemical Evidence of the Existence of 5-HT1A Autoreceptors on Serotoninergic Neurons in the Midbrain Raphe Nuclei. Eur. J. Neurosci. 2, 1144-1154.

Sprouse, J.S., Aghajanian, G.K., 1987. Electrophysiological responses of serotoninergic dorsal raphe neurons to 5-HT1A and 5-HT1B agonists. Synapse 1, 3-9.

Stamford, J.A., Davidson, C., McLaughlin, D.P., Hopwood, S.E., 2000. Control of dorsal raphe 5-HT function by multiple 5-HT(1) autoreceptors: parallel purposes or pointless plurality? Trends Neurosci. 23, 459-465.

Steinbusch, H.W., 1981. Distribution of serotonin-immunoreactivity in the central nervous system of the rat-cell bodies and terminals. Neuroscience 6, 557-618.

Stockmeier, C.A., Shapiro, L.A., Dilley, G.E., Kolli, T.N., Friedman, L., Rajkowska, G., 1998. Increase in serotonin-1A autoreceptors in the midbrain of suicide victims with major depression-postmortem evidence for decreased serotonin activity. J. Neurosci. 18, 7394-7401.

Stopper, C.M., Floresco, S.B., 2014. What's better for me? Fundamental role for lateral habenula in promoting subjective decision biases. Nat. Neurosci. 17, 33-35.

Strazielle, C., Lalonde, R., Hebert, C., Reader, T.A., 1999. Regional brain distribution of noradrenaline uptake sites, and of alpha1-alpha2- and beta-adrenergic receptors in PCD mutant mice: a quantitative autoradiographic study. Neuroscience 94, 287-304.

Strobel, A., Gutknecht, L., Rothe, C., Reif, A., Mossner, R., Zeng, Y., Brocke, B., Lesch, K.P., 2003. Allelic variation in 5-HT1A receptor expression is associated with anxiety- and depression-related personality traits. J. Neural Transm. 110, 1445-1453.

Sui, J.L., Chan, K.W., Logothetis, D.E., 1996. Na+ activation of the muscarinic K+ channel by a G-protein-independent mechanism. J. Gen. Physiol. 108, 381-391.

Sui, J.L., Petit-Jacques, J., Logothetis, D.E., 1998. Activation of the atrial KACh channel by the betagamma subunits of G proteins or intracellular Na+ ions depends on the presence of phosphatidylinositol phosphates. Proc. Natl. Acad. Sci. U. S. A. 95, 1307-1312.

Sun, Q.Q., Huguenard, J.R., Prince, D.A., 2002. Somatostatin inhibits thalamic network oscillations in vitro: actions on the GABAergic neurons of the reticular nucleus. J. Neurosci. 22, 5374-5386.

Suzuki, M., Hurd, Y.L., Sokoloff, P., Schwartz, J.C., Sedvall, G., 1998. D3 dopamine receptor mRNA is widely expressed in the human brain. Brain Res. 779, 58-74.

Szabo, S.T., de Montigny, C., Blier, P., 2000. Progressive attenuation of the firing activity of locus coeruleus noradrenergic neurons by sustained administration of selective serotonin reuptake inhibitors. Int. J. Neuropsychopharmacol. 3, 1-11.

Szymkowicz, S.M., Finnegan, N., Dale, R.M., 2013. A 12-month naturalistic observation of three patients receiving repeat intravenous ketamine infusions for their treatment-resistant depression. J. Affect. Disord. 147, 416-420.

T

Takagishi, M., Chiba, T., 1991. Efferent projections of the infralimbic (area 25) region of the medial prefrontal cortex in the rat: an anterograde tracer PHA-L study. Brain Res. 566, 26-39.

Takahashi, Y., Washiyama, K., Kobayashi, T., Hayashi, S., 2006. Gene expression in the brain from fluoxetine-injected mouse using DNA microarray. Ann. N. Y. Acad. Sci. 1074, 42-51.

Tao, R., Auerbach, S.B., 2002. Opioid receptor subtypes differentially modulate serotonin efflux in the rat central nervous system. J. Pharmacol. Exp. Ther. 303, 549-556.

Tao, R., Auerbach, S.B., 2000. Regulation of serotonin release by GABA and excitatory amino acids. J. Psychopharmacol. 14, 100-113.

Tao, R., Auerbach, S.B., 1994. Increased extracellular serotonin in rat brain after systemic or intraraphe administration of morphine. J. Neurochem. 63, 517-524.

Tao, R., Ma, Z., 2012. Neural Circuit in the Dorsal Raphe Nucleus Responsible for Cannabinoid-Mediated Increases in 5-HT Efflux in the Nucleus Accumbens of the Rat Brain. ISRN Pharmacol. 2012, 276902.

Tao, R., Ma, Z., Auerbach, S.B., 1997. Influence of AMPA/kainate receptors on extracellular 5-hydroxytryptamine in rat midbrain raphe and forebrain. Br. J. Pharmacol. 121, 1707-1715.

Tao, R., Ma, Z., Auerbach, S.B., 1996. Differential regulation of 5-hydroxytryptamine release by GABAA and GABAB receptors in midbrain raphe nuclei and forebrain of rats. Br. J. Pharmacol. 119, 1375-1384.

Thompson, S.M., Gahwiler, B.H., 1992. Comparison of the actions of baclofen at pre- and postsynaptic receptors in the rat hippocampus in vitro. J. Physiol. 451, 329-345.

Tizabi, Y., Bhatti, B.H., Manaye, K.F., Das, J.R., Akinfiresoye, L., 2012. Antidepressant-like effects of low ketamine dose is associated with increased hippocampal AMPA/NMDA receptor density ratio in female Wistar-Kyoto rats. Neuroscience 213, 72-80.

To, Z.P., Bonhaus, D.W., Eglen, R.M., Jakeman, L.B., 1995. Characterization and distribution of putative 5-ht7 receptors in guinea-pig brain. Br. J. Pharmacol. 115, 107-116.

Tork, I., 1990. Anatomy of the serotonergic system. Ann. N. Y. Acad. Sci. 600, 9-34; discussion 34-5.

Torrecilla, M., Fernandez-Aedo, I., Arrue, A., Zumarraga, M., Ugedo, L., 2013. Role of GIRK channels on the noradrenergic transmission in vivo: an electrophysiological and neurochemical study on GIRK2 mutant mice. Int. J. Neuropsychopharmacol. 16, 1093-1104.

Torrecilla, M., Marker, C.L., Cintora, S.C., Stoffel, M., Williams, J.T., Wickman, K., 2002. G-protein-gated potassium channels containing Kir3.2 and Kir3.3 subunits mediate the acute inhibitory effects of opioids on locus ceruleus neurons. J. Neurosci. 22, 4328-4334.

Torrecilla, M., Quillinan, N., Williams, J.T., Wickman, K., 2008. Pre- and postsynaptic regulation of locus coeruleus neurons after chronic morphine treatment: a study of GIRK-knockout mice. Eur. J. Neurosci. 28, 618-624.

Trillat, A.C., Malagie, I., Scearce, K., Pons, D., Anmella, M.C., Jacquot, C., Hen, R., Gardier, A.M., 1997. Regulation of serotonin release in the frontal cortex and ventral hippocampus of homozygous mice lacking 5-HT1B receptors: in vivo microdialysis studies. J. Neurochem. 69, 2019-2025.

Trivedi, M.H., Rush, A.J., Wisniewski, S.R., Nierenberg, A.A., Warden, D., Ritz, L., Norquist, G., Howland, R.H., Lebowitz, B., McGrath, P.J., Shores-Wilson, K., Biggs, M.M., Balasubramani, G.K., Fava, M., STAR*D Study Team, 2006. Evaluation of outcomes with citalopram for depression using measurement-based care in STAR*D: implications for clinical practice. Am. J. Psychiatry 163, 28-40.

Tsankova, N.M., Berton, O., Renthal, W., Kumar, A., Neve, R.L., Nestler, E.J., 2006. Sustained hippocampal chromatin regulation in a mouse model of depression and antidepressant action. Nat. Neurosci. 9, 519-525.

Tso, M.M., Blatchford, K.L., Callado, L.F., McLaughlin, D.P., Stamford, J.A., 2004. Stereoselective effects of ketamine on dopamine, serotonin and noradrenaline release and uptake in rat brain slices. Neurochem. Int. 44, 1-7.

Turrigiano, G., 2012. Homeostatic synaptic plasticity: local and global mechanisms for stabilizing neuronal function. Cold Spring Harb Perspect. Biol. 4, a005736.

U

Unnerstall, J.R., Fernandez, I., Orensanz, L.M., 1985. The alpha-adrenergic receptor: radiohistochemical analysis of functional characteristics and biochemical differences. Pharmacol. Biochem. Behav. 22, 859-874.

V

Valentine, G.W., Mason, G.F., Gomez, R., Fasula, M., Watzl, J., Pittman, B., Krystal, J.H., Sanacora, G., 2011. The antidepressant effect of ketamine is not associated with changes in occipital amino acid neurotransmitter content as measured by [(1)H]-MRS. Psychiatry Res. 191, 122-127.

Van Bockstaele, E.J., Biswas, A., Pickel, V.M., 1993. Topography of serotonin neurons in the dorsal raphe nucleus that send axon collaterals to the rat prefrontal cortex and nucleus accumbens. Brain Res. 624, 188-198.

van Hooft, J.A., Vijverberg, H.P., 2000. 5-HT(3) receptors and neurotransmitter release in the CNS: a nerve ending story? Trends Neurosci. 23, 605-610.

Vandermaelen, C.P., Aghajanian, G.K., 1983. Electrophysiological and pharmacological characterization of serotonergic dorsal raphe neurons

recorded extracellularly and intracellularly in rat brain slices. Brain Res. 289, 109-119.

VanderMaelen, C.P., Matheson, G.K., Wilderman, R.C., Patterson, L.A., 1986. Inhibition of serotonergic dorsal raphe neurons by systemic and iontophoretic administration of buspirone, a non-benzodiazepine anxiolytic drug. Eur. J. Pharmacol. 129, 123-130.

Vasudeva, R.K., Lin, R.C., Simpson, K.L., Waterhouse, B.D., 2011. Functional organization of the dorsal raphe efferent system with special consideration of nitrergic cell groups. J. Chem. Neuroanat. 41, 281-293.

Venzala, E., Garcia-Garcia, A.L., Elizalde, N., Tordera, R.M., 2013. Social vs. environmental stress models of depression from a behavioural and neurochemical approach. Eur. Neuropsychopharmacol. 23, 697-708.

Vilaro, M.T., Cortes, R., Mengod, G., 2005. Serotonin 5-HT4 receptors and their mRNAs in rat and guinea pig brain: distribution and effects of neurotoxic lesions. J. Comp. Neurol. 484, 418-439.

Vyas, A., Pillai, A.G., Chattarji, S., 2004. Recovery after chronic stress fails to reverse amygdaloid neuronal hypertrophy and enhanced anxiety-like behavior. Neuroscience 128, 667-673.

W

Wabno, J., Hess, G., 2013. Repeated administration of imipramine modifies GABAergic transmission in rat frontal cortex. J. Neural Transm. 120, 711-719.

Waldmeier, P.C., Kaupmann, K., Urwyler, S., 2008. Roles of GABAB receptor subtypes in presynaptic auto- and heteroreceptor function regulating GABA and glutamate release. J. Neural Transm. 115, 1401-1411.

Waldmeier, P.C., Wicki, P., Feldtrauer, J.J., Baumann, P.A., 1988. Potential involvement of a baclofen-sensitive autoreceptor in the modulation of the release of endogenous GABA from rat brain slices in vitro. Naunyn Schmiedebergs Arch. Pharmacol. 337, 289-295.

Wang, W., Whorton, M.R., MacKinnon, R., 2014. Quantitative analysis of mammalian GIRK2 channel regulation by G proteins, the signaling lipid PIP2 and Na+ in a reconstituted system. Elife 3, e03671.

Wang, X., Zhao, Y., Zhang, X., Badie, H., Zhou, Y., Mu, Y., Loo, L.S., Cai, L., Thompson, R.C., Yang, B., Chen, Y., Johnson, P.F., Wu, C., Bu, G., Mobley, W.C., Zhang, D., Gage, F.H., Ranscht, B., Zhang, Y.W., Lipton, S.A., Hong, W., Xu, H., 2013. Loss of sorting nexin 27 contributes to excitatory synaptic dysfunction by modulating glutamate receptor recycling in Down's syndrome. Nat. Med. 19, 473-480.

Warden, M.R., Selimbeyoglu, A., Mirzabekov, J.J., Lo, M., Thompson, K.R., Kim, S.Y., Adhikari, A., Tye, K.M., Frank, L.M., Deisseroth, K., 2012. A prefrontal cortex-brainstem neuronal projection that controls response to behavioural challenge. Nature 492, 428-432.

Weigl, L.G., Schreibmayer, W., 2001. G protein-gated inwardly rectifying potassium channels are targets for volatile anesthetics. Mol. Pharmacol. 60, 282-289.

Weissmann, D., Chamba, G., Debure, L., Rousset, C., Richard, F., Maitre, M., Pujol, J.F., 1990. Variation of tryptophan-5-hydroxylase concentration in the rat raphe dorsalis nucleus after p-chlorophenylalanine administration.

II. Anatomical distribution of the tryptophan-5-hydroxylase protein and regional variation of its turnover rate. Brain Res. 536, 46-55.

Wen, W., Wu, W., Romaine, I.M., Kaufmann, K., Du, Y., Sulikowski, G.A., Weaver, C.D., Lindsley, C.W., 2013. Discovery of 'molecular switches' within a GIRK activator scaffold that afford selective GIRK inhibitors. Bioorg. Med. Chem. Lett. 23, 4562-4566.

Whistler, J.L., Chuang, H.H., Chu, P., Jan, L.Y., von Zastrow, M., 1999. Functional dissociation of mu opioid receptor signaling and endocytosis: implications for the biology of opiate tolerance and addiction. Neuron 23, 737-746.

Whorton, M.R., MacKinnon, R., 2013. X-ray structure of the mammalian GIRK2-betagamma G-protein complex. Nature 498, 190-197.

Whorton, M.R., MacKinnon, R., 2011. Crystal structure of the mammalian GIRK2 K+ channel and gating regulation by G proteins, PIP2, and sodium. Cell 147, 199-208.

Wickman, K., Clapham, D.E., 1995. Ion channel regulation by G proteins. Physiol. Rev. 75, 865-885.

Wickman, K., Karschin, C., Karschin, A., Picciotto, M.R., Clapham, D.E., 2000. Brain localization and behavioral impact of the G-protein-gated K+ channel subunit GIRK4. J. Neurosci. 20, 5608-5615.

Wickman, K., Nemec, J., Gendler, S.J., Clapham, D.E., 1998. Abnormal heart rate regulation in GIRK4 knockout mice. Neuron 20, 103-114.

Wickman, K., Pu, W.T., Clapham, D.E., 2002. Structural characterization of the mouse Girk genes. Gene 284, 241-250.

Wickman, K.D., Iniguez-Lluhl, J.A., Davenport, P.A., Taussig, R., Krapivinsky, G.B., Linder, M.E., Gilman, A.G., Clapham, D.E., 1994. Recombinant G-protein beta gamma-subunits activate the muscarinic-gated atrial potassium channel. Nature 368, 255-257.

Wiklund, L., Bjorklund, A., 1980. Mechanisms of regrowth in the bulbospinal serotonin system following 5,6-dihydroxytryptamine induced axotomy. II. Fluorescence histochemical observations. Brain Res. 191, 109-127.

Williams, J.T., Egan, T.M., North, R.A., 1982. Enkephalin opens potassium channels on mammalian central neurones. Nature 299, 74-77.

Woodward, R., Stevens, E.B., Murrell-Lagnado, R.D., 1997. Molecular determinants for assembly of G-protein-activated inwardly rectifying K+ channels. J. Biol. Chem. 272, 10823-10830.

Woolley, M.L., Marsden, C.A., Fone, K.C., 2004. 5-Ht6 Receptors. Curr. Drug Targets CNS Neurol. Disord. 3, 59-79.

Wydeven, N., Marron Fernandez de Velasco, E., Du, Y., Benneyworth, M.A., Hearing, M.C., Fischer, R.A., Thomas, M.J., Weaver, C.D., Wickman, K., 2014. Mechanisms underlying the activation of G-protein-gated inwardly rectifying K+ (GIRK) channels by the novel anxiolytic drug, ML297. Proc. Natl. Acad. Sci. U. S. A. 111, 10755-10760.

Wylie, C.J., Hendricks, T.J., Zhang, B., Wang, L., Lu, P., Leahy, P., Fox, S., Maeno, H., Deneris, E.S., 2010. Distinct transcriptomes define rostral and caudal serotonin neurons. J. Neurosci. 30, 670-684.

X

Xie, Z., Westmoreland, S.V., Miller, G.M., 2008. Modulation of monoamine transporters by common biogenic amines via trace amine-associated receptor 1 and monoamine autoreceptors in human embryonic kidney 293 cells and brain synaptosomes. J. Pharmacol. Exp. Ther. 325, 629-640.

Xu, Z.Q., Zhang, X., Pieribone, V.A., Grillner, S., Hokfelt, T., 1998. Galanin-5-hydroxytryptamine interactions: electrophysiological, immunohistochemical and in situ hybridization studies on rat dorsal raphe neurons with a note on galanin R1 and R2 receptors. Neuroscience 87, 79-94.

Y

Yamada, K., Iwayama, Y., Toyota, T., Ohnishi, T., Ohba, H., Maekawa, M., Yoshikawa, T., 2012. Association study of the KCNJ3 gene as a susceptibility candidate for schizophrenia in the Chinese population. Hum. Genet. 131, 443-451.

Yamada, M., Inanobe, A., Kurachi, Y., 1998. G protein regulation of potassium ion channels. Pharmacol. Rev. 50, 723-760.

Yamakura, T., Lewohl, J.M., Harris, R.A., 2001. Differential effects of general anesthetics on G protein-coupled inwardly rectifying and other potassium channels. Anesthesiology 95, 144-153.

Yamamoto, Y., Kakigi, T., Maeda, K., 1999. Intra-striatal phencyclidine inhibits N-methyl-D-aspartic acid-stimulated increase in glutamate levels of freely moving rats. Prog. Neuropsychopharmacol. Biol. Psychiatry 23, 161-174.

Yokoyama, C., Okamura, H., Nakajima, T., Taguchi, J., Ibata, Y., 1994. Autoradiographic distribution of [3H]YM-09151-2, a high-affinity and selective antagonist ligand for the dopamine D2 receptor group, in the rat brain and spinal cord. J. Comp. Neurol. 344, 121-136.

Yow, T.T., Pera, E., Absalom, N., Heblinski, M., Johnston, G.A., Hanrahan, J.R., Chebib, M., 2011. Naringin directly activates inwardly rectifying potassium channels at an overlapping binding site to tertiapin-Q. Br. J. Pharmacol. 163, 1017-1033.

Yuen, E.Y., Wei, J., Liu, W., Zhong, P., Li, X., Yan, Z., 2012. Repeated stress causes cognitive impairment by suppressing glutamate receptor expression and function in prefrontal cortex. Neuron 73, 962-977.

Z

Zarate, C., Duman, R.S., Liu, G., Sartori, S., Quiroz, J., Murck, H., 2013. New paradigms for treatment-resistant depression. Ann. N. Y. Acad. Sci. 1292, 21-31.

Zarate, C.A.,Jr, Singh, J.B., Carlson, P.J., Brutsche, N.E., Ameli, R., Luckenbaugh, D.A., Charney, D.S., Manji, H.K., 2006. A randomized trial of an N-methyl-D-aspartate antagonist in treatment-resistant major depression. Arch. Gen. Psychiatry 63, 856-864.

Zavitsanou, K., Wang, H., Dalton, V.S., Nguyen, V., 2010. Cannabinoid administration increases 5HT1A receptor binding and mRNA expression in the hippocampus of adult but not adolescent rats. Neuroscience 169, 315-324.

References

Zhong, P., Yan, Z., 2004. Chronic antidepressant treatment alters serotonergic regulation of GABA transmission in prefrontal cortical pyramidal neurons. Neuroscience 129, 65-73.

8. ACCOMPANING MANUSCRIPT

OXFORD UNIVERSITY PRESS | The International Journal of Neuropsychopharmacology

Deletion of GIRK2 subunit of GIRK channels alters 5-HT1A receptor-mediated signaling and results in a depression-resistant behavior

Journal:	*The International Journal of Neuropsychopharmacology*
Manuscript ID:	Draft
Manuscript Type:	Regular Research Article
Date Submitted by the Author:	n/a
Complete List of Authors:	Llamosas, Nerea; University of the Basque Country UPV/EHU, Pharmacology Bruzos-Cidón, Cristina; University of the Basque Country UPV/EHU, Pharmacology Rodríguez, José Julio; IKERBASQUE, Basque Foundation for Science, Achucarro Center for Neuroscience; University of the Basque Country UPV/EHU and CIBERNED, Neuroscience Ugedo, Luisa; University of the Basque Country UPV/EHU, Pharmacology Torrecilla, Maria; University of the Basque Country UPV/EHU, Pharmacology
Research Focus: Choose one or more (maximum 5) that best describe the research focus of your paper:	Psychophysiology < Preclinical, Neuropsychopharmacology - behavioral < Preclinical
Keywords: Enter up to 5 (minimum 3) keywords that best reflect the research reported in your paper.:	Dorsal raphe, GIRK, 5-HT1A, Electrophysiology, Citalopram

To be submitted to *International Journal of Neuropsychopharmacology*.

Regular research article

Deletion of GIRK2 subunit of GIRK channels alters 5-HT$_{1A}$ receptor-mediated signaling and results in a depression-resistant behavior

Llamosas N[1], Bruzos-Cidón C[1], Rodríguez JJ[2, 3], Ugedo L[1] and Torrecilla M[1]

[1] Department of Pharmacology, Faculty of Medicine and Dentistry, University of the Basque Country UPV/EHU, 48940 Leioa, Spain.

[2]Achucarro Center for Neuroscience, IKERBASQUE, Basque Foundation for Science, 48011 Bilbao, Spain.

[3] Department of Neuroscience, University of the Basque Country UPV/EHU and CIBERNED, 48940 Leioa, Spain.

Address for correspondence:
Maria Torrecilla, PhD
Department of Pharmacology, Faculty of Medicine and Dentistry, University of the Basque Country, 48940 Leioa, SPAIN
Telephone number: +34 946013401. Fax number: +34 94 6013220
maria.torrecilla@ehu.es

STATISTICAL SUMMARY:

Abstract: 240 words

Body of the Manuscript: 4994 words

58 References

1 Table

5 Figures

Abstract

Background: Targeting dorsal raphe (DR) 5-HT_{1A} receptors, which are coupled to G-protein inwardly rectifying potassium (GIRK) channels, has revealed their contribution not only to behavioral and functional aspects of depression, but also to the clinical response to its treatment. Although GIRK channels containing GIRK2 subunits play an important role controlling excitability of several brain areas, their impact on the DR activity is still unknown. Thus, the goal of the present study was to investigate *in vivo* the involvement of GIRK2 subunit-containing GIRK channels in depression-related behaviors and physiology of serotonergic (5-HT) neurotransmission. Methods: Behavioral, functional, including *in vivo* extracellular recordings of DR neurons, and neurogenesis studies were carried out in wild-type (WT) and GIRK2 mutant mice. Results: Deletion of the GIRK2 subunit promoted a depression-resistant phenotype and determined the behavioral response to the antidepressant citalopram without altering hippocampal neurogenesis. In the DR neurons of GIRK2 knockout mice ($GIRK2^{-/-}$), and also using GIRK channel blocker tertiapin-Q, the basal firing rate was higher than that obtained in WT animals, although no differences were observed in other firing parameters. 5-HT_{1A} receptors were desensitized in $GIRK2^{-/-}$ mice, as demonstrated by a lower sensitivity of DR neurons to the inhibitory effect of the 5-HT_{1A} receptor agonist, 8-OH-DPAT and the antidepressant citalopram. Conclusions: Our results indicate that GIRK channels formed by GIRK2 subunits determine depression-related behaviors as well as basal and 5-HT_{1A} receptor-mediated DR neuronal activity, becoming alternative therapeutical targets for psychiatric diseases underlying dysfunctional 5-HT transmission.

Keywords

Dorsal raphe, GIRK, 5-HT_{1A}, electrophysiology, citalopram

Introduction

Dysfunctional 5-HT transmission plays a key role in the etiology and treatment of depression. Increasing 5-HT by selectively blocking its reuptake is the main pharmacological strategy to treat it (Krishnan and Nestler, 2008). The major source of 5-HT in the brain is the dorsal raphe nucleus (DR) (Dahlstroem and Fuxe, 1964), and it is highly regulated by the 5-HT_{1A} autoreceptors, which play a critical role in the development, modulation and treatment of depression. A functional polymorphism in the promoter region of the human *Htr1a* gen, which regulates 5-HT_{1A} receptor levels, is linked to predisposition to mental illness, as well as anxiety- and depression-related behaviors and response to antidepressants (Strobel et al., 2003; Lemonde et al., 2004; Lesch and Gutknecht, 2004; Le Francois et al., 2008). Diverse genetic manipulations of 5-HT_{1A} receptor levels have confirmed the role of these receptors in anxiety- and depression-like phenotypes in mice (Heisler et al., 1998; Parks et al., 1998; Richardson-Jones et al., 2010; Ferres-Coy et al., 2013). It is widely accepted that the slow onset of the response to antidepressants is related to the progressive desensitization of the inhibitory effects mediated by activation of 5-HT_{1A} receptors onto 5-HT neurotransmission (Blier and de Montigny, 1994; Artigas et al., 1996). Also the behavioral response to antidepressants has been linked to increased neurogenesis, which is mediated by stimulation of 5-HT_{1A} receptors (Santarelli et al., 2003). The G protein-coupled inwardly rectifying potassium (GIRK) channels are the main inhibitory effectors of 5-HT_{1A} receptors (Williams et al., 1988) and therefore they could be alternative candidates for the study of depression and antidepressant responses involving 5-HT_{1A} receptor-mediated signaling.

Neuronal GIRK channels are tetramers mainly formed by GIRK1-3 subunits, since the expression of GIRK4 subunits is limited in the brain (Karschin et al., 1996). Specifically, the GIRK2 subunit plays a relevant role in GIRK channels function, given that the predominant

form of GIRK channels is a heterotetramer containing GIRK1 and GIRK2 subunits (Liao et al., 1996) and it is the responsible for the generation of G-protein coupled receptor-mediated GIRK currents in several brain areas, including the locus coeruleus (LC) and the hippocampus (HPP) (Luscher et al., 1997; Slesinger et al., 1997; Torrecilla et al., 2002; Labouebe et al., 2007; Cruz et al., 2008). Moreover, mutation of GIRK2 subunits causes a GIRK1 protein down-regulation (Signorini et al., 1997; Torrecilla et al., 2002) and the constitutive activity of GIRK2 subunit-containing GIRK channels reduces neuronal excitability *in vitro* (Luscher et al., 1997; Torrecilla et al., 2002). Recently, it has been demonstrated that the maintenance of the tonic noradrenergic activity, which is another important neurotransmission system widely implicated in mood disorders, is under the control of GIRK2 subunit-containing GIRK channels (Torrecilla et al., 2013). Mice lacking GIRK2 subunits exhibit a reduced anxiety-like phenotype (Blednov et al., 2001; Pravetoni and Wickman, 2008), while mice lacking 5-HT_{1A} receptors display increased anxiety-related behavior (Heisler et al., 1998; Parks et al., 1998; Ramboz et al., 1998). Given the involvement of these receptors in the etiology and treatment of depression, and their functional relationship with GIRK channels, the aim of our study was to investigate the role of GIRK2 subunit-containing GIRK channels in depression-related behaviors, adult neurogenesis, as well as basal and 5-HT_{1A} receptor-mediated electrophysiological activity in DR neurons.

Methods

Animals

We used C57BL6/J wild-type (WT), GIRK2 heterozygous ($GIRK2^{+/-}$), and GIRK2 homozygous ($GIRK2^{-/-}$) mice derived from heterozygote crossing (Signorini et al., 1997). Animals were maintained at 22±2ºC in a 12-h/12-h light/dark cycle with food and water provided *ad libitum*. All procedures were conducted in accordance with European Community

Council Directive on 'The Protection of Animals Used for Experimental and Other Scientific Purposes' (86/609/EEC) and the Spanish Law for the care and use of laboratory animals (RD 1201/2005). Experimental protocols were reviewed and approved by the Local Committee for Animal Experimentation at the University of the Basque Country.

Behavioral tests

All tests were performed between 9:00 and 13:00 h. Mice were transferred to a noise free and temperature-controlled testing room at least one hour before the experiments. No more than one test was performed in each mouse.

Novelty suppressed feeding test

The novelty suppressed feeding test (NSFT) was performed as previously described (Santarelli et al., 2003). Animals were food-deprived 24 h prior to the test (water *ad libitum*). The testing apparatus consisted of a plastic box (45x45x20 cm) with wooden bedding covered floor (approximately 2 cm) illuminated by a 70W lamp and with a white paper platform with a food pellet in the centre. The test was carried out during 10 min and the latency to eat was timed.. Afterwards, animals were transferred to their home cages and the amount of food consumed by each mouse in the subsequent 5 minutes was measured as a control of change in appetite.

Tail suspension test

In the tail suspension test (TST) mice were suspended 60 cm from the surface with adhesive tape placed approximately 2 cm from the tip of the tail. Animals were monitored by video camera for subsequent blind analysis. The test lasted for 6 min and mice were considered immobile when they stood completely motionless or hung passively.

Intraperitoneal administration of citalopram (10 mg/kg) was carried out 30 min prior to the experiments.

In vivo electrophysiological procedures

Mice were anesthetized with chloral hydrate (400 mg/kg, i.p.). In order to maintain a full anesthetic state supplemental doses of chloral hydrate (100 mg/kg, i.p.) were periodically administered. Single-barreled glass micropipettes, tip diameter 1-2 μm, were lowered into the DR (relative to bregma: AP -4.5 mm, ML -1.0 mm, DV -2.5 to -4.0 mm) with a lateral angle of 20° in order to avoid damaging the sagital sinus. DR neurons were identified using established criteria, which included slow (0.5-2.5 Hz) and regular firing rate, and a long duration (0.8-1.5 ms) positive action potential. A burst was defined according to Gartside et al. (2000), and burst-firing neurons in mice were identified as described previously (Gobbi et al., 2007), including a first interspike interval of ≤20 ms and a termination interval ≥160 ms.

Firing patterns analyses were performed using Spike2 software (Cambridge Electronic Design, UK). The following parameters were analyzed offline: firing rate, coefficient of variation, percentage of cells exhibiting burst firing, firing rate of burst firing neurons, number of burst per cell, percentage of spikes in burst, mean spikes per burst, and the response to drug administration. Basal firing rate was recorded for at least 3 min before drug administration. One cell per animal was recorded when any drug was administered. All the recorded neurons met the previously mentioned established criteria and were located within the DR.

Intracerebroventricular administrations were performed using a microsyringe (5μL, Hamilton, Bonaduz, Switzerland) connected to a 30-gauge stainless-steel needle that was perpendicularly inserted into the right lateral ventricle (relative to bregma: AP -0.5 mm, ML -

1.0 mm, DV -2.0 mm). A volume of 1 µL of tertiapin-Q (100 pmol, dissolved in artificial cerebrospinal fluid, ACSF) or ACSF (used as a control group) was injected directly into the right lateral ventricle. Intracerebroventricular administrations were performed 10 min prior to the recordings.

8-OH-DPAT-induced hypothermia

Body temperature was assessed rectally, inserting a lubricated probe (BIO-BRET-3, Cibertec, Spain) approximately 2 cm and monitored with a digital thermometer (CITEC, Cibertec, Spain). Ten minutes after baseline measurements, animals received 8-OH-DPAT (0.5 mg/kg i.p.) or 0.9% saline (i.p.), and body temperature was measured the subsequent 10, 20, 30 and 60 min.

Immunohistochemistry procedures

Fixation and tissue processing

Male adult mice (*n*=6-10/group) were anaesthetized with sodium pentobarbital (200 mg/kg, i.p.). Animals were perfused through the aortic arch with 3.75% acrolein (25 mL, TAAB, UK) in a solution of 2% paraformaldehyde and 0.1 M phosphate buffer (PB) pH 7.4, followed by 2% paraformaldehyde (75 mL). Coronal brain slices were cut into 40-µm thickness using a vibrating microtome (VT1000 S, Leica, Milton Keynes, UK). Coronal sections at levels -1.34 mm/ -2.30 mm posterior to bregma and 1.18 mm/ 0.26 mm anterior to bregma from HPP and subventricular zone (SVZ), respectively, were selected for immunohistochemistry according to the stereotaxic mouse brain atlas of Franklin and Paxinos (1997).

Antibodies

A polyclonal affinity-purified rabbit antibody raised against phosphorylated Histone H3 (HH3) and a monoclonal mouse antiserum generated against glial fibrillary acidic protein (GFAP) were used for the determination of proliferating cells and glia. We determined the number of proliferating cells by the presence of phosphorylated histone H3 that were not colocalized with glial fibrillary acidic protein to exclude glial phenotype. Omission of primary and/or secondary antibodies resulted in a total absence of target labeling (Rodriguez et al., 2008; Rodriguez et al., 2009).

Immunohistochemistry

This procedure was performed as previously described (Rodriguez et al., 2008; Rodriguez et al., 2009). The vibratome sections were first incubated for 30 min in 30% methanol in 0.1 M PB and 30% hydrogen peroxide (H_2O_2), and then rinsed with 0.1 M PB for 5 min and placed in 1% sodium borohydride for 30 min. After incubating brain sections in 0.5% bovine serum albumin, in 0.1 M TS and 0.25% Triton X-for 30 min, they were incubated for 68 h at room temperature in 0.1% bovine serum albumin, in 0.1 M TS and 0.25% Triton X-100 containing rabbit polyclonal antiserum for HH3 (1:1000) and mouse monoclonal antiserum for GFAP (1:60000). For HH3 labeling, sections were placed in 0.1 M TS and 0.25% Triton X-100 containing (1) 1:400 dilutions of biotinylated donkey anti-rabbit IgG (Jackson Immunoresearch, Stratech Scientific Ltd., Soham, UK) for 1 h at room temperature and (2) avidin-bioctin peroxidase complex for 30 min at room temperature. The peroxidase reaction product was visualized in a solution prepared from SGZ kits for 2-3 min. For GFAP labeling, sections were rinsed again in 0.1 M TS for 30 min and incubated in 0.1 M TS and 0.25% Triton X-100 containing (1) 1:400 dilution of biotinylated horse anti-mouse

IgG (Vector Laboratories, Peterborough, UK) for 1 hour at room temperature and (2) avidin-biocytin peroxidase complex for 30 min at room temperature. The GFAP peroxidase reaction was observed by incubation in a solution containing 0.022% 3,3′diaminobenzidine (DAB) and 0.003% H_2O_2 for 1-2 min. With this procedure, the GFAP labeling was seen in brown, allowing us to differentiate it from the HH3 labeled cells (blue). After stopping the reaction by rinsing the sections in 0.1 M TS for 5 min followed by 0.1 M PB for 15 min, sections were mounted onto gelatinized slides and allowed to dry overnight. Sections were then dehydrated in increasing concentrations of ethanol (50%, 70%, 80%, 90%, 95% and 100%) and finally, xylene. Coverslips were applied using Entellan and slides were left overnight before counting.

Cell quantification

The number of HH3-immunoreactive neurons and HH3/GFAP colocalized cells was determined by counting the labeled cells in both hemispheres in coronal vibratome sections taken through representative sections of dentate gyrus (DG) of the HPP, and of the SVZ, at levels previously mentioned. Cells were counted using light microscopy (Nikon Eclipse 80i). The number of HH3 positive cells and the area measurements of the DG and SVZ, bounded by the lateral ventricles, corpus callosum and caudate-putamen nucleus, were determined blindly to ensure consistency and reproducibility.

Drugs

Chloral hydrate, 8-OH-DPAT hydrobromide and WAY100635 maleate were obtained from Sigma-Aldrich, USA. Citalopram hydrobromide and tertiapin-Q from Tocris Bioscience, UK. Tertiapin-Q was prepared in artificial cerebrospinal fluid. Chloral hydrate, 8-OH-DPAT, WAY100635 and citalopram were prepared in 0.9% saline.

Statistical analysis

Behavioral data and immunohistochemical data were compared through genotypes by one-way analysis of variance (ANOVA) followed by Newman-Keuls post-hoc test. For the 8-OH-DPAT hypothermic response analysis, two-way ANOVA followed by Bonferroni post-hoc test was used for statistical comparison. The level of significance was considered as $p<0.05$.

Changes in firing rate induced by 8-OH-DPAT and citalopram are expressed as percentages of the baseline firing rate (mean firing rate during 3 min prior to drug administration). Data compiled from dose-response curves were analyzed for the best simple nonlinear fit to the three-parameter logistic equation (Parker and Waud, 1971) using GraphPad Prism Software (v5.01; GraphPad Software Inc., USA). The following equation was used:

$$E= E_{max} [A]^n / (ED^n_{50}+ [A]^n),$$

Where [A] is the concentration of the drug, E is the effect on the firing rate induced by A, E_{max} is the maximal effect, ED_{50} is the effective dose for eliciting 50% of the Emax and n is the slope factor of the dose-response curve. Extra sum-of-squares F test (GraphPad Prism Software, v5.01, San Diego, USA) was used for statistical comparison of the response to a drug in dose-response curves and for comparison of ED_{50} among groups.

Spontaneous firing rate and coefficient of variation were analyzed in selected pair comparisons using two-tail unpaired t-test. Two-sided χ^2 analysis of contingency tables was used to evaluate differences in the percentage of neurons presenting burst firing. Other parameters derived from burst pattern were analyzed by the non-parametric Kruskal-Wallis test followed by Dunn's post-hoc test.

Results

Behavioral characterization of GIRK2 mutant mice and the response to citalopram

To evaluate whether GIRK2 subunit ablation impacts on depressive-related behaviors, GIRK2 mutant mice were evaluated using two well-established behavioral models of antidepressant activity, the NSFT and TST (Santarelli et al., 2003; Cryan et al., 2005; Heurteaux et al., 2006). In the NSFT, both GIRK2 homozygous ($GIRK2^{-/-}$) and heterozygous ($GIRK2^{+/-}$) mice showed a decreased latency to eat, compared to wild-type (WT) mice ($GIRK2^{-/-}$: 145.60±19.63 s, n=9; $GIRK2^{+/-}$: 154.60±14.30 s, n=20; WT: 212.00±14.85 s, n=22. p<0.05 and p<0.01 for $GIRK2^{-/-}$ and $GIRK2^{+/-}$ mice *vs* WT, respectively, one-way ANOVA following Newman-Keuls test) (Fig. 1a). This decrease in the latency to eat in the mutant groups was not due to an increased appetite (Fig. 1b).

When evaluating the behavioral characteristics in the TST, $GIRK2^{-/-}$ mice showed a lower immobility time than $GIRK2^{+/-}$ and WT mice ($GIRK2^{-/-}$: 115.10±9.08 s, n=16; $GIRK2^{+/-}$: 189.10±3.24 s, n=16; WT: 191.80±8.87 s, n=14. p<0.0001, one-way ANOVA following Newman-Keuls test) (Fig. 1c). Next, we examined the effect of citalopram on the immobility time in the TST. In all groups, the administration of citalopram (10 mg/kg, i.p.) caused a reduction of the immobility time (Fig. 1d). However, in $GIRK2^{-/-}$ and $GIRK2^{+/-}$ mice this reduction was significantly lower than that observed in WT ($GIRK2^{-/-}$: 53.2±9.5 %, n=7; $GIRK2^{+/-}$: 50.5±5.9 %, n=7; WT: 79.2±5.1 %, n=10. p<0.05, one-way ANOVA following Newman-Keuls test).

Electrophysiological properties of DR neurons of GIRK2 mutant mice

To examine the contribution of GIRK2 subunit-containing GIRK channels to the basal activity of DR neurons, firing rate, coefficient of variation and burst activity was recorded in WT and GIRK2 mutant mice *in vivo*.

All neurons recorded from wild-type (WT n=86), GIRK2$^{+/-}$ (n=79), and GIRK2$^{-/-}$ (n=45) mice fitted the standard criteria (see Methods).

Spontaneous firing rate of DR neurons in GIRK2$^{-/-}$ mice was higher than in WT (1.99±0.15 Hz, n=45; 1.68±0.08 Hz, n=86; for GIRK2$^{-/-}$ and WT mice, respectively. p<0.05, two-tailed unpaired t-test). No changes were seen either in the coefficient of variation or in the burst activity among groups (Table 1). A more extended study of the burst pattern (mean firing rate, number of bursts, percentage of spikes firing in bursts, and mean spikes in burst) showed no differences among groups.

Next, the effect of the high affinity GIRK channel blocker, tertiapin-Q (100 pmol, i.c.v.) (Jin and Lu, 1998; Kanjhan et al., 2005), on the electrophysiological properties of DR neurons was assessed. The firing rate of DR neurons in tertiapin-Q-injected WT mice (WT TPN-Q) was statistically higher (38%) than in the WT group (WT TPN-Q: 2.32±0.27 Hz, n=15 and WT: 1.68±0.08 Hz, n=86. p<0.001, two-tailed unpaired t-test). However, no significant changes were seen either in the coefficient of variation or in the burst parameters, compared to WT mice. No differences were observed in firing rate (1.80±0.27 Hz, n=7), coefficient of variation (35.13±4.42 %, n=7) or number of burst firing neurons (14 %) in the intracerebroventricular ACSF-injected WT group compared to WT mice (data not shown).

Effect of Girk2 gene deletion on the 5-HT$_{1A}$ receptor-mediated inhibition of DR neuronal activity

To investigate the role of GIRK2 subunits in the 5-HT$_{1A}$ receptor-mediated transmission, we compared the inhibitory effect of cumulative increasing doses of the 5-HT$_{1A}$ receptor agonist, 8-OH-DPAT (12.5-300 µg/kg, i.p.) onto the firing rate of DR neurons of WT and GIRK2 mutant mice. In all groups, 8-OH-DPAT caused a progressive and dose-dependent inhibition of the firing rate (Fig. 2a and 2b). In GIRK2$^{+/-}$mice, the dose-response curve shifted to the right, so that the ED$_{50}$ mean value was significantly higher than that obtained in WT mice (ED$_{50}$: 42.15±2.89 µg/kg, n=8; ED$_{50}$: 34.93±3.41 µg/kg, n=15, for GIRK2$^{+/-}$ mice and WT, respectively. p<0.05, nonlinear fit analysis, extra sum-of-squares F test). In GIRK2$^{-/-}$ mice, the shift in the dose-response curve was even greater and so the ED$_{50}$ mean value increased 2-fold compared to WT mice (ED$_{50:}$ 69.50±8.57 µg/kg, n=5. p<0.01, nonlinear fit analysis, extra sum-of-squares F test) (Fig. 2c). Subsequent administration of the 5-HT$_{1A}$ receptor antagonist, WAY100635 (1-1.5 mg/kg, i.p.), completely recovered the firing activity in the three groups (WT: 86.22±7.04 %, n=13; GIRK2$^{+/-}$: 92.54±12.98 %, n=6; GIRK2$^{-/-}$: 122.20±23.27 %, n=3). No significant differences were found among groups.

Next, the sensitivity of the 5-HT$_{1A}$ receptor to endogenous 5-HT was tested by using the selective serotonin reuptake inhibitor (SSRI) citalopram (0.5-3 mg/kg, i.p.), which increases 5-HT levels in the synaptic cleft and indirectly activates these receptors (Pineyro and Blier, 1999). For this purpose, citalopram dose-response curves were performed in WT and GIRK2 mutant mice. In all the groups, cumulative doses of citalopram caused a progressive and dose-dependent inhibition of the firing rate. However, citalopram showed less potency inhibiting DR neurons in GIRK2$^{-/-}$ mice, so that the ED$_{50}$ mean value for this group was significantly greater than the values obtained for GIRK2$^{+/-}$ and WT mice (ED$_{50}$:

1.36±0.04 mg/kg, *n*=6; ED_{50}: 1.04±0.04 mg/kg, *n*=7; ED_{50}: 0.97±0.03 mg/kg, *n*=13, for $GIRK2^{-/-}$, $GIRK2^{+/-}$, and WT mice, respectively. $p<0.0001$, nonlinear fit analysis, extra sum-of-squares F test) (Fig. 2d).

Effect of pharmacological blockade of GIRK channels on the citalopram-induced inhibition of DR neuronal activity

To further investigate the 5-HT_{1A}-GIRK signaling pathway we performed a pharmacological blocking of GIRK channels with tertapin-Q and the sensitivity of the 5-HT_{1A} receptor to the effect of the SSRI, citalopram was evaluated in WT TPN-Q mice and in a WT control group (ACSF-injected group, WT control). In both groups, citalopram (0.5-3 mg/kg, i.p) caused a progressive and dose-dependent inhibition of the firing rate (Fig. 3a and 3b), but showed less potency inhibiting DR neurons in WT TPN-Q, so that the ED_{50} mean value for this group was significantly greater than the value obtained for the WT control (ED_{50}: 1.25±0.04 mg/kg, *n*=5; ED_{50}: 0.99±0.06 mg/kg, *n*=4; for WT TPN-Q and the WT control, respectively. $p<0.0001$, nonlinear fit analysis, extra sum-of-squares F test) (Fig. 3c). ED_{50} mean values were similar between $GIRK2^{-/-}$ mice and WT TPN-Q, indicating that citalopram had the same potency in both groups (ED_{50}: 1.25±0.04 mg/kg, *n*=5; ED_{50}: 1.36±0.04 mg/kg, *n*=6; for WT TPN-Q and $GIRK2^{-/-}$ mice, respectively). As expected, the WT control showed similar ED_{50} values to the WT mice.

Characterization of 8-OH-DPAT-induced hypothermia in GIRK2 mutant mice

To further study the functional status of 5-HT_{1A} receptors in GIRK2 mutant mice, we evaluated the 8-OH-DPAT-induced hypothermic response. In all groups, 8-OH-DPAT (0.5mg/kg, i.p.) caused a decrease in temperature (*n*=6-7 per group). $GIRK2^{-/-}$ mice showed a reduced 8-OH-DPAT-induced hypothermia in every different time point, compared to WT

mice. A two-way ANOVA revealed that in the minute 30, the temperature decrease induced by 8-OH-DPAT was significantly smaller in GIRK2$^{-/-}$ mice compared to WT ([$F(2,68)=10.30$, $p<0.05$]) (Fig. 4). In addition, three other groups of GIRK2$^{+/-}$, GIRK2$^{-/-}$ and WT mice were injected with 0.9% saline (saline groups, i.p.), in order to check if the manipulation of the animals or the intraperitoneal injection were causing an effect on the response. No significant changes in the temperature were observed in these groups.

Basal neurogenesis in GIRK2 mutant mice

Finally, we investigated whether GIRK2 subunits are involved in basal adult neurogenesis measuring the area density (#cells/mm^2, Sv) of new proliferating cells in the DG of the HPP and in the SVZ of WT and GIRK2 mutant mice. In both regions of all groups, newly generated cells were observed, as indicated by HH3 immunoreactiviy (HH3-IR). Although GFAP immunoreactivity was detected throughout the DG of the HHP and SVZ, less than 2% of HH3-IR cells expressed GFAP. Quantitative analysis of the Sv of HH3-IR cells showed no differences among genotypes either in the DG (WT: 17.18±1.89; GIRK2$^{+/-}$: 16.69±1.36; and GIRK2$^{-/-}$: 14.71±1.51. Fig. 5a, 5b and 5c) or in the SVZ (WT: 152.43±8.81; GIRK2$^{+/-}$: 154.34± 6.10; and GIRK2$^{-/-}$: 139.99±16. Fig. 5d).

Discussion

The goal of our study was to determine the role that GIRK2 subunit-containing GIRK channels play in depression-related behaviors as well as in the control of 5-HT$_{1A}$-mediated inhibitory effects. We found that mice lacking GIRK2 subunits of GIRK channels display a depression-resistant phenotype combined with a reduced behavioral response to citalopram, an increase in the firing rate of DR neurons and a reduction of 5-HT$_{1A}$ receptor-mediated responses. In addition, GIRK2 subunit deletion does not affect basal adult neurogenesis.

Our findings suggest that *Girk2* gene deletion promotes a depression-resistant behavior and determines the response to the antidepressant citalopram. Thus, GIRK2$^{-/-}$ mice showed a marked decrease in the immobility time in the tail suspension test (TST), and both GIRK2$^{+/-}$ and GIRK2$^{-/-}$ mice presented a lower latency to eat in the novelty suppressed feeding test (NSFT), that was not correlated with an increase in appetite. It is important to remark that general locomotor activity status is a confusing factor in these tests (Blednov et al., 2001). Previous studies showed that GIRK2$^{-/-}$ mice, but not GIRK2$^{+/-}$ mice, have signs of hyperactivity (Blednov et al., 2001; Cruz et al., 2008; Arora et al., 2010) that has been attributed to D1 receptor activation (Blednov et al., 2002). Given that GIRK2$^{+/-}$ mice do not have hyperactivity but showed depression-resistant phenotype in the NSFT, these results might be attributable to a less depressive-like behavior rather than to a more active state. We suggest that the 5-HT$_{1A}$-GIRK signaling may be mediating this depression-resistant phenotype: first, studies in 5-HT$_{1A}$ receptor knockout mice show that they display an antidepressant-like phenotype under baseline conditions (Heisler et al., 1998; Mayorga et al., 2001), as we observed in GIRK2 mutant mice. Secondly, here citalopram was less potent in reducing the immobility in the TST. Similarly, it has been reported that the expression of the antidepressant-like behavioral response of SSRIs in the TST requires the presence of functional 5-HT$_{1A}$ receptors (Mayorga et al., 2001). Additionally, our observations are in line with those showing that chronic administration of fluoxetine exerts a beneficial influence on a rodent model of depression through suppression of GIRK-dependent signaling in the DR (Cornelisse et al., 2007). Interestingly, the depression-resistant phenotype that we observed here is combined with the previously reported reduced anxiety-like behavior that GIRK2 mutant mice display (Blednov et al., 2001; Pravetoni and Wickman, 2008). Therefore, this phenotype represents a great advance over the classic antidepressed-like phenotype of 5-HT$_{1A}$

knockout mice, since they display a robust anxiety-like behavior (Heisler et al., 1998; Parks et al., 1998; Ramboz et al., 1998). Given the constitutive and global nature of the *Girk2* gene deletion, it is not possible to completely identify the circuit(s) or neurotransmitter system(s) that explain this "antidepressive" phenotype. However, we can rule out the involvement of the $GABA_B$-GIRK2 signaling, since, $GABA_B$ mutant mice showed elevated anxiety-related behaviors (Mombereau et al., 2004).

The implication of GIRK2 subunit-containing GIRK channels in the 5-HT_{1A} receptor-mediated neurotransmission is also supported by our *in vivo* electrophysiological findings. First, we observed that the lack of GIRK2 subunits induces an increase in the firing rate of DR neurons. This increase was also observed by the total blocking of GIRK channels with tertiapin-Q. On one hand, these results suggest that the intrinsic activity of GIRK2 subunit-containing GIRK channels controls the transmission in the DR. Similar findings have been obtained in LC neurons, where it has been observed that GIRK2 subunit-containing GIRK channels regulate the tonic activity of LC neurons *in vivo* (Torrecilla et al., 2013). *In vitro* studies have reported that dopaminergic neurons in GIRK2$^{-/-}$ mice exhibit a reduced firing rate (Arora et al., 2010), and in GIRK2/3$^{-/-}$ mice LC neurons show an increased firing rate (Cruz et al., 2008). In addition, the contribution of GIRK2 subunits to the resting membrane potential has been reported in different type of neurons, including LC and HPP neurons (Luscher et al., 1997; Torrecilla et al., 2002; Chen and Johnston, 2005; Koyrakh et al., 2005). Nevertheless, in layer 5/6 pyramidal neurons of the prelimbic cortex of GIRK2$^{-/-}$ mice, intrinsic electrophysiological properties remained unaltered compared to WT mice (Hearing et al., 2013). Taken all together, the contribution of GIRK2 subunits to neuronal excitability seems to vary across cell types and brain regions. On the other hand, the complete blockade of GIRK channels with tertiapin-Q results in a similar increase in the firing rate of DR neurons

to that observed in GIRK2$^{-/-}$ mice. This suggests that GIRK2 subunits, though their expression is low in the DR (Saenz del Burgo et al., 2008), are forming important populations of GIRK channels, which are involved in the control of neuronal tonic activity. Given that GIRK1 subunits are almost absent when deleting GIRK2 subunits (Signorini et al., 1997), both GIRK1 and GIRK2 subunits might be forming functional GIRK channels that control the tonic 5-HT activity of the DR. Alterations in neurotransmitter levels could also affect the firing pattern of DR neurons in GIRK2 mutant mice, since there are decreased and increased levels of 5-HT and 5-HIAA, respectively (Torrecilla et al., 2013). Secondly, our study also reveals that DR 5-HT$_{1A}$ receptors, both endogenously and exogenously activated, are affected by the deletion of GIRK2 subunits, which is shown by reduced receptor functionality. Similar results were observed in an *in vivo* electrophysiological study in LC neurons in GIRK2 mutant mice, showing that μ and α2 receptors were desensitized (Torrecilla et al., 2013). Our results agree with this study, indicating that in the DR, ablation of the *Girk2* gene produces loss of function of the 5-HT$_{1A}$-GIRK signaling pathway. It is important to remark that the reduced function of 5-HT$_{1A}$ and α_2 autoreceptors has been proposed as a key consequence of chronic antidepressant treatments, which would explain the delayed onset effect of antidepressants (McMillen et al., 1980; Lacroix et al., 1991; Artigas et al., 1996; Blier et al., 1998; Szabo et al., 2000; Invernizzi et al., 2001). In fact, new pharmacological or genetic strategies to faster desensitize 5-HT$_{1A}$ and α_2 autoreceptors have been of great interest in the study of depression treatment (Sanacora et al., 2004; Richardson-Jones et al., 2010; Portella et al., 2011). The observation that 8-OH-DPAT and citalopram preserved their maximal inhibitory efficacy is consistent with other studies. In LC neurons in GIRK2 mutant mice, the potency of morphine and clonidine was reduced, yet the inhibitory efficacy remained unaltered *in vivo* (Torrecilla et al., 2013). In hippocampal neurons in GIRK2$^{-/-}$ mice, *in vitro*

postsynaptic GIRK currents induced by stimulation of the 5-HT_{1A} receptor were markedly reduced but not absent (Luscher et al., 1997). Studies conducted to determine the analgesic properties of morphine showed that while the potency of morphine was reduced, its efficacy was preserved in GIRK2$^{-/-}$ and GIRK2/3$^{-/-}$ mice (Mitrovic et al., 2003; Cruz et al., 2008). Also the pharmacological blockade of GIRK channels caused a reduction in the potency but not in the inhibitory efficacy of citalopram, supporting the role of GIRK2 subunit-containing GIRK channels in the inhibitory response of 5-HT_{1A} receptors. The tertiapin-Q dose used was selected according to a previous study, where doses higher than 100 pmol caused dangerous effects (Marker et al., 2004). By testing the 8-OH-DPAT-induced hypothermia, which reflects the sensitivity of 5-HT_{1A} autoreceptors in mice (Goodwin et al., 1985; Richarson-Jones et al., 2011), we confirmed that GIRK2 subunits regulate the functionality of 5-HT_{1A} autoreceptors, as previously reported (Costa et al., 2005). Overall, all the functional findings in our work indicate that in the DR GIRK2 subunits may be forming important GIRK channel populations, in charge of controlling the tonic electrical activity and mediating of 5-HT_{1A} receptor-mediated signaling.

Our findings show that in basal conditions, *Girk2* gene ablation promotes a depression-resistant phenotype without modifying adult neurogenesis in the DG of the HPP or in the SVZ. In line with this, it has also been observed that deletion of the background potassium channel TREK-1 results in a depression-resistant phenotype while the adult neurogenesis is unaltered (Heurteaux et al., 2006). It is worth mentioning that there is a very abundant expression of GIRK2 protein in the HHP and in the SVZ (Saenz del Burgo et al., 2008), and GIRK2 subunit-containing GIRK channels are also coupled to postsynaptic 5-HT_{1A} receptors (Luscher et al., 1997). Taking into consideration the presence and function of GIRK2 subunit-containing GIRK channels in the HPP, we suggest that the absence of

changes in basal neurogenesis observed in GIRK2 mutant mice may be ascribed to the probable requirement of 5-HT_{1A} receptor stimulation to promote neurogenesis (Santarelli et al., 2003)

In conclusion, our results show the specific role of GIRK2 subunit-containing GIRK channels in the promotion of a depression-resistant phenotype, as well as their control of the tonic neuronal activity and mediation of the 5-HT_{1A} receptor inhibitory responses. New strategies targeting the 5-HT_{1A}-GIRK2 pathway could be of great therapeutic interest for the study of pathologies related to an altered 5-HT transmission, such as depression, and development of alternative treatments.

Funding

All the authors are entirely responsible for the scientific content of this paper. This work has been supported by grants from the Government of the Basque Country (S-PE11UN055, IT747-13), the University of the Basque Country (UFI 11/32) and the Spanish Government (FIS PI12/00613) co-financed by FEDER to NL, CB-C, LU and MT. Plan Nacional de I+D+I 2008–2011 and ISCIII-Subdirección General de Evaluación y Fomento de la Investigación co-financed by FEDER (PI10/02738) and the Government of the Basque Country grants (AE-2010-1-28, AEGV10/16 and GV- 2011111020) to JJR. NL has a predoctoral fellowship and CB-C has a postdoctoral fellowship, both from the University of the Basque Country (UPV/EHU).

Acknowledgments

None

Conflict of Interest

None

References

Arora D, Haluk DM, Kourrich S, Pravetoni M, Fernandez-Alacid L, Nicolau JC, Lujan R, Wickman K (2010) Altered neurotransmission in the mesolimbic reward system of girk mice. J Neurochem 114:1487-1497.

Artigas F, Bel N, Casanovas JM, Romero L (1996) Adaptative changes of the serotonergic system after antidepressant treatments. Adv Exp Med Biol 398:51-59.

Blednov YA, Stoffel M, Chang SR, Harris RA (2001) GIRK2 deficient mice. evidence for hyperactivity and reduced anxiety. Physiol Behav 74:109-117.

Blednov YA, Stoffel M, Cooper R, Wallace D, Mane N, Harris RA (2002) Hyperactivity and dopamine D1 receptor activation in mice lacking girk2 channels. Psychopharmacology 159:370-378.

Blier P, de Montigny C (1994) Current advances and trends in the treatment of depression. Trends Pharmacol Sci 15:220-226.

Blier P, Pineyro G, el Mansari M, Bergeron R, de Montigny C (1998) Role of somatodendritic 5-HT autoreceptors in modulating 5-HT neurotransmission. Ann N Y Acad Sci 861:204-216.

Chen X, Johnston D (2005) Constitutively active G-protein-gated inwardly rectifying K+ channels in dendrites of hippocampal CA1 pyramidal neurons. J Neurosci 25:3787-3792.

Cornelisse LN, Van der Harst JE, Lodder JC, Baarendse PJ, Timmerman AJ, Mansvelder HD, Spruijt BM, Brussaard AB (2007) Reduced 5-HT1A- and GABAB receptor function in dorsal

raphe neurons upon chronic fluoxetine treatment of socially stressed rats. J Neurophysiol 98:196-204.

Costa AC, Stasko MR, Stoffel M, Scott-McKean JJ (2005) G-protein-gated potassium (GIRK) channels containing the GIRK2 subunit are control hubs for pharmacologically induced hypothermic responses. J Neurosci 25:7801-7804.

Cruz HG, Berton F, Sollini M, Blanchet C, Pravetoni M, Wickman K, Luscher C (2008) Absence and rescue of morphine withdrawal in GIRK/Kir3 knock-out mice. J Neurosci 28:4069-4077.

Cryan JF, Mombereau C, Vassout A (2005) The tail suspension test as a model for assessing antidepressant activity: Review of pharmacological and genetic studies in mice. Neurosci Biobehav Rev 29:571-625.

Dahlstroem A, Fuxe K (1964) Evidence for the existence of monoamine-containing neurons in the central nervous system. I. demonstration of monoamines in the cell bodies of brain stem neurons. Acta Physiol Scand Suppl 232:1-55.

Ferres-Coy A, Santana N, Castane A, Cortes R, Carmona MC, Toth M, Montefeltro A, Artigas F, Bortolozzi A (2013) Acute 5-HT(1)A autoreceptor knockdown increases antidepressant responses and serotonin release in stressful conditions. Psychopharmacology 225:61-74.

Franklin KBJ, Paxinos G (1997). The Mouse Brain in Stereotaxic Coordinates. Academic Press Inc., San Diego, CA, USA.

Gartside SE, Hajos-Korcsok E, Bagdy E, Harsing LG,Jr, Sharp T, Hajos M (2000) Neurochemical and electrophysiological studies on the functional significance of burst firing in serotonergic neurons. Neuroscience 98:295-300.

Gobbi G, Cassano T, Radja F, Morgese MG, Cuomo V, Santarelli L, Hen R, Blier P (2007) Neurokinin 1 receptor antagonism requires norepinephrine to increase serotonin function. Eur Neuropsychopharmacology. 17:328-338.

Goodwin GM, De Souza RJ, Green AR (1985) The pharmacology of the hypothermic response in mice to 8-hydroxy-2-(di-n-propylamino)tetralin (8-OH-DPAT). A model of presynaptic 5-HT1 function. Neuropharmacology. 24:1187-1194.

Hearing M, Kotecki L, Marron Fernandez de Velasco E, Fajardo-Serrano A, Chung HJ, Lujan R, Wickman K (2013) Repeated cocaine weakens GABA(B)-girk signaling in layer 5/6 pyramidal neurons in the prelimbic cortex. Neuron 80:159-170.

Heisler LK, Chu HM, Brennan TJ, Danao JA, Bajwa P, Parsons LH, Tecott LH (1998) Elevated anxiety and antidepressant-like responses in serotonin 5-HT1A receptor mutant mice. Proc Natl Acad Sci U S A 95:15049-15054.

Heurteaux C, Lucas G, Guy N, El Yacoubi M, Thummler S, Peng XD, Noble F, Blondeau N, Widmann C, Borsotto M, Gobbi G, Vaugeois JM, Debonnel G, Lazdunski M (2006) Deletion of the background potassium channel TREK-1 results in a depression-resistant phenotype. Nat Neurosci 9:1134-1141.

Invernizzi RW, Parini S, Sacchetti G, Fracasso C, Caccia S, Annoni K, Samanin R (2001) Chronic treatment with reboxetine by osmotic pumps facilitates its effect on extracellular

noradrenaline and may desensitize alpha(2)-adrenoceptors in the prefrontal cortex. Br J Pharmacol 132:183-188.

Jin W, Lu Z (1998) A novel high-affinity inhibitor for inward-rectifier K+ channels. Biochemistry 37:13291-13299.

Kanjhan R, Coulson EJ, Adams DJ, Bellingham MC (2005) Tertiapin-Q blocks recombinant and native large conductance K+ channels in a use-dependent manner. J Pharmacol Exp Ther 314:1353-1361.

Karschin C, Dissmann E, Stuhmer W, Karschin A (1996) IRK(1-3) and GIRK(1-4) inwardly rectifying K+ channel mRNAs are differentially expressed in the adult rat brain. J Neurosci 16:3559-3570.

Koyrakh L, Lujan R, Colon J, Karschin C, Kurachi Y, Karschin A, Wickman K (2005) Molecular and cellular diversity of neuronal G-protein-gated potassium channels. J Neurosci 25:11468-11478.

Krishnan V, Nestler EJ (2008) The molecular neurobiology of depression. Nature 455:894-902.

Labouebe G, Lomazzi M, Cruz HG, Creton C, Lujan R, Li M, Yanagawa Y, Obata K, Watanabe M, Wickman K, Boyer SB, Slesinger PA, Luscher C (2007) RGS2 modulates coupling between GABAB receptors and GIRK channels in dopamine neurons of the ventral tegmental area. Nat Neurosci 10:1559-1568.

Lacroix D, Blier P, Curet O, de Montigny C (1991) Effects of long-term desipramine administration on noradrenergic neurotransmission: Electrophysiological studies in the rat brain. J Pharmacol Exp Ther 257:1081-1090.

Le Francois B, Czesak M, Steubl D, Albert PR (2008) Transcriptional regulation at a HTR1A polymorphism associated with mental illness. Neuropharmacology 55:977-985.

Lemonde S, Du L, Bakish D, Hrdina P, Albert PR (2004) Association of the C(-1019)G 5-HT1A functional promoter polymorphism with antidepressant response. Int J Neuropsychopharmacol 7:501-506.

Lesch KP, Gutknecht L (2004) Focus on the 5-HT1A receptor: Emerging role of a gene regulatory variant in psychopathology and pharmacogenetics. Int J Neuropsychopharmacol 7:381-385.

Liao YJ, Jan YN, Jan LY (1996) Heteromultimerization of G-protein-gated inwardly rectifying K+ channel proteins GIRK1 and GIRK2 and their altered expression in weaver brain. J Neurosci 16:7137-7150.

Luscher C, Jan LY, Stoffel M, Malenka RC, Nicoll RA (1997) G protein-coupled inwardly rectifying K+ channels (GIRKs) mediate postsynaptic but not presynaptic transmitter actions in hippocampal neurons. Neuron 19:687-695.

Marker CL, Stoffel M, Wickman K (2004) Spinal G-protein-gated K+ channels formed by GIRK1 and GIRK2 subunits modulate thermal nociception and contribute to morphine analgesia. J Neurosci 24:2806-2812.

Mayorga AJ, Dalvi A, Page ME, Zimov-Levinson S, Hen R, Lucki I (2001) Antidepressant-like behavioral effects in 5-hydroxytryptamine(1A) and 5-hydroxytryptamine(1B) receptor mutant mice. J Pharmacol Exp Ther 298:1101-1107.

McMillen BA, Warnack W, German DC, Shore PA (1980) Effects of chronic desipramine treatment on rat brain noradrenergic responses to alpha-adrenergic drugs. Eur J Pharmacol 61:239-246.

Mitrovic I, Margeta-Mitrovic M, Bader S, Stoffel M, Jan LY, Basbaum AI (2003) Contribution of GIRK2-mediated postsynaptic signaling to opiate and alpha 2-adrenergic analgesia and analgesic sex differences. Proc Natl Acad Sci U S A 100:271-276.

Mombereau C, Kaupmann K, van der Putten H, Cryan JF (2004) Altered response to benzodiazepine anxiolytics in mice lacking GABA B(1) receptors. Eur J Pharmacol 497:119-120.

Parker RB, Waud DR (1971) Pharmacological estimation of drug-receptor dissociation constants. statistical evaluation. I. agonists. J Pharmacol Exp Ther 177:1-12.

Parks CL, Robinson PS, Sibille E, Shenk T, Toth M (1998) Increased anxiety of mice lacking the serotonin1A receptor. Proc Natl Acad Sci U S A 95:10734-10739.

Pineyro G, Blier P (1999) Autoregulation of serotonin neurons: Role in antidepressant drug action. Pharmacol Rev 51:533-591.

Portella MJ, de Diego-Adelino J, Ballesteros J, Puigdemont D, Oller S, Santos B, Alvarez E, Artigas F, Perez V (2011) Can we really accelerate and enhance the selective serotonin

reuptake inhibitor antidepressant effect? A randomized clinical trial and a meta-analysis of pindolol in nonresistant depression. J Clin Psychiatry 72:962-969.

Pravetoni M, Wickman K (2008) Behavioral characterization of mice lacking GIRK/Kir3 channel subunits. Genes Brain Behav 7:523-531.

Ramboz S, Oosting R, Amara DA, Kung HF, Blier P, Mendelsohn M, Mann JJ, Brunner D, Hen R (1998) Serotonin receptor 1A knockout: An animal model of anxiety-related disorder. Proc Natl Acad Sci U S A 95:14476-14481.

Richardson-Jones JW, Craige CP, Nguyen TH, Kung HF, Gardier AM, Dranovsky A, David DJ, Guiard BP, Beck SG, Hen R, Leonardo ED (2011) Serotonin-1A autoreceptors are necessary and sufficient for the normal formation of circuits underlying innate anxiety. J Neurosci 31:6008-6018.

Richardson-Jones JW, Craige CP, Guiard BP, Stephen A, Metzger KL, Kung HF, Gardier AM, Dranovsky A, David DJ, Beck SG, Hen R, Leonardo ED (2010) 5-HT1A autoreceptor levels determine vulnerability to stress and response to antidepressants. Neuron 65:40-52.

Rodriguez JJ, Jones VC, Verkhratsky A (2009) Impaired cell proliferation in the subventricular zone in an alzheimer's disease model. Neuroreport 20:907-912.

Rodriguez JJ, Jones VC, Tabuchi M, Allan SM, Knight EM, LaFerla FM, Oddo S, Verkhratsky A (2008) Impaired adult neurogenesis in the dentate gyrus of a triple transgenic mouse model of alzheimer's disease. PLoS One 3:e2935.

Saenz del Burgo L, Cortes R, Mengod G, Zarate J, Echevarria E, Salles J (2008) Distribution and neurochemical characterization of neurons expressing GIRK channels in the rat brain. J Comp Neurol 510:581-606.

Sanacora G, Berman RM, Cappiello A, Oren DA, Kugaya A, Liu N, Gueorguieva R, Fasula D, Charney DS (2004) Addition of the alpha2-antagonist yohimbine to fluoxetine: Effects on rate of antidepressant response. Neuropsychopharmacology 29:1166-1171.

Santarelli L, Saxe M, Gross C, Surget A, Battaglia F, Dulawa S, Weisstaub N, Lee J, Duman R, Arancio O, Belzung C, Hen R (2003) Requirement of hippocampal neurogenesis for the behavioral effects of antidepressants. Science 301:805-809.

Signorini S, Liao YJ, Duncan SA, Jan LY, Stoffel M (1997) Normal cerebellar development but susceptibility to seizures in mice lacking G protein-coupled, inwardly rectifying K+ channel GIRK2. Proc Natl Acad Sci U S A 94:923-927.

Slesinger PA, Stoffel M, Jan YN, Jan LY (1997) Defective gamma-aminobutyric acid type B receptor-activated inwardly rectifying K+ currents in cerebellar granule cells isolated from weaver and Girk2 null mutant mice. Proc Natl Acad Sci U S A 94:12210-12217.

Strobel A, Gutknecht L, Rothe C, Reif A, Mossner R, Zeng Y, Brocke B, Lesch KP (2003) Allelic variation in 5-HT1A receptor expression is associated with anxiety- and depression-related personality traits. J Neural Transm 110:1445-1453.

Szabo ST, de Montigny C, Blier P (2000) Progressive attenuation of the firing activity of locus coeruleus noradrenergic neurons by sustained administration of selective serotonin reuptake inhibitors. Int J Neuropsychopharmacol 3:1-11.

Torrecilla M, Fernandez-Aedo I, Arrue A, Zumarraga M, Ugedo L (2013) Role of GIRK channels on the noradrenergic transmission in vivo: An electrophysiological and neurochemical study on GIRK2 mutant mice. Int J Neuropsychopharmacol 16:1093-1104.

Torrecilla M, Marker CL, Cintora SC, Stoffel M, Williams JT, Wickman K (2002) G-protein-gated potassium channels containing Kir3.2 and Kir3.3 subunits mediate the acute inhibitory effects of opioids on locus ceruleus neurons. J Neurosci 22:4328-4334.

Williams JT, Colmers WF, Pan ZZ (1988) Voltage- and ligand-activated inwardly rectifying currents in dorsal raphe neurons in vitro. J Neurosci 8:3499-3506.

Figure legends

Figure 1. Behavioral characterization of GIRK2 mutant mice. a) In the novelty suppressed feeding test (NSFT), both GIRK2$^{+/-}$ and GIRK2$^{-/-}$ mice displayed a lower latency to eat compared to wild-type (WT) mice. (*n*=9-22 mice/group; **p*<0.05 and ***p*<0.01 *vs* WT, one-way ANOVA followed by Newman-Keuls test). b) No changes among groups in the amount of food consumed after the NSFT (*n*=9-22 mice/group). c) In the tail suspension test (TST), GIRK2$^{-/-}$ mice displayed a lower immobility time compared to GIRK2$^{+/-}$ and WT mice (*n*=14-16 mice/group; ****p*<0.001 *vs* WT, one-way ANOVA followed by Newman-Keuls test). d) In the TST, 30 minutes after the citalopram injection (10 mg/kg, i.p.), both GIRK2$^{+/-}$ and GIRK2$^{-/-}$ mice showed a lower reduction of the immobility time compared to WT mice (*n*=7-10 mice/group; **p*<0.05 *vs* WT, one-way ANOVA followed by Newman-Keuls test). Bars represent mean±S.E.M. of *n* animals.

Figure 2. Inhibitory effect of 8-OH-DPAT and citalopram on the firing rate of dorsal raphe neurons in wild-type and GIRK2 mutant mice. a) Representative firing rate histograms illustrate the inhibitory effect of 8-OH-DPAT (12.5-300 µg/kg, i.p.) on dorsal raphe (DR) basal activity in wild-type (WT) and b) GIRK2$^{-/-}$ mice. Subsequent adminitration of the 5-HT$_{1A}$ antagonist, WAY100635 (1-1.5 mg/kg, i.p.), completely reversed the 8-OH-DPAT-induced inhibitory effect. c) Dose-response curves for 8-OHDPAT and d) citalopram (0.5-3 mg/kg, i.p.) on DR firing rate in WT, GIRK2$^{+/-}$ and GIRK2$^{-/-}$ mice. Each point represents the mean±S.E.M. of *n* experiments (*n*=5-15 mice/group).

Figure 3. Inhibitory effect of citalopram on the firing rate of dorsal raphe neurons in wild-type and tertiapin-Q injected mice. a) Representative firing rate histograms illustrate the inhibitory effect of citalopram (0.5-2.5 mg/kg, i.p.) on dorsal raphe

(DR) basal activity in artificial cerebrospinal fluid-injected mice (WT control, i.c.v.) and b) tertiapin-Q injected mice (WT TPN-Q, 100 pmol, i.c.v.). c) Dose-response curves for citalopram (0.5-3 mg/kg, i.p.) on DR firing rate in wild-type (WT), WT control, and WT TPN-Q. Each point represents the mean±S.E.M. of *n* experiments (*n*=4-5 mice/group).

Figure 4. Hypothermic response induced by 8-OH-DPAT in wild-type and GIRK2 mutant mice. The temperature decrease induced by 8-OH-DPAT (0.5 mg/kg, i.p.) was significantly lower in GIRK2$^{-/-}$ mice relative to wild-type (WT) mice in minute 30. Mice of each genotype injected with 0.9% saline (saline groups) were used as controls. Each point represents the mean±S.E.M of *n* animals (*n*=6-7 mice/group; **p*<0.05 *vs* WT, two-way ANOVA followed by Bonferroni posttest).

Figure 5. Brightfield micrographs showing phosphorilated Histone H3 (HH3, a proliferating mitotic marker) labelled cells within the dentate gyrus and subventricular zone of wild-type and GIRK2 mutant mice. A-b: Dual labeling of HH3 positive cells (arrows) and glial cells (GFAP, brown) in the hippocampal dentate gyrus (DG) of a) wild-type (WT) and b) GIRK2$^{-/-}$ mice. Bar graphs showing no differences among groups in the area density of HH3 positive cells within c) the DG (all layers included) and d) the subventricular zone (SVZ) of WT and GIRK2 mutant mice. Bars represent mean±S.E.M. of *n* animals (*n*=6-10 mice/group). GCL: Granular Cell Layer, ML: Molecular Layer.

Table 1. *In vivo* electrophysiological properties of dorsal raphe neurons recorded under basal conditions in wild-type and GIRK2 mutant mice.

	WT (*n*=86)	**GIRK2$^{+/-}$ (*n*=79)**	**GIRK2$^{-/-}$ (*n*=45)**	**WT TPN-Q (*n*=15)**
Firing rate (Hz)	1.68±0.08	1.88±0.09	1.99±0.15*	2.33±0.27**
Coefficient of variation (%)	37.64±1.21	36.57±1.21	35.21±1.54	40.38±3.25
Burst firing neurons (%)	7	5	2	13
- Firing rate (Hz)	2.22±0.36	2.01±0.37	4.03	1.49±0.38
- Number of burst	1.33±0.21	4.33±1.85	1.00	2.5±1.50
- Spikes in burst (%)	1.15±0.46	1.01±0.87	0.41	2.8±1.32
- Mean spikes per burst	3.00±0.81	2.00	2.00	3.50±0.50

Each cell was recorded for at least 3 minutes (180 seconds were taken for subsequent analysis). All data are presented as the mean±S.E.M of *n* experiments. WT: wild-type; GIRK2$^{+/-}$: GIRK2 heterozygous mice; GIRK2$^{-/-}$: GIRK2 homozygous mice. WT TPN-Q: tertiapin-Q-injected WT mice. *p<0.05 and **p<0.01 *vs* WT. Two-tailed unpaired t-test.

FIGURE 1

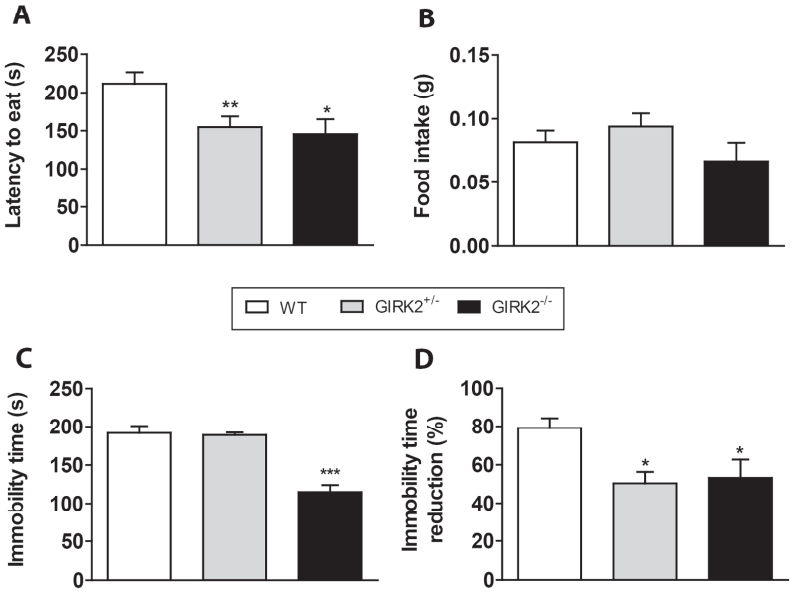

199x168mm (300 x 300 DPI)

FIGURE 2

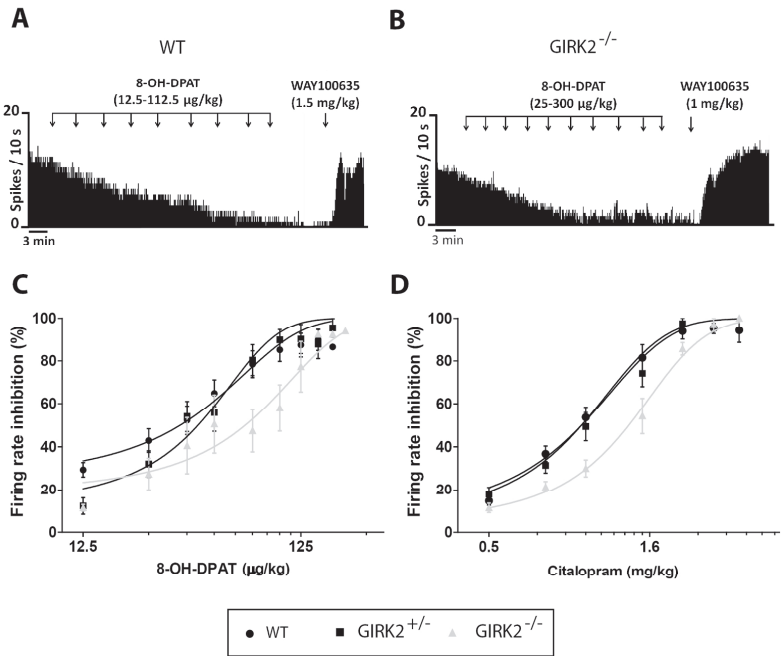

205x193mm (300 x 300 DPI)

FIGURE 3

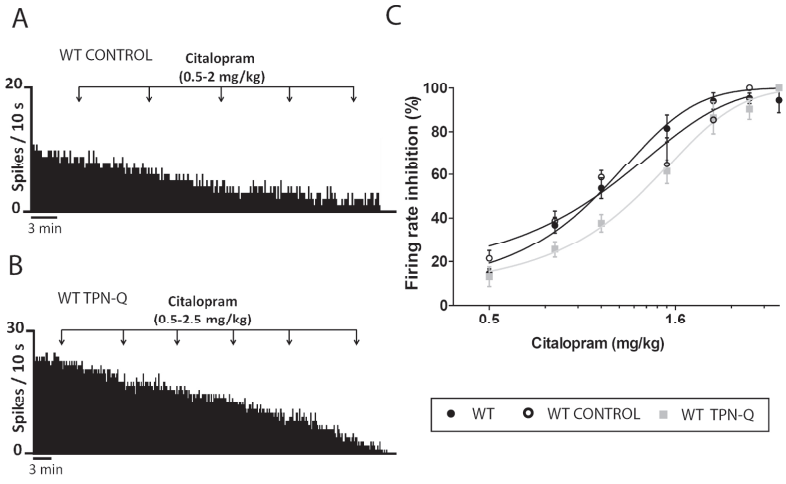

203x143mm (300 x 300 DPI)

FIGURE 4

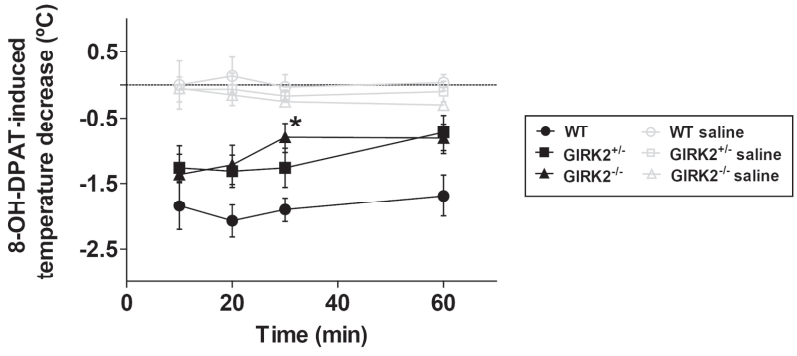

192x110mm (300 x 300 DPI)

FIGURE 5

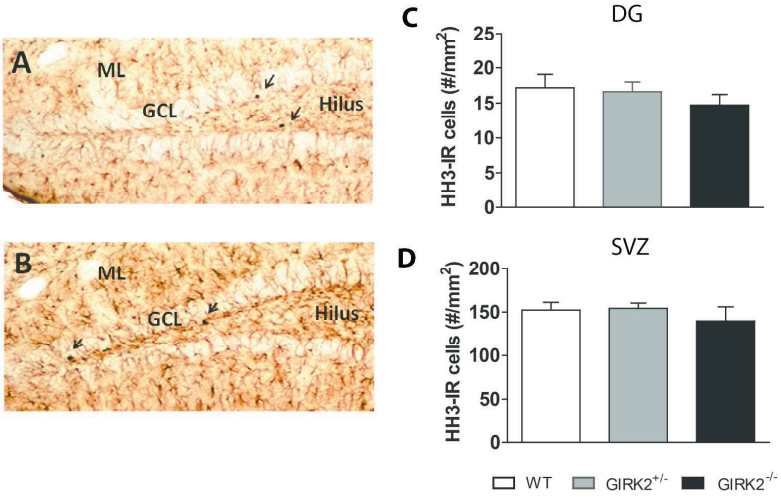

206x139mm (300 x 300 DPI)

The image from the cover and back cover was modified from
www.approximatefield.wordpres.com